2011

Structure-Function Relationships in Poly(3-hexylthiophene)s Formed via Manipulation of Oxidative Coupling Routes

Warren James Solfiell
Louisiana State University and Agricultural and Mechanical College

STRUCTURE-FUNCTION RELATIONSHIPS IN POLY(3-HEXYLTHIOPHENE)S FORMED VIA MANIPULATION OF OXIDATIVE COUPLING ROUTES

A Dissertation

Submitted to the Graduate Faculty of the
Louisiana State University and
Agricultural and Mechanical College
In partial fulfillment of the
Requirements for the degree of
Doctor of Philosophy

In

The Department of Chemistry

By
Warren J. Solfiell
B.S., Framingham State University, 2004
December, 2011

Acknowledgements

I would foremost like to thank my mother, Margaret. You are the one person that has consistently remained in my life through the good times and the bad. There is no question that your love for me is unconditional. You have always provided me the support and compassion that have guided me to where I am today and for these things I thank you. I love you very much.

I would also like to thank Professor Carol Russell, my undergraduate advisor at Framingham State University. You were there when I needed a mentor and a friend and I am very lucky to have met you. Thank you.

I want to express my immense gratitude to Professor Robin McCarley. There is no doubt in my mind that without your guidance, patience, understanding, and kindness I would not have come this far. You are a very special and gifted person on all accounts scientific and otherwise. I thank you from the bottom of my heart.

Each of you never lost your faith in me during the dark times when I could not find the same in myself. For this I am forever grateful.

I would also like to thank Dr. Rafael Cueto. Your help with all things SEC could never be over stated. Thank you.

Table of Contents

List of Tables

List of Figures

List of Abbreviations

$(CH)_x$	poly(acetylene)
Cl^-	chloride ion
DCM	dichloromethane or methylene chloride
HCl	hydrochloric acid
$FeCl_3$	iron(III) chloride or ferric chloride
P3AT	poly(3-alkylthiophene)
P3HT	poly(3-hexylthiophene)
DRI	differential refractive index
PDI	polydispesity index
M_N	number-average molecular weight
M_W	weight-average molecular weight
GC-MS	gas chromatography-mass spectrometer
GPC	gel-permeation chromatography
SEC	size-exclusion chromatography
^{1}H-NMR	proton nuclear magnetic resonance
FT-IR	Fourier-transform infrared spectroscopy
MALDI-ToF-MS	Matrix-assisted laser/desorption time-of-flight mass spectrometry
MALLS	Multi-angle laser light scattering
UV-Vis	Ultraviolet-visible absorption spectroscopy
XPS	X-ray photoelectric spectroscopy
ESR	Electron spin resonance
λ_{max}	Wavelength of maximum absorbance

cm	centimeter
g	gram
mg	milligram
μm	micrometer
μs	microsecond
M	molar
mol	mole
nm	nanometer
m/*z*	mass-to-charge ratio
MW	molecular weight
MWD	molecular weight distribution
S	siemen or ohm^{-1}
V	volt
kV	kilovolt
HT	head-to-tail coupling
HH	head-to-head coupling
TT	tail-to-tail coupling
C	coulombs
mL	milliliter
L	liter
THF	tetrahydrofuran
DCE	1,2-dichloroethane
AN	acceptor number
DN	donor number

Abstract

This investigation focused on the analytical characterization of poly(3-hexylthiophene), a heterocyclic conducting polymer system, with an overall objective of elucidating the effects that the experimental conditions during chemical oxidation using iron(III) chloride as an oxidant impart on the structure of the resulting polymers. Poly(3-alkylthiophene)s are extensively studied materials due to their high electrical conductivities and unique optical properties that make them extremely valuable for use in contemporary technological applications and devices. Specifically, the aim of this research was to determine the dependence of structural characteristics, such as endgroups, molecular weights, and regioregularities, on the solvent employed for the reaction and the temperature the reaction was performed. Matrix-assisted laser desorption/ionization time-of-flight mass spectrometry (MALDI-ToF-MS) was used to characterize the endgroup additions to and obtain molecular weight data about poly(3-hexylthiophene) formed using different experimental conditions. The regioregularity of the materials was evaluated by means of ^{1}H-NMR. Also, average molecular weights and molecular weight distributions were gathered by analytical and semi-preparative size-exclusion chromatography.

In this study it was demonstrated that the physical properties of the solvents employed for chemical oxidation, such as polarity and Lewis acidity and basicity, imparted markedly different structural characteristics to the resulting polymer. It was also shown that the temperature at which the reactions were performed dramatically impacted the extent of chlorination to and the regioregularity of the resulting polymers. Finally, this study revealed for the first time that multiply-charged ion species are formed during the MALDI-ToF-MS analysis of poly(3-alkylthiophene)s and that the presence of these species dramatically affects the accurate determination of molecular weight information for these materials by MALDI-Tof-MS analysis.

Chemical oxidative polymerization remains the most popular and wide-spread method for the preparation of P3ATs, due to the method's affordability, ease, and ability to form large yields of high mass polymer. Therefore, the ability to utilize this synthetic route with a better understanding as to the effects of the experimental conditions–which may be employed in order to augment the materials characteristics–is of utmost importance. The work presented in this Dissertation has demonstrated that through the proper selection of solvent, and/or adjustment to temperature, this simple and convenient synthetic method can be employed to modify the properties of the resulting P3ATs.

Chapter 1

Introduction and Background

1.1 Research Overview

In order for poly(3-alkylthiophene) systems formed by chemical oxidative coupling, to be better employed in a purposeful manner, and become integrated for use in contemporary applications, a better understanding of the basic chemistry and physics that govern their formation and resulting structure is of the utmost importance. It is well known that the structure of these materials directly affects their physical properties that in turn regulate their relevance in modern technological applications and devices.[1,2] The studies presented within this dissertation are focused on garnering an improved understanding of the structural properties of poly(3-hexylthiophene) characteristic of their formation by chemical oxidative coupling by iron(III) chloride. The overall goals of the work are to appraise the influences of variations in chemical oxidative conditions, with the desire of achieving the ability to manipulate structural properties, including regioregularity, average molecular weight, molecular weight distribution, and endgroup substitutions, of the resulting polymer. Specifically, acquiring additional knowledge as to the effects of solvent and temperature, as well as the oxidant-to-monomer ratio, as a function of their influence on the physical properties of the polymer is the aim of this inquiry.

Scientific research involving water-soluble, stimuli-responsive dendrimer systems for use as carriers for guest molecules (Figure 1.1) has been a focus in Professor Robin L. McCarley's research group in the Department of Chemistry at Louisiana State University (LSU).[3,4] These systems are meant to function as carriers as a result of the modification to their periphery/exterior with oligo(pyrrole) units. The capture and release of small guest molecules within the dendrimer system is intended to be achieved by the geometric (steric) changes that occur in the structure upon electron transfer, i.e. reduction and oxidation, of the pyrrole

substituents. Oligo- and poly(pyrrole)s, as well as poly(thiophene)s, have been shown to possess large conformational differences in structure depending on their oxidation state.[1] In an oxidized or cationic form, oligo(pyrrole)s are conformed in a planar and rigid geometry (quinoidal state), which is exploited in a dendrimer system in order to trap guest molecules within the core. Upon reduction, the oligo(pyrrole) returns to a more flexible conformation, which affords the release of the guest from the dendrimer. Enhancement in the effectiveness of these dendrimer systems requires a detailed knowledge of the structure of oligo(pyrrole)s.

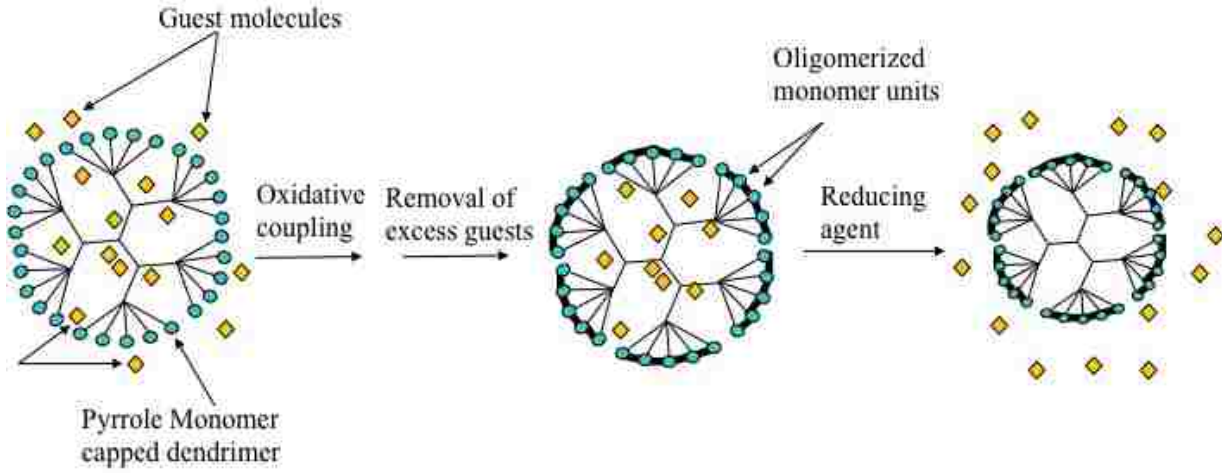

Figure 1.1 Stimuli-responsive dendrimer system.

Prior work involving the elucidation of some experimental conditions influencing the structural characteristics of oligo(pyrrole)s has been performed in these labs.[5] However, because the mechanisms of oxidative polymerization of pyrroles are still not fully understood, and poly(pyrrole)s are more difficult to characterize due to processability issues, oligo- and poly(thiophene)s have been employed as model systems. Some important information regarding the effects that experimental conditions have on these materials has been established concerning the specific solvent and oxidant-to-monomer ratios employed during their formation.[5] Work in this dissertation continues upon the knowledge that has been obtained so far by attempting to clarify such lingering questions as what properties of solvents impact the creation of poly(3-

hexylthiophene) (P3HT)? And, what kinetic and thermodynamic influence does temperature have upon P3HT formation?

Structural characterization of poly(3-hexylthiophene)s, used as model systems for oligo(pyrrole)s, in order to obtain a better understanding of the nature of capture/release dendritic systems is in itself important. Nonetheless, P3HTs have consistently been one of the most intensely investigated, and widely utilized conducting polymers in the world for the past several decades, due to their unique nonlinear and electrically conducting properties. Furthermore, chemical oxidative coupling with iron(III) chloride ($FeCl_3$) remains the most widely employed and popular method for the production of these materials, due to the ease and affordability of the method. Therefore, in the broadest sense, it is of enormous importance to understand the influence that the experimental conditions have on the structure of the resulting polymer, which governs their functionality and usefulness.

The regioregularity, molecular weight (MW), molecular weight distribution (polydispersity or PDI), and nucleophilic addition of substituent groups or atoms have all been shown to directly impact the optical, electrical, and chemical properties of P3HTs,[6-8] and deserve further careful examination as a function of the polymerization environment. A large majority of the work presented herein was acquired by the use of matrix-assisted laser desorption/ionization time-of-flight mass spectrometry, or MALDI-ToF-MS. This technique is utilized for analysis of P3HTs formed by oxidative polymerization, in order to determine repeat (monomer) units, MWs, PDIs, and endgroup structures. To some extent, the limitations of this technique, for the characterization of synthetic conducting polymers, are addressed with an emphasis on the analytical approaches required in order to accurately assess these materials by this means.

1.2 Background

1.2.1 A Historical Viewpoint of the Development of Conjugated Polymers

When Henry Letheby wrote *On the Production of a Blue Substance by the Electrolysis of Sulphate of Aniline*[9] in 1862, he could never have imagined the extent, and breadth, of work that has lead to the current state of understanding that has been established in regards to conjugated aromatic, and other conducting polymers. The advances we have seen in the past several decades concerning conducting polymers have dramatically changed the face of science and technology. Although the pathway that led to this era has been a long and winding road. In fact, for the next fifty years after Letheby first published these findings, the majority of publications with regard to aromatic polymeric materials, such as aniline black and pyrrole black[10,11] (as they are often called), were patents for different methods of using these substances for dies or inks. It was not until the early 20th century and the introduction of more developed analytical techniques that scientific endeavors became focused on understanding the experimental conditions under which these compounds were formed, and the implications these findings had for mankind.[12]

Throughout the 1920s and 1930s, advances in quantum mechanics fostered much thought on theories behind conduction in metals, and solid organic crystals. Historical works by such intellectual giants as Frenkel, Jost, Schottky, Peierls, and Mott led to a more comprehensive understanding of diffusion and conduction of electrons throughout crystal lattice π-structures.[13-19] Concurrently, physicists such as Hund, Huckel, and Mulliken were introducing the world to the Molecular Orbital theory using linear combinations of atomic orbitals (LCAOs) in an attempt to represent molecular orbitals for entire molecules. In conjunction with the development of improved spectroscopy methods, scientists began to explain the absorption of energy within organic substances and how this was related to their molecular structure. In 1939, Mulliken published two extraordinary papers comparing the observed absorption spectra of conjugated

polyenes, and their derivatives, with the theoretical calculations for electronic transitions on various models of butadiene, octatetraene, and β-carotene.[20,21] Mulliken described for each case, unsaturated electrons give rise to a series of electronic transitions which spread over an increasing range of the spectrum with increase in the number of conjugated double bonds; we now know, the effective conjugation length of conducting polymers clearly influences their electrical and optical characteristics.

The same year, Lewis and Calvin attempted to uncover the connection between molecular structure and the position, as well as intensities, of main electronic absorption bands for organic dyes as seen by the spectroscopic methods of the day.[22] Their work aided in trying to simplify the complex band system that is found in many dyes by correlating observed absorption patterns with bond types and molecular structure in order to establish a general set of rules regarding the color of dyes. Complementing their work, in 1943 Zeichmeister interpreted Gillam's work with isomerization of C_{40}-carotenoids,[23,24] and concluded that this phenomenon was a result of spontaneous *cis-trans* rearrangement.[25,26] This was later clarified by spectroscopic means[27] and shown to adhere to Pauling's theoretical treatment of CH-groups adjacent to a double bond with a coplanar *cis* configuration overlap.[28] This work empirically showed that this conformational overlap not only decreased the stability of the molecule, but shifted the molar absorptivity maxima to shorter wavelengths (blue or hypsochromic shift). This is information that is readily accepted today and directly impacts the inherent physical properties of conducting polymers.

A better understanding of molecular orbital overlap, evidenced in the spectral observations for conjugated organic materials, combined with furthering theoretical research into electronic band structure relating to conductance led to an interest in the use of organic compounds as semiconducting materials in the second half of the 1940s. In 1947 Wallace

published *The Band Theory of Graphite*,[29] in which was discussed the material's electrical conductivity, and anisotropy, as well as thermal conductivity, diamagnetic susceptibility, and optical absorption in terms of the band theory of solids. That same year, Akamatu and Nagamatsu reported *A New Suggestion for a Model Representing the Structure of Carbon Black*,[30] in which it was surmised that if the hexagonal planes found in the structure of graphite and amorphous carbon are considered the "molecule" within the structure, then analogous structures could be found among other well-known organic compounds; they further reasoned that if the electrical conductivities seen in graphite are a function of it's molecular structure, then these compounds will exhibit electrical conductance to some degree. Important work towards attempting to elucidate an understanding of the electronic spectra of organic compounds consisting of conjugated double bonds was published by Bayliss in 1948. In his paper *A "Metallic" Model for the Spectra of Conjugated Polyenes,* Bayliss, noting the growing evidence that conjugated materials displayed many of the characteristics of "free" electrons in metals and semiconductors, described his quantitative application of a simple "metallic" model to the electronic spectra of polyenes in the *trans* form.[31] Bayliss confirmed that, despite weaknesses associated with the simplifying assumptions of uniform potential and infinite ionization energies, agreement between theoretical and empirical data was good, particularly in the case of band intensities. Furthermore, he showed that the observations of Mulliken and Rieke,[32] in regards to band intensities and the increase in the number of double bonds for conjugated polyenes, could now be expressed accurately and quantitatively without involving any empirical factors.

In the closing years of the 1940s and the opening of the 1950s, scientific endeavor turned to the correlation between the structure of organic molecules and their function with regard to their electrical conductivities. For instance, Szent-Gyorgyi began to apply this ideology to biological systems and explained that proteins must be likened to these conjugated π-systems

and were associated with biological catalysis and muscle contraction.[33] D. D. Eley investigated the electrical characteristics of metal-free phthalocyanine, comparing it to copper phthalocyanine, determining that phthalocyanine was itself an intrinsic semiconductor.[34] Akamatu et al. began characterizing the electrical conductivities of a series of polycyclic aromatic compounds having analogous structures to graphite including, violanthranone, isoviolanthranone, pyranthranone, and ovalene; these were shown to have electrical conductances of $2.3\times(10^{-10})$ $ohm^{-1}cm^{-1}$, $5.7\times(10^{-9})$ $ohm^{-1}cm^{-1}$, $3.9\times(10^{-15})$ $ohm^{-1}cm^{-1}$, and $4.4\times(10^{-15})$ $ohm^{-1}cm^{-1}$ and were termed "organic semiconductors."[35,36]

In 1954, Akamatu et al. then uncovered a phenomenon which would be key in the development of conducting organic compounds and polymers for decades to come when they discovered that the polycyclic aromatic compound perylene, which they had been characterizing and had been shown to possess semiconducting properties, formed charge-transfer complexes in the presence of halogens.[37] They were able to show that direct exposure of perylene to bromine vapor resulted in a black complex that had conductivities of 10^{-3} ohm^{-1} cm^{-1}, as opposed to perylene alone that possesses a conductivity of 10^{-23} ohm^{-1} cm^{-1}. They noted that the high conductivity must be due to some particular electron state following the formation of the complex, but the mechanism of charge transfer in such a complex still remained unknown. They also made clear that the complexes under study were not stable, a problem that would haunt researchers for some time. By 1956, Akamatu et al. reported that not only did perylene form these complexes with halogens, but most polycyclic aromatic compounds in the presence of bromine or iodine form complexes as well, with conductivities between 10^{0} ohm^{-1} cm^{-1} and 10^{-3} ohm^{-1} cm^{-1}.[38] The most revealing result reported within this publication was that, although most halogen complexes were still quite environmentally unstable, the complex formed between violanthrene and iodine showed high thermal and electrical stability over a period of weeks.

In the later portion of the 1950s, the work with electrical conductivities found within organic semiconducting molecules, resulting from molecular orbital overlap due to their physical structures, turned some research toward the synthesis and characterization of polymers possessing extended π-bond conjugation. Work with pyrolized carbon polymers formed via destructive cyclization and having extended conjugation that could support enhanced electrical properties, had been ongoing since the early 1950s.[39-41] However, it was not until the end of the decade that reports of directly synthesized semiconducting polymers began to appear in the literature. In 1958, Felmayer and Wolf synthesized a polymeric copper phthalocyanine with semiconducting properties.[42] In 1959, Pohl and Itoh prepared a large number of semiconducting phenolphthalein-type polymers, made by treating various phenols with acid anhydrides.[43,44] In that same year, McNeil and Weiss reported the synthesis of xanthene-type polymers with conductivities in the range of $1.4\times(10^{-4})$ ohm^{-1} cm^{-1}.[45]

Concurrently and into the early 1960s, began an age of extensive work towards developing and characterizing conducting polymers with an aggressive effort placed in the direction of garnering a more comprehensive understanding of the mechanisms supporting charge transfer in such materials. From his studies on the absorption spectra of biphenyl derivatives, G. H. Beaven observed a shift to shorter wavelengths (blue shift) of the conjugation band with an increase of the *ortho*-substituent group.[46-48] Beaven explained that the *ortho*-substituents are capable of conjugation with the phenyl groups and that steric interactions prevent coplanarity conditions from being satisfied for either the diphenyl-type or the alternative modes of conjugation. Beaven's findings were being applied to the analysis of conductivities in other conjugated polymers as well. In their paper published in 1963, McNeil et al. reported forming polypyrrole, as an amorphous black insoluble material, via pyrolysis of tetraiodopyrrole.[49] Their material possessed conductivities between 10^{0} ohm^{-1} cm^{-1} and 10^{-2}

ohm^{-1} cm^{-1}. In that paper they argued that steric effects did not play a crucial role in conductivities of the materials as was thought to be the case with amorpous polybenzenes formed in 1956 by Gibson et al.[50]; these materials did not conduct electricity. McNeil referred to other works consisting of the synthesis of conjugated polymers possessing phthalein and quinoxalophenazine units claiming they also lacked coplanarity, but possessed relatively high conductivities in the range of 10^{-4} ohm^{-1} cm^{-1}.[45,51] They surmised that the lack of conductivity in the former may be due to the ionization of lactones to form immobile electron acceptor centers (carboxyl anions) and mobile "holes" (carbonium ions), thus conferring a *p*-type character to the polymer.

In 1962, Pohl and Englehardt, while characterizing the properties of the highly conjugated polymers polyacene quinone, polyquinazones, polyacene, and polyaniline, reported that conduction in semiconducting conjugated polymers do not always meet the criteria for the rigorous application of simple band theory.[44] They argued that electrical conductivity is electronic in nature and not ionic, and that in homologous series conductivity is dependent upon the chemical structure of the material. The homologous series consisted of incorporating 14 aromatic nuclei into the zinc chloride-catalyzed pyromellitic dianhydride-acene polymer, for which a decrease in resistivity was observed as the size of the fused aromatic nuclear portion of the acene component of the polymer increased; that is as effective conjugation length increased, an increase in conductivity was observed.

Other important findings from this era stemmed from further work by Bolto, McNeil, and Weiss concerning the characterization of polypyrroles formed from the pyrolysis of tetraiodopyrrole. Bolto et al. realized that in polypyrroles formed by pyrolysis below a temperature of 500 °C, iodine in various amounts remained present in the polymer depending on the temperature at which the pyrolysis was conducted.[49,52] In these reports, attempts to remove

this excess iodine was performed via treatment with thiosulphate or alkali, solvent extraction, and electrochemical reduction. Through their work concerning the removal of iodine, they determined by electron spin resonance, ESR, that the iodine was present in the form of a charge-transfer complex so weakly held that it could be considered only physically adsorbed. However, in the third installment of their publication concerning this work, it was shown that electrical conductivities as a function of the temperature at which the polymer was formed did not vary greatly from polymers formed from 120 °C to 500 °C; this occurred despite the fact that electron spin resonance showed polymer with varying degrees of iodination.[53] Nonetheless, based on results from their work with electrochemical reduction as a means of iodine removal they showed that the electrical resistivity increased as iodine was "reduced out" of the polymer; they could not say that this was not a result of the reduction of the polymer itself. Although they did not fully understand the mechanisms of doping at the time, they showed that doping of these polymers drastically enhances the physical properties of these materials.

The works of these scientists discussed to this point in time have laid the foundation for the explosion in the area of research concerning the synthesis and characterization of conducting polymers that would begin in the 1970s. The true birth of the contemporary age of electroactive polymers would come in 1977 when Shirakawa et al. published *Synthesis of Electrically Conducting Organic Polymers: Halogen Derivatives of Poly(acetylene), $(CH)_x$*.[54] In that work, remarkably high conductivities for *trans*-poly(acetylene) were observed for polymer exposed to iodine vapors resulting in an increase in conductivity for the material of over seven orders of magnitude (38 S cm^{-1} at room temperature versus $4.4\times(10^{-5})$ S cm^{-1}). A major concern was that these doped poly(acetylene)s were extremely environmentally unstable. This work would later earn Hideki Shirakaw, Alan MacDiarmid, and Alan Heeger the 2000 Nobel Prize in Chemistry.

1.2.2 A Historical Viewpoint and Modern Applications of Poly(thiophene)s

Poly(thiophene)s, as well as poly(pyrrole)s, are in a class of conjugated semiconducting polymers called poly(heterocycle)s. More specifically, thiophene and pyrrole are aromatic 5-membered rings with sulphur and nitrogen as heteroatoms. Poly(thiophene)s and poly(pyrrole)s are two of the most widely investigated conducting polymers to date. This is due to their high electrical conductivities, their unique nonlinear optical properties, their long-term stabilities after doping, and their relatively low toxicities.

The first report indicating the attempts to polymerize thiophene was published in 1956 and appears to use a synthetic route similar to modern day Grignard techniques.[55] However, it was reported that formation of poly(thiophene) was unsuccessful. In 1964, the polymerization of thiophene on the surface of dehydratable silica gel used as a catalyst was reported.[56] The authors noted that the polymerization occurred without ring opening and resulted in a polymer having a chain of conjugated double bonds. In 1971 two international patents were issued for methods of preparing poly(thiophene)s. The first involved refluxing thiophene or terthiophene in the presence of sulfonic acids (RSO_3H; where R= Me or *p*-MeC_6H_4), which was reported to give high molecular weight poly(thiophene); it was to be marketed as a useful self-curing, ultraviolet-absorbing coating for aluminum.[57] The second was a process involving the electrolysis of the aromatic heterocyclic compounds furan, pyrrole, and thiophene in a basic aqueous solution to yield poly(furan), poly(pyrrole), and poly(thiophene).[58]

It was not until the early 1980s that a strong focus was placed on poly(thiophene)s as an electrically semiconducting polymer. Although there were reported attempts of the synthesis of poly(thiophene)s by chemical means in the early 1980s,[59,60] the primary method for forming poly(thiophene)s in this period was electrochemical anodic-oxidative polymerization; this was due to higher conductivities exhibited for polymer produced electrochemically, which was in the

form of polymer films on the surface of a platinum electrode. In 1982, Tourillon and Garnier showed the polymerization of several heterocyclic compounds including azulene, pyrrole, and thiophene in this manner.[61] Through investigations using elemental analysis, infrared spectroscopy, and X-ray photoelectric spectroscopy they were able to determine that typically one counteranion existed per every four monomer units and charges residing on polymer chains were delocalized. That same year, Kaneto et al. investigated the electrical properties of poly(thiophene)s prepared by electrochemical methods.[62] They were able to conclude that the material was doped with 26 mol % perchlorate anion from the electrolye $AgClO_4$ and the greenish film had a conductivity of 0.6 S cm^{-1}. In 1983, Tourillon and Garnier reported that poly(3-methylthiophene) formed by electrochemical means and doped with $CF_3SO_3^-$ was environmentally stable, and maintained equivalent electrical conductivities and doping levels after 8 months of exposure to air.[63] Also by 1983, Kaneto et al. revealed that doping conditions (i.e. the electolyte employed during electrochemical polymerization) played a crucial role in the electrical properties of the resultant poly(thiophene).[64] They reported poly(thiophene)s with conductivities of 106 S cm^{-1} for polymer produced in $LiBF_6$-PhCN. Kaneto et al. were concurrently working towards applications for poly(thiophene)s in such devices as batteries and elecro-optical devices.[65,66]

In the mid 1980s an explosion of research into poly(thiophene)s occurred, and hundreds of reports were published in the literature. Concern turned towards the difficulties involved in the successful characterization of poly(thiophene)s and feasible application of the material, due to the insolubility of the higher molecular weight fraction of the polymer. In 1984 Cao et al.,[67] following procedures outlined by Yamamoto et al.[59] for catalytic coupling of thiophene using thienyl Grinard reagents, realized that Yamamoto was able to isolate low molecular weight materials via extractions with methanol and chloroform; this yielded 20% $CHCl_3$-soluble

polymer. Cao, understanding the worthiness of this soluble material for further studies in view of its processability–that made it more amenable to molecular characterization–was able to acquire a 30% yield of $CHCl_3$-soluble materials.

The fractionation of this poly(thiophene) material opened up a new venue of analytical characterization for these materials, allowing researchers to more coherently characterize their physical properties as a function of their molecular structure; this an on going effort today so as to successfully and fully employ these materials in specific and useful applications. By means of vapor-pressure osmometry, VPO, Cao et al. determined this soluble fraction possessed a number-average molecular weight (M_N) between 1,130 Daltons (Da) and 3,010 Da depending on its preparation prior to VPO analysis. Gel-permeation chromatography, GPC, confirmed the broad molecular weight distribution or polydispersity, PDI, of the material. Mass spectrometric examination of collected GPC fractions revealed that the fractions could be assigned as Br-terminated poly(thiophene) oligomers (Br-$(C_4H_2)_n$-Br with n = 3, 4, and 5). Also, the electrical conductivity of the fraction of $CHCl_3$-soluble polymer upon doping with iodine (exposure to iodine vapor) was observed to be 5 S cm^{-1}, as opposed to 10^{-2} S cm^{-1} for the iodine-doped portion of insoluble poly(thiophene), PT. The importance of the effort and ability to better characterize these materials with a broader range of analytical techniques and therefore more insightfully cannot be over emphasized.

These hindrances and difficulties in characterizing and processing PTs formed to this point of the discussion by chemical and electrochemical methods, due to their insolubility and nonmeltability, was overcome in 1985 with breakthrough work by Elsenbaumer and coworkers.[68-70] Elsenbaumer et al. first reported the synthesis and characterization of a series of melt-mouldable poly(3-alkylthiophene)s, P3ATs, that were soluble in most organic solvents, forming environmentally stable and highly conductive complexes upon exposure to electron

acceptor dopants. Their solubility in organic solvents was due to the introduction of an alkyl chain to the thiophene monomer in the 3-position, and it was noted that solubility increased as the length of the alkyl chain increased. Since any advancement in the direction of realistic and relevant applications of PTs relies solely upon a basic perspective and understanding of the chemical and physical properties controlling the enhancement to the effectiveness of the electronic and optical properties, this work opened a new age in the historical progress of PTs. The development of soluble P3ATs now offered a means by which to better scrutinize the chemistry and physics governing these unique materials at a molecular level.

Besides the chemical method employed by Elsenbaumer et al. to produce P3ATS, which involved a Kumada cross-coupling method similar to that used by Kobayashi et al.,[71] the most important method of chemically preparing P3ATs introduced in the 1980s was reported by Sugimoto et al. in 1986.[72] This method involves the chemical oxidative polymerization of 3-alkylthiophene by utilizing a transition metal halide ($FeCl_3$) as a catalyst. Chemical oxidative coupling is a facile, "one-pot" synthesis that enables yields of high molecular weight polymer in a large scale. As opposed to the former method, with reported yields of P3ATs having an M_N = 5,000 Da and *PDI* = 2, chemical oxidative coupling produced polymer with M_N ranging from 30,000–300,000 Da and *PDI*s ranging from 1.3–5.[1] Chemical oxidative coupling remains the choice for the large-scale synthesis of high molecular weight P3ATs, due to the methods ease and affordability.

By the beginning of the 1990s, much effort was being placed on the development of new synthetic pathways for preparing P3ATs with an emphasis on designing routes that ensure coupling between the 2- and 5-positions of adjacent monomer units. Prominently, the three synthetic routes accomplishing this goal that were developed over the next decade were the Reike,[73-75] the McCullough,[6,76] and the GRIM methods.[77] These pathways employ Kumada cross-

coupling techniques. P3ATs can be formed with exclusively 2-, 5- coupling to an extent ≥ 98% by using organomagnesium or zinc positioned on the number five carbon of the activated alkylthiophene intermediate in the presence of a nickel-complexed catalyst (typically $Ni(dppp)Cl_2$, or $Ni(dppe)Cl_2$; where dppp = 1,2-bis(diphenylphosphino)propane and dppe = 1,2-bis(diphenylphosphino)ethane). These methods, although capable of producing highly conjugated materials, are far more complicated, time consuming, and costly when compared to the chemical oxidative coupling method using $FeCl_3$. In fact, this can be observed in the cost of purchasing such materials commercially. For instance, 1 gram of poly(3-hexylthiophene) formed with 98% 2-, 5- coupling can currently fetch upwards of 1,500 U.S. dollars (Sigma-Aldrich #698997), where as the purchase price for P3ATs forms by less complex methods that produce more regiorandom polymer can be as little as one-third the cost (Sigma-Aldrich #510823; 488.50 USD). Still, given the appropriate environment equivalent amounts of P3HT can be produced by chemical oxidative coupling with iron(III) chloride with the cost of materials being generously estimated to be less than 200 USD.

As mentioned, poly(3-alkylthiophene)s are held in very high regard because of their extremely unique nonlinear optical and electrical properties. For these reasons, they are widely investigated for use and integration into a broad variety of devices and applications. P3ATs have been reported to exhibit exceptional optical qualities, including thermochromic, ionochromic, photochromic, and biochromic properties; these make P3ATs particularly well-suited for sensing applications.[78] These optical properties can be exploited by inducing strain to the backbone of the polymer chains, propagated by steric interactions of the side chains upon introduction of a respective stimuli, which in turn causes a hypsochromic (blue) shift in the absorption maxima resulting from a decrease in the overall effective conjugation length of the material. Optical changes attributable to thermally-induced planar/nonplanar conformational transition of the

conjugated backbone have been well documented.[79-81] Ionochromism seen in P3ATs has been utilized for the development of ionically and chemically selective chemosensors.[79,82-85] Furthermore, Levesque et al. reported on a novel dual photochromism in poly(thiophene) derivatives.[86] Finally, the development of biosensors has been reported based on the biochromic properties that P3ATs possess.[87-89]

Due to their high-quality electroluminescent properties, and the ability to modify this property, P3ATs alone or in polymer blends have been incorporated into electrochromic devices and organic light emitting diodes (OLEDs); electroluminescence ranging the entire visible spectrum has been obtained.[90-96] These properties have been shown to be very important to the realization of modern technologies such as light emitting polymeric (LEP) flat and flexible displays.[97] Also, the charge carrier and field effect mobilities present in P3ATs, along with their solubility and therefore processability, have led to the incorporation of P3AT thin films in devices such as organic field effect transistors (OFETs).[98-104] Modern applications of polymeric thin film OFETs include the development of flexible, active-matrix, electronic-paper displays, and radio frequency identification (RFID) tags.[105] RFID tags are currently and commonly employed for everyday purposes such as electronic vehicle registration, fast-pass payments, product tracking, human and animal identification, and inventory systems.

The unique electrical and charge mobility properties of P3ATs have also fostered their incorporation in photovoltaic devices, or solar cells.[106,107] Because they can be easily patterned and selectively functionalized, and they undergo volume changes during oxidation and reduction, P3ATs have been researched for used in electroactive actuators, such as artificial muscles, molecular switches, and molecular motors.[108,109] The oxidative and reductive properties of P3ATs have made them a common additive for anticorrosive paints and coatings,[110] and an integral component in electrostatic dissipating (ESD) materials for use in electronics and

packaging.[1] The electrical characteristics of P3ATs have even led to studies involving their use in conductive fabrics.[111]

The molecular structure of P3ATs is of main concern when assessing and developing their applicability for realistic and relevant use in modern technologies, as both microscopic and macroscopic structure directly influence the electrical[112-117] and optical[118-121] properties of P3ATs. The first step in designing materials that will exhibit exceptional, controlled properties for these purposes is of course the development of synthetic pathways to form P3ATs having optimum structural homogeneity. Several synthetic pathways have been established in order to create highly ordered P3ATs with outstanding physical properties, such as the McCullough,[122] Rieke,[73] and GRIM[77] methods. However, these methods can be complex, time consuming, and expensive, while the resulting polymers may still require additional postpolymerization treatment.[123-125] Although even more realistic than the proposition and development of new and often complicated synthetic pathways, an understanding of the influences with regards to experimental conditions that lead to more affordable and efficient routes for the formation of these materials is a highly valuable endeavor.

The primary focus of the work presented here revolves around an understanding of the effects on the structure of poly(3-hexylthiophene), P3HT, and therefore the resulting physical properties when P3HTs are formed via chemical oxidative coupling using $FeCl_3$ as an oxidant. Chemical oxidative polymerization of these materials remains the most popular and wide-spread method for the preparation of P3ATs, due to the method's affordability, ease, and ability to form large yields of high mass polymer. Granted, this method does produce less ordered polymer than the former regioregular methods mentioned (McCullough, Rieke, and GRIM), but there is growing evidence that indicates such highly regioregular materials may not be as usefulness as P3ATs formed by chemical oxidation for certain applications. For instance, Woo et al.

compared three samples of poly(3-hexylthiophene) having regioregularities of 86, 90, and 96% to elucidate the effect of regioregularity on polymer-fullerene composite solar cell performance.[126] This work showed that although more regioregular P3HTs do have higher optical densities and charge-carrier mobilities, the 86% regioregular P3HT has sufficient electronic properties to afford high efficiency photovoltaic devices and has the advantage of producing more thermally stable devices because crystallization-induced phase segregation is observed with more regioregular polymer composites.

Furthermore, prior work from these labs indicate that experimental conditions, such as solvent and oxidant-to-monomer ratio, do play an essential role in the resulting structure of polymers formed by chemical oxidation with ferric chloride, most noticeably the extent of nucleophilic additions to the polymer chains.[5] Nonetheless, a finer understanding as to which physical properties of solvents and what kinetic factors are imparted by temperature is needed in order to gain insight into the compatibility of chemical oxidative polymerization as an efficient means for the production of quality P3ATs that may be employed in useful modern applications. This work attempts to fully elucidate answers to these questions.

1.2.3 Regioselective Coupling of Poly(thiophene)s

The extent to which 2-5 coupling is observed in P3ATs is classified as the regioregularity of the substance. Materials formed with a high degree of 2-5 coupling are termed regioregular, and materials with a lesser extent of such coupling are regarded as regioirregular. Because 3-alkylthiophenes are not symmetrical molecules, during their coupling three relative orientations between two adjacent monomers are possible between the 2-, and 5-positions. First, the two individual monomer units can couple at the 2-, and 5-positions as mentioned. This configuration is termed head-to-tail (HT) coupling, and it is the desired coupling to maintain effective conjugation and coplanarity within the structure.

Secondly, the monomer units may couple between the same positions in a 2-2' manner. This configuration is termed head-to-head (HH) coupling, in which steric interactions between the alkyl chains creates a decrease in coplanarity (effective conjugation) upon oxidation (doping) of the material. Studies by McCullough, involving model dimers, trimers, and tetramers of 3-alkylthiophenes, 3ATs, show that any coupling besides HT creates a twisting of thiophene rings away from coplanarity, and decreases the π-orbital overlap thereby leading to an increase in the band gap of these materials.[6] Corroborating the effects of regiochemistry of P3ATs, Elsenbaumer et al. had previously reported the effects of regioregularity on the electrical conducting properties of polymers made from 3-butylthiophene/3'-methylthiophene dimers, concluding that polymer having a 63:37 mixture of HT:HH coupling possessed a three-fold increase in electrical conductivity than material formed via a random copolymerization of butylthiophene and methylthiophene (50:50).[127]

Third, the monomer units can couple in a 5-5' fashion, which is referred to as tail-to-tail (TT) coupling, and this leads to the same consequences as HH coupling when evaluated in context of a triad regioisomer. Defects in coplanarity and conjugation can stem from cross-coupling between the 2- and 4-positions also depending on the synthetic method used to form the P3ATs. Coupling between the 2- and 5-positions of adjacent monomers (i.e. HT, HH, TT, and TH) give rise to four chemically dissimilar triad regioisomers (Figure 1.2).[128,129] Regioregularity is expressed in terms of the percentage of HT coupling found within the material and therefore P3AT possessing 98% HT coupling is regarded as being 98% regioregular.

1.2.4 Analytical Determination of Regioregularity in Poly(3-alkylthiophene)s

Because Poly(3-alkylthiophene)s are soluble in common organic solvents a primary technique of choice for the determination of their regiochemistry has been ^{1}H-NMR spectroscopy (proton nuclear magnetic resonance spectroscopy). In a regioregular polymer,

comprised completely of HT coupling, there appears only one aromatic signal for the proton on the carbon found in the four position of the thiophene ring. Whereas regioirregular polymer consisting of mixtures of the four triad regioisomers possible in random coupling (HT-HT, HT-TT, HT-HH, and TT-HH) will result in the observation of 4 distinct aromatic signals in the ^{1}H-NMR spectrum arising from the proton found of the carbon at the four position of the central ring representing each of the different triad isomers. Sato et al., through the aid of ^{1}H-^{1}H-NOESY and ^{1}H-NOE difference spectroscopy, were able to surmise and assign the chemical shift for the aromatic resonances of the four different triad regioisomers.[128,129] However, the exact ^{1}H-NMR chemical shifts were not explicitly determined until Barbarella et al. successfully synthesized and characterized the four distinct triad regioisomers.[130] As a result, the four distinct peaks were specifically assigned the chemical shifts HT-HT (δ = 6.98 ppm), HT-TT (δ = 7.00 ppm), HT-HH (δ = 7.03 ppm), and TT-HH (δ = 7.05 ppm).

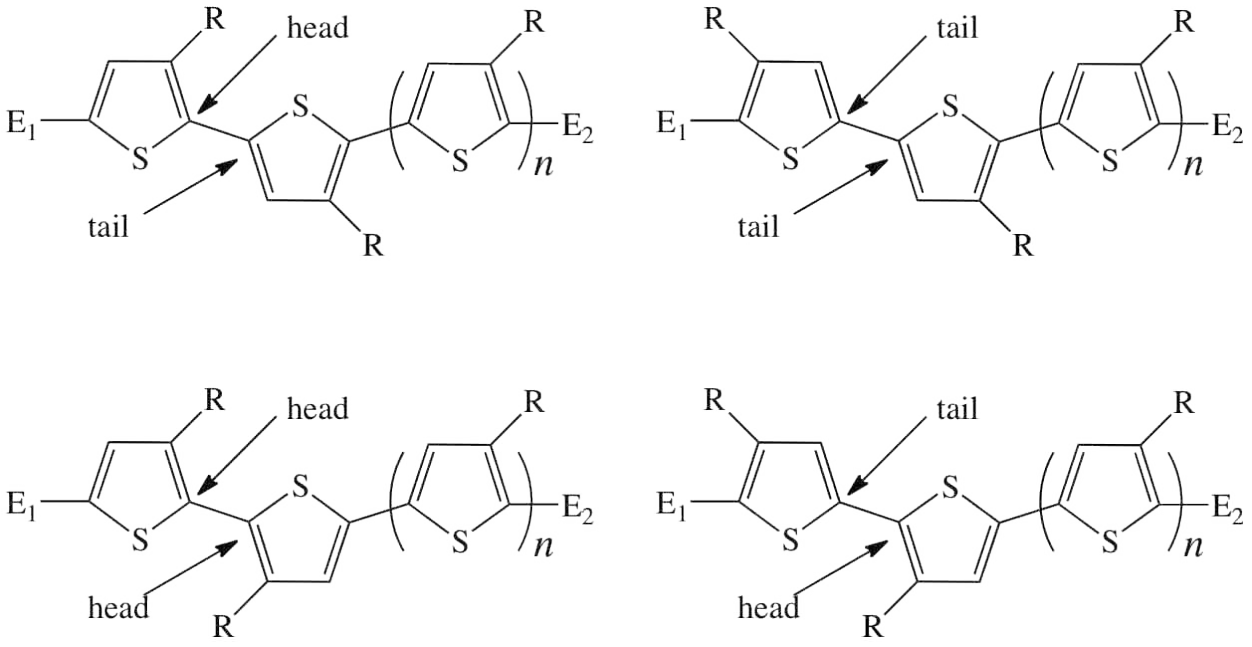

Figure 1.2 Possible regioisomeric coupling of poly(3-alkylthiophene) monomers, showing head-to-tail (HT), tail-to-tail (TT), head-to-head (HH), and tail-to-head (TH).

Another relative method for determination of the ratio of HT-HT coupling compared to non-HT-HT coupling is that which uses comparison of the signal peaks for the α-methylene protons found on the alkyl chain substituent of the thiophene rings of the polymer; this method was first described by Elsenbaumer et al. in 1987.[127] This highly popular method can be used to determine HT content of the polymer by the integration of, and relative ratio between the resonance signals for the α-methylene protons of non-HT-HT and HT-HT materials, which produce signals at $\delta \sim 2.56$ ppm, and $\delta \sim 2.79$ ppm.[127,131] Leclerc et al. confirmed this by ^{1}H-NMR analysis of poly(3,4-dihexylthiophene) a material capable of only HH coupling and resulting in the observation of only one signal at $\delta = 2.50$ ppm for the aryl methylene protons.[131] Likewise, similar information may be obtained by examination of the protons from the β-methylenes of the 3-alkyl substituent, which yield signals at $\delta \sim 1.63$ ppm, and $\delta \sim 1.72$ ppm for β-methylenes in HH coupled polymer and HT coupled polymer, respectively.[128-130]

1.2.5 Regioirregular Poly(3-alkylthiophene)s

The first reports of the chemical synthesis of soluble poly(3-alkylthiophene)s came from Elsenbaumer et al. in 1985. Formation of these soluble materials was done by preparing monomers of 3-ethyl-, 3-*n*-butyl-, and 3-*n*-octylthiophene via the procedure of Kumada.[132] Also prepared was 3-methylthiophene using a method outlined by Gronowitz et al.[133] The monomers were iodinated using the method of Barker et al. to give 3-alkyl substituted 2,5-di-iodothiophenes.[134] The monomers were polymerized by nickel-catalyzed Grignard coupling of the di-iodothiophenes similar to the method outlined by Kobayashi et al.,[71] except that tetrahydrofuran (THF) and 2-methyltetrahydrofuran (2MTHF) were used as reaction solvents. Homopolymers of 3-alkylthiophenes possessing alkyl chains equal to or greater than butyl in size were reported to be readily soluble in common organic solvents, such as THF, 2MTHF, nitropropane, toluene, xylene, methylene chloride, anisole, nitrobenzene, and benzonitrile. ^{1}H-

NMR showed that, although the polymer lacked 2-4 cross-coupling defects, random coupling (HT-HT, HT-TT, HT-HH, and TT-HH) was present. VPO measurements determined these polymers to have M_N between 3,000–8,000 Da and electrical conductivities between 3 and 4 S cm^{-1}.

Curtis et al. coupled 2, 5-bis(chloromercurio)-3-alkylthiophenes using copper powder and catalytic amounts of $PdCl_2$.[135] This method reportly produced regiorandom (but devoid of 2-4 linkages) homo- and copolymer material with an M_N of 26,000 Da, a *PDI* of 2.5, and electrical conductivities from 6×10^2 to 1.9 S cm^{-1}.

Electrochemical anodic oxidation is one means by which regioirregular P3ATs may be produced. This method typically involves growing P3AT films on the surface of a platinum or indium/tin oxide electrode (anode), that is immersed in a monomer/electrolyte solution and then a steady-state or cyclic voltage is applied so as to induce monomer oxidation and polymerization. However, exact experimental parameters for the formation of P3ATs by electrochemical methods vary, and as mentioned previously different electrolytes can have dramatic effects on the properties of the resulting polymers.[131]

Hotta et al.[136] and Leclerc et al.[131] reported similar procedures for the electrochemical production of P3ATs employing a 0.1–0.2 M solution of monomer containing 0.02 M supporting electrolyte (tetrabutylammonium hexafluorophosphate, tetrabutylammonium perchlorate, or tetrabutylammonium trifluoromethanesulfonate) in nitrobenzene or 70:30 mixture of acetonitrile/methylene chloride as a solvent. A voltage was applied in order to maintain a constant current density of 2 mA cm^{-2}, and the temperature of the electrolytic cell was maintained at 5 °C. The electrolytic cell was operated in an oxygen- and moisture-free environment. Oxidative polymerization was performed for periods of 40 seconds in order to create thin films, or up to 6 hours for the production of larger quantities of solid polymer. GPC

analysis of polymers produced over a polymerization period of 2 to 6 hours revealed that the M_N of the materials produced increased from 12,000 Da to 80,000 Da, with *PDI*s of 10.9 and 4.5. Conductivities for polymer films prepared under these conditions were reported to be as high as 40 S cm^{-1}.

In 1986 Sugimoto et al. reported the first instance of chemical oxidative coupling of 3-alkylthiophenes with the transition-metal halide $FeCl_3$ as a catalyst[72] and this route has by far become the most utilized method for the preparation of P3ATs. This facile method has a simple procedure that has been replicated innumerable times with little modification, and historically involves adding a solution of monomer in dry chloroform to a suspension of ferric chloride in dry chloroform while stirring the reactants under an inert gas for a period of hours (typically from 1–24 hours). Until recently,[5] little adjustment to the oxidant-to-monomer ratio has been employed, and usually involves a 4:1–8:1 ratio. This is true of the solvent employed for polymerization also, which arbitrarily has been chloroform except in a very limited number of reports.[5,137] Upon completion, the desired final product would then be washed in methanol, and sometimes acetone. P3ATs formed by means of chemical oxidation under these conditions have reported with M_N ranging from 30,000 to 300,000 and *PDI*s between 1.3 to 5.0.[1]

Leclerc et al. performed structural comparisons between P3ATs formed via electrochemical and chemical oxidative coupling methods.[131] Polymer formed by means of chemical oxidation followed the procedure outlined above by Sugimoto et al. where in 0.003 mol of monomer solubilized in dry chloroform was added dropwise to a suspension of $FeCl_3$ in dry chloroform. The reaction was carried out for 24 hours with stirring under argon atmosphere. The product was washed with methanol, and then acetone. Polymer films were prepared electrochemically at 5 °C by applying a constant current density of 2 mA cm^{-2} on a 6 cm^2 platinum electrode in a one-compartment cell kept under argon. The solvents were either

nitrobenzene, or a 70:30 mixture of acetonitrile:methylene chloride with tetrabutylammonium hexafluorophosphate, tetrabutylammonium perchlorate, or tetrabutylammonium trifluoromethanesulfonate as supporting electrolyte. Polymerization times varied from 1 to 6 hours.

Leclerc reported polymer prepared by chemical oxidation to have M_N of 37,800–55,100 Da, with a *PDI* of 5.0. Whereas polymer prepared via electrochemical methods had M_N between 12,000 and 80,000 Da, with the latter increasing with polymerization time and *PDI*s between 10.9 and 4.5 that decreased with polymerization time. Electrochemically formed polymer was found to have conductivities in the range of 1 to 10 S cm^{-1} and depended on alkyl chain length, and the particular supporting electrolyte employed. Polymer produced chemically gave conductivities between 20 and 30 S cm^{-1}. This can be explained by the increased regioregularity of the chemically-synthesized polymer, with the regioregularity apparently increasing as a function of alkyl chain length due to steric interactions. Upon inspection of ^{1}H-NMR data it was found that polymer created electrochemically had a reioregularity of 60-70% (60-70% HT-HT coupling) by analysis of the peaks for the aryl methylenes, where as the regioregularity for polymer created via chemical oxidation increased to 80%.

Leclerc was also able to obtain important structural information about these materials by means of ^{13}C-NMR. Such ^{13}C-NMR analysis of electrochemically-prepared P3ATs showed that an abundance of small peaks residing between 125 and 150 ppm could be explained from structural defects to the polymers as a result of 2-4 cross-coupling to form branched structures. It was further reasoned that irregular coupling may also be explained by the low selectivity of 2-5 couplings as molecular weight of the materials increased.[138] In addition to this it was noted that during the polymerization of these materials smaller soluble oligomers were produced and that electropolymerization of these smaller oligomers gives rise to material with far greater defects.[139]

X-ray diffraction confirmed that materials prepared via chemical oxidation possessed greater crystallinity than those prepared electrochemically, which is in agreement with the supposition that electrochemically-prepared polymer contains a greater number of 2-4 defects. Also, ultra-violet and visible (UV-vis) spectroscopy results showed that neutral polymers produced electrochemically had absorption maxima (λ_{max}) between 450 and 480 nm depending on whether the solvent employed was acetonitrile/methylene chloride or nitrobenzene, respectively. While polymer produced chemically had a lower band gap, with λ_{max} between 505 and 510 nm for neutral polymer depending on the poly(thiophene) derivative studied. The observed red shift between materials formed by the different synthetic procedures was accounted for by less structural defects (2-4 coupling) in and greater regioregularity of polymer created by chemical oxidation. Leclerc also noted an observable difference in absorption between reduced and oxidized polymers, showing a shift in absorption from the range of 450–510 nm, for neutral materials, to a red-shifted, broad-band absorption in the range of 700–850 nm for oxidized (doped) polymers.

1.2.6 Regioregular Poly(3-alkylthiophene)s

Although some of the former procedures for the production of P3ATs eliminate 2-4 cross-coupled linkages within polymer chains, and some can produce P3ATs with regioregularities around 80%, evidence of the effects caused by the presence of P3ATs with regiorandomness are apparent in Leclerc's work.[131] McCullough et al. and Barbarella et al. went on to investigate this phenomenon by performing theoretical studies by means of gas-phase molecular mechanics and ab initio methods on the model triad regioisomers possible as a result of random coupling (i.e., HT-HT, HT-TT, HT-HH, and TT-HH).[6,130] The molecular mechanics calculations by McCullough et al. showed that for the HT-HT conformation a *trans* coplanar orientation, in which the thiophene rings are *trans* to and within 20° of each other, yield the

lowest energy and are preferred. They noted that the potential energy surface for twisting the rings from a coplanar confirmation to ~20° out of coplanarity is very flat and the structures are within <1 kcal of each other. On the contrary, when a HH defect was introduced to the triad (HT-HH), the thiophene rings maintained a *trans* conformation, but at the defective HH junction the thiophene rings are severely twisted to roughly 40° from planarity. Furthermore, an increasing energy barrier is met that requires more than 5 kcal to achieve even a 20° twist back towards planarity.

J. L. Bredas had already investigated the relationship between band gap and bond length alternation in organic conjugated polymers as a function of increasing quinoidal character and he concluded that π-orbitals must be within 30° of coplanarity in order to overlap in a manner consistent with band gaps of conducting polymers.[115] Thus, noncoplanarity leads to a decrease in conjugation for these materials, which consequently leads to an increase in ionization potentials and band gap widths[114,115] Baughman and Chance also showed that any significant loss in conjugation resulting from noncoplanarity results in portions of polymer chain having localized wave functions and therefore an inhibition of intrachain charge mobility.[140] Hence, a very strong emphasis was placed on the development of synthetic pathways for the production of fully regioregular P3ATS consisting exclusively of HT-HT coupling.

The first reported synthesis of regioregular P3ATs came from McCullough and Lowe in 1992.[122,141,142] In this synthetic route, 2-bromo-5-bromomagnesio-3-alkylthiophene was produced following procedures previously outlined in the literature.[143,144] The 2-bromo-5-(bromomagnesio)-3-alkylthiophene was then polymerized via Kumada cross-coupling in the presence of catalytic amounts of [1,2-bis(diphenylphosphino)propane] nickel (II) chloride $(Ni(dppp)Cl)_2$.[145-149] The ensuing P3ATs were recovered in 44–69% yields having 98–100%

regioregularity (HT-HT coupling) and average molecular weights in the range of 20,000–40,000 Da with a *PDI* of 1.4.[2,76,122,125,142,150,151]

The second method developed to form P3ATs with wholly regioregular coupling is the Rieke method.[73-75,152,153] This route involved the reaction of 2,5-dibromo-3-alkythiophene in a solution of highly reactive "Rieke zinc", at cryogenic temperatures in order to ensure the production of the isomer 2-bromo-5-(bromozincio)-3-alkylthiophene, while reducing the formation of undesirable 5-bromo-2-(bromozincio)-3-alkylthiophene isomer to trace amounts. This intermediate was then polymerized in the presence of catalytic amounts of [1,2-bis(diphenylphosphino)ethane)] nickel(II) chloride ($Ni(dppe)Cl_2$) to form regioregular P3ATs, or reacted with tetrakis(triphenylphosphine) palladium(0) ($Pd(PPh_3)_4$) to form regiorandom polymer. 2-bromo-3-alkyl-5-iodothiophene will also react with "Rieke zinc" to form solely 2-bromo-3-alkyl-5-(iodozincio)thiophene, which will polymerize in the same manner under the same conditions. "Rieke"-prepared P3ATs can be recovered in 75% yields having 98–100% regioregularity (HT-HT coupling) and average molecular weights in the range of 24,000–34,000 Da with a *PDI* of 1.4.

Other less-reported methods for the synthesis of HT-P3ATs include the Stille[154] and the Suzuki methods of cross-coupling polymerization.[155,156] Iraqi et al. developed a method based on Stille chemistry for the production of regioregular poly(3-bromo-alkylthiophene)s, a polythiophene bearing a long alkyl chain terminated with a bromine atom.[157] An extremely important aspect of this synthesis is that the resulting polymer can then be modified into a large variety of polythiophenes by mere nucleophilic displacement of the bromine atom. The method reportedly produced poly(3-bromo-alkylthiophene)s with regioregularity of 94%, having an average molecular weight of 12,300 Da and a *PDI* of 1.5. The Suzuki method involves production of a 2-iodo-3-alkylthiophene precursor and then reacted under cryogenic conditions

with lithium diisopropylamide (LDA), then trimethylborate, which is converted to a stable ester form via stirring in 2,2-dimethyl-1,3-propanediol over anhydrous sodium sulfate to form the polymerizable precursor having the configuration 2-iodo-3-alkyl-5thienylboronic ester. This ester is then polymerized in the presence of a phospine-free palladium catalyst, such as palladium acetate. The Suzuki method resulted in the production of P3ATs having 96–97% regioregularity and average molecular weight of 27,000 Da. Finally, McCullough et al. reported a method employing Grinard Metathesis, simply named the GRIM method, for the production of regioregular P3ATs in 2001.[77] This procedure involved production of an active monomer by reaction of 2,5-dibromo-3-alkylthiophene with any inexpensive and readily available Grignard reagent solution; this results in an 85:15 percent ratio of regioisomers 2-bromo-3-alkyl-5-(manesio-halogen)thiophene, and 2-(magnesio-halogen)-3-alkyl-5-bromothiophene respectively. Treatment of these regioisomers with catalytic amounts of $Ni(dppp)Cl_2$ by refluxing in THF at room temperature, as opposed to cryogenic conditions, produced analytically-pure, highly-ordered P3ATs with a regioregularity between 95–98%.

1.2.7 Mechanism for Polymerization of Five-Membered Ring Aromatic Heterocycles by Oxidative Coupling

The exact nature of polymer growth for P3ATs by chemical oxidation with $FeCl_3$ is still not fully understood. However, as evidence will show the reaction probably proceeds through more than one pathway, the latter depending upon experimental conditions employed. Some information about the mechanics of thiophene coupling has been obtained from investigations of poly(pyrrole)s, which differ from poly(thiophene)s in that the monomer possesses nitrogen as the hetero atom instead of sulphur. Poly(thiophene)s have been employed as model materials for poly(pyrrole)s because they are characteristically similar, but more readily processed after polymerization and thus easier to characterize than poly(pyrrole)s, PPYs.[5] However, many of

the studies into the kinetics and mechanisms involved in the polymerization of these materials tend to yield a variety of results that lead to conflicting conclusions.

Studies on the electropolymerization of dimers as starting materials, as opposed to monomers, have shown that important structural differences are present between the corresponding final materials. It has been reported that poly(bipyrrole), poly(bithiophene), and poly(parabiphenylene) have more structural defects (less HT coupling) than poly(pyrrole), poly(thiophene), and poly(parabiphenylene).[139,158,159] Furthermore, these studies indicate that the extent of structural defects increase when a trimer is introduced as a starting material to the point that polymerization stops after a few coupling steps. This data has been used as an indirect method of concluding that polymer growth occurs mainly by monomer-to-oligomer coupling. Work by Barbarella et al. concerning the oligomerization of 3-(alky-sulfanyl)thiophene by oxidation with $FeCl_3$, and the aid of theoretical calculations, also came to the conclusion that reactions between radical-cation monomers and radical-cation oligomers leads to preferential HT coupling.[160]

Nonetheless, Smie et al. concluded from experimental and theoretical results that coupling between β,β-disubstituted oligo(thiophene)s is favorable during all stages of electropolymerization, and reported that all of their data clearly indicate that electropolymerization is not a chain propagation growth, but a successive series of "dimerization" steps.[161] Baeuerle et al. used nonreactive endcapped oligo(thiophene)s and cyclic voltammetry to show that a series of oligomers (starting with a trimer) formed monocation radicals that were stable within the timescale of the voltammetric experiment, and that oligomers from a tetramer were capable of forming stable dication radicals.[162] Therefore, it would seem that two alternative pathways may exist for the formation of long chain polymers and although it

is more commonly accepted that monomer-oligomer growth predominates, oligomer-oligomer growth probably competes with monomer-oligomer growth during polymerization.

Lacroix et al. realized this fact and investigated C_2-C_2' coupling reactions of radical cations of oligopyrroles of increasing length generated by electrochemical oxidation; in addition, they modeled the reactions with transition state calculations and taking into account the effect of solvent employed during polymerization.[159] Lacroix et al. were able to conclude that the solvent employed in the reactions does in fact affect the stabilities (lifetimes) of various radical cation species. They stated that several pathways for polymer growth are possible, including oligomer-oligomer and monomer-oligomer couplings, as well as the possibility of radical cations coupling with neutral species and other radical cation species. These solvent effects will be further discussed in Chapter 2.

Andrieux et al. later looked into the identification of the first steps of the electrochemical polymerization of pyrroles by means of fast potential-step techniques.[163] The early stages of polymerization were investigated using substituted pyrrole monomers via fast double potential-step chronoamperometry with electrodes having diameters in the micrometer (μm) range. Upon systematic analysis of the reaction kinetics they concluded that radical cations, rather than the neutral radicals that would result from monomer deprotonation, are involved in the carbon-carbon bond formation; they also provided evidence that radical-cation species react with themselves as opposed to neutral monomers. Guyard et al. provided further support of this concept by means of electrochemical, flash pyrolysis, and pulse radiolysis examination of select bipyrroles in order to gain insight into the oxidative polymerization mechanisms of pyrroles and oligo(pyrrole)s.[164] Guyard concluded that only radical cation formation leads to the production of longer oligomers or poly(pyrrole)s. Furthermore, the neutral monomer does not play a part in oligomer formation because deprotonation does not occur before the coupling step; this scenario

leads to dimerization between two radical cations and the formation of a protonated dimer. A proposed scheme of such coupling is shown in Figure 1.3.

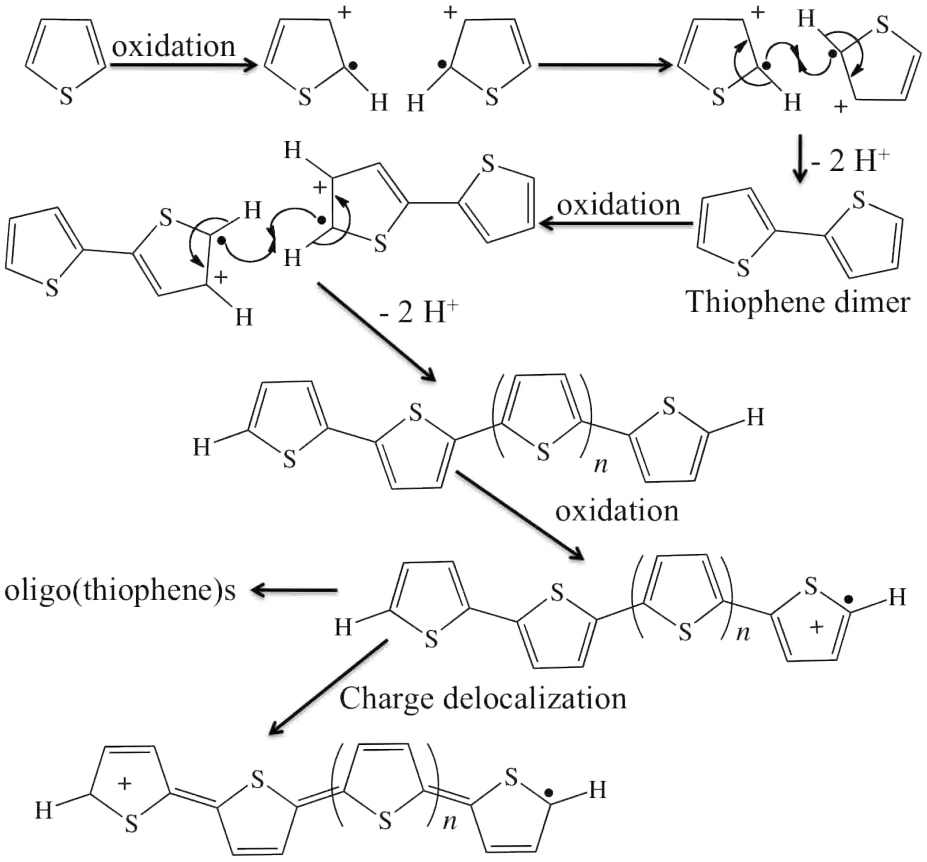

Figure 1.3 Scheme for the proposed radical cation coupling mechanism for chemical oxidative polymerization of thiophene monomers. Adapted from Wei et al., 1991.

Although it has been generally reported in the literature that initiation of chain growth for these materials occurs via coupling of two radical cations followed by addition of monomeric, dimeric, or oligomeric radical-cation species, other studies on the coupling mechanism for thiophenes contradict this generally accepted finding. Wei et al. investigated the kinetics and mechanisms of the polymerization of thiophenes in the presence of bithiophene and terthiophene in order to elucidate information about oligomeric growth of these materials.[165] By electrochemically polymerizing 3-methylthiophene in the presence of small amounts of 2,2'-

bithiophene and 2, 2':5',2"-terthiophene they were able to extract valuable kinetic information. They observed that after the addition of bithiophene or terthiophene the reaction rate increased throughout the entire polymerization period. They noted that if the observed fast reaction were solely due to the addition of bithiophene and terthiophene that the reaction rate would have decreased after these materials were depleted, and the resulting polymer would have a structure more similar to those seen for the polymerization of bithiophene and terthiophene,[139,158,159] and not poly(3-methylthiophene) as was observed. Also, it was shown that the polymerizations conducted in the presence of bithiophene and terthiophene–both having lower oxidation potentials than 3-methylthiophene (1.05, 1.31, and 1.8 V vs. SCE, respectively)–proceeded at an oxidation potential significantly lower than that necessary to polymerize 3-methylthiophene.

Thus it was concluded that oxidation of the monomer was not necessary for the polymerization to proceed and a different mechanism of coupling was proposed to explain these findings, as shown in Figure 1.4. In this theory, when bithiophene or terthiophene are not added, the oxidation of monomer to form a radical cation is the rate determining step because of the higher oxidation potential of the thiophene monomer as compared with the subsequently formed dimer, trimer, oligomer, and polymer.[166,167] The radical cation then undergoes an electrophillic aromatic substitution reaction with a neutral thiophene monomer followed by oxidation and deprotonation to yield a dimer, which is immediately oxidized to a radical cation that then attacks another neutral monomer unit. This reaction is subsequently repeated to form polymer. Wei et al. consequently carried out this experiment for the polymerization of pyrroles in the presence of bipyrrole and obtained similar results, for which they published analogous conclusions.[168]

It has thus been established that for oxidative coupling of poly(heterocycle)s, formation of radical cations is the preliminary step of the polymerization. Subsequent coupling may occur

from adjoining radical cations, or possibly neutral or radical cation monomer units. Coupling of radical-cation oligomers with other radical-cation oligomers may also contribute to chain growth during polymerization. As stated, it is more likely that these various pathways are in kinetic competition with each other during polymerization. There is also evidence that experimental conditions may play a role in supporting one route as compared to another, and changes in the conditions can shift the probability for the production of materials having different physical characteristics.

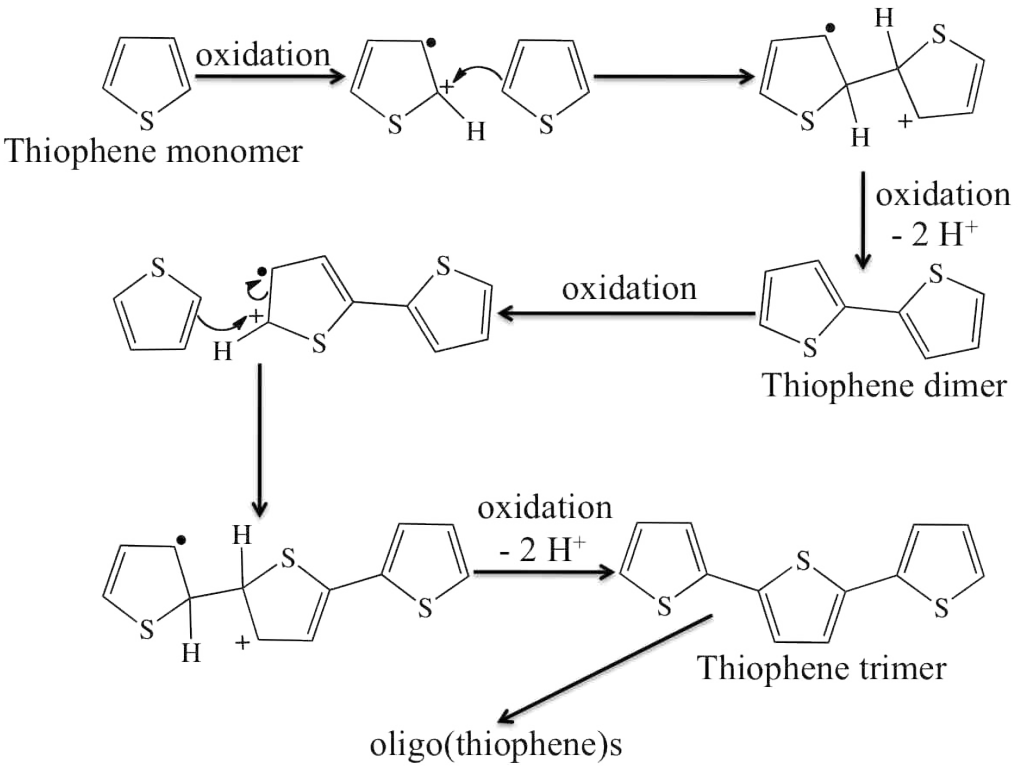

Figure 1.4 Scheme of proposed radical cation-to-neutral monomer coupling mechanism for chemical oxidative polymerization of thiophene monomer. Adapted from Wei et al., 1991.

1.2.8 Mechanism of Charge Transport, and Conductivity in Conjugated Poly(heterocycle)s

The mechanisms involved in the conductivities and charge-transport properties of poly(thiophene)s have been the subject of intense investigation. It has been generally accepted

that charge storage and transport characteristics of conductive poly(heterocycle)s, which are nondegenerate groundstate polymers, result from the formation of self-localized nonlinear excitations (i.e. polarons and bipolarons) depending on the extent to which the material is doped (reversibly oxidized).[169-174] For conducting polymers, interactions between the polymer unit cell with all of its neighbors and the creation of delocalized π-orbital overlap leads to the formation of electronic bands. The highest occupied electronic levels, or highest occupied molecular orbitals (HOMOs), comprise the valence band (VB). The lowest unoccupied electronic levels, or lowest unoccupied molecular orbitals (LUMOs), form the conduction band (CB). The width of the bandgap (E_g), or forbidden gap, between the valence band and the conductance band determines the intrinsic conductivity of the material.

In 1977, Shirakawa et al. showed that the conductivity of poly(acetylene) could be increased from $\sim 10^{-5}$ to $\sim 10^{3}$ S cm^{-1} by exposing it to oxidizing or reducing agents.[54] This process is often called "doping" and can simply be considered a reversible reduction or oxidation reaction. The doping of a conducting polymer results in the conversion of a neutral polymeric species to a polymeric cationic or anionic complex, with a balancing counter ion generated from the reduced oxidant or the oxidized reducing agent. Use of an oxidizing agent is typically referred to as *p*-type doping and that of a reducing agent is termed *n*-type doping. With regards to conducting polymers, the ease with which the material is oxidized or reduced is a crucial consideration.

Poly(thiophene)s may be *p*-doped or oxidized by chemical, electrochemical, and photochemical means. The oxidation of poly(thiophene)s to remove one electron results in the formation of a radical cation (spin ½), called a polaron. It has been reported by Bredas et al. that in an organic polymer chain it can be energetically favorable to localize the charge that appears on the chain. As a result, there is a local distortion of the lattice around the charge which has an

associated thermodynamic cost called a distortion energy.[112,114,115,175,176] It is further explained that this process causes the presence of localized electronic states in the bandgap due to an upward shift ($\Delta\varepsilon$) of the HOMO and downward shifts of the LUMO, thereby lowering the ionization energy. Furthermore, Bredas explains that if $\Delta\varepsilon$ is larger than the energy needed to distort the lattice around the charge the charge localization is favorable. The formation of a polaron in a P3AT chain results in the formation of a quinoidal resonance structure, as shown in Figure 1.5. The presence of a polaron necessitates that a coplanar orientation of rings be readily accessible in order for a small band gap and high conductivity to be achieved. If high energy constraints prevent this coplanar arrangement, then lower conductivities are the result.[177]

Evidence shows that the loss of a second electron from the polymer chain results in the formation of a polymeric dication, which may be in the form of a spinless pair of like charges associated with a strong local lattice distortion called a bipolaron, or the formation of two individual polarons (i.e. a polaron pair); the individual stabilities of which are determined by the length of the polymer chain.[178,179] Fichou et al.[178] examined the stabilities of polarons and bipolarons in extended model thiophene oligomers and they concluded that for oligomers where $n \leq 5$ oxidation by means of stoichiometric amounts of $FeCl_3$ results in solely polaron formation. However, oligomers where $n = 6$ with sufficient oxidation show absorption spectra consistent with multiple charge formation, attesting to the minimum chain length necessary in order for bipolaron formation to occur.

Bredas et al. used theoretical calculations to compare the energy costs for the formation of bipolarons, as compared to a polaron pair, and concluded that the distortion energy to form one bipolaron is roughly equal to that to form two polarons.[175,176] They went on to explain that the formation of a bipolaron leads to a species that is far more thermodynamically stable, despite the possible Coulombic repulsion between the two like charges because of the greater decrease in

the ionization energy associated with a bipolaron as opposed to a polaron. They noted that this stabilization was further assisted by screening effects of the counter anion due to the greater binding energy of the bipolaron.

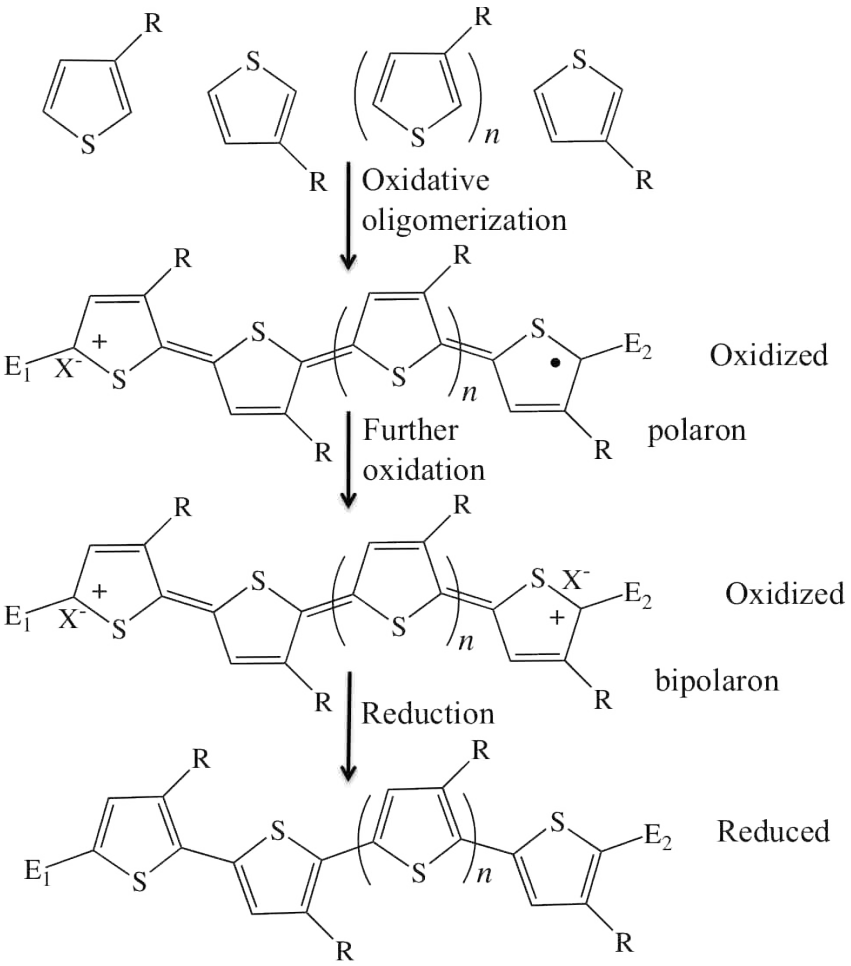

Figure 1.5 Effect of oxidation-reduction reactions on oligo(thiophene)s leading to formation of polarons and bipolarons.

Conversely, Zade and Bendikov performed a theoretical study of long oligothiophene dications and compared the stabilities of bipolaron versus polaron pairs.[179] Their investigation concluded that for short oligothiophene dications, such as $n = 6$, the polaron pair state only slightly contributes to the electronic structure of the dication with a major contribution coming from the bipolaron state. In medium-sized oligomers, such as $n = 14$, the contribution from the polaron pair state begins to become significant and in long chain oligo(thiophene)s, such as $n =$

30–50, the contribution from the polaron pair state becomes dominant; these molecules can be considered as consisting of two independent cation radicals. They went on to clarify that their calculations were performed in the gas-phase in the absence of counter-anions and that only single chain oligomers were considered, thus eliminating possible π-stacking.

Nonetheless, the higher conductivities seen in poly(thiophene)s upon doping are accepted as a result of the extreme change in the electronic band structure of the material, appearing as a unique midgap state and a localized quinoidal resonance structure.[1] This structure allows for the formation of bipolarons as mobile charge carriers along the length of the quasi one-dimensional chain.[1] Simply put, the oxidation of poly(thiophene)s leads to a reduction in the band gap, which in turn increases electrical conductivity in one-dimension. However, 3-dimensional morphology resulting from processing and structure, which can influence the packing density of the material, can also have a great influence on the electrical conductivity seen in poly(thiophene)s.

It has been shown that macroscopic charge transport in conducting polymers not only occurs along the polymer chain itself (intrachain transport), but also via charge "hopping" between polymer chains (interchain transport).[175,176] Efficient interchain transport is dependent on the molecular weight[180] and orientation[180,181] (i.e. anisotropy) of the material and these characteristics are influenced by the density of packing (crystallinity) of the materials, which is directly influenced by the structure of the polymer chains. An explanation of interchain transport was reported by Hill et al.[182] Using endcapped oligo(thiophene)s (dimers and trimers) and absorption spectroscopy, along with electron spin resonance spectroscopy, they showed that radical cations of these oligomers formed dimers (π-dimers). They went on to explain that in such a structure one (or more) cationic thiophene ring(s) form a π-complex in which the radical electron spins are paired. This work was concurrently supported from reports by Zinger et al. using photoxidation to form stable radical cations from small endcapped oligo(thiophene)s that

displayed similar π-stacking behavior so as to form π-dimers.[183] The phenomenon of π-stacking has been further explored and substantiated in the literature by use of various oligomeric species under different chemical conditions.[184,185]

1.2.9 Structure-Function Relationships in Poly(alkylthiophene)s

Poly(alkylthiophene)s are extremely valuable materials and have been the subject of intense scientific investigation for the past several decades due to their unique nonlinear optical and tremendous electrically conductive properties. These properties are directly dependent on the microscopic and macroscopic structures of the polymer itself. Structural characteristics that strongly influence the physical properties of poly(alkylthiphene)s include the material's molecular weight, regioregularity, and the endgroup or backbone substitutions that occur during polymer chain formation.

Initial investigations into the influence of molecular weight on the physical properties of poly(thiophene)s involved the synthesis and/or isolation of smaller thiophene oligomers and alkyl-substituted thiophene oligomers. For reasons of insolubility or nonreactivity in the specific chemical environments employed, oligomers up to octathiophene have been the longest *unsubstituted* group of thiophenes investigated.[186-189] However, a series of alkyl-substituted oligo(thiophene)s were prepared and studied with repeat units up to $n = 48$.[167,190-197] Ten Hoeve et al. prepared a series of oligo(thiophene)s (n = 3–11) carrying a limited number of dodecyl-aliphatic side chains and having exclusively HT coupling in order to investigate the dependence of conjugation length on the chain length.[167] With oligomers having repeat units of $n = 3, 5, 7, 9$, and 11, Ten Hoeve reported conductivities for iodine-doped oligomers that steadily increased as chain length increased, with the 11-mer possessing the maximum conductivity of 20 S cm^{-1}. An increasing red shift in absorption maximum (λ_{max}) correlating with increasing chain length was also observed, with λ_{max} = 345 (n = 3), 412 (n = 5), 440 (n = 7), 455 (n = 9), and 462 (n = 11) nm.

Similarly, Otsubo et al. reported the preparation of regioregular oligo(thiophene)s having limited attachment of octyl-chains consisting of n = 5, 10, 15, and 20 monomer units.[197] Otsubo et al found that for oligomers with n = 5, 10, 15, and 20 conductivities for iodine-doped oligomers were 0.69, 0.73, 11–13, and 21–36 S cm^{-1}, with a red-shift in absorption maximum as chain length increased, with λ_{max} = 411, 452, 466, and 468 nm. Further more, cyclic voltammetry showed that oxidation potentials for oligomers decreased in proportion to increasing chain length, having $E_{1/2}$ of 0.92, 0.72, and ~0.6 volts (V) vs. a Ag/AgCl reference electrode for oligomers of n = 5, 10, and 15 respectively. Voltammetric measurements for oligomers of n = 20 were not possible due to poor solubility. Otsubo et al. also prepared regioregular oligo(thiophene)s with limited octyl side chains having monomer repeat units up to n = 48.[197] They concluded that because no additional red shifting in absorption maxima for oligomers was observed beyond n = 20 the limitation on the extensive conjugation (i.e. effective conjugation length) is around 20 monomer units. These results are in agreement with prior work by Meier et al. concerning the effective conjugation length for oligomers of dialkoxy-substituted phenylene ethylenes.[198]

Trznadel et al. further studied the effect of molecular weight on the spectroscopic and spectroelectrochemical properties of regioregular poly(3-hexylthiophene).[7] In this work, regioregular poly(3-hexylthiophene), P3HT, was prepared by means of a modified McCullough method[122,141] and it was then fractionated via sequential soxhlet extractions in acetone, hexane, methylene chloride, tetrahydrofuran (THF), and chloroform. The resulting fractions had M_N of 2,280, 4,380, 8,370, 17,700, and 10,800 Da respectively, with *PDI*s of 1.38, 1.22, 1.33, 1.45, and 1.97. The absorption maximum for these materials was shown to have a red-shift with an increase in molecular weight with λ_{max} = 421, 438, 441, and 447 nm for the acetone, hexane, methylene chloride, and THF fractions; the measurements were performed in THF solvent.

Regioregularity was also noticed to increase with an increase in molecular weight, although ^{1}H-NMR measurements were not quantified.

Voltammetric behavior for these P3HTs was shown to depend on their molecular weight. Samples of the materials extracted in hexane, methylene chloride, and THF were examined by means of spectroelectrochemical techniques, and it was found that potentials for initiating oxidation were at 0.55, 0.5, and 0.45 V vs. a Ag/AgCl reference electrode, respectively.

Osawa et al. investigated the effect of molecular weight on the electrical properties of electrochemically-synthesized P3HTs and found that the electrical conductivities for these polymers increases as a function of increasing molecular weight up to a $M_N \sim 25{,}000$ Da, but no observable difference in conductivities could be established above this weight.[199] Consistent with these findings, there was no appreciable differences observed in absorption spectra for λ_{max} beyond molecular weights of 25,000 Da, as opposed to the more prominent differences seen in smaller weight materials.

Because interchain charge transfer influences the optical and electrical properties of these materials, the density and order of packing for the bulk polymer is important and the crystallinity of bulk P3ATs has been shown to impact these properties.[99-102] Zen et al. studied the conductivities of P3HT as a function of their bulk morphologies for several solvent-extracted fractions of polymer having molecular weights ranging between 2,500–27,000 Da.[100] By means of differential scanning calorimetry (DSC), X-ray diffraction, and transmission electron scpectroscopy Zen et al. showed that the crystalline state morphology increased as a function of molecular weight. This was compared to the charge mobility characteristics for the different morphologies and the mobility was found to increase over four orders of magnitude for an increase in crystallinity from 5% to 20%. Frechet et al. have also shown field effect mobilities of regioregular P3HTs increase from 1.7×10^{-6} cm^2 V^{-1} s^{-1} to 9.4×10^{-3} cm^2 V^{-1} s^{-1} in field effect

transistors, FETs, as the molecular weight increases from 3,200 to 31,100 Da; this is a result of differences in the morphologies seen for increasing molecular weight materials.[98,99,200]

Nucleophilic addition of substituent groups either as endgroups or backbone additions during oxidative polymerization of alkylthiophenes and pyrroles has been shown to have dramatic effects on the electrochemical and optical properties of the resulting materials.[201,202] Qi et al. performed several studies in order to elucidate these effects.[8,203,204] In one study of the reactivation of poly(3-methylthiophene) following overoxidation in the presence of chloride anion (nucleophile), it was determined that oxidative degradation of poly(3-methylthiophene) is promoted in the presence of chloride.[8] In that work it was shown that the polymer became electrochemically inactive after a single cycle of the potential to +1.3 V in a chloride solution, while in the absence of chloride the polymer was electrochemically stable to potentials to +1.4 V. In situ conductivity measurements confirmed that this deactivation results in ~100 fold decrease in conductivity and X-ray spectroscopy showed the result of covalent binding of chloride to be approximately occurring every other thiophene ring caused by nucleophilic substitution,[8,203,204] as illustrated in Figure 1.6.

Restoration of the conjugation within the material (i.e., reactivating the electrochemical properties of the material) was achieved by oxidation at +1.3 V, which results in the deprotonation of the material at the chlorinated position. Qi reports that the reactivation returns the conductivity of the polymer to approximately 20–50% of the pristine polymer. Nonetheless, the oxidation potential of the chlorinated material was shown to be 0.5 V more positive than that of the virgin polymer. Qi later noted the oxidative substitution to poly(thiophene)s and poly(pyrrole)s by nucleophiles to be quite a general reaction, depending on the degree of oxidation of the polymer and the reactivity of the nucleophile.[204] His group confirmed their

finding with oxidative substitutions in the presence of chloride, bromide, and some alcohols, which readily occurred upon overoxidation of the polymers.

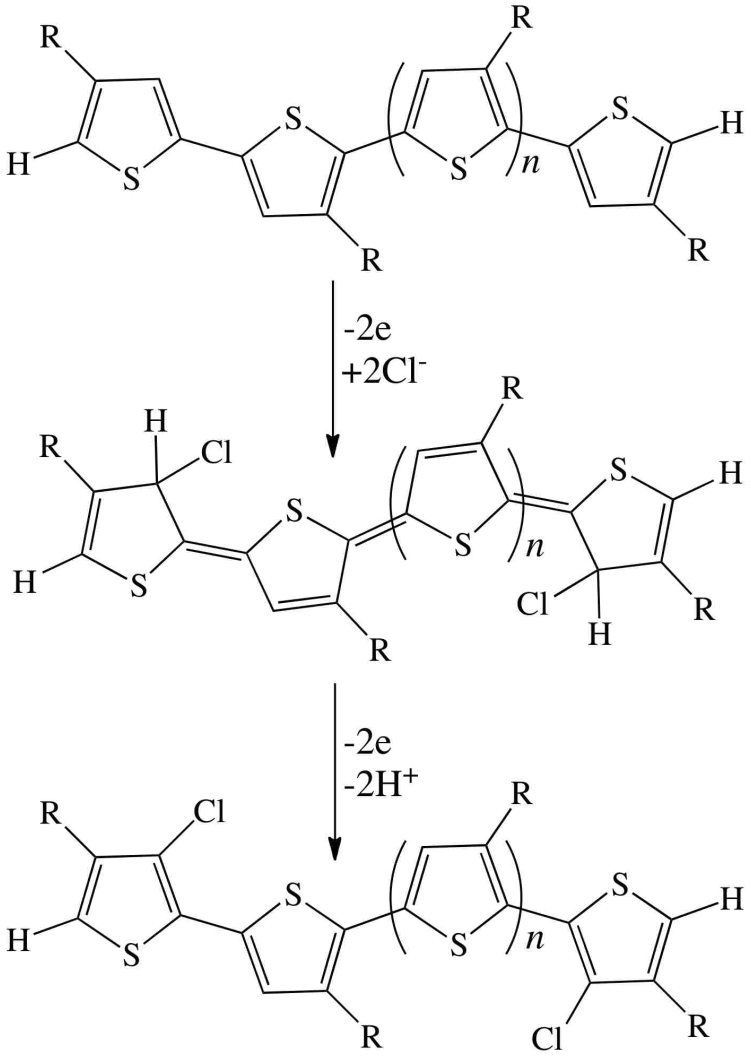

Figure 1.6 Scheme of proposed mechanism for nucleophilic addition of chlorine to P3HT. Adapted from Qi et al., 1993.

Garcia et al. examined the effect of endgroup substitution on the electrochemical and optical properties on poly(thiophene)s by preparing a series of oligo(thiophene)s with n = 2–6, which carried endgroup substitutions including methoxy and nitro groups, and bromine atoms.[205] Electrochemical studies indicate that, besides the decrease in oxidation potential attributable to

an increase in oligomer chain length, chemical substituents such as methoxy and bromine stabilized the increased lifetime of radical-cation species and also lowered the oxidation potentials for these oligomers. Likewise, bathochromic (red) shifts were seen for the absorption maximum of substituted oligomers, as compared with the unsubstituted species.

Demanze et al. also worked towards the tuning of the electronic and optical properties of oligo(thiophene) dimers and trimers via cyano group substitutions as either endgroup additions or addtions to the central ring of the oligomer.[206] From this work it was concluded that the electrochemical properties of these oligomers followed the general trend that oxidation potentials increased with (i) the decrease in chain length of the oligomer, (ii) the increase in the number of substitution sites, and (iii) the substitution being located on a central ring as opposed to a terminal ring. Similarly, ultraviolet-visible spectroscopy (UV-Vis) measurements indicated an overall trend of bathochromic shifts when the number of substituted sites increased, with a hypsochromic (blue) shift in the mono- or disubstituted series when the substituent group moved from a terminal to a central position.

Finally, Andrieux et al. studied the substituent effects on the electrochemical properties of pyrroles and small pyrrole oligomers via the electrochemical oxidation of several oligo(pyrrole)s, either unprotected, partially blocked, or totally blocked on their α-positions, or substituted in the *N*-position.[207] As observed with various oligo(thiophene) series the oxidation potential of unsubstituted oligo(pyrrole)s was shown to decrease linearly with increasing chain length. Substitution on the *N*-position with the strong electron withdrawing groups of butoxycarbonyl (BOC) or the sulfonyl group -SO_2Ph shifted the oxidation potential to more positive values. However, it was noted that the large positive shifts did not result in an increase in reactivity for these materials. The properties of pyrrole monomer and bipyrrole substituted on the terminal α-positions with electron withdrawing methyl or *tert*-butyl groups showed

significant decrease in the oxidation potentials for all species investigated. Although there was no appreciably observable increase in the radical cation stabilities for the methyl-substituted materials, a large stabilization of radical cations was observed for the bi-*tert*-butylated compounds.

1.3 MALDI-TOF Mass Spectrometry of Synthetic Polymers

1.3.1 Background of MALDI-ToF Mass Spectrometry of Synthetic Polymers

Although mass spectrometry has been an invaluable tool for the determination of molar masses for over 50 years, it has only been since the development of soft ionization techniques, such as matrix-assisted laser desorption/ionization (MALDI), that mass spectrometry has become a priceless technique for the characterization of synthetic polymers. Issues such as the low volatility and the thermal instability of most of these materials had previously hindered their characterization by means of mass spectrometry.[208] The first two reports for the use of techniques that would come to be known as matrix-assisted laser/desorption ionization time-of-flight mass spectrometry, MALDI-ToF-MS, came almost simultaneously from Tanaka et al.,[209] and Karas and Hillenkamp.[210] Koichi Tanaka would later receive the 2002 Nobel Prize in Chemistry for these efforts. MALDI-ToF-MS has since become a critical means for the determination of molecular weights and molecular weight distributions and structural information with respect to repeat units and additives, such as endgroups, or impurities.[123,125,211,212] MALDI-ToF-MS is the most employed mass spectrometric technique, as compared to other modern methods such as atmospheric-pressure/chemical-ionization (APCI) and electrospray-ionization (ESI), for the analysis of synthetic polymers, because the latter may be hindered by molecular mass or polarity issues and convoluted by multiple charging, as well as solvent restrictions.[208,212]

Polymers may be unambiguously identified via determination of the mass number for the repeat (monomer) units that are characteristic of the chemical composition of the polymer chains. This can only be reliably accomplished from observations of mass spectra in the mass-to-charge (m/z) range where adequate resolution of single oligomers can be achieved or by the use of Fourier-transform analysis. In 1992, Danis et al. were able to sufficiently resolve oligomers of low molecular weight poly(acrylic acid)s and poly(styrene sulfonic acid)s in order to correctly ascertain the mass number of the repeat units, as well as the masses for the endgroups.[213] That same year, Castro et al. investigated the matrix-assisted laser desorption/ionization of higher mass molecules by Fourier-transform mass spectrometry and they satisfactorily resolved oligomers of poly(ethylene glycol), PEG, having masses up to 10,000 Da.[214]

The average molecular weights of synthetic polymers play a significant role in the morphology and resulting physical properties of bulk polymer systems, as explained for poly(thiophene)s in section 1.2.9. MALDI-ToF-MS is very well matched for the analysis of the molecular weights of synthetic polymers for several reasons. First mass spectrometry in general is an absolute method for the reason that exact mass measurements may be obtained. This is in opposition to other classical methods for molecular weight determination, such as gel-permeation chromatography (GPC) or size-exclusion chromatography (SEC), which are relative techniques generally requiring molecular weight calibration in order to obtain comparable molar masses. Secondly, MALDI-ToF-MS analysis requires very little sample and has a large throughput as it requires very little time to acquire a large amount of data. Finally, MALDI-ToF-MS is a soft ionization technique that produces almost no fragmentation of analyte during analysis and for the most part produces singly-charged species.

Since its inception, MALDI-ToF-MS has been shown to have the ability to detect organic molecules of very high molar mass. Tanaka et al. reported the observation of doubly-charged

clusters of lysozyme from chicken egg whites with a mass over 100,000 Da.[209] Karas et al. investigated the laser-desorption/ionization mass spectra of poly(styrene) and showed that polymer as large as 70,000 Da could be easily detected.[210] Bahr et al. also showed the method to be a an invaluable analytical tool capable of obtaining mass spectra for a variety of synthetic polymers from 1,000 to 80,000 Da, while noting that protonated species of biopolymers with molecular weights up to 300,000 are easily produced.[215] In fact, MALDI-ToF-MS has been shown to have the ability to detect and characterize monodisperse polymer samples with molecular weights as high as 1.5 million Daltons.[216]

Monodisperse polymers are those that have a solely distinct molar mass that can be calculated if the chemical composition of the repeat (monomer) unit is known. The degree of polymerization, *DP*, for an ideally monodisperse polymer is defined as the number of repeat units within the polymer; $DP = M/M_0$, where M is the total molecular weight of the sample and M_0 is the molar mass of the repeat unit. Nonetheless, most polymers are polydisperse or heterogeneous with respect to molecular weight to some extent, due to the nature of most polymerization reactions. Therefore, a polydispersity index, *PDI*, is employed in order to effectively categorize the extent of a polymer's heterogeneity regarding molecular weight or molecular weight distribution (MWD). The *PDI* is the ratio of the number-average molecular weight (M_N) to the weight-average molecular weight (M_W) of the polymer (Equation 1.3). The larger the disparity between M_W and M_N, the broader the molecular weight distribution is within the polymer sample.

The number-average molecular weight is the arithmetic mean (average) of the molecular weight, M_i, of the individual polymer molecules determined by measuring the molecular weight of N_i molecules. In other words M_N is the average M_i weighted according to number fraction and is mathematically defined in Equation 1.1. The M_N is determined by colligative analytical

methods, such as osmometry or differential refractivity, which are sensitive to the number of molecules present. The weight-average molecular weight depends not only on the number of polymer molecules but also the molecular weight of each polymer molecule. Therefore the M_W is the average M_i weighted according to weight fractions. To derive the weight-average molecular weight the number of polymer molecules of molecular weight i, or N_i, in the mathematical function for the number-average molecular weight is replaced with the weight of the polymer having molecular weight I, or N_iM_i; this is mathematically illustrated in Equation 1.2. The M_W is established by techniques that are sensitive to the weight or size of the material, such as light scattering. Every individual polymer sample has a unique value for M_N and M_W.

Equation 1.1

$$M_N = \frac{\sum_{i=1}^{\infty} M_i N_i}{\sum_{i=1}^{\infty} N_i}$$

Equation 1.2

$$M_W = \frac{\sum_{i=1}^{\infty} (M_i)^2 N_i}{\sum_{i=1}^{\infty} M_i N_i}$$

Equation 1.3

$$PDI = \frac{M_W}{M_N}$$

As discussed in section 1.2.9, the addition of substituent groups or atoms to the terminal ends (α-position) or backbone (β-position) of poly(thiophene)s can have a dramatic effect on the physical properties of those materials. Moreover, other studies have demonstrated that the endgroup of a polymer affects the physical and chemical properties of that polymer, such as the surface reactivity,[217] phase behavior,[218] and light-emitting qualities.[219] Therefore, the determination and quantification of endgroups and/or other functional moieties bound to a polymer is crucial in assessing the material's physical properties and applicability. Because of

the far greater mass resolving capabilities of MALDI-ToF-MS it is with out a doubt superior to all other means for the analysis of types of attached functional groups and the chemical composition of synthetic polymers.

If the exact chemical composition of the repeat unit comprising the polymer chain is unknown, it may be determined through examination of the mass spectrum of that polymer in the mass to charge (m/z) range where the oligomers are sufficiently resolved. By subtracting the m/z of an oligomer immediately preceeding (M_{olig1}) another from the m/z of the oligomer immediately following the preceeding (M_{olig2}), the molar mass of the repeat unit (M_{rep}) can be correctly established; $M_{rep} = M_{olig2} - M_{olig1}$. This is assuming that all ionization events–or reactions, such as cationization, protonation, or electron loss–are equivalent between the two. Likewise, if the molar mass of the repeat unit is known, the molar mass of an endgroup or other addition can be readily determined. The molar mass of the endgroup (M_{end}) is calculated by taking the molar mass of a signal peak (M_{peak}) for a given repeat number and subtracting the molar mass for the given number of cations (xM_{cat}) involved in ionization of the analyte (or anions, or electrons for negative mode evaluation) as well as the molar mass for the number of repeat units (nM_{rep}) comprising the oligomer.[220] This idea is further clarified in Equations 1.4, and 1.5.

Equation 1.4 $$M_{end} = M_{peak} - M_{cat} - nM_{rep}$$

Equation 1.6 $$M_{end} = M_{peak} - M_{elec} - M_{rep}$$

1.3.2 Limitations of MALDI-ToF Mass Spectrometry for Analysis of Synthetic Polymers

Although MALDI-ToF-MS is theoretically well suited for the analysis of molecular weights of synthetic polymers, the analysis of polymers with *PDI* values greater than 1.1 (broader molecular weight distributions) often times leads to discrepancies when compared to other classical methods of obtaining molecular weights, such as size-exclusion chromatography (SEC).[221-224] Montaudo et al. investigated the effects of polydispersity on the MALDI-ToF-MS

estimates for molecular weight and molecular weight distribution of a variety of synthetic polymers with differing *PDI*s.[221] They reported that their measurements for molecular weight agreed with the results obtained by GPC only when polymers having very narrow molecular weight distributions were examined. When polydispersity values reached around 1.10 it was noted that the difference between the observed molecular weights measured by SEC and MALDI-ToF-MS were underestimated up to 20% for the latter. For *PDI* values greater than 2.0 evaluations of the MALDI-ToF-MS spectra fail to yield reliable results. It is currently advisable that mass spectrometric measurements for molecular weights and molecular weight distributions of synthetic polymer samples having *PDI*s greater than 1.10 be considered with caution.[221-226]

The factors contributing to the phenomenon of high or low mass discrimination encountered in MALDI-ToF-MS analysis of polydisperse polymer samples are abundant, but all are attributed to the fact that there are many variables to be considered during analysis via this method.[221-226] Still, they can be summarized into two primary categories: sample preparation and instrumental effects. Sample preparation issues that must be considered include the selection of appropriate matrix, the consistent use of the appropriate solvent, consistent optimization of mixing ratios and concentrations, the addition of cationizing agents or salts, and the method of sample preparation (i.e., the dried-drop method, spin coating, or electrospray deposition).[208,222,223,225] Instrumental issues that contribute to observed discrimination include the applied laser power, variables integral to the ToF analyzer, such as ion acceleration and ion focusing, and detector issues, such as limited dynamic range and saturation.[208,222,224,225]

The choice of appropriate matrix is crucial to induce sufficient ionization of the analyte, in the appropriate manner (i.e., for positive mode investigations: protonation, cationization, electron loss). Physical properties of the matrix that should be considered include the ability of the matrix to induce the appropriate ionization for a particular analyte on the basis of its chemical

composition, the electronic absorption maximum of the matrix, the solubility of the matrix in the appropriate solvents, the miscibility of the analyte with the matrix, and the crystallinity of the matrix/analyte blend when dried. Belu et al. showed the dramatic effects of matrix on the observable mass spectra for samples of poly(styrene), while holding all other variables constant.[227] Samples prepared with matrices of indole acrylic acid (IAA) and nitrophenyl octyl ether (NPOE) yielded mass spectra having low ion signal intensities and poorly resolved oligomer peaks. Those prepared with dithranol matrix resulted in spectra with an abundance of very well resolved oligomer ion signals.

Unlike biopolymers or proteins, the final ionization of synthetic polymers in the MALDI process is usually accomplished by cationization not protonation. As a result, the proper choice of matrix and the correct use of a cationizing agent, usually a metal salt, must be evaluated.[208,222,223,227] The cationizing salt will form adducts with the polymer during ionization and the molar mass of the adduct must be accounted for in the evaluation of the respective mass spectra. Lloyd et al. studied the utilization of different cation salts as potential adducts for ionization of poly(methylmethacrylate), PMMA.[228] In the respective mass spectra an increasing shift in the distribution of low mass oligomer ion signals, upwards of 1000 *m/z*, was observed for samples produced in the presence of cesium salts, as opposed to those produced by adduction with sodium salts.

With regard to instrumental factors affecting the mass discrimination seen in mass spectra of synthetic polymers obtained by MALDI-ToF-MS, desorption/ionization, transmission, and detection issues can all be possibilities.[208,222,224,225] For instance, desorption/ionization is dependent on the laser power employed to initiate these events and the preferable laser power would be one that gives equal probability of ionization to the entire distribution of molecular weights. Unfortunately this is typically not the case, as it is often observable that polymer

chains of differing molar mass require higher laser powers in order to reach the threshold fluence for ionization and detection.[222,223] Sakurada et al. observed that the average molecular weight for PMMA samples determined by MALDI-ToF-MS was overestimated significantly when compared with results obtained from supercritical fluid chromatography and size-exclusion chromatography, because of the high laser power required for optimal mass spectrometric detection.[229] Also, higher laser powers have been shown to be responsible for the dimerization and formation of clusters in the gas phase during desorption/ionization. Such species were found to be are responsible for increasing shifts in molecular weight distributions.[230]

Mass discrimination can be caused by detection factors as well. Microchannel plate, MCP, detectors are typically employed in MALDI-ToF mass spectrometers and are limited by dynamic range. Also, they are easily saturated by low molecular weight oligomers in the presence of very polydisperse polymer samples with a large concentration of low molecular weight material.[222,224,230-232] McEwen et al. showed that deflection of lower mass ions did indeed result in the detection of higher mass ions, which proved population-induced mass discrimination is prevalent in the analysis of polymer samples with large *PDI*s.[232] Furthermore, for MCPs and MCP hybrid detection systems there exists a mass dependency for ion detection, where the efficiency of ion-to-electron conversion decreases as a function of increasing molecular weight due to a decrease in impact velocity.[222,224,230,232,233] This issue has been addressed by the use of post/secondary acceleration, which instills an extra velocity component to ions and improves the ratio of ion-to-electron conversion at the detector.[230] Finally, mass discrimination of polydisperse polymer samples occurring during ion transmission has been reported and it is argued to be caused by extended flight tube length combined with small detector surface area, as well as with the lensing action provided by the source electrodes.[230,234]

Size-exclusion chromatography (SEC) has classically been employed for determination of the accuracy of MALDI-ToF-MS analysis and it is often used in conjunction with MALDI-ToF-MS for more insightful elucidation of structural characteristics of synthetic polymers. Issues encountered by mass discrimination of polydisperse polymer samples observed in MALDI-ToF mass spectra have been addressed in limited reports of polymer fractionation through sequential solvent soxhlet extractions[125] or by means of SEC.[235,236] Fractionation is an attempt to narrow the molecular weight distributions, providing more accurate MALDI-ToF mass spectra for the individual fractions. However, molecular weight data obtained from MALDI-ToF-MS analysis of fractionated polymers may still be inaccurate due to the variables involved and it must be considered with caution.

The possibility of endgroup specific discrimination must also be considered when analyzing synthetic polymers by means of MALDI-ToF-MS. Lui et al. proposed and investigated the endgroup fragmentation of Bromine atoms during the MALDI-ToF-MS analysis of P3HTs via observation of endgroup intensities as a function of laser power fluence.[125] It was noticed that during analysis of low weight materials, the proportion of the relative abundance for solely hydrogen-terminated oligomers (H-H) increased compared to oligomers possessing one hydrogen-terminated end and one bromine-terminated end (H-Br) as the laser power was increased. The increase in H-H signal intensities was theorized to be a result of the liberation (fragmentation) of bromine atoms, which was consequently increasing the observable signal intensities for H-H oligomers. However, mass spectra obtained when the same samples were run in negative ion mode did not indicate the presence of bromine anions and the same spectra could not account for the presence of bromine radicals. Furthermore, mass spectra of higher weight materials run at increasing laser powers did not indicate any variations in the observable intensities for oligomers having different endgroups.

Puglisi et al. performed studies designed to use MALDI-ToF-MS to determine the composition of an equimolar blend of Nylon 6, Ny6, and polybutyleneterephthalate, PBT, and they noticed that a strong imbalance between the two components was observable in the respective mass spectra.[237,238] Despite the fact that the molar mass and polydispersity of each sample were determined to be equivalent, the signal intensities observed for the Ny6 fraction were greater than that observed for the PBT, which was terminated with hydroxyl endgroups. Variations in endgroups that terminated either compound revealed that the proportion of dominant signal intensities could be shifted between the compounds depending on the endgroup substituent terminating that respective material. This clearly indicated that the ionization efficiency for either compound is dependent on the nature of the endgroup introduced to that polymer. However, it was shown that this effect was more prevalent for polymers having a lower molecular weight.

In a similar study but with significantly different outcome, Guttman et al. set out to perform an experiment where a series of blended poly(styrene)s, PS, were prepared from two species of poly(styrene) having different endgroups and mixed in increasingly different molar ratios. The samples were then outsourced to 14 different third-party laboratories for MALDI-ToF-MS analysis.[239] The poly(styrene)s had a molecular weight of ~9,000 Da and were terminated with either hydrogen atoms (PSH) or hydroxyethylene groups (PSOH). Five mixtures were created with mass ratios between 95:5 and 10:90 PSOH/PSH. The results did not indicate any effect of the endgroup polarity for determining the proper mass fractions. The work did establish that differences in the quantitative analysis amongst laboratories could be accounted for by improper mass calibrations, data analysis techniques, and failure to optimize the instrumental parameters.

Nonetheless, it is unreasonable to dismiss the roles that chemical composition of other polymers and endgroups, as well as molecular weights, have on possible endgroup discrimination observable in the MALDI-ToF-MS analysis of synthetic polymers, as Puglisi et al.[237,238] have indicated. Also, considering the effects that endgroups and other substituents have on the oxidation potentials of poly(thiophene)s (cf. section 1.2.9), as well as the possible effects to the morphology of these materials that may occur due to endgroup effects, it is reasonable to expect some degree of endgroup dependent ionization efficiency during their MALDI-ToF-MS analysis.

1.3.3 MALDI-ToF Mass Spectrometry of Poly(3-alkylthiophene)s

Given its tremendous applicability for the characterization of synthetic polymers, the importance of MALDI-ToF-MS analysis has not been lost in the investigations for structural characterization of conducting polymers. Because it has been established that the structure of conducting polymers is directly responsible for their optical and electrical properties it is crucial to their development that MALDI-ToF-MS be routinely used for the evaluation of repeat units, endgroups, and molecular weights of conducting polymers. It has thus been used extensively to elucidate this critical information for many different varieties of conducting polymers.[1,123-125,240-250]

MALDI-ToF-MS has been used to characterize an array of poly(alkylthiophene)s formed by several various regioregular and regioirregular synthetic pathways. Poly(3-alkylthiophene)s formed by regioregular synthesis (cf. section 1.2.6) and investigated by means of MALDI-ToF-MS include the McCullough, Reike, and GRIM methods.[5,123-125,220] It was reported that P3ATs created via the McCullough method possess three distinct endgroup patterns, including those terminated on both ends with hydrogen atoms (H-H), those terminated on both ends with bromine atoms (Br-Br), and those possessing one hydrogen endgroup and one bromine endgroup (H-Br). Also, it was found that polymer made by the Reike method possesses either H-H, or H-

Br endgroups, while GRIM method led to material containing either H-Br endgroups or oligomers having one hydrogen endgroup with the other end terminated by a methyl group (H-CH_3).

Liu et al. reported work concerning the methodic fractionation of regioregular P3HTs by sequential soxhlet extractions using various organic solvents in order to compare the accuracy of molecular weights for those fractions as determined by MALDI-ToF-MS and SEC.[125] Comparison of the M_N and M_W for five fractions of P3HT differing in molecular weight range showed that both values are overestimated by SEC analysis by a factor ranging from 1.2–2.3. These results indicate that for low weight polymer fractions the overestimation is in the range of a factor between 1.2–1.5; for higher weight materials the overestimation is 1.5–2.3 times. The authors noted that these findings were in agreement with similar work done for the analysis of rigid-rod oligo(thiophene)-ethynylene systems M_N and M_W, which were overestimated by SEC by a factor of 1.5–2.0.[251] Liu et al. thus concluded that conducting polymers, like poly(thiophene)s, adopt a rod-like conformation in solution, which is responsible for the anomalous SEC results.

Regioirregular poly(thiophene)s formed by chemical oxidation using iron(III) chloride have been characterized by MALDI-ToF-MS as well. McCarley et al. showed that P3HT chains formed by this method contained 2–4 chloride additions and did not possess hydrogen terminated endgroups.[240] In order to verify the source of the chloride, which was thought to be attributable to the solvent ($CHCl_3$) or the $FeCl_3$ oxidant, polymer was formed in chloroform using $FeBr_3$ as an oxidant. The resulting polymer chains contained 2–3 Bromine additions, with no hydrogen terminated endgroups and the conclusion was drawn that oxidant is the origin of the chloride added to the polymer chains.

1.4 References

(1) Skotheim, T. A.; Elsenbaumer, R. L.; Reynolds, J. R. *Handbook of Conducting Polymers*; 2 ed.; Marcel Dekker Inc.: New York, 1998.

(2) McCullough, R. D. The Chemistry of Conducting Polythiophenes. *Advanced Materials (Weinheim, Germany)*. **1998**, *10*, 93-116.

(3) Morara, A. D. Characterization of a Modified Poly(Propylene Imine) Dendrimer-Host Sytem. Ph.D. Dissertation, Louisiana State University and A&M College, Baton Rouge, 2005.

(4) Morara, A. D.; McCarley, R. L. Encapsulation of Neutral Guests by Tri(Ethylene Oxide)-Pyrrole-Terminated Dendrimer Hosts in Water. *Organic Letters*. **2006**, *8*, 1999-2002.

(5) Brauch, R. M. Structural Characterization of Poly (Heterocycle)S Formed Using Oxidative Methods. Ph.D. Louisiana State University and A&M College, Baton Rouge, 2006.

(6) McCullough, R. D.; Lowe, R. D.; Jayaraman, M.; Anderson, D. L. Design, Synthesis, and Control of Conducting Polymer Architectures: Structurally Homogeneous Poly(3-Alkylthiophenes). *Journal of Organic Chemistry*. **1993**, *58*, 904-912.

(7) Trznadel, M.; Pron, A.; Zagorska, M.; Chrzaszcz, R.; Pielichowski, J. Effect of Molecular Weight on Spectroscopic and Spectroelectrochemical Properties of Regioregular Poly(3-Hexylthiophene). *Macromolecules*. **1998**, *31*, 5051-5058.

(8) Qi, Z.; Pickup, P. G. Reactivation of Poly(3-Methylthiophene) Following Overoxidation in the Presence of Chloride. *Journal of the Chemical Society, Chemical Communications*. **1992**, 1675-1676.

(9) Letheby, H. On the Production of a Blue Substance by the Electrolysis of Sulphate of Aniline. *Journal of the Chemical Society, Transactions*. **1862**, *15*, 161-163.

(10) Angeli, A. Pyrrole Black. Preliminary Note. I. *Gazzetta Chimica Italiana*. **1916**, *46*, 279-283.

(11) Angeli, A.; Alessandri, L. Pyrrole Black. Preliminary Note. II. *Gazzetta Chimica Italiana*. **1916**, *46*, 283-300.

(12) Gilchrist, L. The Electrolysis of Acid Solutions of Aniline. *Journal of Physical Chemistry*. **1904**, *8*, 539-547.

(13) Frenkel, J. The Theory of Metals. *Zeitschrift fuer Physik*. **1924**, *29*, 214-240.

(14) Frenkel, Y. I. Thermal Agitation in Solids and Liquids. *Zeitschrift fuer Physik*. **1926**, *35*, 652-669.

(15) Jost, W. Diffusion and Electrolytic Conduction in Crystals (Ionic Semiconductors). *Journal of Chemical Physics*. **1933**, *1*, 466-475.

(16) Schottky, W. The Mechanism of Ionic Motion in Solid Electrolytes. *Z. physik. Chem*. **1935**, *B29*, 335-355.

(17) Peierls, R. Statistical Theory of Superlattices with Unequal Concentrations of the Components. *Proceedings of the Royal Society of London, Series A: Mathematical, Physical and Engineering Sciences*. **1936**, *154*, 207-222.

(18) Mott, N. F.; Littleton, M. J. Conduction in Polar Crystals. I. Electrolytic Conduction in Solid Salts. *Transactions of the Faraday Society*. **1938**, *34*, 485-499.

(19) Mott, N. F. Conduction in Polar Crystals. II. The Conduction Band and Ultraviolet Absorption of Alkali Halide Crystals. *Transactions of the Faraday Society*. **1938**, *34*, 500-506.

(20) Mulliken, R. S. Intensities of Electronic Transitions in Molecular Spectra. VII. Conjugated Polyenes and Carotenoids. *Journal of Chemical Physics*. **1939**, *7*, 364-373.

(21) Mulliken, R. S. Intensities of Electronic Transitions in Molecular Spectra. VIIIa. Odd-Numbered Conjugated Polyene Chain Molecules and Organic Dyes (with Notes on Optical Anisotropy and Raman Intensities). *Journal of Chemical Physics*. **1939**, *7*, 570-572.

(22) Lewis, G. N.; Calvin, M. The Color of Organic Substances. *Chemical Reviews*. **1939**, *25*, 273-328.

(23) Gillam, A. E.; El Ridi, M. S. Carotenoids and Vitamin a in Cow Blood Serum. *Biochemical Journal*. **1935**, *29*, 2465-2468.

(24) Gillam, A. E.; Ridi, M. S. E. The Isomerization of Carotenes by Chromatographic Adsorption. I. Pseudo-β-Carotene. *Biochemical Journal*. **1936**, *30*, 1735-1742.

(25) Zechmeister, L.; Tuzson, P. Reversible Isomerization of Carotenoids by Iodine Catalysis. *Berichte der Deutschen Chemischen Gesellschaft [Abteilung] B: Abhandlungen*. **1939**, *72B*, 1340-1346.

(26) Zechmeister, L.; v. Cholnoky, L.; Polgar, A. The Isomerization of Zeaxanthin and Physaliene. *Berichte der Deutschen Chemischen Gesellschaft [Abteilung] B: Abhandlungen*. **1939**, *72B*, 1678-1685.

(27) Zechmeister, L.; Polgar, A. Cis-Trans Isomerization and Spectral Characteristics of Carotenoids and Some Related Compounds. *Journal of the American Chemical Society*. **1943**, *65*, 1522-1528.

(28) Pauling, L. Recent Work on the Configuration and Electronic Structure of Molecules, with Some Applications to Natural Products. *Fortschr. Chem. org. Naturstoffe*. **1939**, *3*, 203-285.

(29) Wallace, P. R. The Band Theory of Graphite. *Physical Review*. **1947**, *71*, 622-634.

(30) Akamatu, H.; Nagamatsu, K. A New Suggestion for a Model Representing the Structure of Carbon Black. *Journal of Colloid Science*. **1947**, *2*, 593-598.

(31) Bayliss, N. S. A "Metallic" Model for the Spectra of Conjugated Polyenes. *Journal of Chemical Physics*. **1948**, *16*, 287-292.

(32) Mulliken, R. S.; Rieke, C. A. Molecular Electronic Spectra, Dispersion and Polarization. Theoretical Interpretation and Computation of Oscillator Strengths and Intensities. *Phys. Soc. Rept. Progress Physics*. **1941**, *8*, 231-273.

(33) Szent-Gyorgyi, A. Internal Photoelectric Effect and Band Spectra in Proteins. *Nature (London, United Kingdom)*. **1946**, *157*, 875.

(34) Eley, D. D. Phthalocyanines as Semiconductors. *Nature*. **1948**, *162*, 819.

(35) Akamatu, H.; Inokuchi, H. The Electrical Conductivity of Violanthrone, Isoviolanthrone, and Pyranthrone. *Journal of Chemical Physics*. **1950**, *18*, 810-811.

(36) Akamatsu, H.; Inokuchi, H.; Handa, T. Electric Conductivity and Magnetic Susceptibility of Ovalene. *Nature (London, United Kingdom)*. **1951**, *168*, 520-521.

(37) Akamatsu, H.; Inokuchi, H.; Matsunaga, Y. Electrical Conductivity of the Perylene-Bromine Complex. *Nature (London, United Kingdom)*. **1954**, *173*, 168-169.

(38) Akamatsu, H.; Inokuchi, H.; Matsunaga, Y. Organic Semiconductors with High Conductivity. I. Complexes between Polycyclic Aromatic Hydrocarbons and Halogens. *Bulletin of the Chemical Society of Japan*. **1956**, *29*, 213-218.

(39) Mrozowski, S. Semiconductivity and Diamagnetism of Polycrystalline Graphite and Condensed Ring Systems. *Physical Review*. **1952**, *85*, 609-620.

(40) Mrozowski, S. Electric Resistivity of Interstitial Compounds of Graphite. *Journal of Chemical Physics*. **1953**, *21*, 492-495.

(41) Winslow, F. H.; Baker, W. O.; Pape, N. R.; Matreyek, W. Formation and Properties of Polymer Carbon. *Journal of Polymer Science*. **1955**, *16*, 101-120.

(42) Felmayer, W.; Wolf, I. Conductivity and Energy-Gap Measurements of Some Relatives of Phthalocyanine. *Journal of the Electrochemical Society*. **1958**, *105*, 141-145.

(43) Pohl, H. A.; Bornmann, J. A.; Itoh, W. Semiconducting Polymers. *Polymer Preprints (American Chemical Society, Division of Polymer Chemistry)*. **1961**, *2*, 211-219.

(44) Pohl, H. A.; Engelhardt, E. H. Synthesis and Characterization of Some Highly Conjugated Semiconducting Polymers. *Journal of Physical Chemistry*. **1962**, *66*, 2085-2095.

(45) McNeil, R.; Weiss, D. E. A Xanthene Polymer with Semiconducting Properties. *Australian Journal of Chemistry*. **1959**, *12*, 643-656.

(46) Beaven, G. H.; Bird, G. R.; Hall, D. M.; Johnson, E. A.; Ladbury, J. E.; Lesslie, M. S.; Turner, E. E. The Relation between Configuration and Conjugation in Biphenyl Derivatives. V. 2,2'-Bridged Compounds with Seven- and Eight-Membered Rings. *Journal of the Chemical Society*. **1955**, 2708-2713.

(47) Beaven, G. H.; James, A. T.; Johnson, E. A. Steric Effects in the Gas-Liquid Chromatography of Some Alkylbiphenyls. *Nature (London, United Kingdom)*. **1957**, *179*, 490-491.

(48) Beaven, G. H.; Johnson, E. A. The Relation between Configuration and Conjugation in Biphenyl Derivatives. VIII. Some Compounds Derived from 2,2'-Diacetylbiphenyl. *Journal of the Chemical Society*. **1957**, 651-658.

(49) McNeill, R.; Siudak, R.; Wardlaw, J. H.; Weiss, D. E. Electronic Conduction in Polymers. I. Chemical Structure of Polypyrrole. *Australian Journal of Chemistry*. **1963**, *16*, 1056-1075.

(50) Gibson, J.; Holohan, M.; Riley, H. L. *Journal of the Chemical Society*. **1956**, *456*

(51) Bolto, B. A.; Weiss, D. E. Semiconducting Polymers Containing Coordinated Metal Ions. *Australian Journal of Chemistry*. **1962**, *15*, 653-667.

(52) Bolto, B. A.; Weiss, D. E. Electronic Conduction in Polymers. II. Electrochemical Reduction of Polypyrrole at Controlled Potential. *Australian Journal of Chemistry*. **1963**, *16*, 1076-1089.

(53) Bolto, B. A.; McNeill, R.; Weiss, D. E. Electronic Conduction in Polymers. III. Electronic Properties of Polypyrrole. *Australian Journal of Chemistry*. **1963**, *16*, 1090-1103.

(54) Shirakawa, H.; Louis, E. J.; MacDiarmid, A. G.; Chiang, C. K.; Heeger, A. J. Synthesis of Electrically Conducting Organic Polymers: Halogen Derivatives of Polyacetylene, (Ch)X. *Journal of the Chemical Society, Chemical Communications*. **1977**, 578-580.

(55) Schmitt, J.; Fallard, R.; Suquet, M. Arylthiophenes. *Bulletin de la Societe Chimique de France*. **1956**, 1147-1151.

(56) Strelko, V. V.; Vysotskii, Z. Z. Polymerization of Thiophene on the Surface of Dehydratable Silica Gel. *Sintez i Fiz.-Khim. Polimerov, Akad. Nauk Ukr. SSR, Inst. Khim. Vysokomolekul. Soedin., Sb. Statei*. **1964**, 80-82.

(57) Huber, L. K.; (Pennwalt Corp.). Thiophene Polymers. US, 1968-702203-3557068, 1971.

(58) Louvar, J. J.; (Universal Oil Products Co.). Polymerization of Heterocyclic Compounds. US, 1968-718334-3574072, 1971.

(59) Yamamoto, T.; Sanechika, K.; Yamamoto, A. Preparation of Thermostable and Electric-Conducting Poly(2,5-Thienylene). *Journal of Polymer Science, Polymer Letters Edition*. **1980**, *18*, 9-12.

(60) Kossmehl, G.; Chatzitheodorou, G. Electrical Conductivity of Poly(2,5-Thiophenediyl)-Arsenic Pentafluoride-Complexes. *Makromolekulare Chemie, Rapid Communications*. **1981**, *2*, 551-555.

(61) Tourillon, G.; Garnier, F. New Electrochemically Generated Organic Conducting Polymers. *Journal of Electroanalytical Chemistry and Interfacial Electrochemistry*. **1982**, *135*, 173-178.

(62) Kaneto, K.; Yoshino, K.; Inuishi, Y. Electrical Properties of Conducting Polymer, Polythiophene, Prepared by Electrochemical Polymerization. *Japanese Journal of Applied Physics, Part 2: Letters*. **1982**, *21*, 567-568.

(63) Tourillon, G.; Garnier, F. Stability of Conducting Polythiophene and Derivatives. *Journal of the Electrochemical Society*. **1983**, *130*, 2042-2044.

(64) Kaneto, K.; Kohno, Y.; Yoshino, K.; Inuishi, Y. Electrochemical Preparation of a Metallic Polythiophene Film. *Journal of the Chemical Society, Chemical Communications*. **1983**, 382-383.

(65) Kaneto, K.; Yoshino, K.; Inuishi, Y. Characteristics of Polythiophene Battery. *Japanese Journal of Applied Physics, Part 2: Letters*. **1983**, *22*, 567-568.

(66) Kaneto, K.; Yoshino, K.; Inuishi, Y. Characteristics of Electrooptic Device Using Conducting Polymers, Polythiophene and Polypyrrole Films. *Japanese Journal of Applied Physics, Part 2: Letters*. **1983**, *22*, 412-414.

(67) Cao, Y.; Wu, Q.; Guo, K.; Qian, R. Studies on the Methyl Chloride-Soluble Fraction of Polythiophene and Its Conductivity on Doping with Iodine. *Makromolekulare Chemie*. **1984**, *185*, 389-396.

(68) Elsenbaumer, R. L.; Jen, K. Y.; Oboodi, R. Processible and Environmentally Stable Conducting Polymers. *Synthetic Metals*. **1986**, *15*, 169-174.

(69) Jen, K. Y.; Miller, G. G.; Elsenbaumer, R. L. Highly Conducting, Soluble, and Environmentally-Stable Poly(3-Alkylthiophenes). *Journal of the Chemical Society, Chemical Communications*. **1986**, 1346-1347.

(70) Jen, K. Y.; Oboodi, R.; Elsenbaumer, R. L. Processible and Environmentally Stable Conducting Polymers. *Polymeric Materials Science and Engineering*. **1985**, *53*, 79-83.

(71) Kobayashi, M.; Chen, J.; Chung, T. C.; Moraes, F.; Heeger, A. J.; Wudl, F. Synthesis and Properties of Chemically Coupled Poly(Thiophene). *Synthetic Metals*. **1984**, *9*, 77-86.

(72) Sugimoto, R.; Takeda, S.; Gu, H. B.; Yoshino, K. Preparation of Soluble Polythiophene Derivatives Utilizing Transition Metal Halides as Catalysts and Their Property. *Chemistry Express*. **1986**, *1*, 635-638.

(73) Chen, T. A.; Rieke, R. D. The First Regioregular Head-to-Tail Poly(3-Hexylthiophene-2,5-Diyl) and a Regiorandom Isopolymer: Nickel Versus Palladium Catalysis of 2(5)-Bromo-5(2)-(Bromozincio)-3-Hexylthiophene Polymerization. *Journal of the American Chemical Society*. **1992**, *114*, 10087-10088.

(74) Chen, T. A.; O'Brien, R. A.; Rieke, R. D. Use of Highly Reactive Zinc Leads to a New, Facile Synthesis for Polyarylenes. *Macromolecules*. **1993**, *26*, 3462-3463.

(75) Chen, T.-A.; Wu, X.; Rieke, R. D. Regiocontrolled Synthesis of Poly(3-Alkylthiophenes) Mediated by Rieke Zinc: Their Characterization and Solid-State Properties. *Journal of the American Chemical Society*. **1995**, *117*, 233-244.

(76) McCullough, R. D.; Williams, S. P. Toward Tuning Electrical and Optical Properties in Conjugated Polymers Using Side-Chains: Highly Conductive Head-to-Tail, Heteroatom Functionalized Polythiophenes. *Journal of the American Chemical Society*. **1993**, *115*, 11608-11609.

(77) Loewe, R. S.; Ewbank, P. C.; Liu, J.; Zhai, L.; McCullough, R. D. Regioregular, Head-to-Tail Coupled Poly(3-Alkylthiophenes) Made Easy by the Grim Method: Investigation of the Reaction and the Origin of Regioselectivity. *Macromolecules*. **2001**, *34*, 4324-4333.

(78) Leclerc, M.; Faid, K. Electrical and Optical Properties of Processable Polythiophene Derivatives. Structure-Property Relationships. *Advanced Materials (Weinheim, Germany)*. **1997**, *9*, 1087-1094.

(79) Levesque, I.; Leclerc, M. Ionochromic and Thermochromic Phenomena in a Regioregular Polythiophene Derivative Bearing Oligo(Oxyethylene) Side Chains. *Chemistry of Materials*. **1996**, *8*, 2843-2849.

(80) Balamurugan, S. S.; Bantchev, G. B.; Yang, Y.; McCarley, R. L. Highly Water-Soluble Thermally Responsive Poly(Thiophene)-Based Brushes. *Angewandte Chemie, International Edition*. **2005**, *44*, 4872-4876.

(81) Inganaes, O.; Gustafsson, G.; Salaneck, W. R.; Oesterholm, J. E.; Laakso, J. Thermochromism in Thin Films of Poly(3-Alkylthiophenes). *Synthetic Metals*. **1989**, *28*, C377-C384.

(82) Bobacka, J.; Ivaska, A.; Lewenstam, A. Potentiometric Ion Sensors. *Chemical Reviews (Washington, DC, United States)*. **2008**, *108*, 329-351.

(83) Lange, U.; Roznyatovskaya, N. V.; Mirsky, V. M. Conducting Polymers in Chemical Sensors and Arrays. *Analytica Chimica Acta*. **2008**, *614*, 1-26.

(84) Marsella, M. J.; Newland, R. J.; Carroll, P. J.; Swager, T. M. Ionoresistivity as a Highly Sensitive Sensory Probe: Investigations of Polythiophenes Functionalized with Calix[4]Arene-Based Ion Receptors. *Journal of the American Chemical Society*. **1995**, *117*, 9842-9848.

(85) Marsella, M. J.; Swager, T. M. Designing Conducting Polymer-Based Sensors: Selective Ionochromic Response in Crown Ether-Containing Polythiophenes. *Journal of the American Chemical Society*. **1993**, *115*, 12214-12215.

(86) Levesque, I.; Leclerc, M. Novel Dual Photochromism in Polythiophene Derivatives. *Macromolecules*. **1997**, *30*, 4347-4352.

(87) Faid, K.; Leclerc, M. Functionalized Regioregular Polythiophenes: Towards the Development of Biochromic Sensors. *Chemical Communications (Cambridge)*. **1996**, 2761-2762.

(88) Kim, H.-C.; Lee, S.-K.; Jeon, W. B.; Lyu, H.-K.; Lee, S. W.; Jeong, S. W. Detection of C-Reactive Protein on a Functional Poly(Thiophene) Self-Assembled Monolayer Using Surface Plasmon Resonance. *Ultramicroscopy*. **2008**, *108*, 1379-1383.

(89) Odaci, D.; Kiralp Kayahan, S.; Timur, S.; Toppare, L. Use of a Thiophene-Based Conducting Polymer in Microbial Biosensing. *Electrochimica Acta*. **2008**, *53*, 4104-4108.

(90) Berggren, M.; Gustafsson, G.; Inganaes, O.; Andersson, M. R.; Wennerstroem, O.; Hjertberg, T. Green Electroluminescence in Poly-(3-Cyclohexylthiophene) Light-Emitting Diodes. *Advanced Materials (Weinheim, Germany)*. **1994**, *6*, 488-490.

(91) Berggren, M.; Inganas, O.; Gustafsson, G.; Rasmusson, J.; Andersson, M. R.; Hjertberg, T.; Wennerstrom, O. Light-Emitting Diodes with Variable Colors from Polymer Blends. *Nature (London)*. **1994**, *372*, 444-446.

(92) Yamamoto, T.; Wakayama, H.; Fukuda, T.; Kanbara, T. Electrochemical and Electric Properties of Vacuum-Deposited Poly(Arylene)S: Electrochemical Activity, Diode, and Electroluminescence. *Journal of Physical Chemistry*. **1992**, *96*, 8677-8679.

(93) Argun, A. A.; Aubert, P.-H.; Thompson, B. C.; Schwendeman, I.; Gaupp, C. L.; Hwang, J.; Pinto, N. J.; Tanner, D. B.; MacDiarmid, A. G.; Reynolds, J. R. Multicolored Electrochromism in Polymers: Structures and Devices. *Chemistry of Materials*. **2004**, *16*, 4401-4412.

(94) Liu, Y.; Xu, Y.; Zhu, D. Synthesis and Characterization of Poly(3-Alkyl Thiophene)s for Light-Emitting Diodes. *Macromolecular Chemistry and Physics*. **2001**, *202*, 1010-1015.

(95) Granstrom, M. Novel Polymer Light-Emitting Diode Designs Using Poly(Thiophenes). *Polymers for Advanced Technologies*. **1997**, *8*, 424-430.

(96) Kraft, A.; Grimsdale, A. C.; Holmes, A. B. Electroluminescent Conjugated Polymers-Seeing Polymers in a New Light. *Angewandte Chemie, International Edition*. **1998**, *37*, 403-428.

(97) Oullette, J. Semiconducting Polymers on Display. *The Industrial Physicist*; American Institute of Physics. June/July, **2001**, *7* (3), 22-25.

(98) Kline, R. J.; McGehee, M. D.; Kadnikova, E. N.; Liu, J.; Frechet, J. M. J. Controlling the Field-Effect Mobility of Regioregular Polythiophene by Changing the Molecular Weight. *Advanced Materials (Weinheim, Germany)*. **2003**, *15*, 1519-1522.

(99) Kline, R. J.; McGehee, M. D.; Kadnikova, E. N.; Liu, J.; Frechet, J. M. J.; Toney, M. F. Dependence of Regioregular Poly(3-Hexylthiophene) Film Morphology and Field-Effect Mobility on Molecular Weight. *Macromolecules*. **2005**, *38*, 3312-3319.

(100) Zen, A.; Saphiannikova, M.; Neher, D.; Grenzer, J.; Grigorian, S.; Pietsch, U.; Asawapirom, U.; Janietz, S.; Scherf, U.; Lieberwirth, I.; Wegner, G. Effect of Molecular Weight on the Structure and Crystallinity of Poly(3-Hexylthiophene). *Macromolecules*. **2006**, *39*, 2162-2171.

(101) Yang, H.; Shin, T. J.; Bao, Z.; Ryu, C. Y. Structural Transitions of Nanocrystalline Domains in Regioregular Poly(3-Hexyl Thiophene) Thin Films. *Journal of Polymer Science, Part B: Polymer Physics*. **2007**, *45*, 1303-1312.

(102) Yang, H.; LeFevre, S. W.; Ryu, C. Y.; Bao, Z. Solubility-Driven Thin Film Structures of Regioregular Poly(3-Hexyl Thiophene) Using Volatile Solvents. *Applied Physics Letters*. **2007**, *90*, 172116/172111-172116/172113.

(103) Zhang, R.; Li, B.; Iovu, M. C.; Jeffries-El, M.; Sauve, G.; Cooper, J.; Jia, S.; Tristram-Nagle, S.; Smilgies, D. M.; Lambeth, D. N.; McCullough, R. D.; Kowalewski, T. Nanostructure Dependence of Field-Effect Mobility in Regioregular Poly(3-Hexylthiophene) Thin Film Field Effect Transistors. *PMSE Preprints*. **2006**, *95*, 862-863.

(104) Sandberg, H. G. O.; Baecklund, T. G.; Oesterbacka, R.; Jussila, S.; Maekelae, T.; Stubb, H. Applications of an All-Polymer Solution-Processed High-Performance, Transistor. *Synthetic Metals*. **2005**, *155*, 662-665.

(105) Sirringhaus, H. Device Physics of Solution-Processed Organic Field-Effect Transistors. *Advanced Materials (Weinheim, Germany)*. **2005**, *17*, 2411-2425.

(106) Zhang, Q.; Cirpan, A.; Russell, T. P.; Emrick, T. Donor-Acceptor Poly(Thiophene-Block-Perylene Diimide) Copolymers: Synthesis and Solar Cell Fabrication. *Macromolecules (Washington, DC, United States)*. **2009**, *42*, 1079-1082.

(107) Gunes, S.; Marjanovic, N.; Nedeljkovic, J. M.; Sariciftci, N. S. Photovoltaic Characterization of Hybrid Solar Cells Using Surface Modified TiO_2 Nanoparticles and Poly(3-Hexyl)Thiophene. *Nanotechnology*. **2008**, *19*, 424009/424001-424009/424005.

(108) Jager, E. W. H.; Smela, E.; Inganas, O. Microfabricating Conjugated Polymer Actuators. *Science (Washington, D. C.)*. **2000**, *290*, 1540-1546.

(109) Scherlis Damian, A.; Marzari, N. Pi-Stacking in Thiophene Oligomers as the Driving Force for Electroactive Materials and Devices. *J Am Chem Soc*. **2005**, *127*, 3207-3212.

(110) Iribarren, J. I.; Ocampo, C.; Armelin, E.; Liesa, F.; Aleman, C. Poly(3-Alkylthiophene)S as Anticorrosive Additive for Paints: Influence of the Main Chain Stereoregularity. *Journal of Applied Polymer Science*. **2008**, *108*, 3291-3297.

(111) Daoud, W. A.; Xin, J. H. Regioregular Poly(3-Alkylthiophenes): Synthesis, Characterization, and Application in Conductive Fabrics. *Journal of Applied Polymer Science*. **2004**, *93*, 2131-2135.

(112) Bredas, J. L.; Street, G. B. Polarons, Bipolarons, and Solitons in Conducting Polymers. *Accounts of Chemical Research*. **1985**, *18*, 309-315.

(113) Cowan, D. O.; Wiygul, F. M. The Organic Solid State. *Chemical & Engineering News*. **1986**, *64*, 28-31, 34-45.

(114) Bredas, J. L. Relationship between Band Gap and Bond Length Alternation in Organic Conjugated Polymers. *Journal of Chemical Physics*. **1985**, *82*, 3808-3811.

(115) Bredas, J. L.; Street, G. B.; Themans, B.; Andre, J. M. Organic Polymers Based on Aromatic Rings (Polyparaphenylene, Polypyrrole, Polythiophene): Evolution of the Electronic Properties as a Function of the Torsion Angle between Adjacent Rings. *Journal of Chemical Physics*. **1985**, *83*, 1323-1329.

(116) Pranata, J.; Grubbs, R. H.; Dougherty, D. A. Band Structures of Polyfulvene and Related Polymers. A Model for the Effects of Benzannelation on the Band Structures of Polythiophene, Polypyrrole, and Polyfulvene. *Journal of the American Chemical Society*. **1988**, *110*, 3430-3435.

(117) Lee, Y. S.; Kertesz, M.; Elsenbaumer, R. L. Importance of Energetics in the Design of Small Bandgap Conducting Polymers. *Chemistry of Materials*. **1990**, *2*, 526-530.

(118) Williams, D. J. Organic Polymers and Nonpolymeric Materials with Good Nonlinear Optical Properties. *Angewandte Chemie*. **1984**, *96*, 637-651.

(119) De Melo, C. P.; Silbey, R. Nonlinear Polarizabilities of Conjugated Chains: Regular Polyenes, Solitons, and Polarons. *Chemical Physics Letters*. **1987**, *140*, 537-541.

(120) Ramasesha, S.; Soos, Z. G. Exact Dynamic Nonlinear Susceptibilities of Finite Correlated Models. *Chemical Physics Letters*. **1988**, *153*, 171-175.

(121) De Melo, C. P.; Silbey, R. Variational-Perturbational Treatment for the Polarizabilities of Conjugated Chains. II. Hyperpolarizabilities of Polyenic Chains. *Journal of Chemical Physics*. **1988**, *88*, 2567-2571.

(122) McCullough, R. D.; Lowe, R. D. Enhanced Electrical Conductivity in Regioselectively Synthesized Poly(3-Alkylthiophenes). *Journal of the Chemical Society, Chemical Communications*. **1992**, 70-72.

(123) Liu, J.; McCullough, R. D. End Group Modification of Regioregular Polythiophene through Postpolymerization Functionalization. *Macromolecules*. **2002**, *35*, 9882-9889.

(124) Langeveld-Voss, B. M. W.; Janssen, R. A. J.; Spiering, A. J. H.; van Dongen, J. L. J.; Vonk, E. C.; Claessens, H. A. End-Group Modification of Regioregular Poly(3-Alkylthiophene)S. *Chemical Communications (Cambridge)*. **2000**, 81-82.

(125) Liu, J.; Loewe, R. S.; McCullough, R. D. Employing Maldi-Ms on Poly(Alkylthiophenes): Analysis of Molecular Weights, Molecular Weight Distributions, End-Group Structures, and End-Group Modifications. *Macromolecules*. **1999**, *32*, 5777-5785.

(126) Woo, C. H.; Thompson, B. C.; Kim, B. J.; Toney, M. F.; Frechet, J. M. J. The Influence of Poly(3-Hexylthiophene) Regioregularity on Fullerene-Composite Solar Cell Performance. *Journal of the American Chemical Society*. **2008**, *130*, 16324-16329.

(127) Elsenbaumer, R. L.; Jen, K. Y.; Miller, G. G.; Eckhardt, H.; Shacklette, L. W.; Jow, R. In Electronic Properties of Conjugated Polymers, *Springer Series Solid State Science*; Kuzmany, H., Mehring, M., Roth, S., Eds.; Springer: New York, 1987; Vol. 76.

(128) Sato, M.; Morii, H. Configurational Feature of Electrochemically Prepared Poly(3-Dodecylthiophene). *Polymer Communications*. **1991**, *32*, 42-44.

(129) Sato, M.; Morii, H. Nuclear Magnetic Resonance Studies on Electrochemically Prepared Poly(3-Dodecylthiophene). *Macromolecules*. **1991**, *24*, 1196-1200.

(130) Barbarella, G.; Bongini, A.; Zambianchi, M. Regiochemistry and Conformation of Poly(3-Hexylthiophene) Via the Synthesis and the Spectroscopic Characterization of the Model Configurational Triads. *Macromolecules*. **1994**, *27*, 3039-3045.

(131) Leclerc, M.; Martinez Diaz, F.; Wegner, G. Structural Analysis of Poly(3-Alkylthiophenes). *Makromolekulare Chemie*. **1989**, *190*, 3105-3116.

(132) Tamao, K.; Kodama, S.; Nakajima, I.; Kumada, M.; Minato, A.; Suzuki, K. Nickel-Phosphine Complex-Catalyzed Grignard Coupling. II. Grignard Coupling of Heterocyclic Compounds. *Tetrahedron*. **1982**, *38*, 3347-3354.

(133) Gronowitz, S.; Hoffman, R. A. Proton Magnetic Resonance (Nmr) of Thiophenes. VII. Monosubstituted Thiophenes: Chemical Shifts and Substituent Effects. *Arkiv foer Kemi*. **1960**, *16*, 539-562.

(134) Barker, J. M.; Huddleston, P. R.; Wood, M. L. Mannich Reactions of Methoxythiophenes. *Synthetic Communications*. **1975**, *5*, 59-64.

(135) McClain, M. D.; Whittington, D. A.; Mitchell, D. J.; Curtis, M. D. Novel Poly(3-Alkylthiophene) and Poly(3- Alkylthienyl Ketone) Syntheses Via Organomercurials. *Journal of the American Chemical Society*. **1995**, *117*, 3887-3888.

(136) Hotta, S.; Rughooputh, S. D. D. V.; Heeger, A. J.; Wudl, F. Spectroscopic Studies of Soluble Poly(3-Alkylthienylenes). *Macromolecules*. **1987**, *20*, 212-215.

(137) Stanke, D.; Hallensleben, M. L.; Toppare, L. Oxidative Polymerization of Some N-Alkylpyrroles with Ferric Chloride. *Synthetic Metals*. **1995**, *73*, 267-272.

(138) Waltman, R. J.; Bargon, J. Reactivity/Structure Correlations for the Electropolymerization of Pyrrole: An Indo/Cndo Study of the Reactive Sites of Oligomeric Radical Cations. *Tetrahedron*. **1984**, *40*, 3963-3970.

(139) Roncali, J.; Garnier, F.; Lemaire, M.; Garreau, R. Poly Mono-, Bi-, and Trithiophene: Effect of Oligomer Chain Length on the Polymer Properties. *Synthetic Metals*. **1986**, *15*, 323-331.

(140) Baughman, R. H.; Chance, R. R. Point Defects in Fully Conjugated Polymers. *Journal of Applied Physics*. **1976**, *47*, 4295-4300.

(141) McCullough, R. D.; Lowe, R. D. The Synthesis of Well-Defined Conducting Poly(3-Alkylthiophenes). *Polymer Preprints (American Chemical Society, Division of Polymer Chemistry)*. **1992**, *33*, 195-196.

(142) McCullough, R. D.; Lowe, R. D.; Jayaraman, M.; Ewbank, P. C.; Anderson, D. L.; Tristram-Nagle, S. Synthesis and Physical Properties of Regiochemically Well-Defined, Head-to-Tail Coupled Poly(3-Alkylthiophenes). *Synthetic Metals*. **1993**, *55*, 1198-1203.

(143) Pham, C. V.; Mark, H. B., Jr.; Zimmer, H. A Convenient Synthesis of 3-Alkylthiophenes. *Synthetic Communications*. **1986**, *16*, 689-696.

(144) Consiglio, G.; Gronowitz, S.; Hornfeldt, A. B.; Maltesson, B.; Noto, R.; Spinelli, D. Nucleophilic Substitutions in Five-Membered Rings. Evidence for Primary Steric Effects in Alkylthiophene Derivatives. *Chemica Scripta*. **1977**, *11*, 175-179.

(145) Tamao, K.; Kiso, Y.; Sumitani, K.; Kumada, M. Alkyl Group Isomerization in the Cross-Coupling Reaction of Secondary Alkyl Grignard Reagents with Organic Halides in the Presence of Nickel-Phosphine Complexes as Catalysts. *Journal of the American Chemical Society*. **1972**, *94*, 9268-9269.

(146) Kumada, M. Nickel and Palladium Complex Catalyzed Cross-Coupling Reactions of Organometallic Reagents with Organic Halides. *Pure and Applied Chemistry*. **1980**, *52*, 669-679.

(147) Negishi, E. Bimetallic Catalytic Systems Containing Titanium, Zirconium, Nickel and Palladium. Their Applications to Selective Organic Syntheses. *Pure and Applied Chemistry*. **1981**, *53*, 2333-2356.

(148) Kalinin, V. N. Carbon-Carbon Bond Formation in Heterocycles Using Nickel and Palladium Catalyzed Reactions. *Synthesis*. **1992**, 413-432.

(149) Negishi, E.; Takahashi, T.; Baba, S.; Van Horn, D. E.; Okukado, N. Nickel- or Palladium-Catalyzed Cross Coupling. 31. Palladium- or Nickel-Catalyzed Reactions of Alkenylmetals with Unsaturated Organic Halides as a Selective Route to Arylated Alkenes and Conjugated Dienes: Scope, Limitations, and Mechanism. *Journal of the American Chemical Society*. **1987**, *109*, 2393-2401.

(150) McCullough, R. D.; Tristram-Nagle, S.; Williams, S. P.; Lowe, R. D.; Jayaraman, M. Self-Orienting Head-to-Tail Poly(3-Alkylthiophenes): New Insights on Structure-Property Relationships in Conducting Polymers. *Journal of the American Chemical Society*. **1993**, *115*, 4910-4911.

(151) McCullough, R. D.; Jayaraman, M. The Tuning of Conjugation by Recipe: The Synthesis and Properties of Random Head-to-Tail Poly(3-Alkylthiophene) Copolymers. *Journal of the Chemical Society, Chemical Communications*. **1995**, 135-136.

(152) Chen, T.-A.; Rieke, R. D. Polyalkylthiophenes with the Smallest Bandgap and the Highest Intrinsic Conductivity. *Synthetic Metals*. **1993**, *60*, 175-177.

(153) Wu, X.; Chen, T.-A.; Rieke, R. D. Synthesis of Regioregular Head-to-Tail Poly[3-(Alkylthio)Thiophenes]. A Highly Electroconductive Polymer. *Macromolecules*. **1995**, *28*, 2101-2102.

(154) Iraqi, A.; Barker, G. W. Synthesis and Characterization of Telechelic Regioregular Head-to-Tail Poly(3-Alkylthiophenes). *Journal of Materials Chemistry*. **1998**, *8*, 25-29.

(155) Miyaura, N.; Ishiyama, T.; Sasaki, H.; Ishikawa, M.; Sato, M.; Suzuki, A. Palladium-Catalyzed Inter- and Intramolecular Cross-Coupling Reactions of β-Alkyl-9-Borabicyclo[3.3.1]Nonane Derivatives with 1-Halo-1-Alkenes or Haloarenes. Syntheses of Functionalized Alkenes, Arenes, and Cycloalkenes Via a Hydroboration-Coupling Sequence. *Journal of the American Chemical Society*. **1989**, *111*, 314-321.

(156) Guillerez, S.; Bidan, G. New Convenient Synthesis of Highly Regioregular Poly(3-Octylthiophene) Based on the Suzuki Coupling Reaction. *Synthetic Metals*. **1998**, *93*, 123-126.

(157) Iraqi, A.; Crayston, J. A.; Walton, J. C. Covalent Binding of Redox Active Centers to Preformed Regioregular Polythiophenes. *Journal of Materials Chemistry*. **1998**, *8*, 31-36.

(158) *Handbook of Organic Conductive Molecules and Polymers*; Nalva, H. S.; John Wiley and Sons: New York, 1997; Vol. 2.

(159) Lacroix, J.-C.; Maurel, F.; Lacaze, P.-C. Oligomer-Oligomer Versus Oligomer-Monomer C2-C2' Coupling Reactions in Polypyrrole Growth. *Journal of the American Chemical Society*. **2001**, *123*, 1989-1996.

(160) Barbarella, G.; Zambianchi, M.; Toro, R. D.; Colonna, M., Jr.; Iarossi, D.; Goldoni, F.; Bongini, A. Regioselective Oligomerization of 3-(Alkylsulfanyl)Thiophenes with Ferric Chloride. *Journal of Organic Chemistry*. **1996**, *61*, 8285-8292.

(161) Smie, A.; Synowczyk, A.; Heinze, J.; Alle, R.; Tschuncky, P.; Gotz, G.; Bauerle, P. β,β-Disubstituted Oligothiophenes, a New Oligomeric Approach Towards the Synthesis of Conducting Polymers. *Journal of Electroanalytical Chemistry*. **1998**, *452*, 87-95.

(162) Baeuerle, P.; Segelbacher, U.; Maier, A.; Mehring, M. Electronic Structure of Mono- and Dimeric Cation Radicals in End-Capped Oligothiophenes. *Journal of the American Chemical Society*. **1993**, *115*, 10217-10223.

(163) Andrieux, C. P.; Audebert, P.; Hapiot, P.; Saveant, J. M. Identification of the First Steps of the Electrochemical Polymerization of Pyrroles by Means of Fast Potential Step Techniques. *Journal of Physical Chemistry*. **1991**, *95*, 10158-10164.

(164) Guyard, L.; Hapiot, P.; Neta, P. Redox Chemistry of Bipyrroles: Further Insights into the Oxidative Polymerization Mechanism of Pyrrole and Oligopyrroles. *Journal of Physical Chemistry B*. **1997**, *101*, 5698-5706.

(165) Wei, Y.; Chan, C. C.; Tian, J.; Jang, G. W.; Hsueh, K. F. Electrochemical Polymerization of Thiophenes in the Presence of Bithiophene or Terthiophene: Kinetics and Mechanism of the Polymerization. *Chemistry of Materials*. **1991**, *3*, 888-897.

(166) Diaz, A. F.; Crowley, J.; Bargon, J.; Gardini, G. P.; Torrance, J. B. Electrooxidation of Aromatic Oligomers and Conducting Polymers. *Journal of Electroanalytical Chemistry and Interfacial Electrochemistry*. **1981**, *121*, 355-361.

(167) Ten Hoeve, W.; Wynberg, H.; Havinga, E. E.; Meijer, E. W. Substituted 2,2':5',2":5",2"':5"',2"":5"",2""':5""',2""":5""",2"""':5"""',2""":5""",2"""':5"""',2""""':5""""',2""""- Undecithiophenes, the Longest Characterized Oligothiophenes. *Journal of the American Chemical Society*. **1991**, *113*, 5887-5889.

(168) Wei, Y.; Tian, J.; Yang, D. A New Method for Polymerization of Pyrrole and Derivatives. *Makromolekulare Chemie, Rapid Communications*. **1991**, *12*, 617-623.

(169) Patil, A. O.; Heeger, A. J.; Wudl, F. Optical Properties of Conducting Polymers. *Chemical Reviews*. **1988**, *88*, 183-200.

(170) Chung, T. C.; Kaufman, J. H.; Heeger, A. J.; Wudl, F. Charge Storage in Doped Poly(Thiophene): Optical and Electrochemical Studies. *Physical Review B: Condensed Matter and Materials Physics*. **1984**, *30*, 702-710.

(171) Kaneto, K.; Ura, S.; Yoshino, K.; Inuishi, Y. Optical and Electrical Properties of Electrochemically Doped N- and P-Type Polythiophenes. *Japanese Journal of Applied Physics, Part 2: Letters*. **1984**, *23*, 189-191.

(172) Bredas, J. L.; Themans, B.; Fripiat, J. G.; Andre, J. M.; Chance, R. R. Highly Conducting Polyparaphenylene, Polypyrrole, and Polythiophene Chains: An Ab Initio Study of the Geometry and Electronic-Structure Modifications Upon Doping. *Physical Review B: Condensed Matter and Materials Physics*. **1984**, *29*, 6761-6773.

(173) Vardeny, Z.; Ehrenfreund, E.; Shinar, J.; Wudl, F. Photoexcitation Spectroscopy of Polythiophene. *Physical Review B: Condensed Matter and Materials Physics*. **1987**, *35*, 2498-2500.

(174) Heeger, A. J.; Kivelson, S.; Schrieffer, J. R.; Su, W. P. Solitons in Conducting Polymers. *Reviews of Modern Physics*. **1988**, *60*, 781-850.

(175) Bredas, J. L.; Chance, R. R.; Silbey, R. Comparative Theoretical Study of the Doping of Conjugated Polymers: Polarons in Polyacetylene and Polyparaphenylene. *Physical Review B: Condensed Matter and Materials Physics*. **1982**, *26*, 5843-5854.

(176) Bredas, J. L.; Scott, J. C.; Yakushi, K.; Street, G. B. Polarons and Bipolarons in Polypyrrole: Evolution of the Band Structure and Optical Spectrum Upon Doping. *Physical Review B: Condensed Matter and Materials Physics*. **1984**, *30*, 1023-1025.

(177) Baughman, R. H.; Bredas, J. L.; Chance, R. R.; Elsenbaumer, R. L.; Shacklette, L. W. Structural Basis for Semiconducting and Metallic Polymer Dopant Systems. *Chemical Reviews*. **1982**, *82*, 209-222.

(178) Fichou, D.; Xu, B.; Horowitz, G.; Garnier, F. Generation of Stabilized Polarons and Bipolarons on Extended Model Thiophene Oligomers. *Synthetic Metals*. **1991**, *41*, 463-469.

(179) Zade, S. S.; Bendikov, M. Theoretical Study of Long Oligothiophene Dications: Bipolaron Vs Polaron Pair Vs Triplet State. *Journal of Physical Chemistry B*. **2006**, *110*, 15839-15846.

(180) Pearson, D. S.; Pincus, P. A.; Heffner, G. W.; Dahman, S. J. Effect of Molecular Weight and Orientation on the Conductivity of Conjugated Polymers. *Macromolecules*. **1993**, *26*, 1570-1575.

(181) Jeon, D.; Kim, J.; Gallagher, M. C.; Willis, R. F. Scanning Tunneling Spectroscopic Evidence for Granular Metallic Conductivity in Conducting Polymeric Polyaniline. *Science (Washington, DC, United States)*. **1992**, *256*, 1662-1664.

(182) Hill, M. G.; Penneau, J. F.; Zinger, B.; Mann, K. R.; Miller, L. L. Oligothiophene Cation Radicals. π-Dimers as Alternatives to Bipolarons in Oxidized Polythiophenes. *Chemistry of Materials*. **1992**, *4*, 1106-1113.

(183) Zinger, B.; Mann, K. R.; Hill, M. G.; Miller, L. L. Photochemical Formation of Oligothiophene Cation Radicals in Acidic Solution and Nafion. *Chemistry of Materials*. **1992**, *4*, 1113-1118.

(184) Hapiot, P.; Audebert, P.; Monnier, K.; Pernaut, J. M.; Garcia, P. Electrochemical Evidence of π-Dimerization with Short Thiophene Oligomers. *Chemistry of Materials*. **1994**, *6*, 1549-1555.

(185) Hong, Y.; Yu, Y.; Miller, L. L. An Oxidized Oligothiophene That Forms π-Stacks. *Synthetic Metals*. **1995**, *74*, 133-135.

(186) Xu, Z.; Fichou, D.; Horowitz, G.; Garnier, F. Electrochemical Synthesis of Alpha-Conjugated Octi- and Decithienyl Oligomers. *Journal of Electroanalytical Chemistry and Interfacial Electrochemistry*. **1989**, *267*, 339-342.

(187) Fichou, D.; Bachet, B.; Demanze, F.; Billy, I.; Horowitz, G.; Garnier, F. Growth and Structural Characterization of the Quasi-2D Single Crystal of α-Octithiophene (α-8t). *Advanced Materials (Weinheim, Germany)*. **1996**, *8*, 500-504.

(188) Fichou, D.; Demanze, P.; Horowitz, G.; Hajlaoui, R.; Constant, M.; Garnier, F. Structural, Spectroscopic, and Device Characteristics of Octithiophene. *Synthetic Metals*. **1997**, *85*, 1309-1312.

(189) Fichou, D.; Teulade-Fichou, M. P.; Horowitz, G.; Demanze, F. Thermal and Optical Characterization of High Purity α-Octithiophene. *Advanced Materials (Weinheim, Germany)*. **1997**, *9*, 75-80.

(190) Zotti, G.; Schiavon, G.; Berlin, A.; Pagani, G. Thiophene Oligomers as Polythiophene Models. 1. Anodic Coupling of Thiophene Oligomers to Dimers: A Kinetic Investigation. *Chemistry of Materials*. **1993**, *5*, 430-436.

(191) Zotti, G.; Schiavon, G.; Berlin, A.; Pagani, G. Thiophene Oligomers as Polythiophene Models. 2. Electrochemistry and in Situ ESR of End-Capped Oligothienyls in the Solid State. Evidence for π-Dimerization of Hexameric Polarons in Polythiophene. *Chemistry of Materials*. **1993**, *5*, 620-624.

(192) Zotti, G.; Schiavon, G.; Berlin, A.; Pagani, G. Thiophene Oligomers as Polythiophene Models. 3. Conductive and Capacitive Behavior of End-Capped Oligothienyls as Thin Films. A Contribution to the Conduction Mechanism and to the Faradaic-Capacitive Debate of Conducting Polymers. *Advanced Materials. (Weinheim, Fed. Repub. Ger.)*. **1993**, *5*, 551-554.

(193) Sato, M.-a.; Hiroi, M. Preparation of Long Alkyl-Substituted Oligothiophenes. *Chemistry Letters*. **1994**, 985-988.

(194) Sato, M.-a.; Hiroi, M. Synthesis and Properties of Hexyl-Substituted Oligothiophenes. *Synthetic Metals*. **1995**, *71*, 2085-2086.

(195) Baeuerle, P.; Fischer, T.; Bidlingmeier, B.; Stabel, A.; Rabe, J. P. Oligothiophehes - yet Longer? Synthesis, Characterization, and Scanning Tunneling Microscopy Images of Homologous, Isomerically Pure Oligo(Alkylthiophenes). *Angewandte Chemie, International Edition in English*. **1995**, *34*, 303-307.

(196) Nakanishi, H.; Aso, Y.; Otsubo, T. The Longest Class of Oligothiophenes. *Synthetic Metals*. **1999**, *101*, 604-605.

(197) Otsubo, T.; Aso, Y.; Takimiya, K.; Nakanishi, H.; Sumi, N. Synthetic Studies of Extraordinarily Long Oligothiophenes. *Synthetic Metals*. **2003**, *133-134*, 325-328.

(198) Meier, H.; Stalmach, U.; Kolshorn, H. Effective Conjugation Length and Uv/Vis Spectra of Oligomers. *Acta Polymerica*. **1997**, *48*, 379-384.

(199) Osawa, S.; Ito, M.; Iwase, S.; Yajima, H.; Endo, R.; Tanaka, K. Effects of Molecular Weight on the Electrical Properties of Electrochemically Synthesized Poly(3-Hexylthiophene). *Polymer*. **1992**, *33*, 914-919.

(200) Goh, C.; Kline, R. J.; McGehee, M. D.; Kadnikova, E. N.; Frechet, J. M. J. Molecular-Weight-Dependent Mobilities in Regioregular Poly(3-Hexyl-Thiophene) Diodes. *Applied Physics Letters*. **2005**, *86*, 122110/122111-122110/122113.

(201) Tsai, E. W.; Basak, S.; Ruiz, J. P.; Reynolds, J. R.; Rajeshwar, K. Electrochemistry of Some β-Substituted Polythiophenes. Anodic Oxidation, Electrochromism, and Electrochemical Deactivation. *Journal of the Electrochemical Society*. **1989**, *136*, 3683-3689.

(202) Christensen, P. A.; Hamnett, A. In Situ Spectroscopic Investigations of the Growth, Electrochemical Cycling and Overoxidation of Polypyrrole in Aqueous Solution. *Electrochimica Acta*. **1991**, *36*, 1263-1286.

(203) Qi, Z.; Pickup, P. G. X-Ray Emission Analysis of Thin Poly(3-Methylthiophene) and Poly{(3-Methylthiophene)-Co-[1-Methyl-3-(Pyrrol-1-Ylmethyl)Pyridinium]} Films. Composition, Oxidation Level, and Overoxidation. *Analytical Chemistry*. **1993**, *65*, 696-703.

(204) Qi, Z.; Rees, N. G.; Pickup, P. G. Electrochemically Induced Substitution of Polythiophenes and Polypyrrole. *Chemistry of Materials*. **1996**, *8*, 701-707.

(205) Garcia, P.; Pernaut, J. M.; Hapiot, P.; Wintgens, V.; Valat, P.; Garnier, F.; Delabouglise, D. Effect of End Substitution on Electrochemical and Optical Properties of Oligothiophenes. *Journal of Physical Chemistry*. **1993**, *97*, 513-516.

(206) Demanze, F.; Cornil, J.; Garnier, F.; Horowitz, G.; Valat, P.; Yassar, A.; Lazzaroni, R.; Bredas, J.-L. Tuning of the Electronic and Optical Properties of Oligothiophenes Via Cyano Substitution: A Joint Experimental and Theoretical Study. *Journal of Physical Chemistry B*. **1997**, *101*, 4553-4558.

(207) Andrieux, C. P.; Hapiot, P.; Audebert, P.; Guyard, L.; An, M. N. D.; Groenendaal, L.; Meijer, E. W. Substituent Effects on the Electrochemical Properties of Pyrroles and Small Oligopyrroles. *Chemistry of Materials*. **1997**, *9*, 723-729.

(208) *Maldi-Tof Mass Spectrometry of Synthetic Polymers*; Pasch, H., Schrepp, W.; Springer: New York, 2003.

(209) Tanaka, K.; Waki, H.; Ido, Y.; Akita, S.; Yoshida, Y.; Yohida, T. Protein and Polymer Analyses up to *m/z* 100,000 by Laser Ionization Time-of-Flight Mass Spectrometry. *Rapid Communications in Mass Spectrometry*. **1988**, *2*, 151-153.

(210) Karas, M.; Hillenkamp, F. Laser Desorption Ionization of Proteins with Molecular Masses Exceeding 10,000 Daltons. *Analytical Chemistry*. **1988**, *60*, 2299-2301.

(211) Smith, C. G.; Nyquist, R. A.; Smith, P. B.; Pasztor, A. J., Jr.; Martin, S. J. Analysis of Synthetic Polymers. *Analytical Chemistry*. **1991**, *63*, 11R-32R.

(212) Peacock, P. M.; McEwen, C. N. Mass Spectrometry of Synthetic Polymers. *Analytical Chemistry*. **2006**, *78*, 3957-3964.

(213) Danis, P. O.; Karr, D. E.; Mayer, F.; Holle, A.; Watson, C. H. The Analysis of Water-Soluble Polymers by Matrix-Assisted Laser Desorption Time-of-Flight Mass Spectrometry. *Organic Mass Spectrometry*. **1992**, *27*, 843-846.

(214) Castro, J. A.; Koester, C.; Wilkins, C. Matrix-Assisted Laser Desorption/Ionization of High-Mass Molecules by Fourier-Transform Mass Spectrometry. *Rapid Communications in Mass Spectrometry*. **1992**, *6*, 239-241.

(215) Bahr, U.; Deppe, A.; Karas, M.; Hillenkamp, F.; Giessmann, U. Mass Spectrometry of Synthetic Polymers by UV-Matrix-Assisted Laser Desorption/Ionization. *Analytical Chemistry*. **1992**, *64*, 2866-2869.

(216) Schriemer, D. C.; Li, L. Detection of High Molecular Weight Narrow Polydisperse Polymers up to 1.5 Million Daltons by Maldi Mass Spectrometry. *Analytical Chemistry*. **1996**, *68*, 2721-2725.

(217) Eng, S. J.; Motekaitis, R. J.; Martell, A. E. The Effect of End-Group Substitutions and Use of a Mixed Solvent System on Diketones and Their Iron Complexes. *Inorganica Chimica Acta*. **1998**, *278*, 170-177.

(218) Qian, C.; Grigoras, S.; Kennan, L. D. End Group Effects on the Phase Behavior of Polymer Blends: Poly(Dimethylsiloxane) and Poly(Methylphenylsiloxane) Blend. *Macromolecules*. **1996**, *29*, 1260-1265.

(219) Tao, Y.; Donat-Bouillud, A.; D'Iorio, M.; Lam, J.; Gorjanc, T. C.; Py, C.; Wong, M. S.; Li, Z. H. Organic Light Emitting Diodes Based on End-Substituted Oligo(Phenylenevinylene)S. *Thin Solid Films*. **2000**, *363*, 298-301.

(220) Chen, H.; He, M.; Pei, J.; Liu, B. End-Group Analysis of Blue Light-Emitting Polymers Using Matrix-Assisted Laser Desorption/Ionization Time-of-Flight Mass Spectrometry. *Analytical Chemistry*. **2002**, *74*, 6252-6258.

(221) Montaudo, G.; Montaudo, M. S.; Puglisi, C.; Samperi, F. Characterization of Polymers by Matrix-Assisted Laser Desorption/Ionization Time-of-Flight Mass Spectrometry: Molecular Weight Estimates in Samples of Varying Polydispersity. *Rapid Communications in Mass Spectrometry*. **1995**, *9*, 453-460.

(222) Nielen, M. W. F. Maldi Time-of-Flight Mass Spectrometry of Synthetic Polymers. *Mass Spectrometry Reviews*. **1999**, *18*, 309-344.

(223) Schriemer, D. C.; Li, L. Mass Discrimination in the Analysis of Polydisperse Polymers by Maldi Time-of-Flight Mass Spectrometry. 1. Sample Preparation and Desorption/Ionization Issues. *Analytical Chemistry*. **1997**, *69*, 4169-4175.

(224) Schriemer, D. C.; Li, L. Mass Discrimination in the Analysis of Polydisperse Polymers by Maldi Time-of-Flight Mass Spectrometry. 2. Instrumental Issues. *Analytical Chemistry*. **1997**, *69*, 4176-4183.

(225) Hanton, S. D. Mass Spectrometry of Polymers and Polymer Surfaces. *Chemical Reviews (Washington, D. C.)*. **2001**, *101*, 527-569.

(226) Lloyd, P. M.; Suddaby, K. G.; Varney, J. E.; Scrivener, E.; Derrick, P. J.; Haddleton, D. M. A Comparison between Matrix-Assisted Laser Desorption/Ionization Time-of-Flight Mass Spectrometry and Size Exclusion Chromatography in the Mass Characterization of Synthetic Polymers with Narrow Molecular-Mass Distributions: Poly(Methyl Methacrylate) and Poly(Styrene). *European Mass Spectrometry*. **1995**, *1*, 293-300.

(227) Belu, A. M.; DeSimone, J. M.; Linton, R. W.; Lange, G. W.; Friedman, R. M. Evaluation of Matrix-Assisted Laser Desorption Ionization Mass Spectrometry for Polymer Characterization. *Journal of the American Society for Mass Spectrometry*. **1996**, *7*, 11-24.

(228) Lloyd, P. M.; Scrivener, E.; Maloney, D. R.; Haddleton, D. M.; Derrick, P. J. Cation Attachment to Synthetic Polymers in Matrix-Assisted Laser Desorption/Ionization Mass Spectrometry. *Polymer Preprints (American Chemical Society, Division of Polymer Chemistry)*. **1996**, *37*, 847-848.

(229) Sakurada, N.; Fukuo, T.; Arakawa, R.; Ute, K.; Hatada, K. Characterization of Poly(Methyl Methacrylate) by Matrix-Assisted Laser Desorption/Ionization Mass Spectrometry. A Comparison with Supercritical Fluid Chromatography and Gel Permeation Chromatography. *Rapid Communications in Mass Spectrometry*. **1998**, *12*, 1895-1898.

(230) Axelsson, J.; Scrivener, E.; Haddleton, D. M.; Derrick, P. J. Mass Discrimination Effects in an Ion Detector and Other Causes for Shifts in Polymer Mass Distributions Measured by Matrix-Assisted Laser Desorption/Ionization Time-of-Flight Mass Spectrometry. *Macromolecules*. **1996**, *29*, 8875-8882.

(231) McEwen, C.; Jackson, C.; Larsen, B. The Fundamentals of Characterizing Polymers Using Maldi Mass Spectrometry. *Polymer Preprints (American Chemical Society, Division of Polymer Chemistry)*. **1996**, *37*, 314-315.

(232) McEwen, C. N.; Jackson, C.; Larsen, B. S. Instrumental Effects in the Analysis of Polymers of Wide Polydispersity by Maldi Mass Spectrometry. *International Journal of Mass Spectrometry and Ion Processes*. **1997**, *160*, 387-394.

(233) Larsen, B. S.; Simonsick, W. J., Jr.; McEwen, C. N. Fundamentals of the Application of Matrix-Assisted Laser Desorption-Ionization Mass Spectrometry to Low Mass Poly(Methyl Methacrylate) Polymers. *Journal of the American Society for Mass Spectrometry*. **1996**, *7*, 287-292.

(234) Guo, B.; Chen, H.; Rashidzadeh, H.; Liu, X. Observation of Varying Molecular Weight Distributions in Matrix-Assisted Laser Desorption/Ionization Time-of-Flight Analysis of Polymethyl Methacrylate. *Rapid Communications in Mass Spectrometry*. **1997**, *11*, 781-785.

(235) Montaudo, G.; Garozzo, D.; Montaudo, M. S.; Puglisi, C.; Samperi, F. Molecular and Structural Characterization of Polydisperse Polymers and Copolymers by Combining Maldi-Tof Mass Spectrometry with Gpc Fractionation. *Macromolecules*. **1995**, *28*, 7983-7989.

(236) Vitalini, D.; Mineo, P.; Scamporrino, E. Further Application of a Procedure for Molecular Weight and Molecular Weight Distribution Measurement of Polydisperse Polymers from Their Matrix-Assisted Laser Desorption/Ionization Time-of-Flight Mass Spectra. *Macromolecules*. **1997**, *30*, 5285-5289.

(237) Puglisi, C.; Samperi, F.; Alicata, R.; Montaudo, G. End-Groups-Dependent Maldi Spectra of Polymer Mixtures. *Macromolecules*. **2002**, *35*, 3000-3007.

(238) Alicata, R.; Montaudo, G.; Puglisi, C.; Samperi, F. Influence of Chain End Groups on the Matrix-Assisted Laser Desorption/Ionization Spectra of Polymer Blends. *Rapid Communications in Mass Spectrometry*. **2002**, *16*, 248-260.

(239) Guttman, C. M.; Wetzel, S. J.; Flynn, K. M.; Fanconi, B. M.; VanderHart, D. L.; Wallace, W. E. Matrix-Assisted Laser Desorption/Ionization Time-of-Flight Mass Spectrometry Interlaboratory Comparison of Mixtures of Polystyrene with Different End Groups: Statistical Analysis of Mass Fractions and Mass Moments. *Analytical Chemistry*. **2005**, *77*, 4539-4548.

(240) McCarley, T. D.; Noble, C. O.; DuBois, C. J., Jr.; McCarley, R. L. Maldi-Ms Evaluation of Poly(3-Hexylthiophene) Synthesized by Chemical Oxidation with $FeCl_3$. *Macromolecules*. **2001**, *34*, 7999-8004.

(241) Scherman, O. A.; Rutenberg, I. M.; Grubbs, R. H. Direct Synthesis of Soluble, End-Functionalized Polyenes and Polyacetylene Block Copolymers. *Journal of the American Chemical Society*. **2003**, *125*, 8515-8522.

(242) Fouad, I.; Mechbal, Z.; Chane-Ching, K. I.; Adenier, A.; Maurel, F.; Aaron, J.-J.; Vodicka, P.; Cernovska, K.; Kozmik, V.; Svoboda, J. Polythienobenzothiophenes, a New Family of Electroactive Polymers: Electrosynthesis, Spectral Characterization and Modelling. *Journal of Materials Chemistry*. **2004**, *14*, 1711-1721.

(243) Lo, C.; Adenier, A.; Chane-Ching, K. I.; Maurel, F.; Aaron, J. J.; Kosata, B.; Svoboda, J. A Novel Fluorescent, Conducting Polymer: Poly[1-(Thiophene-2-Yl)Benzothieno[3,2-B]Benzothiophene] Electrosynthesis, Characterization and Optical Properties. *Synthetic Metals*. **2006**, *156*, 256-269.

(244) Gutierrez-Llorente, A.; Horowitz, G.; Perez-Casero, R.; Perriere, J.; Fave, J. L.; Yassar, A.; Sant, C. Growth of Polyalkylthiophene Films by Matrix Assisted Pulsed Laser Evaporation. *Organic Electronics*. **2004**, *5*, 29-34.

(245) Mezlova, M.; Aaron, J. J.; Svoboda, J.; Adenier, A.; Maurel, F.; Chane-Ching, K. Novel Conducting Polymers Based on Thieno[3,2-B]Indoles: Electrochemical Properties and Molecular Structure. *Journal of Electroanalytical Chemistry*. **2005**, *581*, 93-103.

(246) Zotti, G.; Zecchin, S.; Schiavon, G.; Vercelli, B.; Berlin, A.; Porzio, W. Electrostatically Self-Assembled Multilayers of Novel Symmetrical Rigid-Rod Polyanionic and Polycationic Polythiophenes on Ito/Glass and Gold Electrodes. *Chemistry of Materials*. **2004**, *16*, 2091-2100.

(247) Visy, C.; Lukkari, J.; Kankare, J. Electrochemically Polymerized Terthiophene Derivatives Carrying Aromatic Substituents. *Macromolecules*. **1994**, *27*, 3322-3329.

(248) Camalet, J. L.; Lacroix, J. C.; Aeiyach, S.; Chane-Ching, K.; Lacaze, P. C. Electrosynthesis of Adherent Polyaniline Films on Iron and Mild Steel in Aqueous Oxalic Acid Medium. *Synthetic Metals*. **1998**, *93*, 133-142.

(249) Folch, I.; Borros, S.; Amabilino, D. B.; Veciana, J. Matrix-Assisted Laser Desorption/Ionization Time-of-Flight Mass Spectrometric Analysis of Some Conducting Polymers. *Journal of Mass Spectrometry*. **2000**, *35*, 550-555.

(250) Dolan, A. R.; Wood, T. D. Analysis of Polyaniline Oligomers by Laser Desorption Ionization and Solventless Maldi. *Journal of the American Society for Mass Spectrometry*. **2004**, *15*, 893-899.

(251) Pearson, D. L.; Schumm, J. S.; Tour, J. M. Iterative Divergent/Convergent Approach to Conjugated Oligomers by a Doubling of Molecular Length at Each Iteration. A Rapid Route to Potential Molecular Wires. *Macromolecules*. **1994**, *27*, 2348-2350.

Chapter 2

Characterization of P3HTs Formed by Chemical Oxidation in Various Solvents

2.1 Introduction

2.1.1 An Overview of the Use of Various Solvents in Chemical Oxidative Polymerization

Sugimoto et al. were the first to report the preparation and characterization of soluble poly(thiophene) derivatives using transition metal halides as catalysts in 1986.[1] Since then, chemical oxidation has remained the most utilized method for the production of poly(3-alkylthiophene)s, P3ATs.[2] This is due to the method's ability to produce large yields of high molecular weight material with relatively good regioregularity in an affordable, facile manner. As noted in Chapter 1, there are other synthetic methods for the production of highly-ordered P3ATs that have regioregularities on the order of 98+ %. Nonetheless, these methods are far more complicated and expensive than the chemical oxidative coupling to form P3ATs. The works presented here are an in-depth investigation into the effects of the physical properties of poly(3-hexylthiophene)s, P3HTs, formed by chemical oxidation with $FeCl_3$ as a function of variation in the solvents that are employed during the formation of P3HTs.

Chemical oxidation with $FeCl_3$ has been reported for use in producing P3ATs an innumerable number of times. The procedures outlined by Sugimoto et al. for production of P3ATs by this method have been repeatedly employed and they have changed very little throughout the past two decades. Almost indiscriminately, little thought has been placed on development and manipulation of this procedure in order to acquire the ability to tailor and better understand the P3ATs that are formed via this route. Historically, this synthesis involves the addition of a solvated monomer in dry chloroform as a solvent to a suspension of iron(III) chloride in dry chloroform as a solvent. The amounts of oxidant and monomer used depend on the desired yield, although the oxidant-to-monomer ratio is generally maintained within the

range of 4:1–8:1. The reaction is stirred and kept under a blanket of inert gas for a period of hours, up to 24 hours. The crude polymer is then washed with methanol and acetone, resulting in a black solid. The empirical characterization of the physical properties for P3ATs formed by these means is discussed in Section 1.25 and elsewhere throughout Chapter 1.

Very little evidence of studies considering the importance of the particular solvent employed during chemical oxidative polymerization of P3ATs can be found in the literature. Although a few reports do exist, chloroform has classically been the sole choice of solvent for chemical oxidation of P3ATs without regard as to why. In part, this may be due to the fact that chloroform works well for the production of P3ATs by this means, which satisfies the expectations in regards to physical properties of those utilizing the method. Still, the trend for the use of chloroform may also be partly attributed to reports by Niemi et al. that concluded chloroform to be a superior solvent for chemical oxidative polymerization, because they argued ferric chloride must be in a solid or crystalline state in order for the polymerization of 3-alkylthiophenes to proceed via chemical oxidation.[3]

Niemi et al.[3] investigated the role of iron(III) chloride as an oxidant with two intentions: (i) to attempt to elucidate the attributes of iron(III) chloride that enable it to be an active oxidant for chemical oxidation; and (ii) to attempt to derive the mechanism of coupling involved in the chemical oxidative polymerization process of P3ATs. In order to do so, they performed a series of chemical oxidative polymerizations of P3ATs in several different solvents.

The criteria that were accounted for between the solvents used for polymerization were the solubility of iron(III) chloride in the given solvent. Their choice of solvents in which they reported ferric chloride was not at all soluble included carbon tetrachloride, pentane, and hexane. Solvents they chose that dissolved ferric chloride to a very limited extent were chloroform, and toluene. Solvents they chose that in which ferric chloride was reported completely soluble

included diethyl ether, xylene, acetone, and formic acid. The results reported indicate that only solvents in which $FeCl_3$ is either somewhat soluble or completely insoluble are capable of generating polymer.

From these studies, Niemi et al. concluded that ferric chloride must be solid to be active as a polymerization oxidant for 3-alkylthiophenes and that soluble $FeCl_3$ must be inert towards polymerization. In support of these conclusions, they referenced the crystalline state of $FeCl_3$ and argued that inside solid ferric chloride the iron(III) ions are mostly hidden within the crystal structure and each chloride ion is coordinated by two iron(III) ions, where the iron(III) ions are inert. Niemi et al. further explain that in order for the total charge of the crystal surface to be neutral there must exist a deficiency of chloride ions, where some of the chloride ions are coordinated to only one iron(III) ion. Thus, each iron(III) ion at the surface of the crystal has one unshared chloride ion and one free orbital. This allows thiophene monomers within close proximity of the crystalline surface to easily coordinate through the free electron pair of the heteroatom on the monomer with the free orbital of the iron(III) ion; oxidization of the monomer species to a radical cation results. Thus, Niemi et al. conclude polymerization must proceed on the surface of the oxidant, which must be in a solid state.

On the contrary, earlier work by Myers et al. with respect to the effect of the reaction medium for the chemical oxidative polymerization of pyrroles with ferric chloride showed that solubility of the oxidant did not directly impact the initiation of polymerization to form poly(pyrrole)s, PPYs.[4] Reactions performed in solvents in which ferric chloride is soluble, such as nitromethane, diethyl ether, tetrahydrofuran, and acetonitrile, afforded PPYs; so did solvents in which ferric chloride is insoluble, such as benzene, hexane, and carbon tetrachloride. However, it was observed that the nature of the reaction medium had a marked effect on the physical properties (e.g. conductivity) and yields of the final polymer.

Myers et al.[4] proposed that a necessary pyrrole-$FeCl_3$ intermediate is formed in the polymerization process and that the yields of PPY were dependent on the extent of the $FeCl_3$-solvent complexation, which influenced the amount of $FeCl_3$-pyrrole interaction. In order to test the theory, they observed the dissolution exotherms upon addition of ferric chloride to the various solvents, and then monitored the exotherms upon addition of monomer solution to the oxidant mixtures. They noted that solvents possessing strong Lewis base (donor) characteristics–such as dimethylsulfoxide and pyridine–exhibited strong exotherms when ferric chloride was added. These observations were suggested to be associated with the formation of $FeCl_3$-solvent complexes. Upon addition of monomer to these solutions there was no observable second exotherm that could be attributed to monomer-$FeCl_3$ interactions; in addition no polymerization occurred. It was surmised that the Lewis basicity of these solvents enhanced the stability of the $FeCl_3$-solvent complex to such an extent as to prevent $FeCl_3$-pyrrole interaction. Thus, it is apparent that there are properties of solvents besides those that facilitate solubility that play a crucial role in whether or not a solvent can be useful for chemical oxidative polymerization.

Olinga et al. also later showed in 1995, while doing comparison studies on the kinetics of polymerizations of thiophene by chemical oxidation with $FeCl_3$ in both chloroform and acetonitrile that polymerization of thiophenes does occur in the absence of solid oxidant, contrary to the claims of Niemi et al.[5] They reported that although the polymerization yield is limited, polymer is formed in acetonitrile; a solvent in which ferric chloride is completely soluble.

Finally, studies from the McCarley labs at Louisiana State University, LSU, performed by Brauch have shown that poly(3-hexylthiophene)s, P3HTs, can be successfully formed in solvents other than chloroform (in which $FeCl_3$ is completely soluble). Also, the influence of

such solvents results in structural characteristics of the final polymer that can impact the physical properties of the material and thus such solvents may hold promise for tailoring the functionality of P3ATs made by chemical oxidative polymerization with ferric chloride.[6] Brauch, while forming P3HTs by means of chemical oxidation with ferric chloride and nitromethane as a solvent observed a dramatic decrease in the extent of nucleophilic addition of chlorine to the final P3HTs; this occurred when limited oxidant-to-monomer ratios were used. The effects of specific endgroup or backbone addition to the physical properties of P3ATs have been discussed in Sections 1.2.9 and 1.3.2, and the importance of the implications to manipulating the physical characteristics of P3ATs formed by chemical oxidation cannot be overemphasized.

For these reasons, an in-depth investigation attempting to garner further insight into what physical properties of solvents influence the structural properties of P3ATs formed by chemical oxidation is of utmost importance to the realistic and purposeful application of these materials in modern technologies. As was explained in Chapter 1, the structure of these materials directly impacts their physical characteristics, which in turn determines their functionality. Chemical oxidative polymerization is the most utilized method for the preparation of P3ATs because of its ease and affordability. Therefore, the ability to optimize and tailor the functionality of polymers created by these means offers much promise for the use of chemical oxidation for the production of P3ATs. Such a route could be employed in order to affordably and in large scale produce devices relevant to the needs of mankind in the 21st century.

Thus, the studies found within this Chapter deal with the elucidation of the effects on the physical properties of P3HTs that stem from the specific solvent employed for chemical oxidative polymerization. An array of solvents has been utilized for these purposes. The physical characteristics of the solvents examined here were their dielectric constant, as well as their Lewis acidity and basicity (electron acceptor and donor) characteristics. The physical

attributes imparted on the final polymer prepared using these various solvents include yield, molecular weight, molecular weight distributions, regioregularities, and endgroup or backbone additions.

2.1.2 Physical Properties of Solvents

The physical properties of solvents investigated in these works were polarity, as well as Lewis acid and base characteristics. In the limited references within the literature concerning solvent effects of chemical oxidation to form P3ATs emphasis has been placed on the solubility of iron(III) chloride in such solvents (cf. Section 2.1). A major contribution from a particular solvent that determines the solubility of ferric chloride is solvent polarity. The polarity or relative static permittivity of a given solvent is determined by the nature of the bonds within solvent molecules, which are characterized by the differences in electronegativity between the bonding atoms. The polarity or the differences in electronegativity found within a molecule may also depend on the arrangement of molecular orbitals comprising the bonds within a molecule. For instance, an asymmetrical arrangement of nonpolar covalent bonds combined with nonbonding electron pairs may impart a difference in electronegativity within the molecule as a whole, giving that molecule a certain amount of relative polarity.

The polarity of different molecules is addressed in a relative fashion compared to either more-polar or less-polar materials. Compounds are designated with a dielectric constant that is based on their electric susceptibility to polarize. For instance, water is one of the most polar substances known with a dielectric constant near 80. On the other hand, carbon tetrachloride, due to its relatively nonpolar covalent bonds that are symmetrically arranged, is very nonpolar and has a dielectric constant of 2.2. Compounds having dielectric constants between this range are often classified as polar or nonpolar, although such classification is done so as compared relative to other substances. Iron(III) chloride is soluble in more polar solvents, due in part to the

strong electrostatic stabilizing ability imparted from the dipoles found within the structure of those solvents. However, less polar solvents are unable to electronically interact with the charges integral to the different ionic species of ferric chloride leading to its dissolution in more polar solvents.

Nonetheless, the solubility of ferric chloride is not solely dependent on the polarity of a given solvent. For instance, ferric chloride is completely soluble in diethyl ether, which is relatively nonpolar and possesses a dielectric constant of 4.3. This is in comparison to chloroform–in which ferric chloride is almost completely insoluble–that has a dielectric constant of 4.8. Therefore, there are other characteristics inherent to a particular solvent that determine the solubility of iron(III) chloride. In fact, a solvent may also possess strong Lewis acid and base properties.

A Lewis acid is defined as a molecule or ion whose incomplete electronic arrangement allows it to bind to another species by accepting an electron pair from that species. A Lewis base is a molecule or ion capable of donating an electron pair to a Lewis acid, resulting in the formation of a coordinate covalent bond.[7-10] Viktor Gutmann emphasized the fact that because the actual behavior of a molecule is the result of unique matching of its electronic structure with the electronic structures of other constituents composing the system, it is necessary to treat each system as a whole rather than its isolated constituents.[10] Lewis acids (electron acceptors) and Lewis bases (electron donors) interact very strongly with other compounds possessing opposite characteristics to the donor or acceptor. The terms nucleophilic and electrophilic are also used to characterize the properties of Lewis bases (electron donor), and Lewis acids (electron acceptor), respectively.

Regardless, intermolecular interactions between Lewis acids and bases induce charge density rearrangements within the molecules due to charge transfer and polarization effects

between the electron acceptor and electron donor; the terms donor and acceptor indicate the function involved in the process of charge transfer.[10] Furthermore, the change in polarity exhibited by these complexes induces variation from the original bond distances and bond angles of the individual components that changes the chemical properties and reactivity of the complex compound.[10] In other words, Lewis acids and bases can interact very strongly with other Lewis bases and acids, respectively, to form very stable complexes. Their stability depends on the extent of their Lewis characteristics.

Gutmann related this concept to the process for the solvation of ions in electrolyte solutions in either water or nonaqueous solvents, as opposed to an entirely electrostatic explanation based on solvent polarity. In 1960, Lindqvist and Zackriss reported a qualitative order of solvent donor strength based on enthalpy changes observed from calorimetric data on antimony (V) chloride, $SbCl_5$, emphasizing the changes in bond properties resulting from coordination.[11,12] Gutmann later termed the "donor number" (DN) concept that addressed donor strengths of solvents in a more quantitative fashion, and the concept was successfully applied to ionization processes in aprotic solvents.[13,14] In 1976, Mayer et al. were empirically able to quantitatively describe the acceptor properties of a solvent and define this capability using an "acceptor number" (AN).[15]

The donor number or donicity of a molecule is defined as the molar enthalpy value for the reaction of the donor (D) with $SbCl_5$ as a reference acceptor in a 10^{-3} M solution of 1,2-dichloroethane (DCE).[10,13] The molar enthalpy of a 1:1 molar adduct formation in dichloroethane is taken as an approximate measure of the energy of the coordinate bond between the donor atom and the Sb atom of $SbCl_5$.[10,13] The thermodynamic stability of the 1:1 D-$SbCl_5$ complex is defined by the free enthalpy $\Delta G° = -RT \ln K$, and $\Delta G°$can be used alternatively as a measure of the donor number of a solvent as long as a linear relationship exists between $\Delta G°$ and ΔH.[10,13]

$SbCl_5$ is preferable as a reference acceptor for several reasons, such as: (i) adducts are formed in a 1:1 molar ratio with all donor molecules; (ii) adduct formation leads to a change in the $SbCl_5$ acceptor from a bipyramidal to a distorted octahedral configuration, thus involving similar hybridization energies; (iii) $SbCl_5$ is a very strong acceptor with negligible donor properties, leading to complete adduct formation even with very weak donors; and (iv) the Sb-Cl bonds are not easily broken into oppositely charged fragments.[10,13] Solvents possessing higher donor strengths are designated with higher donor numbers, and solvents with less donor strength are given smaller donor numbers. For instance, benzene has a donor number of 0.1, whereas ammonia has been assigned a donor number of 59.

Mayer et al. developed an empirical parameter for the acceptor properties of solvents that is based on the ^{31}P-NMR chemical shift observed in triethylphosphine oxide (Et_3PO) in the respective pure solvent.[10,15] It bases itself on the premise that when the acceptor solvent interacts with a Et_3PO molecule at the basic oxygen atom, the electron density at the phosphorous atom decreases, resulting in an observable downfield chemical shift.[10,15] Hexane is used as a reference solvent to which the acceptor number of zero has been assigned. To emphasize the relationship between acceptor properties and conjugate donor properties, $SbCl_5$ in DCE is used as a standard for both parameters (AN and DN) and it is arbitrarily assigned an AN of 100.[10,15] Therefore, the acceptor number (AN) is defined as a dimensionless number related to the relative chemical shift (δ) of ^{31}P in Et_3PO in a particular solvent, with hexane as a reference solvent assigned an AN of 0 and $Et_3PO{\bullet}SbCl_5$ in 1,2-dichloroethane to which the acceptor number of 100 has been assigned.[10,15] In general, solvents that have little or no interactions stemming from inherent Lewis acid characteristics with the basic oxygen of the Et_3PO molecule, such as hexane, are designated as having a low acceptor number and solvents that interact more strongly with the Et_3PO molecule are given a higher AN on a scale from 0–100.

It is important to consider both the donor number as well as the acceptor number when considering and interpreting coordinating interactions in solutions. Referring back to the fact that $FeCl_3$ dissolves in diethyl ether, which has a dielectric constant less than that of chloroform in which $FeCl_3$ does not dissolve, it may be interpreted that the donicity (Lewis basicity) of diethyl ether is the contributing factor influencing the solubility of ferric chloride. In fact, diethyl ether has a DN of 19.2, whereas chloroform has negligible Lewis base characteristics.

2.1.3 State of Iron(III) Chloride in Nonaqueous Solvents

It has been shown that the state of iron(III) chloride in nonaqueous solvents is dependent on the physical properties of the solvent in which it is introduced.[16-24] Evidence from studies using electron spin resonance (ESR) and ultraviolet-visible spectroscopy (UV-Vis) reveal that iron(III) chloride exists in the dimeric form ($Fe_2Cl_5^+$) in solvents of low dielectric constant and weak Lewis basicity.[25] Likewise, these reports indicate that $FeCl_3$ exists in a solvated monomeric form ($FeCl_2^+$) in solvents of high dielectric constant and strong Lewis basicity.[25] Nonetheless, the physical state of iron(III) chloride in various nonaqueous solvents, and especially the equilibrium associated with its solvation, is a complicated matter that is still not fully understood. Still, it is accepted that there are two different species of iron(III) chloride that may exist in nonaqueous solvents depending on the nature of the solvent employed. These species are represented in Equations 2.1 and 2.2.[16]

Equation 2.1 $2FeCl_3 \longrightarrow FeCl_2^+ + FeCl_4^-$ or

Equation 2.2 $2FeCl_3 \longrightarrow Fe_2Cl_5^+ + FeCl_4^-$

The production of the tetrachloferrate anion ($FeCl_4^-$) is indicative of the monomeric species and its presence has been attributed to interactions with solvents having high dielectric constants.[20] However, Vertes et al. have indicated by means of Mössbauer spectrometry that the

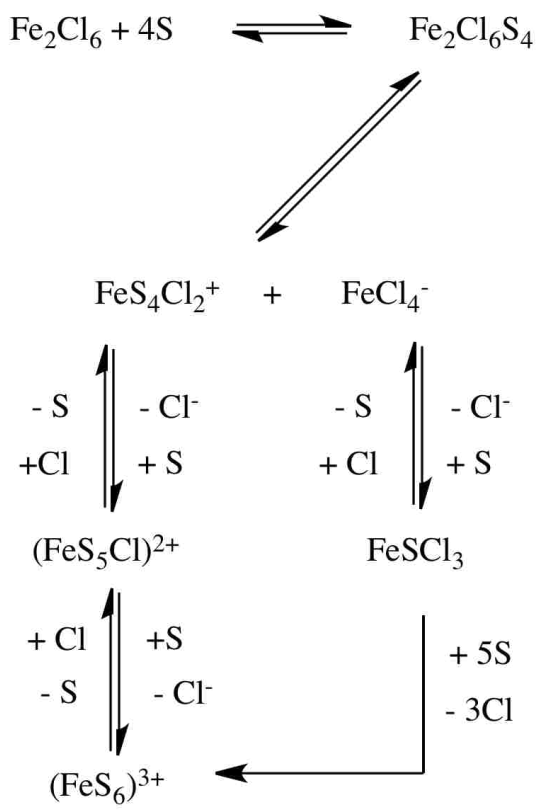

Figure 2.1 Illustration of a general scheme by which $FeCl_3$ may undergo autocomplex formation in various nonaqueous solvents. Adapted from Vertes et al., 1978.

dimeric species of iron(III) chloride is also present in polar solvents, such as nitromethane.[22] Furthermore, Fajer et al. and Work et al. have reported the presence of monomeric species in solvents of low polarity, such as benzene, by means of infrared spectroscopy.[17,23] Therefore, to reason that one species or the other exists in solution depending on the nature of the solution dramatically oversimplifies the scenario.

Thus, it further stands to reason that in any given nonaqueous solvent both species of iron(III) chloride exist to some extent and within the system exists a complicated equilibrium of ferric chloride species, whose population distribution is dependent on the exact physical properties of the solvent employed. In fact, Drago et al. reported that solvents possessing greater donicity (Lewis basicity) impart more chloride dissociation from $FeCl_3$ than solvents with less donor strength and charge separation is facilitated by solvents having higher dielectric constants, while it is inhibited by those solvents possessing low dielectric constants.[19] It thus becomes clear that all three properties of solvents under investigation–dielectric constant, donor number, and acceptor number–play a role in controlling the distribution of species residing in solutions or mixtures of iron(III) chloride in nonaqueous solvents.

Gutmann clarified that this equilibrium is far more complicated when the substrate ($FeCl_3$) possesses more than one ionizable bond, and in particular when anions are formed that

compete with the donor molecules for coordination of the substrate.[10] He went on to further explain that if the donor properties of the competing ligands are not vastly different both complex cations and complex anions are formed simultaneously, resulting in autocomplex formation.[10] Gutmann described this autocomplex formation in Equation 2.3, which can be divided into two competing steps for the formation of complex cations and complex anions as described in Equations 2.3.1 and 2.3.2; in these equations M is the metal substrate, X is the salt of the metal, and D is a molecule of donor solvent.[10] Gutmann added that in a strong donor solvent a solute will undergo autocomplex formation if the M-X bond is not easily ionized, whereas in a weak donor solvent a compound which is easily ionized will give autocomplex ions.[10] Vertes et al.[22] illustrated a general scheme by which $FeCl_3$ may undergo autocomplex formation in various nonaqueous solvents, which has been adapted and shown in Figure 2.1, where S denotes a solvent molecule.

Equation 2.3 $$n\mathrm{D} + 2\mathrm{MX} \longleftrightarrow \mathrm{D}_n\mathrm{M}^+ + \mathrm{MX}_2^-$$

(i) Formation of a complex cation:

Equation 2.3.1 $$n\mathrm{D} + \mathrm{MX} \longleftrightarrow \mathrm{D}_n\mathrm{M}^+ + \mathrm{X}^-$$

(ii) Formation of a complex anion:

Equation 2.3.2 $$\mathrm{X}^- + \mathrm{MX} \longleftrightarrow \mathrm{MX}_2^-$$

2.2 Methods and Materials

2.2.1 Chemicals

Solvents employed for the purposes of polymerization and analytical characterization of P3HTs were either chromatographic or reagent grade, and were used as received unless noted otherwise. Once opened, solvents used for polymerization and characterization were stored over activated molecular sieves (4Å, 8–12 mesh, beads, Fisher Chemical) and degassed with argon for one hour prior to use. 3-*n*-hexylthiophene monomer was purchased from Sigma-Aldrich

(#399051, 99%) and distilled under vacuum prior to use. Ferric chloride was purchased from Sigma-Aldrich (#451649, anhydrous, powder, ≥99.9%, trace metal basis) and was opened under argon in a glove bag, then stored under argon in a dessicator. Matrices employed for MALDI-ToF-MS analysis were either 2,2':5',2''-terthiophene or *trans*-2-[3-(4-tert-butylphenyl)-2-methyl-2-propenylidine]malonitrile (DCTB). Both matrices were purchased from Sigma-Aldrich (#311073, 99%, and #727881, ≥98% respectively) and used as received.

2.2.2 Synthetic Methods: Chemical Oxidation of 3-Hexylthiophene

Polymerizations were carried out according to previously reported procedures in the literature for chemical oxidative polymerization of thiophenes and pyrroles[1,6,26] with some modifications. The reactions were performed in a 250mL round bottom flask (RBF). The solvents employed varied depending on their physical properties for the individual experiments. The molar ratio of oxidant-to-monomer remained constant, at 1:1 throughout all polymerizations. Oxidant-to-monomer ratios employed for these polymerizations are small compared to those used for typical oxidative polymerizations of P3ATs found throughout the literature. This was done to minimize excess chlorination to the polymer from the oxidant in order to better observe the effect that various solvents have on these processes. It has been shown that the oxidant-to-monomer ratio directly impacts the extent of chlorination to P3HTs and by decreasing the oxidant-to-monomer ratio the amount of chlorination to P3HTs can be somewhat decreased.[6] However, using a low oxidant-to-monomer ratio does kinetically hinder the reaction, which decreases the yields of polymer produced in the time frame of the reaction. 3-*n*-hexylthiophene was purified prior to experiments, via vacuum distillation. Iron(III) chloride consistently remained under a blanket of argon from the moment it was opened as received from the supplier. All solvents used were degassed with argon for a period of one hour prior to the reactions.

First, an oxidant solution or suspension, depending on the nature of the solvent, was prepared by the addition of 162.2 mg (1.0 mmol) of iron(III) chloride into 12.5 mL of a given solvent. The mixture was allowed to stir for one hour at room temperature under a blanket of argon. A monomer solution was prepared by the addition of 168.3 mg (1.0 mmol) of 3-*n*-hexylthiophene to 12.5 mL of the same solvent used for preparation of the iron(III) mixture. This was allowed to stir at room temperature under argon for one hour. The monomer solution was then cannulated into the stirred oxidant mixture under argon. The reaction was then allowed to proceed for one hour, while stirring at room temperature under a blanket of argon.

After one hour, the reaction was quenched by the addition of 200 mL of anhydrous methanol and allowed to stir at room temperature under argon for 24 hours; during which time the polymer is reduced and precipitates out of solution. The solid polymer was then thoroughly separated by vacuum filtration and rinsed well with methanol in order to remove residual $FeCl_3$. The solid polymer was then redissolved in 250 mL of chloroform. The polymer solution in chloroform was next washed three times in a separatory funnel with 250 mL 2.0 N HCl. The chloroform was then rotary-evaporated to leave a thin, reddish-violet film of polymer that was then vacuum-dried to constant-mass overnight.

In the above procedure, polymer that remained soluble after quenching with 200 mL of anhydrous methanol and therefore residing in the filtrate following vacuum filtration was not used for the characterization of experimental effects on P3HTs formed by chemical oxidation. Previous studies employed a method where soluble and solid portions of materials produced in this matter were combined during the chloroform extraction and subsequent washing stages of the procedure, which were then analyzed together.[6] Nonetheless, it has been revealed in this work that the soluble portion of the polymerized material formed by chemical oxidation with ferric chloride using nitromethane as a solvent is solely comprised of small oligomers with repeat

units of n = 5, 6, and 7 having hydrogen endgroups [H-($C_{10}H_{14}S)_n$-H]. These oligomers were shown to be highly defective, with regioregularities of ~26%. The soluble portion comprised roughly ~20% of the total yield for these polymers when soluble and solid portions are mixed. The solid polymer portions still contain a large population of these oligomers, as seen by MALDI-ToF-MS, which have predominantly hydrogen end groups, but also a limited population of oligomers having one hydrogen and one chlorine endgroup [H-($C_{10}H_{14}S)_n$-Cl].

The reasons that some of these small oligomers remain in solution while others do not is still not fully understood. Although, it is likely that such small oligomers found in solid fractions of polymer are sequestered within larger oligomer and polymer chains during precipitation. Because endgroup analysis by MALDI-ToF-MS can only be performed by examination of oligomers in a m/z range where isotopic resolution is achieved, and mass discrimination and resolution are dependent on populations of ions encountering the detector (saturation), it was decided that soluble materials would not be included in the overall evaluation for polymers formed by manipulation of the experimental parameters. Furthermore, the extreme regioirregularity of the isolated soluble materials is thought to not be representative of those found in solid material.

2.3 Characterization

2.3.1 Endgroup Analysis

Endgroup analysis of poly(3-hexylthiophene)s was done by use of matrix-assisted laser desorption/ionization time-of-flight mass spectrometry (MALDI-ToF-MS). Some perspective of the use of MALDI-ToF-MS for the characterization of synthetic and conducting polymers has been discussed in Sections 1.3.1 and 1.3.3. Some limitations of MALDI-ToF-MS have also been discussed in Section 1.3.2. MALDI-ToF-MS has become an essential tool for the characterization of synthetic polymers because it has the ability to detect large polymers and

biomolecules with limited fragmentation, as well as generally imparting single charges to such molecules when compared to other methods of ionization used for mass spectrometric analysis.[27]

Preparation of the analyte sample for examination via MALDI-ToF-MS involves mixing a dilute analyte with a concentrated matrix solution, usually in a 1:100–1:1,000 molar ratio. The matrix serves to absorb energy from the incident laser beam and then impart this energy to the analyte in the mixture. It may also help to crystallize the analyte in a preferential manner, which assists in desorption of the analyte into the gas phase. In the gas phase, the matrix also assists in the ionization of the analyte within the MALDI desorption plume, which will be discussed shortly. The analyte/matrix mixture can be prepared on the MALDI plate or target–that serves as the desorption platform at which the incident laser beam is directed–in several ways. Sample preparation can be done via two variations of the dried-drop method that is used for these studies. The first variation involves a drop (~1–2 μL) of matrix mixture being applied to the MALDI target that is allowed to dry, followed by a drop (~1–2 μL) of analyte being placed on top of the dried matrix and then being allowed to dry. The variation of the dried-drop method employed for these studies involves mixing the analyte and matrix mixtures together, then spotting a 1–2 μL drop onto the MALDI target and allowing the spot to dry.

The exact nature of the ionization mechanism involved in the ion formation process of MALDI-ToF-MS is still not fully understood. However, three categories for ion formation are agreed upon in the literature and these include proton-transfer, cation adduction (by use of metal salts), and electron-transfer. Proton-transfer ionization is typically observed in the MALDI-ToF-MS analysis of peptides, and proteins. As mentioned in Section 1.3.1, cationization is the most commonly seen ionization pathway for detection of synthetic polymers.[28,29] Still, electroactive compounds having low ionization energies can also form molecular radical cations due to electron-transfer reactions between the analyte sample and the matrix.[30,31] Furthermore, electron-

transfer has been shown to be the pathway of ion formation during MALDI-ToF-MS for electrically conducting polymers, such as poly(3-alkylthiophene)s.[32,33] Still, this pathway for ion formation of P3HTs was confirmed in these experiments by the use of internal standards, and verified by the production of molecular radical cations ($M^{\bullet+}$) in the observed MALDI-ToF mass spectra.

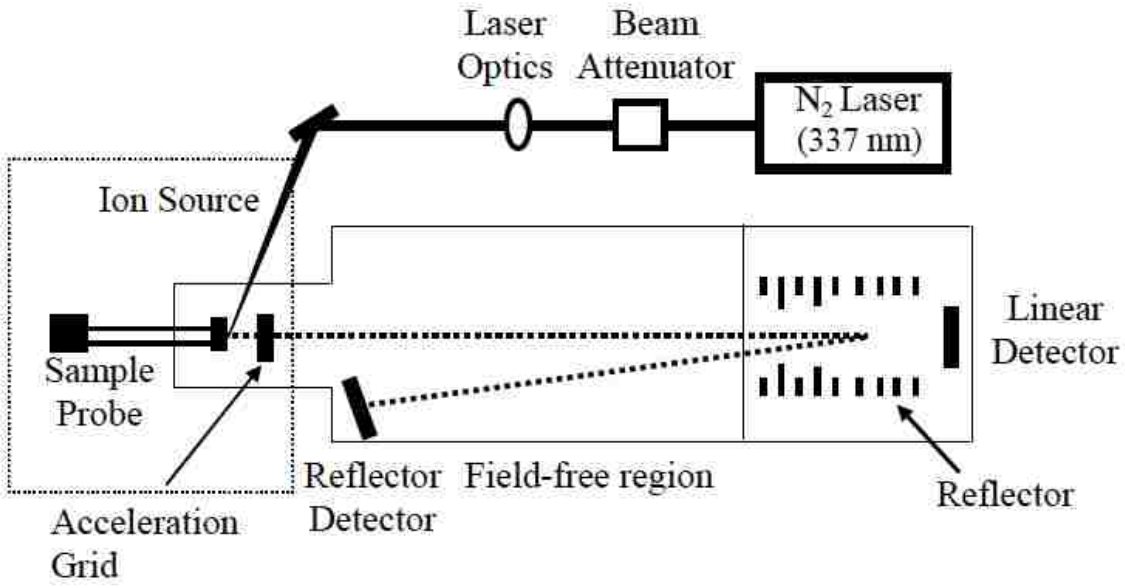

Figure 2.2 Diagram of a generic MALDI-ToF mass spectrometer with linear and reflectron detectors. Adapted from Dass, C., 2001.

A complete description of the mechanics and physics of the MALDI-ToF mass spectrometer has been described elsewhere.[28,34,35] The basic schematic diagram of a typical MALDI-ToF mass spectrometer with an ion reflector is shown in Figure 2.2. Once the MALDI target has been prepared with the dried sample and then placed into the instrument, the target source containing the sample is brought to a low pressure (~10^{-6} torr) matching that of the flight tube of the instrument. A pulsed laser beam, in this case a 337-nm nitrogen laser, is focused and directed through a series of electric lenses and mirrors onto the analyte/matrix mixture that is spotted on the sample target. The laser power is typically adjusted to a point just above the

threshold necessary in order to obtain a viable ion signal, because reports show that signal-to-noise ratios begin to decline at powers of 20% above this threshold.[28,36] Higher laser powers have also been shown to cause dimerization and cluster formation of polymers that can be responsible for increasing shifts in molecular weight distributions.[37] The incident beam ablates and vaporizes the sample/matrix mixture into a hot, very chemically reactive, gas-phase plume. Primary ions are formed during the laser pulse or within the excited state lifetime of the matrix (a few nanoseconds).[38,39] However, in the plume reactions between ions and neutrals will continue as long as there are collisions.[38]

Ions remaining in the MALDI plume are then focused and accelerated into the flight tube of the mass spectrometer by application of a voltage potential. Ideally, they are accelerated and enter the flight tube having consistent kinetic energies, where they are left to travel in this field-free region. Ions in the field-free region are separated by the premise that larger molecular ions travel more slowly than smaller molecular ions and therefore are differentiated by their velocities. However, the velocity of a given ion is also influenced by its mass-to-charge (m/z) ratio, where additional charges impart additional velocities to molecular ions of identical mass upon voltage acceleration. Given these facts, the time it takes for a molecular ion to travel the distance of a flight tube of a known length may be used to determine the molecular weight of that material. This relationship is shown in Equation 2.4, where t is the time required for the ion to transverse the flight tube, L is the length of the flight tube, v is the velocity of the ion, m is the mass of the ion, z is the charge associated with the ion, and V is the accelerating potential. In order to calibrate the instrument for correct analysis of m/z for the analyte, standards having known masses, such as peptide standards, are analyzed prior to characterization of the analyte.

Equation 2.4

$$t = \frac{L}{v} = L\left(\frac{m}{2zV}\right)^{\frac{1}{2}}$$

The mass resolution of ions detected in linear mode–meaning after a straight, single flight down the length of a flight tube–can be limited. This is due to the fact that although ions are ideally accelerated with potentials that are meant to impart constant kinetic energies, similar ions do not always enter the field-free region with similar, consistent properties. Ions may be formed in different locations within the MALDI plume (spatial issues), or they may be formed at differing times (temporal issues), and they may be formed having different vectors of velocity, as well as being formed with differing initial kinetic energies.[28] In order to overcome these issues, MALDI-ToF mass spectrometers have been developed with reflectors, otherwise known as reflectrons.

A reflectron is composed of a series of electrical lenses that have increasing repelling potentials and it is located at the linear end of the flight tube. The instrument can then be used in one of either two spatial modes. The linear mode allows analyte ions to travel from the source directly to the opposite end of the flight tube to be detected at the linear detector (cf. Figure 2.1) and this mode is preferable for the detection of higher weight materials; However, there are limitations in mass resolution.[35] The instrument can also operate in the reflectron mode, wherein the traveling ions that have been accelerated at the source enter the reflectron mirror at the end of the flight tube. They are consequently slowed down within the reflectron field where they come to a stop and are redirected by the reflectron voltage back into a field-free drift zone again, and then detected at the reflectron detector (cf. Figure 2.1). The initial separation of these ions in the first drift zone, their reacceleration by the reflectron mirror, and subsequent further separation in the second drift zone accounts for the far greater resolution that is achievable in this mode. The reflectron mirror is helpful in overcoming the spatial, temporal, and kinetic issues created at the source of the instrument because it compensates for differing kinetic energies and velocities of ions having similar masses and allows for these isomass ions to reach the reflectron detector at

the same time, which allows better resolution; this mode is not preferable for detection of large molecular weight materials.[35]

The MALDI-ToF-MS analysis of synthetic and conducting polymers has been further discussed in Section 1.3 along with some limitations of MALDI-ToF-MS for this purpose. This method of analysis is employed in these studies for the verification of endgroup (α-) and backbone (β-) additions to the chains of P3HTs formed by chemical oxidative polymerization. To reiterate though, if the exact chemical composition of the repeat unit comprising the polymer chain is unknown, then it may be determined through examination of the mass spectrum of that polymer in the mass-to-charge (m/z) range where the oligomers are sufficiently resolved. By subtracting the m/z of an oligomer immediately preceeding (M_{olig1}) the m/z of the oligomer immediately following the preceeding (M_{olig2}) the molar mass of the repeat unit (M_{rep}) can be correctly established (i.e. $M_{rep} = M_{olig2} - M_{olig1}$). This is assuming that all ionization events or reactions–such as cationization, protonation, or electron loss–are equivalent between the two. Likewise, if the molar mass of the repeat unit is known, then the molar mass of an endgroup or other addition can be simply determined. The molar mass of the endgroup (M_{end}) is calculated by considering the molar mass of a signal peak (M_{peak}) and subtracting the molar mass for the given number of cations (nM_{cat}) involved in ionization of the analyte (or anions, or electrons for negative mode evaluation), as well as the molar mass for the number of repeat units (nM_{rep}) comprising the oligomer.[40] This idea is further clarified in Equations 1.4 and 1.5.

2.3.2 Molecular Weight Analysis

Molecular weight measurements were done by means of gel-permeation chromatography (GPC), also referred to as size-exclusion chromatography (SEC), using a multiangle laser light scattering (MALLS) detector in conjunction with a differential refractive index (DRI) detector. MALLS, and light scattering in general, is a method that is sensitive to not only the

concentration of a material but also the size or hydrodynamic volume of the material and it can be used to determine the weight-average molecular weight (M_W) of a material (cf. Section 1.3.1 and Equation 1.2). The DRI detector is solely a concentration detector and it is used for the determination of the number-average molecular weight (M_N) of a material (cf. Section 1.3.1 and Equation 1.1). These values enable the calculation of the molecular weight distribution or polydispersity index (*PDI*) of a sample (cf. Equation 1.3). The use of a DRI detector in conjunction with a MALLS detector also enables the determination of hydrodynamic volumes for analyte samples without calibrating the instrument with a molecular weight standard.

SEC is the most widely utilized method for the determination of molecular weights for synthetic polymers due to its convenience and high throughput. SEC separates materials in solution based on their hydrodynamic volumes. The analyte is thoroughly dissolved in an appropriate solvent and passed through a column packed with small (~10 μm diameter) porous beads made of silica or polymer blends through which the solvent and analyte may freely diffuse. Higher molecular weight material that cannot interact within the small (50 Å–10^6 Å) pores, elutes first within the void volume (V_0) of the column (i.e. the volume of effluent found between the packing material). Lower weight materials that can interact with the pores of the beads elute at later times, an effect that is dependent on analyte size (i.e. the smaller the molecular volume of the analyte, the longer it will interact with the packing material). Analyte that is small enough to diffuse freely within the pores of the packing material elutes last and may interact with the entire pore volume (V_i) of the beads. Thus, the elution volume of the smallest molecules may require the total volume ($V_t = V_0 + V_i$) of the mobile-phase within the column. Thus the retention volume (V_R) for a specific molecular weight species is dependent on the extent to which it entropically interacts with the packing material and enthalpic interactions are not suppose to play a role in the separation of materials by molecular volume by this means.

As noted, DRI detection is a colligative means of detection. That is, it measures the concentration of a material based on empirically-determined, concentration-dependent changes in refractive index called the specific refractive index increment, SSRI, also known as the $\delta n/\delta c$. Historically, the use of this method of detection–or any other colligative means of detection, such as ultraviolet-visible absorption (UV-Vis) spectroscopy–solely by itself for the determination of weight-average molecular weights, M_W, using SEC required that the instrument be calibrated with a standard of known and distinct molecular weight in order for the estimation of hydrodynamic volumes to be made. Differences in the physical conformation of the standard can impart error in the correct determination of molecular volumes of the analyte if the physical conformation of the analyte varies greatly from that of the standard. This has been reported to be the case for poly(thiophene)s. Typically, calibrations are made using poly(styrene) that has a randon coil or spherical conformation. Whereas poly(thiophene)s and other conducting polymers have been reported to have a rigid-rod conformation.[33,41,42] For this reason, molecular weights of poly(thiophene)s tend to be overestimated when determined by use of poly(styrene) calibration standards in conjunction with concentration-based detection methods alone.

Therefore, MALLS detection is employed along with DRI detection in order to make molecular weight determination possible without the need for calibration of the instrument with standard material. Multiangle laser light scattering is a commonly employed technique to assess the molecular mass of an analyte by detecting how that analyte scatters incident light. The collimated light source in MALLS is generated using a laser and it is passed through a cell containing the solvent and solute. In general, light scattering is based on the fact that the incident light induces a dipole within the analyte that is then released as an electromagnetic wave of the same frequency as the incident light. The ratio of the intensity of emitted light in excess to that of the solvent is termed the Rayleigh ratio (R_θ). The molecular weight of the material is in

turn calculated using data for the concentration of analyte at a given time determined by DRI using the empirically measured SSRI ($\delta n/\delta c$) of the material. The relationship between these factors and molecular mass is explained in Equation 2.5.[43]

Equation 2.5

$$\frac{R_\theta}{Kc} = M_W P(\theta) - 2A_2 M^2 P^2(\theta) c$$

Equation 2.6

$$K = \frac{4\pi^2 n_0^2}{N_A \lambda_0^4}\left(\frac{\delta n}{\delta c}\right)^2$$

In Equation 2.5, R_θ is the Rayleigh ratio, K is the optical constant that is in part determined by the SSRI and concentration information obtained via the DRI detector and it is defined in Equation 2.6.[43] Furthermore, c is the concentration of the species scattering light, M_W is the molecular weight, $P(\theta)$ is the form factor of the scattering function that relates the variation in angular scattering intensities with the mean-square-radius of the analyte. A_2 is the second viral coefficient, a thermodynamic measure of solvent-solute interactions that can often be assumed to be negligible due to the relatively low concentration of analyte found within SEC fractions.[43] In Equation 2.6, n_0 is the refractive index for the solvent, N_A is Avogadro's number, and λ is the wavelength of the incident light.[43]

Equation 2.7

$$P(\theta) = 1 - \left(\frac{16\pi^2}{3\lambda^2}\right)\langle r_{rms}\rangle^2 \sin^2\left(\frac{\theta}{2}\right)$$

Equation 2.8

$$\frac{R_\theta}{Kc} = M_W$$

In equation 2.7 is shown the simplification of the form factor, $P(\theta)$, upon the assumption that the scattering angle is low or the mean-square-radius is negligible compared to the wavelength of incident light.[43] In Equation 2.7, λ is the wavelength of incident light, θ is the angle between the incident beam and the scattered light, and r_{rms} is the root-mean-square radius of the analyte. Since the light scattering measurements are taken at multiple angles, the Rayleigh

ratio R_θ may be extrapolated to an angle of zero and Equations 2.5 and 2.7 can be combined and simplified to Equation 2.8.[43] Thus, the molecular weight of the analyte can be readily calculated.

2.3.3 Determination of Regioregularity

The pattern of coupling between monomers of 3-*n*-hexylthiophene by means of chemical oxidative polymerization, called regioregularity, has been discussed in Section 1.2.3. The regioregularity of P3ATs has a marked impact on the materials electrical and optical properties, as has been outlined in depth throughout Chapter 1. The analytical method for the determination of the materials presented here is ^{1}H-NMR. With this technique, the integration and comparison of the relative ratio between the signal peaks for the α-methylenes (aryl methylenes) of polymer chains is used for this determination. Signals for these α-methylene peaks are typically present at a chemical shift of $\delta \sim 2.8$, or $\delta \sim 2.6$ if the coupling is regioregular or regiorandom, respectively. The extent of regioregularity is defined as the percentage of the ratio between the two peaks. A more extensive look at this application is found within Section 1.2.4.

2.4 Instrumentation

2.4.1 MALDI-ToF-MS

Mass spectrometric measurements were obtained in part by use of a Bruker OmniFlex MALDI-ToF mass specrometer. The instrument was equipped with a 337-nm nitrogen laser and it is capable of both linear and reflectron time-of-flight detection. The OmniFlex possesses multichannel plate (MCP) detectors with a limit of detection (LOD) of 1 fmol ACTH and is capable of mass resolutions up to 10,000 depending on the *m/z* observed. Measurements were also performed using a Bruker ProFlexx III, which was also equipped with a 337-nm nitrogen laser, MCP detectors with a LOD of 100 fmol ACTH and capable of linear and reflectron detection. The mass resolution of this instrument is up to 8,000 depending on the *m/z* investigated.

The matrices employed for MALDI-ToF-MS inquiries were either terthiophene or *trans*-2-[3-(4-tert-butylphenyl)-2-methyl-2-propenylidine]malonitrile, DCTB. DCTB was used for the majority of the experiments, as far greater signal intensities and signal-to-noise ratios were achieved employing this matrix. Samples were prepared by dissolving the analyte and the matrix in chloroform or methylene chloride. A saturated solution of matrix was prepared in these solvents in matrix:analyte ratios > 1000:1. A small aliquot (~ 2 μL) of analyte sample was added to the matrix solution (~ 4–6 μL) and mixed thoroughly prior to spotting onto the target plate using the dried drop method, where a 1 μL drop of a given sample was spotted on the target plate and allowed to air dry. The instrument was calibrated prior to each measurement using peptide standards (Bruker, #222570) in the molecular weight range of *m/z* 700–3200 for analysis performed in reflectron mode. Internal standards were used for some measurements in order to compare the isotopic measurements obtained experimentally to those of their calculated isotopic mass. The internal standards were oligo(ferrocenyldimethylsilanes), specifically $Fe[Si(CH_3)_2Fc]_3H$, $Fe[Si(CH_3)_2Fc]_5H$, and $Fe[Si(CH_3)_2Fc]_7H$, which were provided by Professor Ian Manners at the University of Toronto. The use of internal standards allowed the verification of electron-transfer as the means of ionization for the observed oligomers of P3HT, as seen in MALDI-ToF-MS (cf. Section 2.3.1). However, internal standards were not used for all experiments after consistent verification of the identity of the species being observed in the mass spectra, as oligo(ferrocenyldimethylsilane)s ionize much more readily than the P3HTs under investigation. Because of their low ionization potentials, there appeared large ionization discrimination of the analyte compared to the internal standards and the use of internal standards was limited.

Bruker's Xmass software was employed in order to calculate the isotopic masses and patterns for oligo(3-hexylthiophene)s having different endgroup (α-) and backbone (β-)

substituents. The calculated patterns were used in conjunction with Equations 1.4 and 1.5 for the determination of α- and β-substituents, and also referred to for mass accuracy determinations. The observed experimental signal intensities (relative abundances) were used as pseudo-N_i measurements and the m/z values were applied as pseudo-M_i measurements for the relative comparison of populations or extent of substitution (cf. Section 1.3.1). Observed experimental signal peaks were designated to be molecular radical cations ($M^{+\bullet}$) as a result of electron-loss ionization, as described in Section 2.3.1.

2.4.2 Size-Exclusion Chromatography (SEC)

Size-exclusion chromatography experiments were performed through the use of an Agilent 1100 series autosampler and isocratic pump system. In some experiments, ultraviolet-visible absorption measurements were taken using a Waters 490E ultraviolet-visible detector (set to 430 nm). Light scattering measurements were obtained with a Wyatt Dawn Heleos (Wyatt Technologies Corporation, Santa Barbara, California) thermostatically-controlled, multiangle laser light scattering (MALLS) detector, with a 50-mW GaAs linearly-polarized laser (658 nm) and a K5 cell. The MALLS detectors were calibrated using toluene and then their signals were normalized with poly(styrene) standards having a distinct monodisperse molecular weight of 30,000 Da prior to experiments. A Wyatt Optilab Rex refractive index detector was used in conjunction with light scattering measurements and it was positioned after the Dawn Helios MALLS detector. The two inline columns that were employed for these purposes were Phenogel columns (30 cm × 7.8 mm) from Phenomenex. Both columns possessed packing material consisting of 10-μm diameter particles. The first column contained a linear bed of packing material having mixed pore sizes in the range of 50–10^6 Å and the second column contained beads with solely 10^5 Å pores. These columns were preceded by a Phenomenex guard (10-μm diameter) guard-column. The solvent employed for the separations was tetrahydrofuran, THF,

that was degassed prior to experiments using helium sparging and/or an inline vacuum degasser. The flow rate of the solvent for these analytical analyses was maintained at 1.0 mL min^{-1} and the injection volume for the investigated samples was 100 μL. The collected data was processed using the Astra V software provided from Wyatt Technologies Corporation.

2.4.3 Specific Refractive Index Increment (SRII) Measurements

Determination of $\delta n/\delta c$ for bulk and fractionated P3HTs was done using the Wyatt Optilab Rex refractive index detector (Wyatt Technologies Corporation, Santa Barbara, California) used for SEC analysis (cf. Section 2.4.1). Measurements were made on a bulk polymer sample at a wavelength of 658 nm and a temperature of 25 °C. The $\delta n/\delta c$ that was determined and employed for these experiments was 0.227.

2.4.4 Proton Nuclear Magnetic Resonance (^{1}H-NMR)

^{1}H-NMR analyses were performed on either a Bruker DPX-400 (400 MHz) or AV-4 (400 MHz) liquid spectrometer. Samples of P3HTs were dissolved in deuterated chloroform ($CDCl_3$) purchased from Sigma-Aldrich for all ^{1}H-NMR experiments.

2.5 Results

2.5.1 P3HTs Formed in Chloroform

P3HTs investigated in this Section were prepared via the procedure outlined in Section 2.2.2 using chloroform ($CHCl_3$) as the solvent medium. Chloroform has historically been the solvent employed for chemical oxidative polymerization of P3ATs without much regard or explanation as to its qualifications for these purposes. Chloroform is a very nonpolar solvent with a dielectric constant of 4.8 at 25 °C (cf. Section 2.1.2). Iron(III) chloride is only slightly soluble in chloroform, remaining for the most part in the solid state, but imparting a slight yellowish tint to the suspension. Chloroform has very strong Lewis acid characteristics and is assigned a Gutmann Acceptor number, AN, (cf. Section 2.1.2) of 23. It has virtually negligible

Lewis base characteristics and therefore has a Guttman donor number, DN, (cf. Section 2.1.2) very near zero. Mass yields of polymer recovered from the preparation of P3HTs formed following the procedures outlined in Section 2.2.2 with chloroform were on the order of ~ 30%. As noted in Section 2.2.2, polymer yields are in general lower than others reported in the literature for the production of P3HTs by this method as a result of the low oxidant-to-monomer ratio used in order to minimize excess chlorination to the materials so as to better recognize the effects solvents have on this process. Mass yields of P3HTs for the purposes of this work were regarded in a relative manner, but mass yields in general were not overly scrutinized in order to account specifically for the extent of chlorination to the materials.

The MALDI-ToF mass spectra observed during the endgroup analysis of these materials indicate the presence of oligomers possessing α-terminal ends consisting of two hydrogens [H-$(C_{10}H_{14}S)_n$-H], as well as oligomers possessing one hydrogen and one chlorine [H-$(C_{10}H_{14}S)_n$-Cl], along with oligomers possessing α-terminal ends consisting of two chlorine atoms [Cl-$(C_{10}H_{14}S)_n$-Cl], where the population of the latter two are comparable to the former, as shown in Figure 2.3. There are also ion peaks indicating the presence of oligomers with 3–4 chloride additions that are indicative of oligomers possessing two chlorinated α-terminal ends and between 1–2 β-substitutions. These oliogmers are observed in greater abundance than the previously mentioned species. The upper spectrum in Figure 2.3 is the MALDI-ToF mass spectrum of oligomers in the range of m/z 0–5300, by use of reflectron mode (cf. Section 2.3.1). There are an abundance of interstitial peaks between those indicated by their repeat units (n = 1,2,3….) that are indicative of molecular radical cations ($M^{\bullet+}$) having α-hydrogen substituents with solely hydrogen-terminated endgroups.

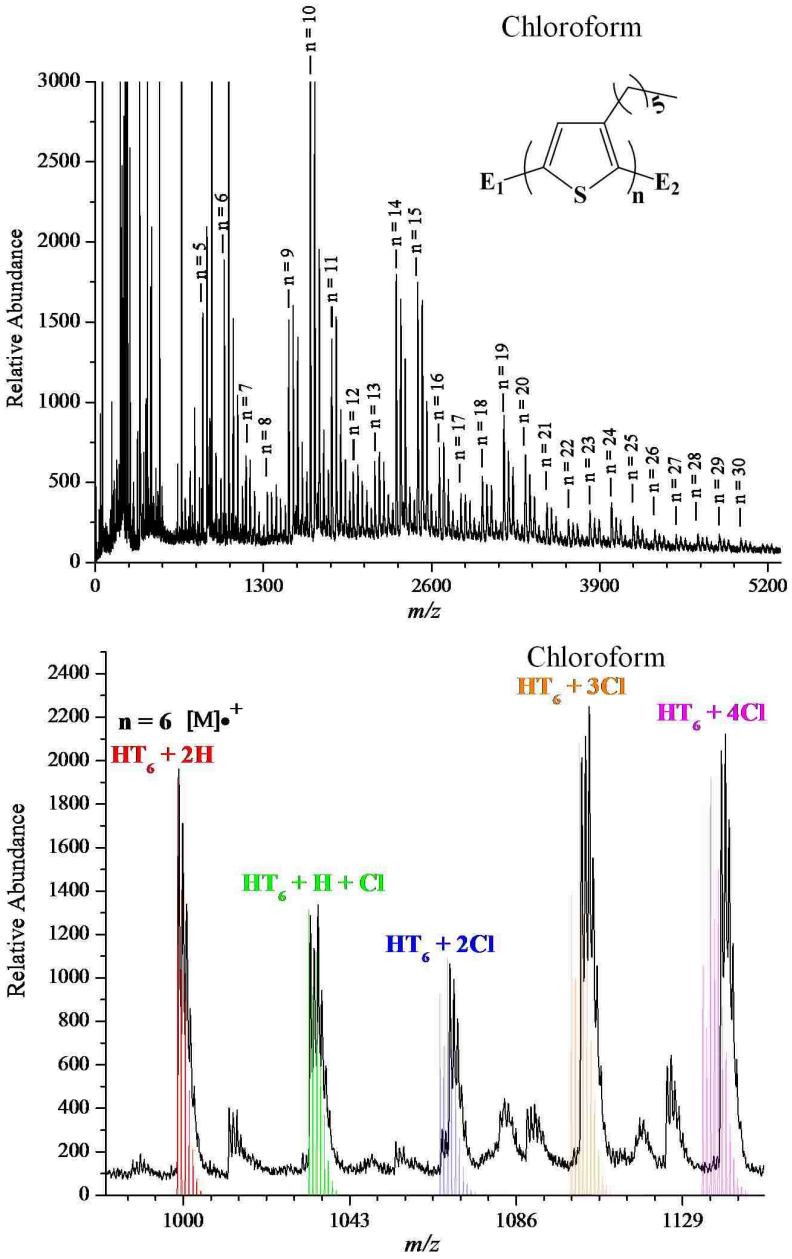

Figure 2.3 MALDI-ToF mass spectra of P3HT formed in chloroform observed by use of reflectron mode (upper). The inset (lower) shows expanded 6-mer region of the spectrum with colored peaks indicating the calculated isotope patterns of the 6-mer having different chlorine additions.

The lower spectrum in Figure 2.3 is an inset to the spectrum for P3HT formed by chemical oxidation with ferric chloride using chloroform as a solvent and focuses on the $M^{\bullet+}$ peak for the oligomer n = 6. The overlays shown in various colors are the calculated isotopic

patterns for the representation of the given species that were produced by the Bruker Xmass software. The calculated peaks are labeled in their respective color denoting the chemical composition of the calculated patterns, where HT_n indicates the repeat unit, which is a 3-*n*-hexylthiophene monomer unit minus 2 hydrogen atoms with a molar mass of 166.3 amu. These are shown in comparison to the experimental peaks observed for the polymer sample in the background. The spectrum shows excellent agreement with oligomers representing the hydrogen terminated molecular radical cation, as well as the ion pattern indicating the presence of oligomers possessing one chlorine termination and one hydrogen endgroup. There is also good evidence shown in this spectrum for the presence of oligomers having 3–4 chlorine additions.

The calculated patterns for oligomers having two or more chlorine additions do show some disagreement with the observed patterns. The differences seen in the calculated and observed patterns for the oligomers containing more than two chlorine additions may be accounted for by the lack of deprotonation during polymerization. The mechanism for nucleophilic addition of chlorine is discussed in Section 1.2.8. Specifically, Qi and Pickup proposed a pathway for the nucleophilic addition of chlorine during electrochemical polymerization of P3ATs where at lower oxidation potentials chlorine may be added to an oligomer chain without deprotonation at the addition site, which rendered the polymer electrically inactive.[44]

The scheme for this nucleophilic addition of chloride is shown in Figure 1.6. This scenario may be the case for oligomers of P3HT formed by chemical oxidation having two or more chlorine additions. This is a reasonable assumption because Qi and Pickup noted that the oxidation potentials for materials having chloride additions after deprotonation by means of overoxidation increased by 0.5 V. Therefore, if the oxidation potential of such oligomers increases after chlorination, it is reasonable to assume that further additions may occur in which

deprotonation does not. The MALDI-ToF mass spectrum in the inset for the 6-mer shown in Figure 2.3 is in good agreement with this hypothesis. Furthermore, this spectrum indicates evidence of more extensive chlorination as shown by the series of convoluted peaks within the recognized peaks, which may be the result of excessive chlorination of oligomers of different repeat units.

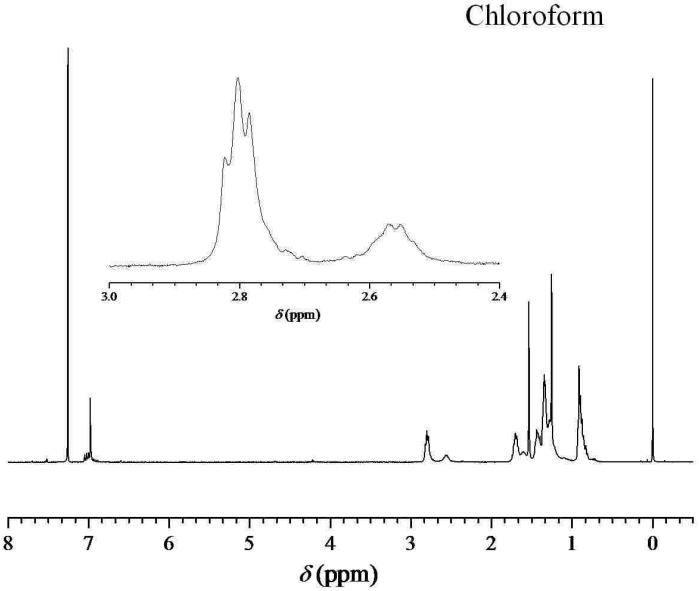

Figure 2.4 ^{1}H-NMR spectrum of P3HT formed in chloroform. The inset shows the α-methylene region used to determine the material's regioregularity of 77%.

The ^{1}H-NMR analysis of P3HTs formed by chemical oxidation with ferric chloride using chloroform is shown in Figure 2.4**.** The inset shows the peaks for signals arising from the α-methylene (aryl methylene) groups found at chemical shifts of $\delta \sim 2.8$ ppm and $\delta \sim 2.58$ ppm, indicating signal response from regioregular and regioirregular material, respectively (cf. Section 1.2.3). The analysis of structural regularity by integration and relative comparison of these peaks is discussed in Section 1.2.4. From integration of the peak found at $\delta \sim 2.8$ ppm normalized as one (1.0) and integration of the peak found at $\delta \sim 2.58$ ppm, which was determined to be 0.30 as compared to the normalized peak, the percentage of the peak at $\delta \sim 2.8$ ppm is found to be 77%

of the combined areas of the two peaks. Therefore, the regioregularity of P3HT formed by this chemical oxidative polymerization (cf. Section 2.2.2) using chloroform as a solvent can be regarded as 77% regioregular material.

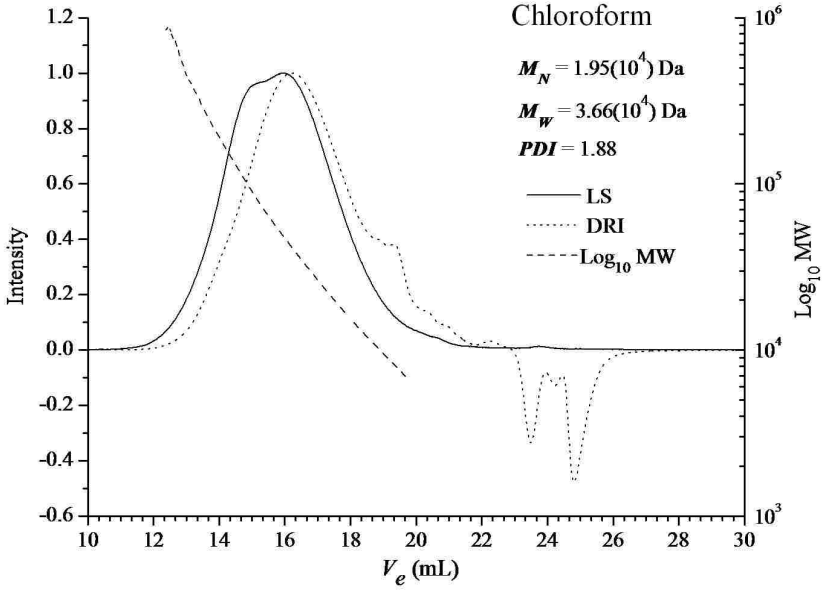

Figure 2.5 Plot of elution volume vs. Log_{10} of molar mass (dashed) and LS (solid) and DRI (dotted) chromatograms of P3HT formed in chloroform.

In Figure 2.5 is shown the chromatogram from the analytical GPC analysis of P3HT formed in chloroform; light scattering (LS) data is represented by the solid line trace, differential refractive index (DRI) data is traced with a dotted line, and the logarithm base 10 of the distribution of molecular weight data is shown by a dashed line. The number-average molecular weight (M_N) for this material as determined from the DRI data is found to be 19,500 Da, and the weight-average molecular weight, M_W, calculated from light scattering (LS) data is 36,700 Da. Thus, the *PDI* for P3HTs formed by oxidative polymerization with iron(III) chloride using chloroform as a solvent is calculated to be 1.88.

2.5.2 P3HTs Formed in Carbon Tetrachloride

P3HTs investigated in this section were prepared via the procedure outlined in Section 2.2.2 using carbon tetrachloride (CCl_4) as the solvent medium. Carbon tetrachloride is a more

nonpolar solvent than chloroform with a dielectric constant at 25 °C (cf. Section 2.1.2) of 2.2. Iron(III) chloride is less soluble in carbon tetrachloride than it is in chloroform, remaining for the most part in the solid state and imparting a very slight yellowish tint to the suspension. Carbon tetrachloride has more than two times less Lewis acid strength than chloroform and is assigned a Gutmann Acceptor number, AN, (cf. Section 2.1.2) of 8.6. Carbon tetrachloride has negligible Lewis base characteristics. Mass yields of polymer recovered from the preparation of P3HTs formed following the procedures outlined in Section 2.2.2 using carbon tetrachloride were on the order of ~ 30%.

The MALDI-ToF mass spectra observed during the endgroup analysis of these materials indicate the presence of oligomers possessing α-terminal ends consisting of two hydrogens [H-$(C_{10}H_{14}S)_n$-H], along with oligomers having one hydrogen, and one chlorine [H-$(C_{10}H_{14}S)_n$-Cl] at the α-terminals, and oligomers possessing α-terminal ends consisting of two chlorine atoms [Cl-$(C_{10}H_{14}S)_n$-Cl], where the population of the latter two exceeds the former as shown in Figure 2.6. The upper spectrum in Figure 2.6 is the MALDI-ToF mass spectrum of oligomers in the range of m/z 0–5300 by use of reflectron mode (cf. Section 2.3.1). The overall ion pattern indicated in the upper spectrum of Figure 2.6 indicates an abundance of interstitial peaks between those of the hydrogen-terminated molecular radical cations, where the trend is observed that oligomers having one chlorine addition are in greater abundance than those with no chlorine additions, and oligomers with two chlorine additions are in greater abundance than those having one chlorine addition. This of course assumes equal ionization efficiency of the different species indicated (cf. Section 1.3.2)

The lower spectrum in Figure 2.6 is an inset to the spectrum for P3HT formed by chemical oxidation with ferric chloride using carbon tetrachloride as a solvent and it focuses on the $M^{\bullet+}$ peak for the oligomer $n = 6$. The overlays shown in various colors are the calculated

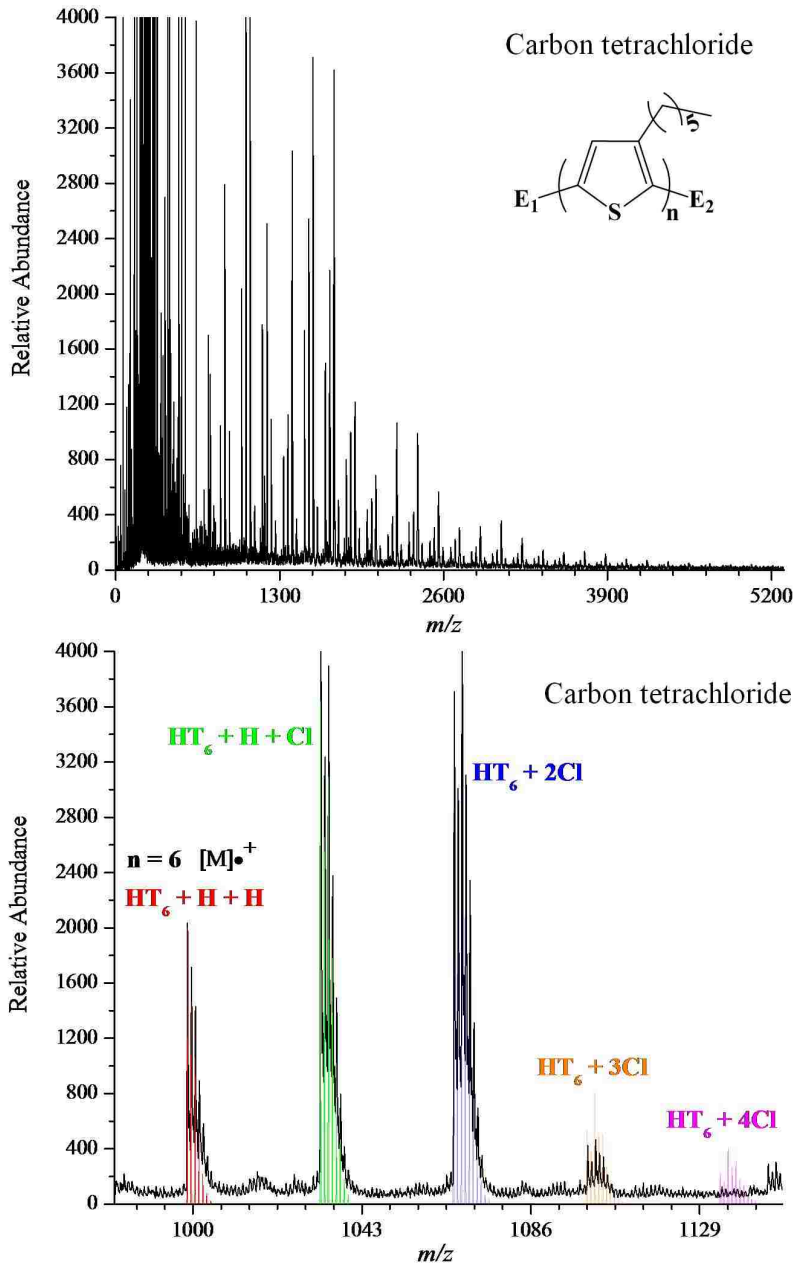

Figure 2.6 MALDI-ToF mass spectra of P3HT formed in carbon tetrachloride observed by use of reflectron mode (upper). The inset (lower) shows expanded 6-mer region of the spectrum with colored peaks indicating the calculated isotope patterns of the 6-mer having different chlorine additions.

isotopic patterns for the representation of the given species, which were produced by the Bruker Xmass software. The calculated peaks are labeled in their respective color denoting the chemical composition of the calculated patterns, where HT_n indicates the repeat unit, which is a 3-*n*-

hexylthiophene monomer unit minus 2 hydrogen atoms and has a molar mass of 166.3 amu. These are shown in comparison to the experimental peaks observed for the polymer sample in the background. The spectrum shows excellent agreement with oligomers representing the hydrogen-terminated molecular radical cation, as well as ion patterns indicating oligomers possessing one chlorine termination, and one hydrogen endgroup. There is also excellent agreement between the calculated and observed ion patterns for oligomers possessing two and three chlorine additions. The extent of chlorination is greater than that seen for polymer formed in chloroform, indicated by the relative abundances of oligomers with one and two chloride additions. The abundance of oligomers with three chlorine additions is minimal compared to the former, although this could be indicative of mass discrimination as a result of instrumental limitations (cf. Section 1.3.2).

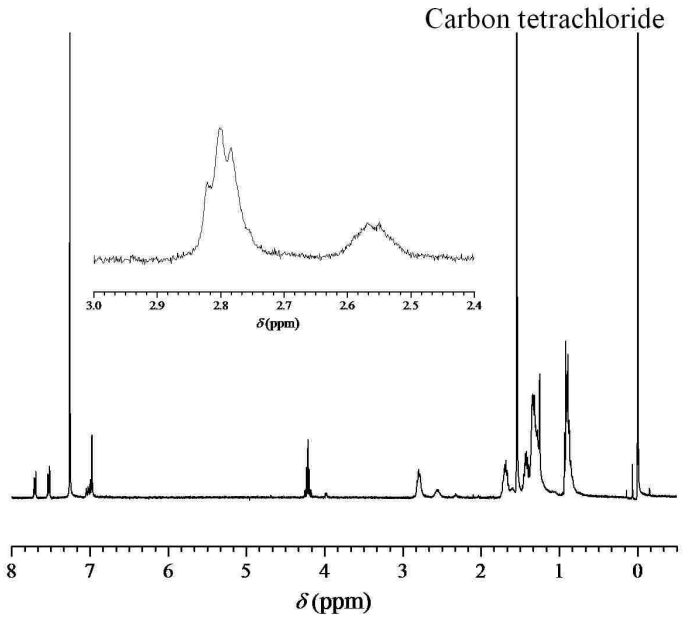

Figure 2.7 ^{1}H-NMR spectrum of P3HT formed in carbon tetrachloride. The inset shows the α-methylene region used to determine the material's regioregularity of 74%.

The ^{1}H-NMR analysis of P3HTs formed by chemical oxidation with ferric chloride using carbon tetrachloride is shown in Figure 2.7. The inset shows the peaks for signals arising from

the α-methylene (aryl methylene) groups found at chemical shifts of $\delta \sim 2.8$ ppm and $\delta \sim 2.58$ ppm, indicating signal response from regioregular and regioirregular material, respectively (cf. Section 1.2.3). The analysis of structural regularity by integration and relative comparison of these peaks is discussed in Section 1.2.4. From integration of the peak found at $\delta \sim 2.8$ ppm normalized as one (1.0) and integration of the peak found at $\delta \sim 2.58$ ppm, which was determined to be 0.35 as compared to the normalized peak, the percentage of the peak at $\delta \sim 2.8$ ppm is found to be 74% of the combined areas of the two peaks. Therefore, the regioregularity of P3HT formed by this chemical oxidative polymerization (cf. Section 2.2.2) using carbon tetrachloride as a solvent can be regarded as 74% regioregular material.

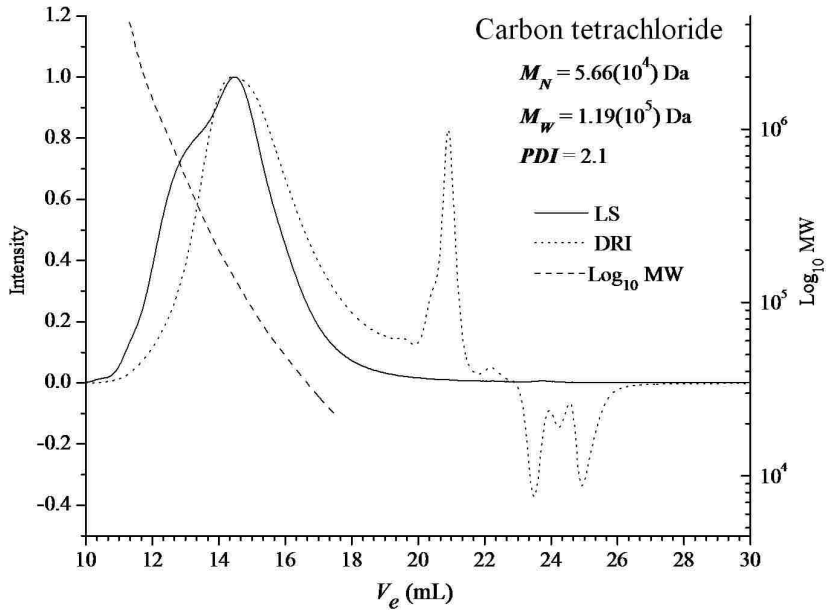

Figure 2.8 Plot of elution volume vs. Log_{10} of molar mass (dashed) and LS (solid) and DRI (dotted) chromatograms of P3HT formed in carbon tetrachloride.

In Figure 2.8 is shown the chromatogram from the analytical GPC analysis of P3HT formed in carbon tetrachloride; light scattering (LS) data is represented with solid line trace, differential refractive index (DRI) data is denoted by a dotted line, and the logarithm base 10 of

the distribution of molecular weight data is shown by a dashed line. The number-average molecular weight (M_N) for this material, as determined from the DRI data, is found to be 56,600 Da, and the weight-average molecular weight, calculated from light scattering (LS) data is 119,000 Da. Thus, the *PDI* for P3HTs formed by oxidative polymerization with iron(III) chloride using carbon tetrachloride as a solvent is calculated to be 2.1.

2.5.3 P3HTs Formed in Methylene Chloride

P3HTs investigated in this section were prepared via the procedure outlined in Section 2.2.2 using methylene chloride (CH_2Cl_2) as the solvent medium. Methylene chloride is more than two times as polar as chloroform with a dielectric constant at 25 °C (cf. Section 2.1.2) of 9.1. Iron(III) chloride is more soluble in methylene chloride than it is in chloroform, although $FeCl_3$ still remains for the most part in the solid state and imparts a slightly more yellowish tint to the suspension than when mixed in chloroform. Methylene chloride has a Lewis acid strength slightly less than chloroform and is assigned a Gutmann Acceptor number, AN, (cf. Section 2.1.2) of 20.4. Likewise, it has negligible Lewis base characteristics and is assigned a DN of 1. Mass yields of polymer recovered from the preparation of P3HTs formed following the procedures outlined in Section 2.2.2 using methylene chloride were on the order of ~ 25%.

The MALDI-ToF mass spectra observed during the endgroup analysis of these materials indicate the presence of oligomers possessing α-terminal ends consisting of two hydrogens [H-$(C_{10}H_{14}S)_n$-H], along with oligomers having one hydrogen, and one chlorinated [H-$(C_{10}H_{14}S)_n$-Cl] α-terminals and oligomers possessing α-terminal ends consisting of two chlorine atoms [Cl-$(C_{10}H_{14}S)_n$-Cl], where the extent of chlorination is relatively comparable to the extent of chlorination observed for material formed in chloroform as shown in Figure 2.9. The upper spectrum in Figure 2.9 is the MALDI-ToF mass spectrum of oligomers in the range of m/z 0–5300 by use of reflectron mode (cf. Section 2.3.1).

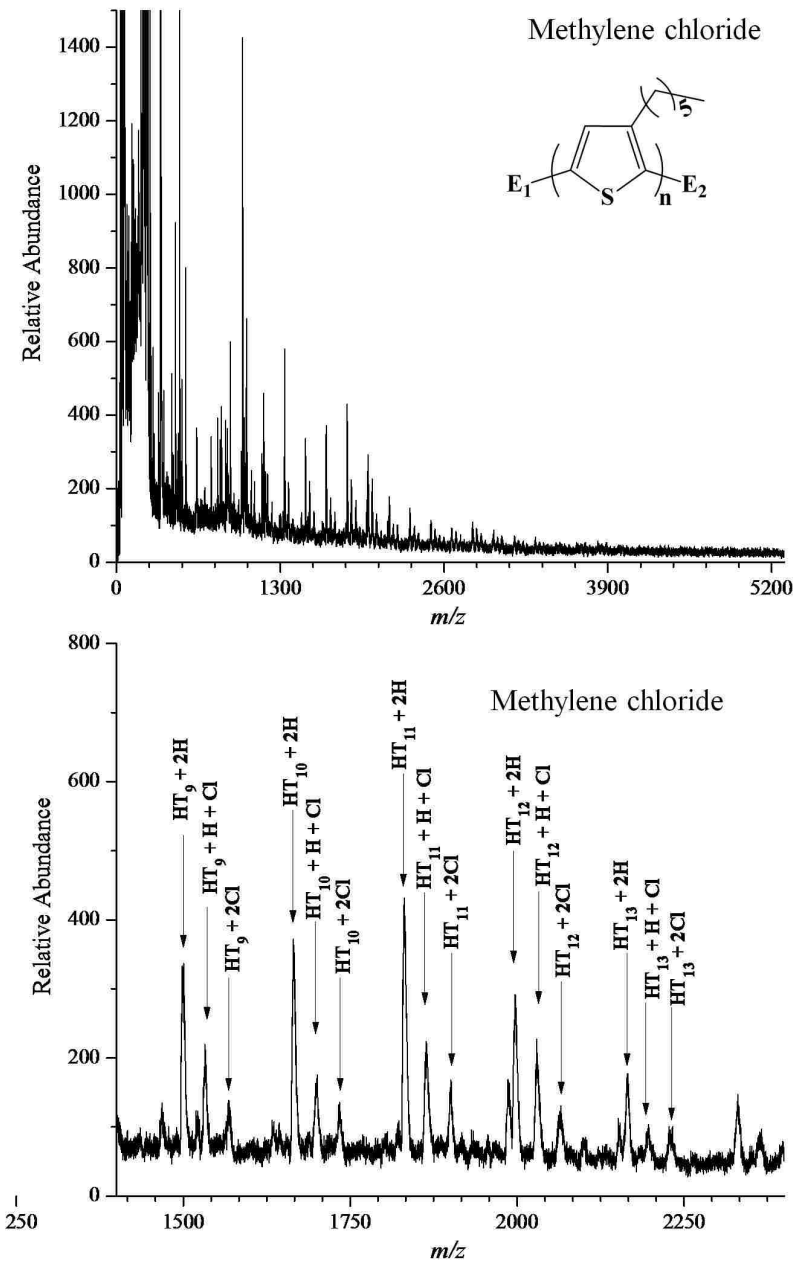

Figure 2.9 MALDI-ToF mass spectra of P3HT formed in methylene chloride observed by use of reflectron mode (upper). The inset (lower) shows the expanded region of the spectrum between *m/z* 1400-2400 with peaks representing oligomers possessing different nucleophilic substitutions indicated with the appropriate endgroup additions.

The lower spectrum in Figure 2.9 is an inset to the spectrum for P3HT formed by chemical oxidation with ferric chloride using methylene chloride as a solvent. Ionization in the given *m/z* range of oligomers was limited and did not produce spectra in which reasonable

resolution was achieved in order to accurately discern the addition of chlorine between oligomers by isotopic patterns. This may have been due to instrumental issues, because the physical characteristics of the polymer produced in methylene chloride did not differ much from those produced in chloroform. The inset shows oligomers ionized in the range of *m*/*z* 1400–2400. The spectrum shows good agreement with oligomers representing the hydrogen-terminated molecular radical cation, as well as ion patterns indicating oligomers possessing one chlorine termination and one hydrogen endgroup, along with oligomers possessing two chlorine additions. The extent of chlorination is comparable to that found in oligomers produced in chloroform as a solvent.

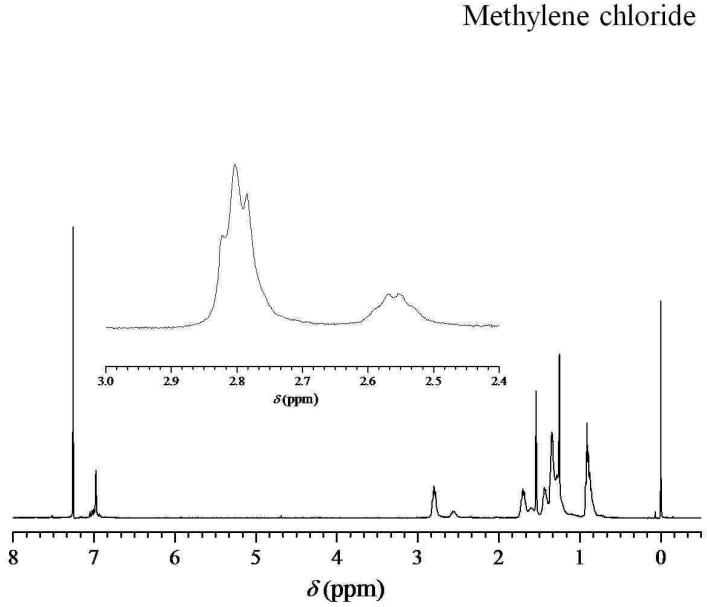

Figure 2.10 ^{1}H-NMR spectrum of P3HT formed in methylene chloride. The inset shows the α-methylene region used to determine the material's regioregularity of 75%.

The ^{1}H-NMR analysis of P3HTs formed by chemical oxidation with ferric chloride using methylene chloride is shown in Figure 2.10. The inset shows the peaks for signals arising from the α-methylene (aryl methylene) groups found at chemical shifts of $\delta \sim 2.8$ ppm and $\delta \sim 2.58$

ppm, indicating signal response from regioregular and regioirregular material respectively (cf. Section 1.2.3). The analysis of structural regularity by integration, and relative comparison of these peaks is discussed in Section 1.2.4. From integration of the peak found at $\delta \sim 2.8$ ppm normalized as one (1.0) and integration of the peak found at $\delta \sim 2.58$ ppm, which was determined to be 0.33 as compared to the normalized peak, the percentage of the peak at $\delta \sim 2.8$ ppm is found to be 75% of the combined areas of the two peaks. Therefore, the regioregularity of P3HT formed by this chemical oxidative polymerization (cf. Section 2.2.2) using methylene chloride as a solvent is regarded as 75% regioregular material.

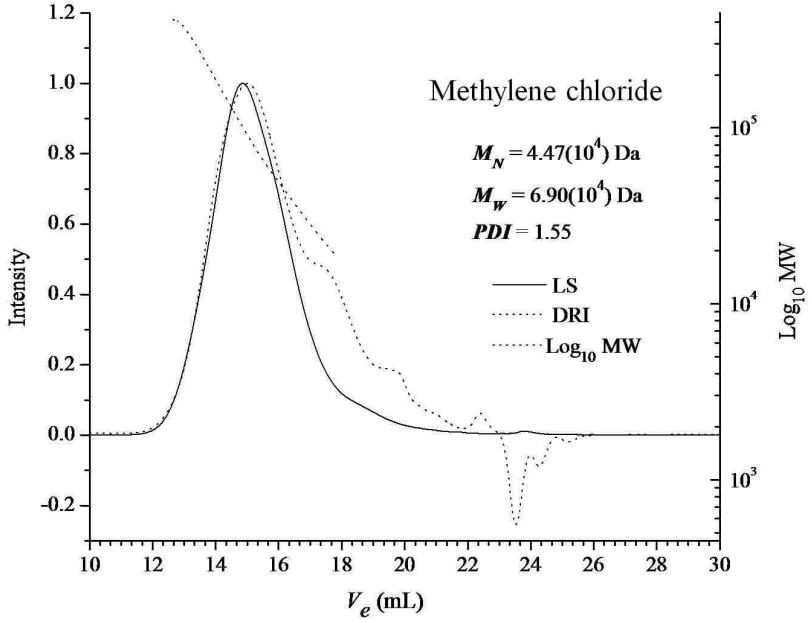

Figure 2.11 Plot of elution volume vs. Log_{10} of molar mass (dashed) and LS (solid) and DRI (dotted) chromatograms of P3HT formed in methylene chloride.

Figure 2.11 shows the chromatogram from the analytical GPC analysis of P3HT formed in methylene chloride; light scattering (LS) data is represented by the solid line trace, differential refractive index (DRI) data is traced with a dotted line, and the logarithm base 10 of the distribution of molecular weight data is shown by a dashed line. The number-average molecular weight (M_N) for this material as determined from the DRI data is found to be 44,700 Da and the

weight-average molecular weight calculated from light scattering (LS) data is 69,000 Da. Thus, the *PDI* for P3HTs formed by oxidative polymerization with iron(III) chloride using methylene chloride as a solvent is calculated to be 1.55.

2.5.4 P3HTs Formed in 1,2-Dichloroethane

P3HTs investigated in this section were prepared via the procedure outlined in Section 2.2.2 using 1,2-dichloroethane, (DCE, $C_2H_4Cl_2$) as the solvent medium. DCE is more than two times as polar as chloroform with a dielectric constant of 10.4 at 25 °C (cf. Section 2.1.2). Iron(III) chloride is more soluble in DCE than it is in chloroform and comparable in solubility as when added to methylene chloride, remaining for the most part in the solid state and imparting slightly more yellowish tint to the suspension as compared to chloroform. DCE is used as a reference, with antimony (V) chloride, for empirical determination of Guttman acceptor numbers and has arbitrarily been assigned an AN of 100 in that state (cf. Section 2.1.2) and is considered to have strong Lewis acid characteristics. It is also used as a supporting medium for determination of Guttman donor numbers (cf. Section 2.1.2) and is regarded as having negligible Lewis base strengths. Mass yields of polymer recovered from the preparation of P3HTs formed following the procedures outlined in Section 2.2.2 using DCE were on the order of ~ 30%.

The MALDI-ToF mass spectra observed during the endgroup analysis of these materials indicate the presence of oligomers possessing α-terminal ends consisting of primarily two hydrogens [H-$(C_{10}H_{14}S)_n$-H] and oligomers having one hydrogen and one chlorine [H-$(C_{10}H_{14}S)_n$-Cl] α-terminal groups as shown in Figure 2.12. The upper spectrum in Figure 2.12 is the MALDI-ToF mass spectrum of oligomers in the range of m/z 0–5300 by use of reflectron mode (cf. Section 2.3.1).

The lower spectrum in Figure 2.12 is an inset to the spectrum for P3HT formed by chemical oxidation with ferric chloride using DCE as a solvent and focuses on the $M^{\bullet+}$ peak for

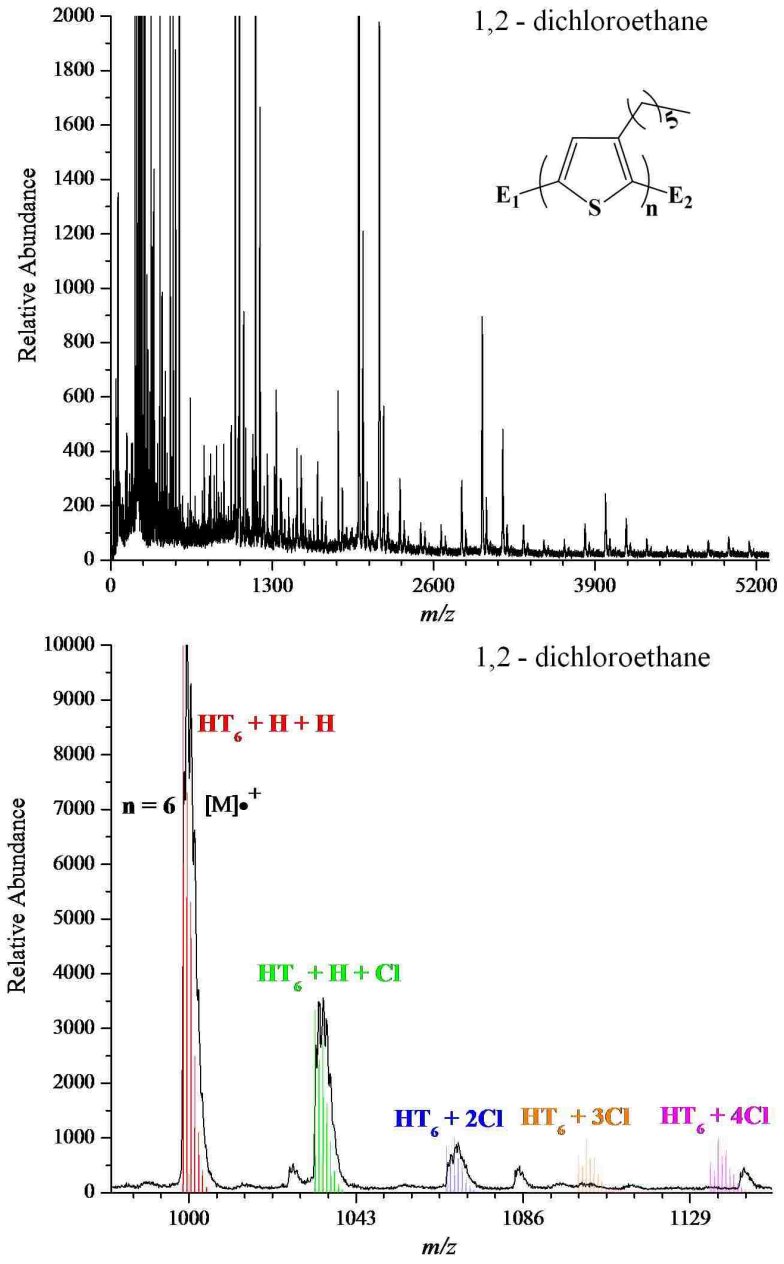

Figure 2.12 MALDI-ToF mass spectra of P3HT formed in 1,2-dichloroethane observed by use of reflectron mode (upper). The inset (lower) shows expanded 6-mer region of the spectrum with colored peaks indicating the calculated isotope patterns of the 6-mer having different chlorine additions.

the oligomer $n = 6$. The overlays shown in various colors are the calculated isotopic patterns for the representation of the given species, which were produced by the Bruker Xmass software. The calculated peaks are labeled in their respective color denoting the chemical composition of

the calculated patterns, where HT_n indicates the repeat unit, which is a 3-*n*-hexylthiophene monomer unit minus 2 hydrogen atoms and has a molar mass of 166.3 amu. These are shown in comparison to the experimental peaks observed for the polymer sample in the background.

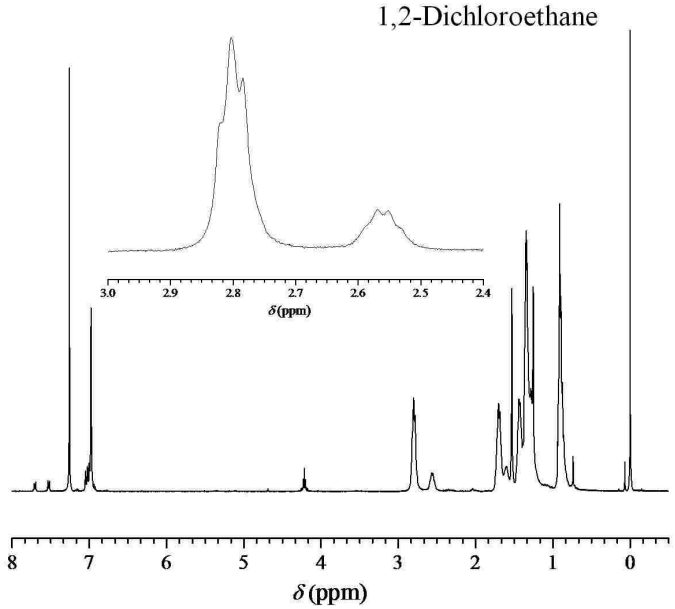

Figure 2.13 ^{1}H-NMR spectrum of P3HT formed in 1,2-dichloroethane. The inset shows the α-methylene region used to determine the material's regioregularity of 81%.

The spectrum shows good agreement with oligomers representing the hydrogen-terminated molecular radical cation, as well as ion patterns indicating oligomers possessing one chlorine termination and one hydrogen endgroup. There is also indication by comparison of calculated and observed ion patterns for oligomers possessing two chlorine additions. There is limited chlorination as compared to materials formed using chloroform as a solvent. In fact, the majority of chlorination is in the form of the addition of one chlorine atom and the relative abundance as observed by MALDI-ToF-MS of this species is less than half that of the hydrogen-terminated oligomers. Furthermore, the amount of oligomers possessing two chlorine additions is extremely limited, being less than 1/10th of material possessing solely hydrogen endgroups,

making hydrogen-terminated P3HT the primary species observed during MALDI-ToF-MS analysis of material formed using DCE as a solvent.

The ^{1}H-NMR analysis of P3HTs formed by chemical oxidation with ferric chloride using 1,2-dichloroethane is shown in Figure 2.13. The inset shows the peaks for signals arising from the α-methylene (aryl methylene) groups found at chemical shifts of $\delta \sim 2.8$ ppm and $\delta \sim 2.58$ ppm, indicating signal response from regioregular and regioirregular material, respectively (cf. Section 1.2.3). The analysis of structural regularity by integration and relative comparison of these peaks is discussed in Section 1.2.4. From integration of the peak found at $\delta \sim 2.8$ ppm normalized as one (1.0) and integration of the peak found at $\delta \sim 2.58$ ppm, which was determined to be 0.24 as compared to the normalized peak, the percentage of the peak at $\delta \sim 2.8$ ppm is found to be 81% of the combined areas of the two peaks. Therefore, the regioregularity of P3HT formed by this chemical oxidative polymerization (cf. Section 2.2.2) using DCE as a solvent can be regarded as 81% regioregular material.

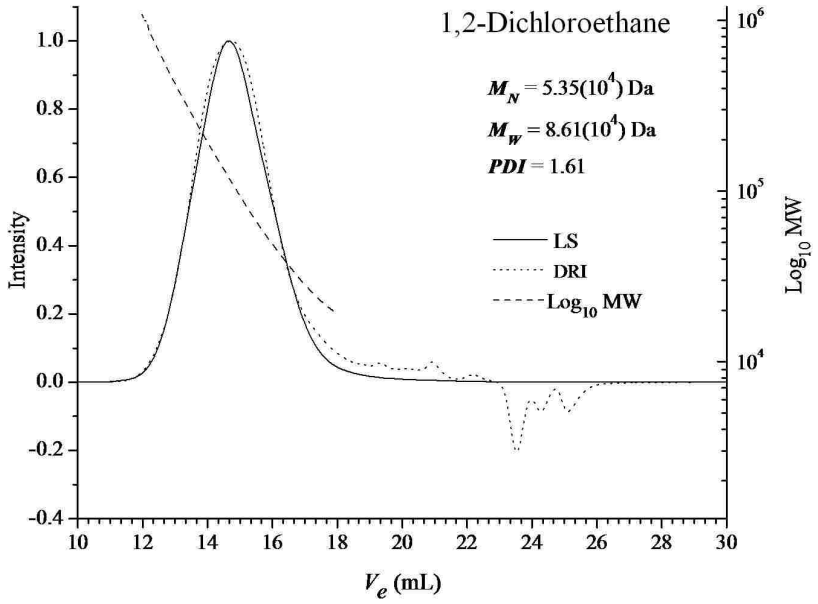

Figure 2.14 Plot of elution volume vs. Log_{10} of molar mass (dashed) and LS (solid) and DRI (dotted) chromatograms of P3HT formed in 1,2-dichloroethane.

In Figure 2.14 is shown the chromatogram from the analytical GPC analysis of P3HT formed in DCE; light scattering (LS) data is represented by the solid line trace, differential refractive index (DRI) data is traced with a dotted line, and the logarithm base 10 of the distribution of molecular weight data is shown by a dashed line. The number-average molecular weight (M_N) for this material as determined from the DRI data is found to be 53,500 Da and the weight-average molecular weight, M_W, calculated from light scattering (LS) data is 86,000 Da. Thus, the *PDI* for P3HTs formed by oxidative polymerization with iron(III) chloride using DCE as a solvent is calculated to be 1.61.

2.5.5 P3HTs Formed in Nitromethane

P3HTs investigated in this section were prepared via the procedure outlined in Section 2.2.2 using nitromethane (CH_3NO_2) as the solvent medium. Nitromethane is a very polar solvent with a dielectric constant of 37 at 25 °C (cf. Section 2.1.2). Iron(III) chloride is completely soluble in nitromethane, forming a yellow/orange solution almost immediately upon addition of $FeCl_3$. Nitromethane is a strong Lewis acid strength and is assigned a Gutmann Acceptor number (AN) (cf. Section 2.1.2) of 20.5, slightly less than chloroform. Nitromethane has little Lewis base characteristics and has a Guttman donor number, DN, (cf. Section 2.1.2) of 2.7. Mass yields of polymer recovered from the preparation of P3HTs formed following the procedures outlined in Section 2.2.2 using nitromethane were on the order of ~ 25%.

The MALDI-ToF mass spectra observed during the endgroup analysis of these materials indicate the presence of oligomers possessing α-terminal ends consisting of primarily two hydrogens [H-$(C_{10}H_{14}S)_n$-H] and a limited number of oligomers having one hydrogen and one chlorine [H-$(C_{10}H_{14}S)_n$-Cl] α-terminal groups as shown in Figure 2.15. The upper spectrum in Figure 2.15 is the MALDI-ToF mass spectrum of oligomers in the range of m/z 0–6500 by use of reflectron mode (cf. Section 2.3.1). There is a very limited abundance of interstitial peaks

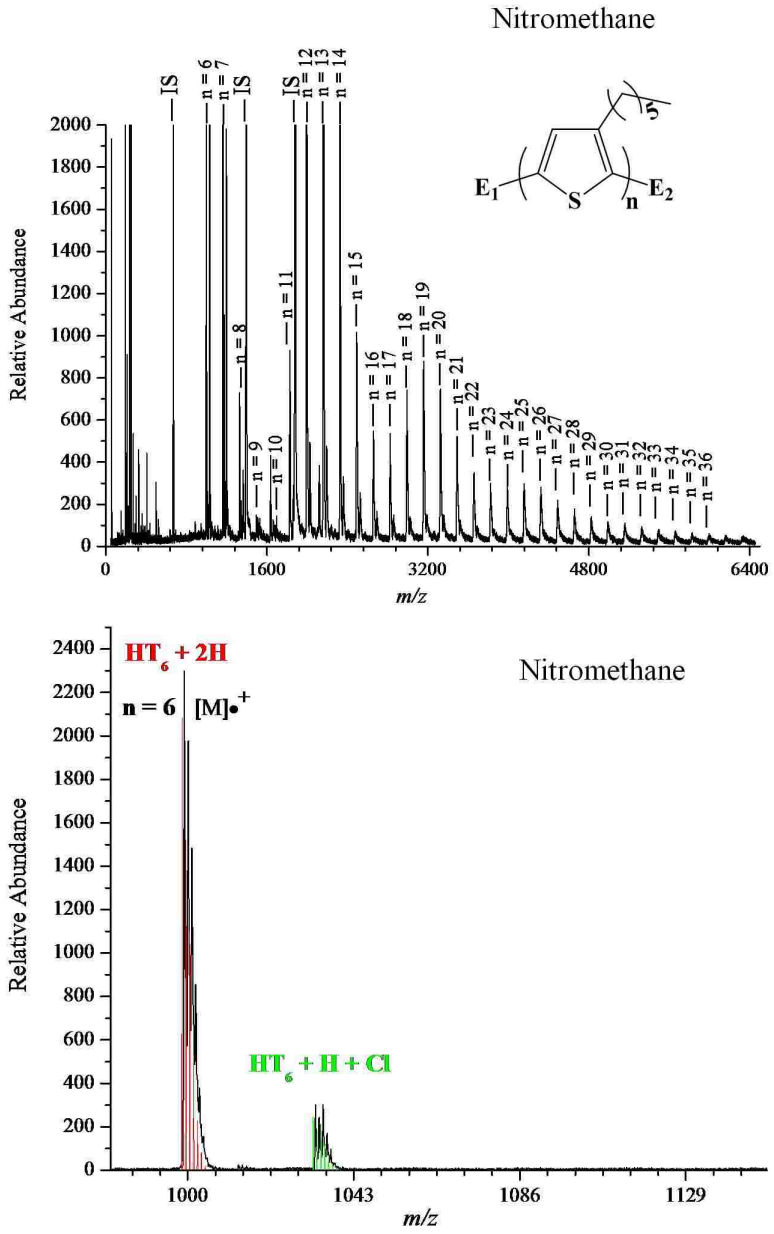

Figure 2.15 MALDI-ToF mass spectra of P3HT formed in nitromethane observed by use of reflectron mode (upper). The inset (lower) shows expanded 6-mer region of the spectrum with colored peaks indicating the calculated isotope patterns of the 6-mer having different chlorine additions.

between those indicated by their repeat units (n = 1,2,3….), indicative of molecular radical cations ($M^{\bullet+}$) having α-terminal substituents with solely hydrogen-terminated endgroups. This spectrum was taken using internal standards (cf. Section 2.4.1), which did not inhibit the degree of ionization for this material as chlorination is very limited.

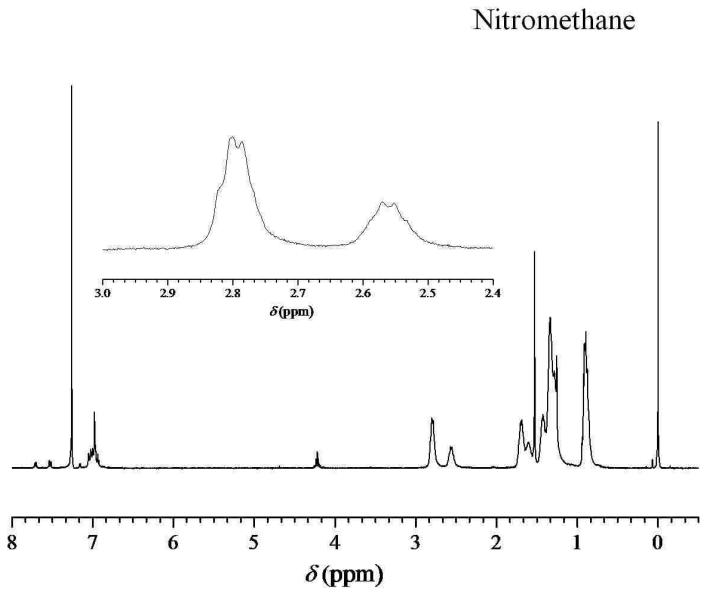

Figure 2.16 ^{1}H-NMR spectrum of P3HT formed in nitromethane. The inset shows the α-methylene region used to determine the material's regioregularity of 67%.

The lower spectrum in Figure 2.15 is an inset to the spectrum for P3HT formed by chemical oxidation with ferric chloride using nitromethane as a solvent and it focuses on the $M^{\bullet+}$ peak for the oligomer $n = 6$. The overlays shown in various colors are the calculated isotopic patterns for the representation of the given species, which were produced by the Bruker Xmass software. The calculated peaks are labeled in their respective color denoting the chemical composition of the calculated patterns, where HT_n indicates the repeat unit, which is a 3-*n*-hexylthiophene monomer unit minus 2 hydrogen atoms and has a molar mass of 166.3 amu. These are shown in comparison to the experimental peaks observed for the polymer sample in the background. The spectrum shows excellent agreement with oligomers representing the hydrogen terminated molecular radical cations [H-$(C_{10}H_{14}S)_n$-H], as well as ion patterns indicating oligomers possessing one chlorine termination and one hydrogen endgroup [H-$(C_{10}H_{14}S)_n$-Cl]. There is extremely limited chlorination as compared to materials formed using most of the other solvents employed for these studies. In fact, all chlorination is in the form of

the addition of one chlorine atom and the relative abundance as observed by MALDI-ToF-MS of this species is 1/7th that of the hydrogen-terminated oligomers. Polymer formed by use of nitromethane as a solvent exhibited the least amount of chlorination compared to all other solvents employed, as observed by MALDI-ToF-MS.

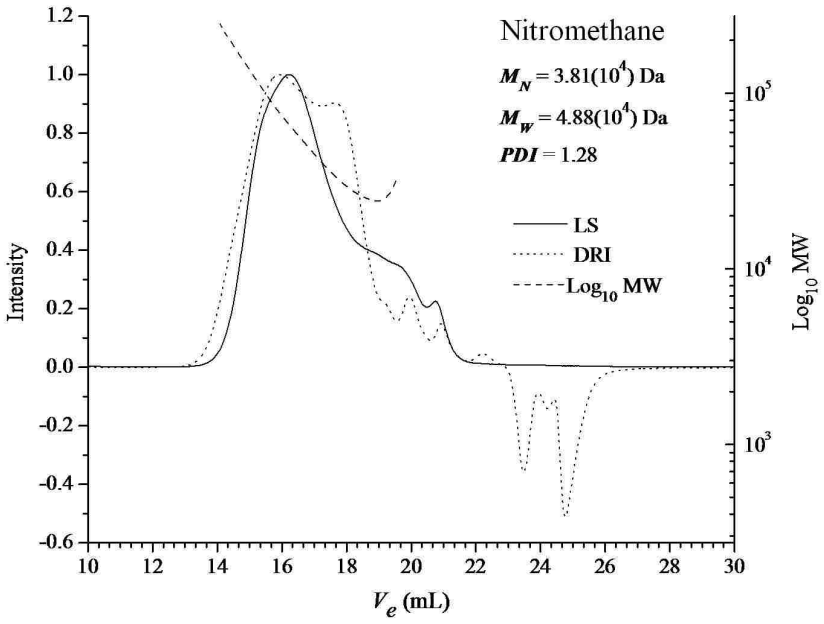

Figure 2.17 Plot of elution volume vs. Log_{10} of molar mass (dashed) and LS (solid) and DRI (dotted) chromatograms of P3HT formed in nitromethane.

The ^{1}H-NMR analysis of P3HTs formed by chemical oxidation with ferric chloride using nitromethane is shown in Figure 2.16. The inset shows the peaks for signals arising from the α-methylene (aryl methylene) groups found at chemical shifts of $\delta \sim 2.8$ ppm and $\delta \sim 2.58$ ppm, indicating signal response from regioregular and regioirregular material, respectively (cf. Section 1.2.3). The analysis of structural regularity by integration and relative comparison of these peaks is discussed in Section 1.2.4. From integration of the peak found at $\delta \sim 2.8$ ppm normalized as one (1.0) and integration of the peak found at $\delta \sim 2.58$ ppm, which was determined to be 0.5 as compared to the normalized peak, the percentage of the peak at $\delta \sim 2.8$ ppm is found to be 67% of the combined areas of the two peaks. Therefore, the regioregularity of P3HT formed by this

chemical oxidative polymerization (cf. Section 2.2.2) using nitromethane as a solvent can be regarded as 67% regioregular material.

In Figure 2.17 is shown the chromatogram from the analytical GPC analysis of P3HT formed in nitromethane; light scattering (LS) data is represented by the solid line trace, differential refractive index (DRI) data is traced with a dotted line, and the logarithm base 10 of the distribution of molecular weight data is shown by a dashed line. The number-average molecular weight (M_N) for this material as determined from the DRI data is found to be 38,100 Da and the weight-average molecular weight, M_W, calculated from light scattering (LS) data is 48,800 Da. Thus, the *PDI* for P3HTs formed by oxidative polymerization with iron(III) chloride using nitromethane as a solvent is calculated to be 1.28.

2.5.6 P3HTs Formed in Nitrobenzene

P3HTs investigated in this section were prepared via the procedure outlined in Section 2.2.2 using nitrobenzene ($C_6H_5NO_2$) as the solvent medium. Nitrobenzene is a slightly less polar solvent than nitromethane with a dielectric constant of 35.7 at 25 °C (cf. Section 2.1.2). Iron(III) chloride is completely soluble in nitrobenzene, forming a yellow/orange solution almost immediately upon addition of $FeCl_3$. Nitrobenzene possesses less Lewis acid strength than nitromethane and it is assigned a Gutmann Acceptor number, AN, (cf. Section 2.1.2) of 14.8. Nitrobenzene has slightly stronger Lewis base characteristics than nitromethane and has a Guttman donor number, DN, (cf. Section 2.1.2) of 4.4. Mass yields of polymer recovered from the preparation of P3HTs formed following the procedures outlined in Section 2.2.2 using nitorbenzene were on the order of ~ 20%.

The MALDI-ToF mass spectra observed during the endgroup analysis of these materials indicate the presence of oligomers possessing α-terminal ends consisting of primarily two hydrogens [H-$(C_{10}H_{14}S)_n$-H] and a limited number oligomers having one hydrogen and one

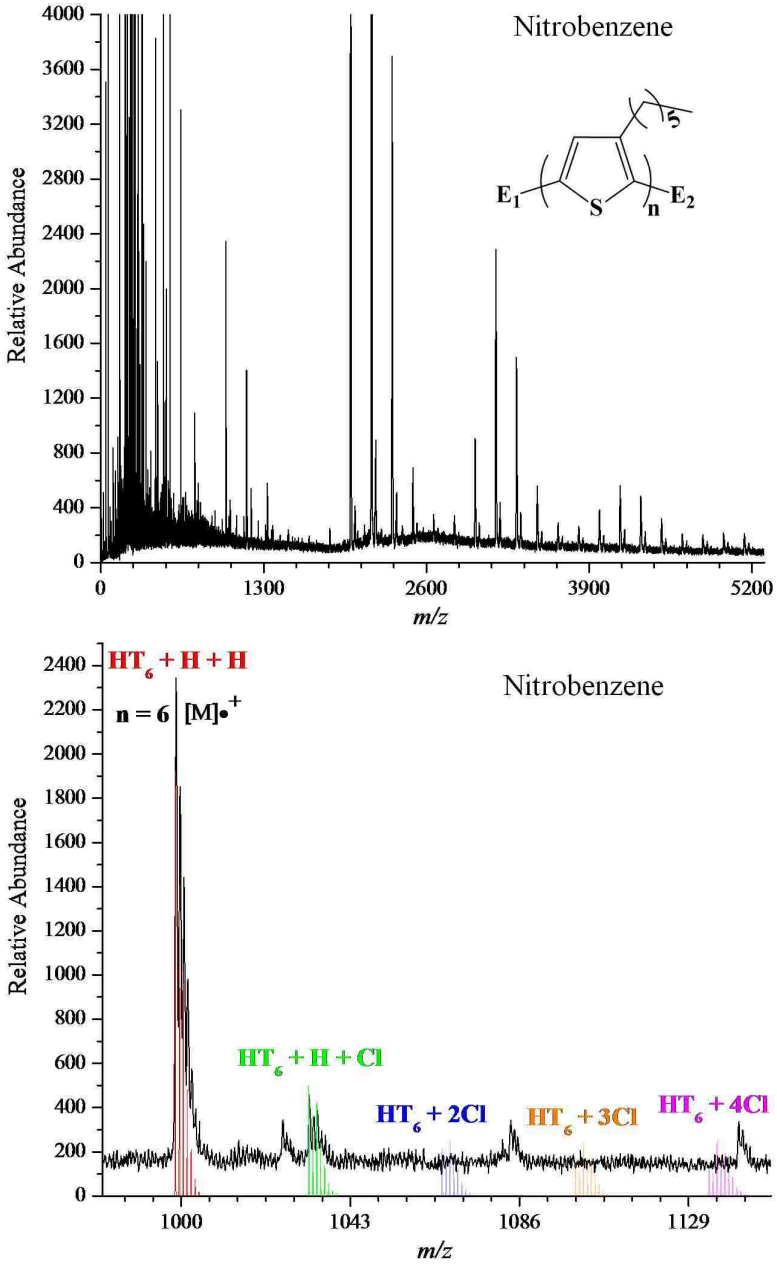

Figure 2.18 MALDI-ToF mass spectra of P3HT formed in nitrobenzene observed by use of reflectron mode (upper). The inset (lower) shows expanded 6-mer region of the spectrum with colored peaks indicating the calculated isotope patterns of the 6-mer having different chlorine additions.

chlorine [H-$(C_{10}H_{14}S)_n$-Cl] α-terminal groups as shown in Figure 2.18. The upper spectrum in Figure 2.18 is the MALDI-ToF mass spectrum of oligomers in the range of *m/z* 0–5300 by use of reflectron mode (cf. Section 2.3.1). There is a very limited abundance of interstitial peaks

between those indicative of molecular radical cations ($M^{\bullet+}$) having α-terminal substituents with solely hydrogen-terminated endgroups.

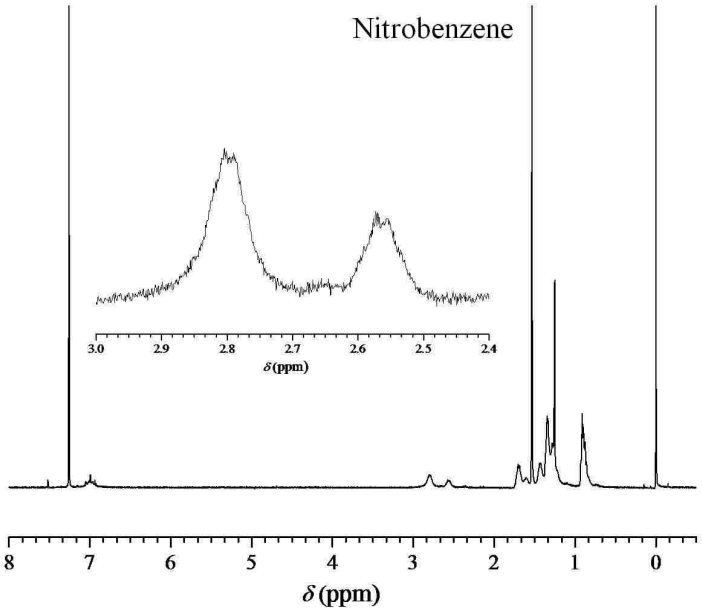

Figure 2.19 ^{1}H-NMR spectrum of P3HT formed in nitrobenzene. The inset shows the α-methylene region used to determine the material's regioregularity of 64%.

The lower spectrum in Figure 2.18 is an inset to the spectrum for P3HT formed by chemical oxidation with ferric chloride using nitrobenzene as a solvent and it focuses on the $M^{\bullet+}$ peak for the oligomer n = 6. The overlays shown in various colors are the calculated isotopic patterns for the representation of the given species, which were produced by the Bruker Xmass software. The calculated peaks are labeled in their respective color denoting the chemical composition of the calculated patterns, where HT_n indicates the repeat unit, which is a 3-*n*-hexylthiophene monomer unit minus 2 hydrogen atoms and has a molar mass of 166.3 amu. These are shown in comparison to the experimental peaks observed for the polymer sample in the background. The spectrum shows excellent agreement with oligomers representing the hydrogen-terminated molecular radical cations [H-$(C_{10}H_{14}S)_n$-H], as well as ion patterns indicating oligomers possessing one chlorine termination and one hydrogen endgroup [H-

$(C_{10}H_{14}S)_n$-Cl]. There is extremely limited chlorination as compared to materials formed using most other solvents employed for these studies. In fact, all chlorination is in the form of the addition of one chlorine atom and the relative abundance as observed by MALDI-ToF-MS of this species is 1/5th that of the hydrogen-terminated oligomers. Polymer formed by use of nitrobenzene as a solvent exhibited the least amount of chlorination as observed by MALDI-ToF-MS, with the exception of polymer formed in nitromethane.

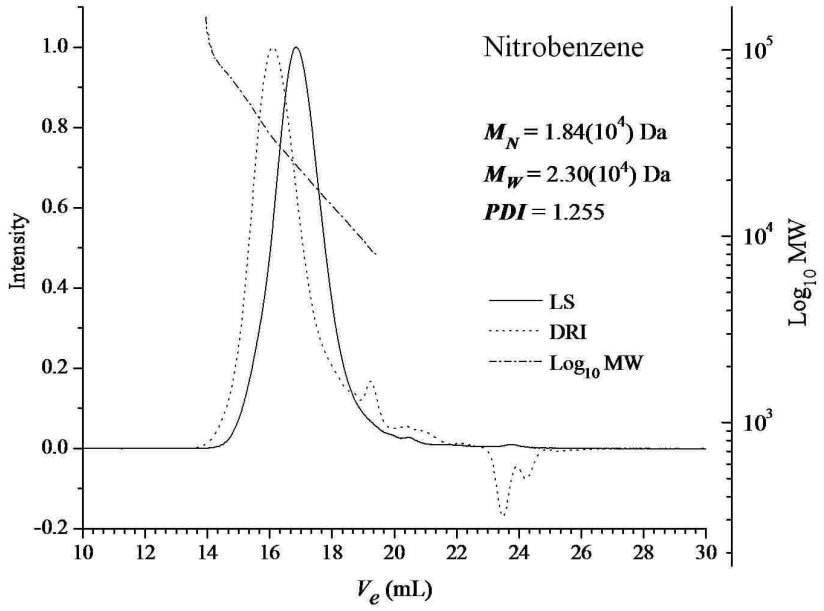

Figure 2.20 Plot of elution volume vs. Log_{10} of molar mass (dashed) and LS (solid) and DRI (dotted) chromatograms of P3HT formed in nitrobenzene.

The ^{1}H-NMR analysis of P3HTs formed by chemical oxidation with ferric chloride using nitrobenzene is shown in Figure 2.19. The inset shows the peaks for signals arising from the α-methylene (aryl methylene) groups found at chemical shifts of $\delta \sim 2.8$ ppm and $\delta \sim 2.58$ ppm, indicating signal response from regioregular and regioirregular material, respectively (cf. Section 1.2.3). The analysis of structural regularity by integration and relative comparison of these peaks is discussed in Section 1.2.4. From integration of the peak found at $\delta \sim 2.8$ ppm normalized as one (1.0) and integration of the peak found at $\delta \sim 2.58$ ppm, which was determined to be 0.6 as

compared to the normalized peak, the percentage of the peak at $\delta \sim 2.8$ ppm is found to be 64% of the combined areas of the two peaks. Therefore, the regioregularity of P3HT formed by this chemical oxidative polymerization (cf. Section 2.2.2) using nitrobenzene as a solvent can be regarded as 64% regioregular material.

In Figure 2.20 is shown the chromatogram from the analytical GPC analysis of P3HT formed in nitrobenzene; light scattering (LS) data is represented by the solid line trace, differential refractive index (DRI) data is traced with a dotted line, and the logarithm base 10 of the distribution of molecular weight data is shown by a dashed line. The number-average molecular weight (M_N) for this material as determined from the DRI data is found to be 18,400 Da and the weight-average molecular weight, M_W, calculated from light scattering (LS) data is 23,000 Da. Thus, the *PDI* for P3HTs formed by oxidative polymerization with iron(III) chloride using nitrobenzene as a solvent is calculated to be 1.26.

2.5.7 P3HTs Formed in Acetonitrile

P3HTs investigated in this section were prepared via the procedure outlined in Section 2.2.2 using acetonitrile (C_2H_5CN) as the solvent medium. Acetonitrile is a very polar solvent comparable to nitromethane in dielectric strength, having a dielectric constant of 36.6 at 25 °C (cf. Section 2.1.2). Iron(III) chloride is completely soluble in acetonitrile, forming a yellow/orange solution almost immediately upon addition of $FeCl_3$. Acetonitrile possesses strong Lewis acid characteristics and it is assigned a Gutmann Acceptor number, AN, (cf. Section 2.1.2) of 19.3. Acetonitrile has stronger Lewis base characteristics than nitromethane and nitrobenzene and has a Guttman donor number, DN, (cf. Section 2.1.2) of 14.1. Mass yields of polymer recovered from the preparation of P3HTs formed following the procedures outlined in Section 2.2.2 using acetonitrile were on the order of ~ 25%.

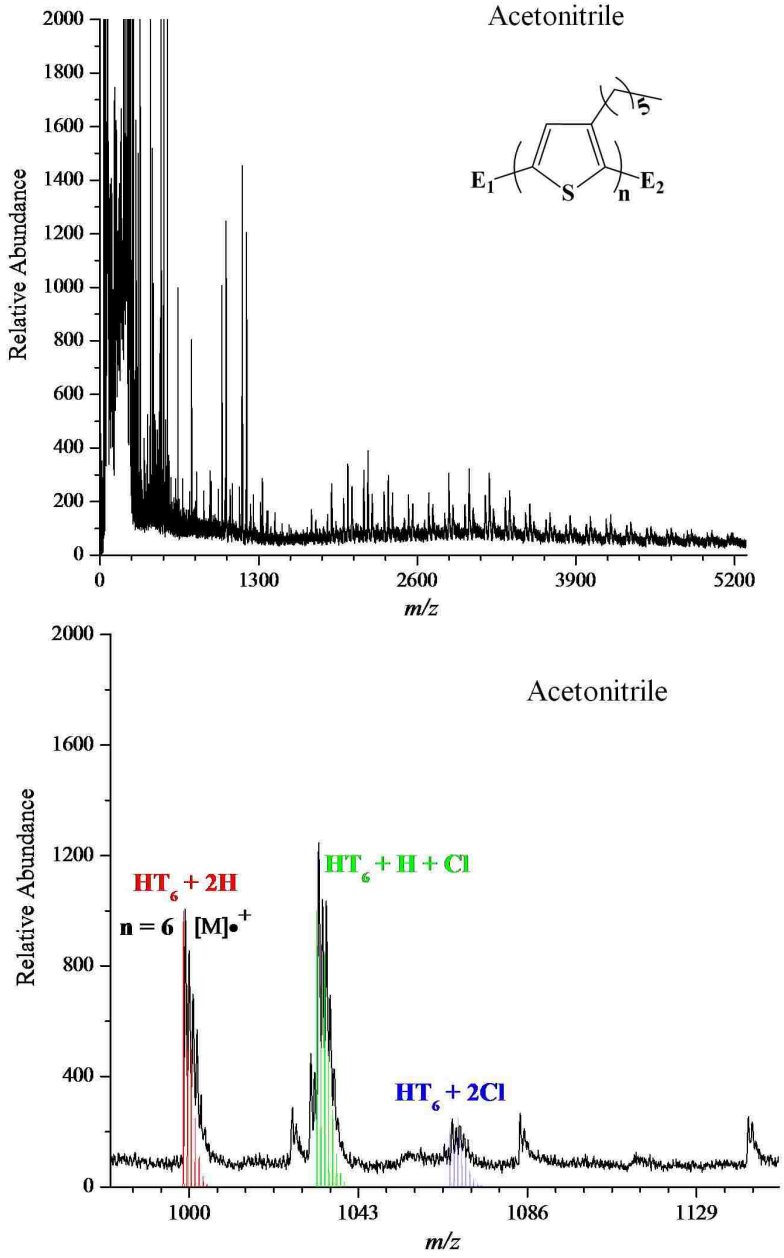

Figure 2.21 MALDI-ToF mass spectra of P3HT formed in acetonitrile observed by use of reflectron mode (upper). The inset (lower) shows expanded 6-mer region of the spectrum with colored peaks indicating the calculated isotope patterns of the 6-mer having different chlorine additions.

The MALDI-ToF mass spectra observed during the endgroup analysis of these materials indicate the presence of oligomers possessing α-terminal ends consisting of two hydrogens [H-$(C_{10}H_{14}S)_n$-H] and a greater number oligomers having one hydrogen and one chlorine [H-

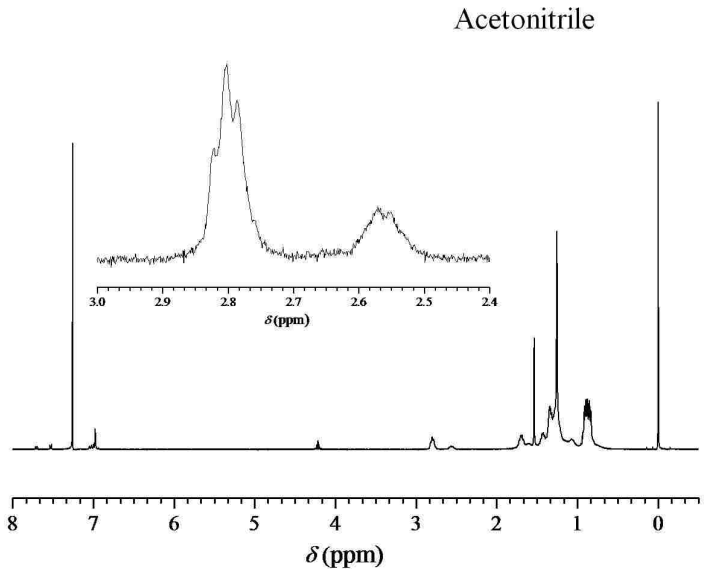

Figure 2.22 ^{1}H-NMR spectrum of P3HT formed in acetonitrile. The inset shows the α-methylene region used to determine the material's regioregularity of 75%.

$(C_{10}H_{14}S)_n$-Cl] α-terminal groups as shown in Figure 2.21. The upper spectrum in Figure 2.21 is the MALDI-ToF mass spectrum of oligomers in the range of m/z 0–5300 by use of reflectron mode (cf. Section 2.3.1).

The lower spectrum in Figure 2.21 is an inset to the spectrum for P3HT formed by chemical oxidation with ferric chloride using acetonitrile as a solvent and focuses on the $M^{\bullet+}$ peak for the oligomer n = 6. The overlays shown in various colors are the calculated isotopic patterns for the representation of the given species, which were produced by the Bruker Xmass software. The calculated peaks are labeled in their respective color denoting the chemical composition of the calculated patterns, where HT_n indicates the repeat unit, which is a 3-*n*-hexylthiophene monomer unit minus 2 hydrogen atoms and has a molar mass of 166.3 amu. These are shown in comparison to the experimental peaks observed for the polymer sample in the background. The spectrum shows excellent agreement with oligomers representing the hydrogen-terminated molecular radical cations [H-$(C_{10}H_{14}S)_n$-H], as well as ion patterns

indicating oligomers possessing one chlorine termination and one hydrogen endgroup [H-$(C_{10}H_{14}S)_n$-Cl]. There is also an ion pattern representing oligomers having two chlorine additions, although to a very limited extent. Chlorination, as indicated by the ion pattern for oligomers possessing one chlorine addition [H-$(C_{10}H_{14}S)_n$-Cl], is more prevalent than that seen for other polymers formed in solvents with high dielectric constants, but less than that seen for more nonpolar solvents. However, the relative abundance of material with one chlorine addition exceeds that of material with solely hydrogen terminated endgroups.

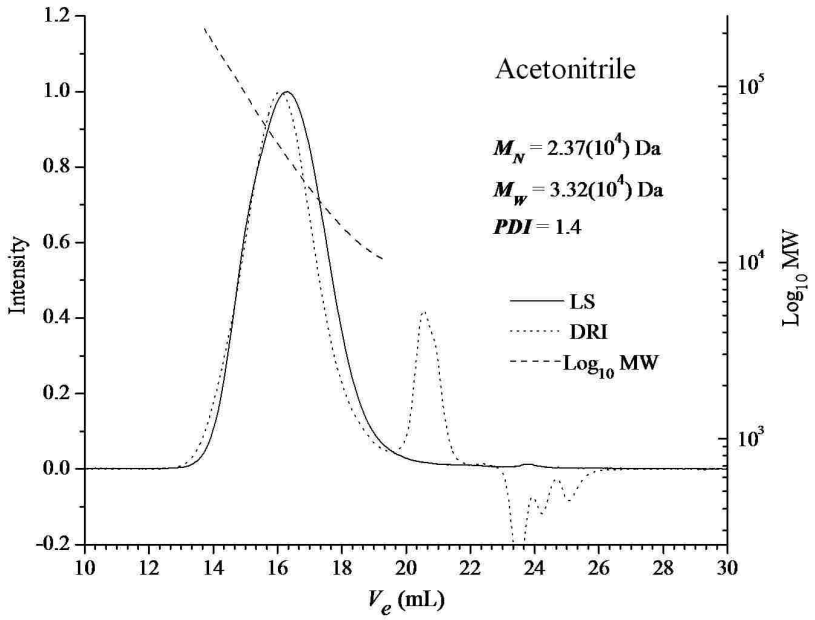

Figure 2.23 Plot of elution volume vs. Log_{10} of molar mass (dashed) and LS (solid) and DRI (dotted) chromatograms of P3HT formed in acetonitrile.

The ^{1}H-NMR analysis of P3HTs formed by chemical oxidation with ferric chloride using acetonitrile is shown in Figure 2.22. The inset shows the peaks for signals arising from the α-methylene (aryl methylene) groups found at chemical shifts of $\delta \sim 2.8$ ppm and $\delta \sim 2.58$ ppm, indicating signal response from regioregular and regioirregular material, respectively (cf. Section 1.2.3). The analysis of structural regularity by integration and relative comparison of these peaks is discussed in Section 1.2.4. From integration of the peak found at $\delta \sim 2.8$ ppm normalized as

one (1.0) and integration of the peak found at $\delta \sim 2.58$ ppm, which was determined to be 0.33 as compared to the normalized peak, the percentage of the peak at $\delta \sim 2.8$ ppm is found to be 75% of the combined areas of the two peaks. Therefore, the regioregularity of P3HT formed by this chemical oxidative polymerization (cf. Section 2.2.2) using acetonitrile as a solvent can be regarded as 75% regioregular material.

In Figure 2.23 is shown the chromatogram from the analytical GPC analysis of P3HT formed in acetonitrile; light scattering (LS) data is represented by the solid line trace, differential refractive index (DRI) data is traced with a dotted line, and the logarithm base 10 of the distribution of molecular weight data is shown by a dashed line. The number-average molecular weight (M_N) for this material as determined from the DRI data is found to be 23,700 Da and the weight-average molecular weight, M_W, calculated from light scattering (LS) data is 33,200 Da. Thus, the *PDI* for P3HTs formed by oxidative polymerization with iron(III) chloride using acetonitrile as a solvent is calculated to be 1.4.

2.5.8 P3HTs Formed in Benzene

P3HTs investigated in this section were prepared via the procedure outlined in Section 2.2.2 using benzene (C_6H_6) as the solvent medium. Benzene is a very nonpolar solvent, having a dielectric constant of 2.27 at 25 °C (cf. Section 2.1.2). Iron(III) chloride is completely insoluble in benzene, remaining a colorless suspension upon addition of $FeCl_3$. Benzene possesses some Lewis acid characteristics and it is assigned a Gutmann Acceptor number, AN, (cf. Section 2.1.2) of 8.2. Benzene has negligible Lewis base characteristics and has a Guttman donor number, DN, (cf. Section 2.1.2) of 0.1. Mass yields of polymer recovered from the preparation of P3HTs formed following the procedures outlined in Section 2.2.2 using Benzene were on the order of ~ 8%.

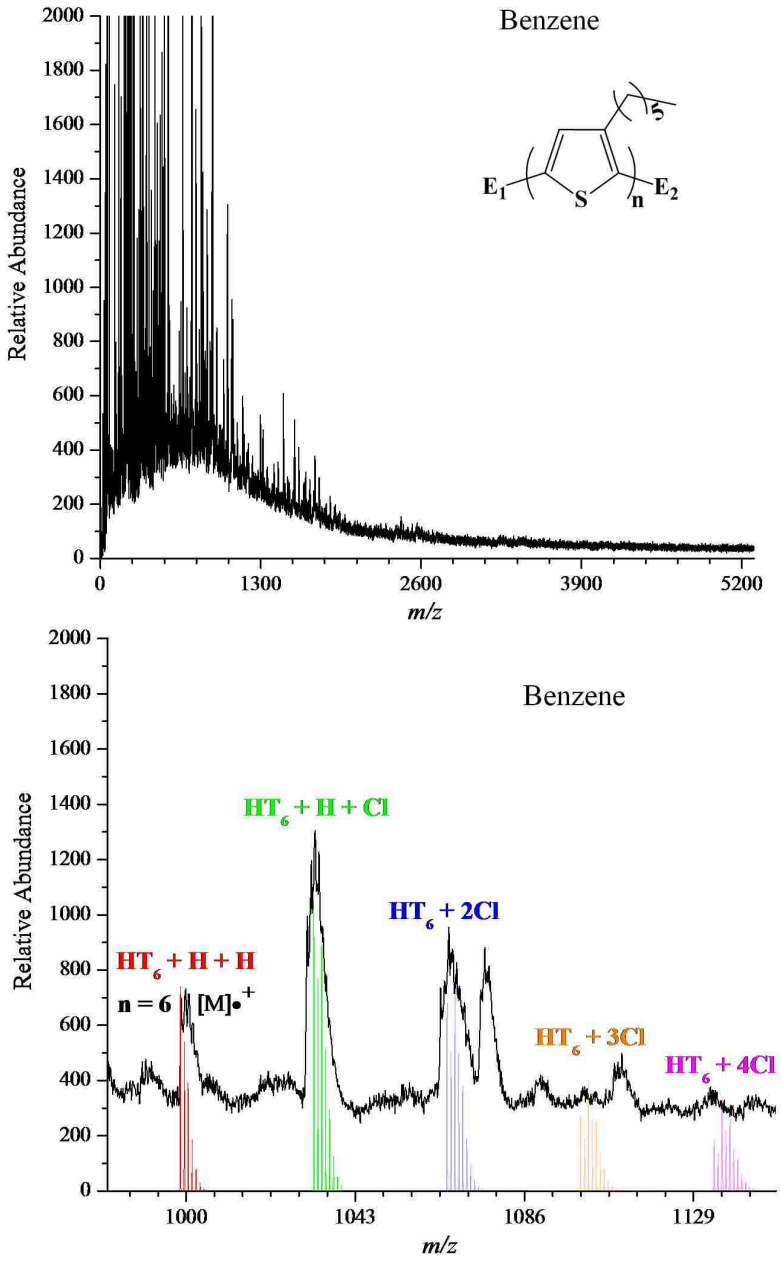

Figure 2.24 MALDI-ToF mass spectra of P3HT formed in benzene observed by use of reflectron mode (upper). The inset (lower) shows expanded 6-mer region of the spectrum with colored peaks indicating the calculated isotope patterns of the 6-mer having different chlorine additions.

MALDI-ToF-MS analysis of materials produced in benzene as a solvent was difficult and there was a limited detection of materials in the mass range observable by use of reflectron mode. Use of linear mode did not produce detectable ions either. The MALDI-ToF mass

spectra observed during the endgroup analysis of these materials indicate the presence of oligomers possessing α-terminal ends consisting of two hydrogens [H-$(C_{10}H_{14}S)_n$-H] and a greater number oligomers having one hydrogen and one chlorine [H-$(C_{10}H_{14}S)_n$-Cl] or two chlorine [Cl-$(C_{10}H_{14}S)_n$-Cl] α-terminal groups as shown in Figure 2.24. The upper spectrum in Figure 2.24 is the MALDI-ToF mass spectrum of oligomers in the range of m/z 0–5300 by use of reflectron mode (cf. Section 2.3.1).

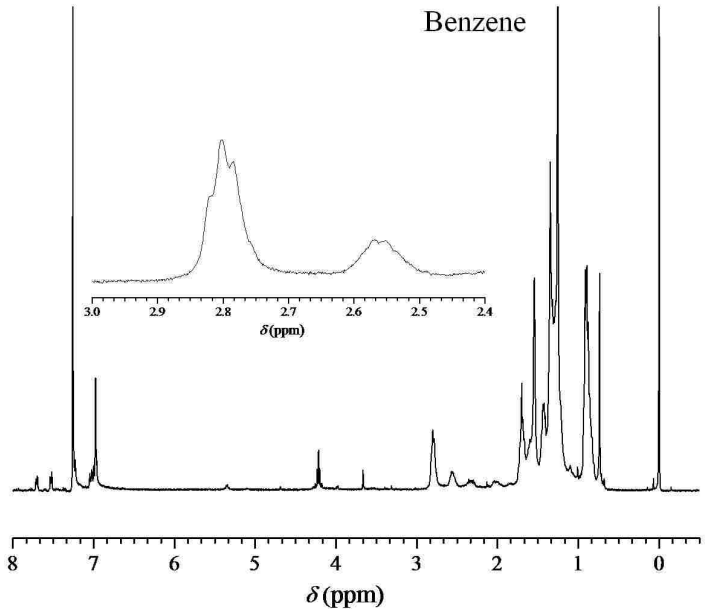

Figure 2.25 ^{1}H-NMR spectrum of P3HT formed in benzene. The inset shows the α-methylene region used to determine the material's regioregularity of 71%.

The lower spectrum in Figure 2.24 is an inset to the spectrum for P3HT formed by chemical oxidation with ferric chloride using benzene as a solvent and it focuses on the $M^{\bullet+}$ peak for the oligomer $n = 6$. The overlays shown in various colors are the calculated isotopic patterns for the representation of the given species, which were produced by the Bruker Xmass software. The calculated peaks are labeled in their respective color denoting the chemical composition of the calculated patterns, where HT_n indicates the repeat unit, which is a 3-*n*-hexylthiophene monomer unit minus 2 hydrogen atoms and has a molar mass of 166.3 amu. These are shown in

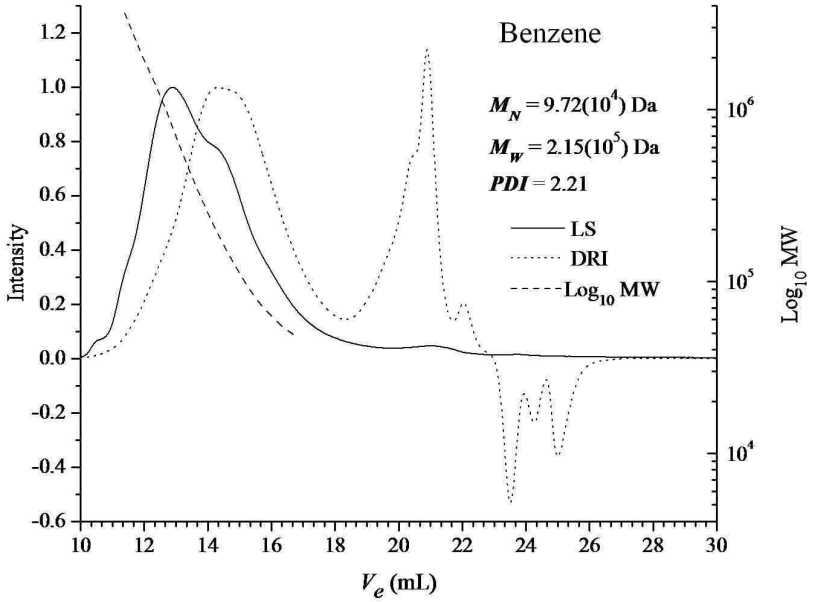

Figure 2.26 Plot of elution volume vs. Log_{10} of molar mass (dashed) and LS (solid) and DRI (dotted) chromatograms of P3HT formed in benzene.

comparison to the experimental peaks observed for the polymer sample in the background. The spectrum shows good agreement with oligomers representing the hydrogen-terminated molecular radical cations [H-$(C_{10}H_{14}S)_n$-H], as well as ion patterns indicating oligomers possessing one chlorine termination and one hydrogen endgroup [H-$(C_{10}H_{14}S)_n$-Cl], as well as those possessing two chlorine additions [Cl-$(C_{10}H_{14}S)_n$-Cl]. The abundances of the latter two patterns exceed that of the hydrogen-terminated oligomer pattern. The difficulty in obtaining the spectrum is indicated by the excessive baseline signal.

The ^{1}H-NMR analysis of P3HTs formed by chemical oxidation with ferric chloride using benzene is shown in Figure 2.25. The inset shows the peaks for signals arising from the α-methylene (aryl methylene) groups found at chemical shifts of $\delta \sim 2.8$ ppm and $\delta \sim 2.58$ ppm, indicating signal response from regioregular and regioirregular material, respectively (cf. Section 1.2.3). The analysis of structural regularity by integration and relative comparison of these peaks is discussed in Section 1.2.4. From integration of the peak found at $\delta \sim 2.8$ ppm normalized as

one (1.0) and integration of the peak found at $\delta \sim 2.58$ ppm, which was determined to be 0.4 as compared to the normalized peak, the percentage of the peak at $\delta \sim 2.8$ ppm is found to be 71% of the combined areas of the two peaks. Therefore, the regioregularity of P3HT formed by this chemical oxidative polymerization (cf. Section 2.2.2) using benzene as a solvent is regarded as 71% regioregular material.

In Figure 2.26 is shown the chromatogram from the analytical GPC analysis of P3HT formed in benzene; light scattering (LS) data is represented by the solid line trace, differential refractive index (DRI) data is traced with a dotted line, and the logarithm base 10 of the distribution of molecular weight data is shown by a dashed line. The number-average molecular weight (M_N) for this material as determined from the DRI data is found to be 92,000 Da and the weight-average molecular weight, M_W, calculated from light scattering (LS) data is 215,000 Da. Thus, the *PDI* for P3HTs formed by oxidative polymerization with iron(III) chloride using benzene as a solvent is calculated to be 2.21.

2.5.9 P3HTs Formed in Hexane

P3HTs investigated in this section were prepared via the procedure outlined in Section 2.2.2 using *n*-hexane (C_6H_{14}) as the solvent medium. *n*-Hexane is a very nonpolar solvent, having a dielectric constant of 1.9 at 25 °C (cf. Section 2.1.2). Iron(III) chloride is completely insoluble in *n*-hexane, remaining a colorless suspension upon addition of $FeCl_3$. *n*-Hexane is a very inert solvent. *n*-Hexane possesses no appreciable Lewis acid characteristics and it is used as a reference solvent for empirical AN determination in which it is arbitrarily assigned a Gutmann Acceptor number, AN, (cf. Section 2.1.2) of 0. *n*-Hexane has no appreciable Lewis base characteristics and has a Guttman donor number, DN, (cf. Section 2.1.2) of 0. Mass yields of polymer recovered from the preparation of P3HTs formed following the procedures outlined in Section 2.2.2 using *n*-hexane were on the order of ~ 5%.

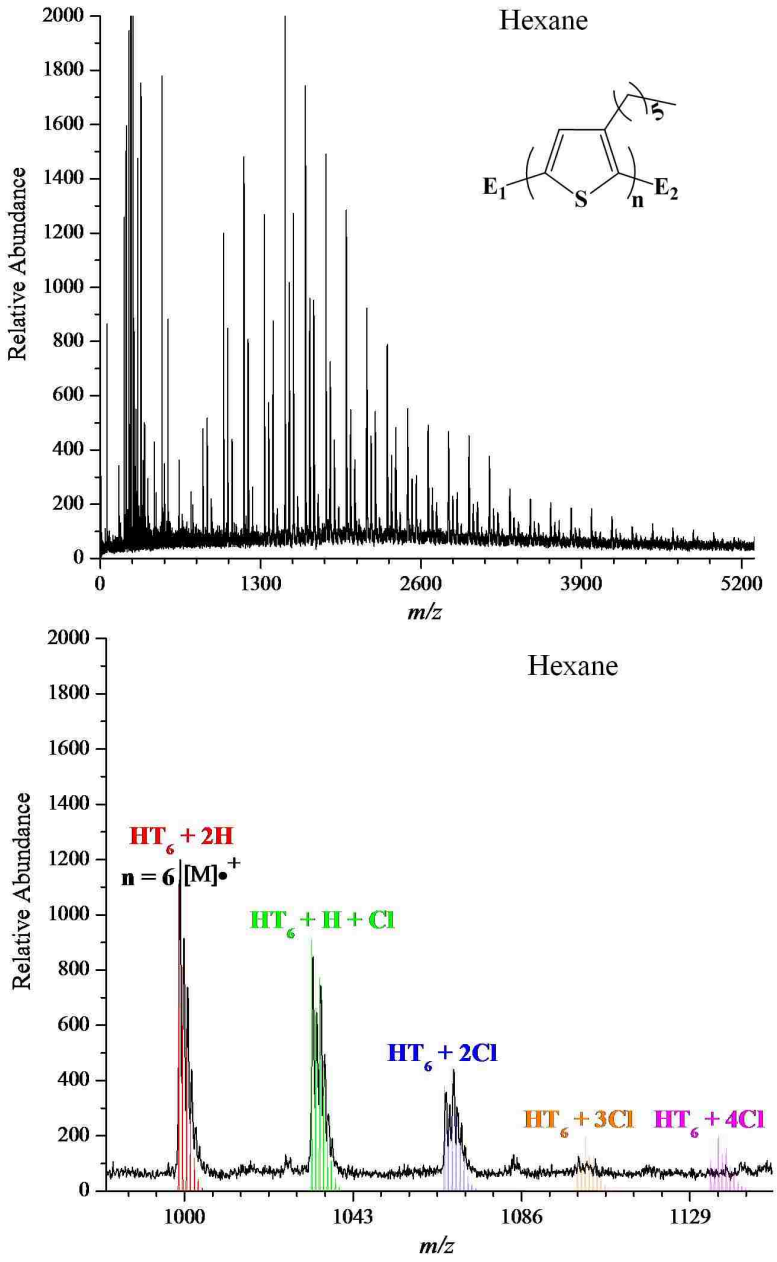

Figure 2.27 MALDI-ToF mass spectra of P3HT formed in hexane observed by use of reflectron mode (upper). The inset (lower) shows expanded 6-mer region of the spectrum with colored peaks indicating the calculated isotope patterns of the 6-mer having different chlorine additions.

The MALDI-ToF mass spectra observed during the endgroup analysis of these materials indicate the presence of oligomers possessing α-terminal ends consisting of two hydrogens [H-$(C_{10}H_{14}S)_n$-H], oligomers having one hydrogen and one chlorine [H-$(C_{10}H_{14}S)_n$-Cl] or two

chlorine [Cl-$(C_{10}H_{14}S)_n$-Cl] α-terminal groups as shown in Figure 2.27. The upper spectrum in Figure 2.27 is the MALDI-ToF mass spectrum of oligomers in the range of *m*/*z* 0–5300 by use of reflectron mode (cf. Section 2.3.1). The *m*/*z* of the interstitial peaks between those representing molecular radical cations for solely hydrogen-terminated oligomers indicate a fair extent of chlorination to this material.

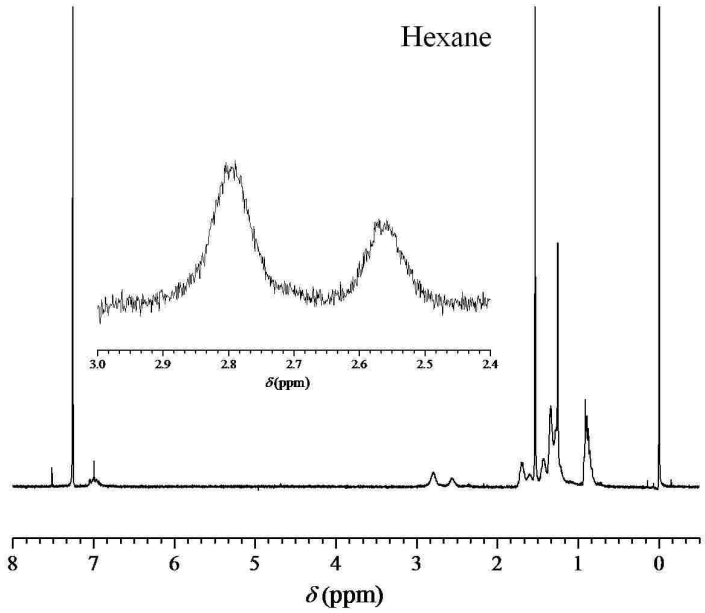

Figure 2.28 ^{1}H-NMR spectrum of P3HT formed in hexane. The inset shows the α-methylene region used to determine the material's regioregularity of 58%.

The lower spectrum in Figure 2.27 is an inset to the spectrum for P3HT formed by chemical oxidation with ferric chloride using hexane as a solvent and focuses on the $M^{\bullet+}$ peak for the oligomer $n = 6$. The overlays shown in various colors are the calculated isotopic patterns for the representation of the given species, which were produced by the Bruker Xmass software. The calculated peaks are labeled in their respective color denoting the chemical composition of the calculated patterns, where HT_n indicates the repeat unit, which is a 3-*n*-hexylthiophene monomer unit minus 2 hydrogen atoms and has a molar mass of 166.3 amu. These are shown in comparison to the experimental peaks observed for the polymer sample in the background. The

spectrum shows excellent agreement with oligomers representing the hydrogen-terminated molecular radical cations [H-($C_{10}H_{14}S)_n$-H], as well as ion patterns indicating oligomers possessing one chlorine termination and one hydrogen endgroup [H-($C_{10}H_{14}S)_n$-Cl], along with those possessing two chlorine additions [Cl-($C_{10}H_{14}S)_n$-Cl]. The abundances of the latter two patterns do not exceed that of the hydrogen-terminated oligomer pattern, although there is a high ratio of these peaks relative to the peak for the hydrogen-terminated oligomer, indicating a fairly large extent of chlorination for materials produced in hexane. Nonetheless, the extent of chlorination is not as great as other nonpolar solvents, such as chloroform and carbon tetrachloride.

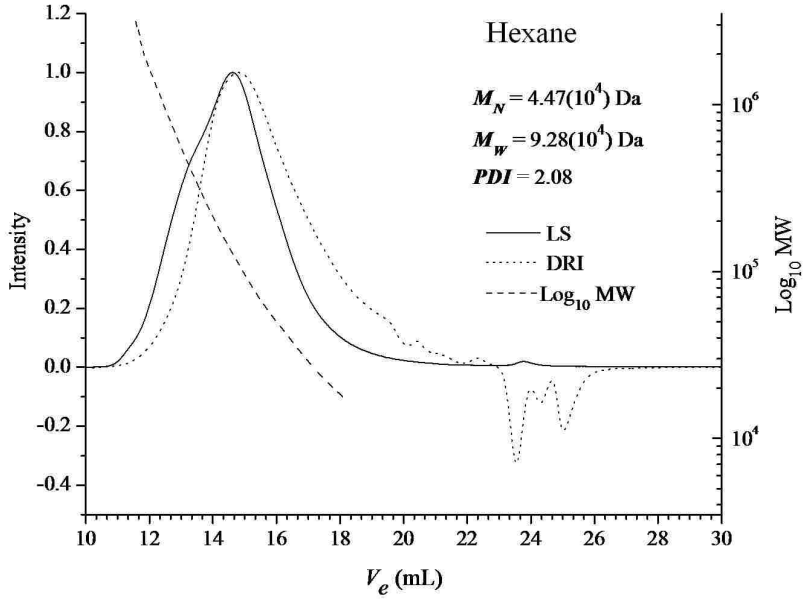

Figure 2.29 Plot of elution volume vs. Log_{10} of molar mass (dashed) and LS (solid) and DRI (dotted) chromatograms of P3HT formed in hexane.

The ^{1}H-NMR analysis of P3HTs formed by chemical oxidation with ferric chloride using *n*-hexane is shown in Figure 2.28. The inset shows the peaks for signals arising from the α-methylene (aryl methylene) groups found at chemical shifts of $\delta \sim 2.8$ ppm and $\delta \sim 2.58$ ppm, indicating signal response from regioregular and regioirregular material, respectively (cf. Section

1.2.3). The analysis of structural regularity by integration and relative comparison of these peaks is discussed in Section 1.2.4. From integration of the peak found at $\delta \sim 2.8$ ppm normalized as one (1.0) and integration of the peak found at $\delta \sim 2.58$ ppm, which was determined to be 0.72 as compared to the normalized peak, the percentage of the peak at $\delta \sim 2.8$ ppm is found to be 58% of the combined areas of the two peaks. Therefore, the regioregularity of P3HT formed by this chemical oxidative polymerization (cf. Section 2.2.2) using *n*-hexane as a solvent is regarded as 58% regioregular material.

In Figure 2.29 is shown the chromatogram from the analytical GPC analysis of P3HT formed in *n*-hexane; light scattering (LS) data is represented by the solid line trace, differential refractive index (DRI) data is traced with a dotted line, and the logarithm base 10 of the distribution of molecular weight data is shown by a dashed line. The number-average molecular weight (M_N) for this material as determined from the DRI data is found to be 44,700 Da and the weight-average molecular weight, M_W, calculated from light scattering (LS) data is 92,800 Da. Thus, the *PDI* for P3HTs formed by oxidative polymerization with iron(III) chloride using *n*-hexane as a solvent is calculated to be 2.08.

2.6 Discussion

2.6.1 Solvent Influences on the Addition of Chlorine to P3HTs Made by Means of Chemical Oxidation

As discussed in Section 2.1.1, previous reports indicated that certain nonaqueous solvents used as reaction medium are more conducive to propagating polymerization of poly(3-hexylthiophene) by means of chemical oxidative coupling using ferric chloride as an oxidant.[3] These earlier studies indicate that nonpolar solvents are a requirement for polymerization and they showed that some polar solvents in which the oxidant is soluble were unable to support polymerization to form P3HTs (cf. Section 2.1.1). On the contrary, certain other studies

indicated successful polymerizations of 3-alkylthiophenes and other similar conducting polymer systems in solvents in which ferric chloride is completely soluble, such as acetonitrile and nitromethane.[5,6,26] Nonetheless, Niemi et al. did show that some solvents, such as diethyl ether in which iron(III) chloride is fully soluble, do not support polymerization, due to strong interactions between the solvent and oxidant.[3] Furthermore, Brauch's work revealed that P3HTs formed in nitromethane using limited oxidant-to-monomer ratios possess far less chlorine addition as compared to those formed using chloroform.[6]

It has been surmised herein that the physical state of iron(III) chloride (cf. Section 2.1.3) –that is dependent on the nature of the nonaqueous solvent in which the reaction is performed[16-24]–strongly contributes to the physical properties of the resulting polymer. This is due in part to the interactions of the solvent with the particular species of oxidant in solution, which can differ depending on the physical properties of the solvent (cf. Section 2.1) and imparts specific structural characteristics to the resulting polymer. MALDI-ToF-MS analysis of P3HTs formed in various solvents has shown this to be true in these studies and the resulting extent of chlorination to these materials may be explained in terms of the solvent polarity, in conjunction with solvent Lewis acid and base characteristics.

For instance, P3ATs formed in the very nonpolar solvent chloroform display heavy α- and possibly β- chlorine additions (cf. Section 2.5.1, Figure 2.3). However, polymer formed in the very polar solvent nitromethane exhibits a dramatic decrease in chlorination to the polymer chains (cf. Section 2.5.5, Figure 2.15). These results suggest that P3ATs formed in solvents in which ferric chloride is more soluble and therefore more so in the monomeric state (cf. Section 2.1.3, Equations 2.1 and 2.2) will result in less chlorination than those formed in less polar solvents, which sustain a large population of the dimeric species of the oxidant. This is a reasonable inference considering that the dimeric form of ferric chloride is countered by a

chloride anion, having very strong lewis basicity (DN ~ 27), thus making it a formidable nucleophile. Although, it can be safely argued that because some chlorination occurs in polar solvents that better support the monomeric form of the oxidant, the dimeric form of ferric chloride exists to some degree in such solvents simultaneously.

As previously mentioned in Section 2.1.3, ESR and ultraviolet-visible spectroscopy studies have shown that the presence of the tetrachloroferrate ion, indicative of the monomeric species of ferric chloride, is solvent dependent. Generally speaking, the monomeric species has been shown to be found in solvents with large dielectric constants.[20] Conversely, Mössbauer spectroscopy experiments have indicated that dimeric species exist in polar solvents such as nitrobenzene,[22] and infrared spectroscopy studies have reported that the monomeric form of ferric chloride can be found in inert solvents such as benzene.[17,23] These studies, along with the work herein, provide convincing evidence that both species of oxidant exist in a given solvent and the distribution of the population of either species is directly dependent on the physical properties of the solvent.

This scenario undoubtedly oversimplifies the physical state of ferric chloride in nonaqueous solvents and in particular oversimplifies the situation corresponding to the role that the solvent plays in the chemical oxidation of 3-hexylthiophene, and thus the physical properties of the resulting polymers. It has been made clear that solvents in which ferric chloride is soluble, as well as those it is not, will support this reaction and the two general species of oxidant found in different solvents to varying degrees impart structural differences to the product. However, the interaction between solvent and oxidant is far more complicated as indicated by the fact that certain solvents do not support chemical oxidation of P3ATs regardless of the physical state of iron(III) chloride, such as is the case with diethyl ether. Furthermore, polymerizations performed in acetonitrile, which has a dielectric constant comparable to nitromethane and hence should

have a large population of monomeric species (lack of free chloride anions), produced heavily-chlorinated P3ATs (cf. Section 2.5.7, Figure 2.21). Thus, it becomes clear that although a solvent's polarity may contribute to the state of iron(III) chloride in solution, the solvent's Lewis basicity and acidity contribute to the activity of such species as an oxidant for these polymerizations as well as influencing the materials final structural characteristics.

It has been reported that strong donor solvents, such as diethyl ether or pyridine, form strongly solvated monomers of iron(III) chloride and that solvents having weak dononicity, such as benzene or chloroform, will cause formation of dimers.[25] Because it is also clear that solvents having high dielectric constants and low donor ability, such as nitromethane, also form the monomeric species of ferric chloride,[19,20] it is reasonable to assume that both properties influence solvation and complexation of iron(III) chloride, which creates an equilibrium of active species that influence the polymerization of 3-hexylthiophene. This is in agreement with the results seen for polymer formed in acetonitrile; a solvent which has been reported to form the tetrachloroferrate ion (monomeric species),[22] has a high dielectric constant (comparable to nitromethane), but possesses a donor number more than twice that of nitromethane. In fact, Drago et al. did report that solvents of higher donicity will result in more chloride dissociation from $FeCl_3$ than weak ones and that charge separation is facilitated by solvents of higher dielectric constant, while inhibited by those with a low dielectric constant.[19]

The lack of polymerization in diethyl ether can be explained by the same phenomena. In a similar study working with poly(pyrrole)s using iron(III) chloride as an oxidant, Myers noted that no polymerization reactions occurred in very strong donor solvents.[4] In this study by Myers, the solvents included pyridine and DMSO. Contrary to the studies performed in the works presented herein, Myers reported polymerization to occur in diethyl ether albeit limited. Myer's study measured the primary and secondary exotherms exhibited for the addition of iron(III)

chloride to the solvent, followed by the addition of monomer to the solvent-$FeCl_3$ complex. He was able to show a direct correlation between the intensity of the secondary exotherms and the yields of polymers produced. In solutions with high donor solvents, a very strong primary exotherm was produced followed by no secondary exotherm and consequently no polymerization. In the case of diethyl ether, a moderate primary and secondary exotherm were exhibited thus leading to a small yield of product. Hence there appears to be a competition between solvent and monomer for interaction with the oxidant. Iron(III) chloride is a strong Lewis acid. Therefore, if the solvent possesses strong donicity (Lewis basicity), then there is a strong interaction between the two. In the case of a weakly basic monomer, such as the pyrrole, there will be limited interaction with the oxidant to form a minimal amount of polymer. The complete lack of polymerization encountered when using 3-hexylthiophene as a monomer may then be explained by the fact that it is a softer Lewis base than the pyrrole monomer under the same conditions.

In order to investigate this matter, several solvents (cf. Table 2.1) varying in polarity, Lewis acidity (AN), and basicity (DN) were chosen as the solvents in which to perform polymerizations of 3-hexylthiophene. The oxidant-to-monomer ratio for these reactions was held constant at 1:1 (cf. Section 2.2.2), thus limiting chlorination directly from oxidant. It has already been shown in our labs that the oxidant-to-monomer ratio directly affects the extent of chlorination seen in P3ATs formed in chloroform and nitromethane.[6] Both of these solvents vary greatly in dielectric constants (4.8 and 38 at 25 °C) and have appreciably large acceptor numbers (23.1 and 20.5). They are both also weak donors (negligible and 2.7). Because chloroform and nitromethane only vary greatly in their dielectric constants, an in-depth study of solvents with larger variances in other physical properties was of utmost importance. Obviously, it would have been desirable to investigate solvents that exhibit trends where two of the three variables remain

constant throughout, thereby varying only one of the physical properties. Unfortunately, this is a relatively difficult proposition as most solvents exhibit differences in all three physical characteristics.

Solvent	Dielectric Constant @ 25 °C	AN[1]	DN[2]	$E_T(30)$	M_N (Da)	M_W (Da)	*PDI*	Regioregularity
chloroform	4.8	23	negligible	39.1	19,500	36,600	1.88	77%
carbon tetrachloride	2.2	8.6	negligible	32.4	56,600	119,000	2.1	74%
methylene chloride	9.1	20.4	1	40.7	44,700	69,000	1.55	75%
1,2-dichloroethane	10.4	100*	–	41.3	53,500	86,100	1.61	81%
acetonitrile	36.6	19.3	14.1	45.6	23,700	33,200	1.4	75%
nitromethane	37	20.5	2.7	46.3	38,100	48,800	1.28	67%
nitrobenzene	35.7	14.8	4.4	41.2	18,400	23,000	1.26	64%
benzene	2.27	8.2	0.1	34.3	97,200	215,000	2.21	71%
n-hexane	1.9	0	0	31	44,700	92,800	2.08	58%

*1,2-dichloroethane is used as a reference solvent with $SbCl_5$ for empirical DN measurements.
[1]acceptor number
[2]donor number

Table 2.1 Solvents employed for the production of P3HTs by chemical oxidation with ferric chloride. The physical properties of solvents are included, along with physical properties of polymers resulting from polymerizations performed in each solvent.

For instance, carbon tetrachloride, chloroform, and methylene chloride were employed for polymerizations as each differs by singular addition of chlorine atoms. Additionally, 1,2-dichloroethane was used because of the additional carbon atom while still remaining adequately chlorinated, as well as the fact that 1,2-dichloroethane is used as a reference solvent with $SbCl_5$ for empirical measurements of donicity for other solvents and this solvent is arbitrarily given the acceptor number assignment of 100. As a result, it is considered to be a strong Lewis acid with negligible donor strength. Both carbon tetrachloride and chloroform are extremely nonpolar and

considered inert solvents. Their dielectric constants are similar at 2.7 and 4.8, but there is a large difference in acceptor numbers, specifically 8.6 (CCl_4) and 23.1 ($CHCl_3$). P3ATs formed in carbon tetrachloride, as qualitatively analyzed with MALDI-ToF-MS, possess a greater abundance of oligomers having one and two chlorine additions than solely hydrogen-terminated oligomers (cf. Figure 2.6) compared to those formed in chloroform (cf. Figure 2.3). Notably, polymer produced in chloroform exhibits possible additions of three and four chlorines. Although polymer formed in carbon tetrachloride may also possess multiple chlorination that could not be observed in the MALDI-ToF mass spectrum, due to discrimination attributed to the excessive extent of the observable chlorination. Ionization discrimination is likely occurring due to the excessive chlorination of materials formed in carbon tetrachloride, which is obscuring the detection of oligomers possessing 3–4 chlorine additions. Furthermore, the oligomers representing the addition of 3–4 chlorines seen in the spectrum for polymer produced in chloroform (cf. Figure 2.3) do not have complete isotopic agreement between the calculated isotopic patterns compared to the experimental patterns and chlorine atoms may not be covalently bonded to the oligomer chains or may be bonded without deprotonation occurring. For this reason, the comparison of the extent of chlorination between the materials formed in chloroform and carbon tetrachloride is based on oligomer patterns representing one and two chlorine additions. Chloroform and methylene chloride have similar acceptor numbers of 23.1 and 20.4, but methylene chloride has a dielectric constant roughly twice that of chloroform (10.7 versus 4.8). The MALDI-ToF mass spectra of P3HTs made with methylene chloride (cf. Figure 2.9) exhibited observably less chlorination than those made in chloroform (cf. Figure 2.3).

The additional chlorination of P3ATs formed in CCl_4 as compared to $CHCl_3$, taking into account oligomer patterns for the addition of one and two chlorines, may be accounted for by the much smaller AN for carbon tetrachloride. Both solvents are very nonpolar and weakly basic,

therefore the majority of iron(III) chloride species present should be in the dimeric state. Thus, the prominent anion in solution should be the chloride ion, which is reported to have a DN of 26.6 in aprotic solvents.[10] Because the donor strength of the chloride anion is lowered by an increase in AN of the solvent,[10] it makes sense that the P3ATs formed in CCl_4 are more chlorinated. Less chlorination of P3ATs formed in methylene chloride may be attributed to the differences in polarity between the two solvents. Both solvents have large acceptor numbers, causing more or less equal reduction in the basicity of the chloride anion. However, CH_2Cl_2 is twice as polar as $CHCl_3$ and CH_2Cl_2 shifts the equilibrium of the population distribution of ferric chloride species to the monomeric form (tetrachloroferrate anion). Thus, less chloride anions present in CH_2Cl_2 solution should result in the formation of P3HT with less chlorination as observed in the MALDI-ToF mass spectrum of the material formed in methylene chloride.

Polymers formed by chemical oxidation using 1,2-dichloroethane (DCE) provided interesting results. DCE has a dielectric constant similar to that of methylene chloride (10.4 and 10.7 at 25 °C, respectively), but as explained in Section 2.1.2 its acceptor number is arbitrarily assigned for reference purposes. However, for the purposes of this work the AN was considered to be such as to reflect strong Lewis acid characteristics. Chlorination levels of P3ATs formed in DCE (cf. Figure 2.12) were approximately equivalent to those for polymer formed in CH_2Cl_2 (cf. Figure 2.9). This phenomenon may indicate that the acceptor strengths for both solvents are similar (AN ~ 20), although this conclusion is unsupported.

Conversely, other solvents studied had much larger dielectric constants than those solvents mentioned above; these include nitromethane, nitrobenzene, and acetonitrile. Nitromethane has a dielectric constant of 38 (at 25 °C) and an AN of 20.5 with a DN of 2.7. Previous work in our labs showed that the use of nitromethane combined with lowering the oxidant to monomer ratio (2.58:1) dramatically diminished the extent of chlorination to P3HTs

compared to those formed in chloroform.[6] Nitrobenzene has a dielectric constant of 35.7 (at 25 °C), slightly lower than that of nitromethane, and it has an acceptor number of 14.8 and a donor number of 4.4. Acetonitrile possesses a dielectric constant of 36.6 (at 25 °C), an AN of 19.3 and a DN of 14.1. Overall chlorination in these solvents was considerably less than the previously discussed much less polar solvents; this observation is presumed to be due to the fact that the prominent oxidant species in polar solvents will be monomeric, having a majority of tetrachloroferrate anions present in solution.

The extent of chlorination for P3HTs formed in nitromethane (cf. Figure 2.15) is quite close to that found in materials formed in nitrobenzene (cf. Figure 2.18). However, there appears to be slightly less chlorination in materials formed in nitromethane as qualitatively observed in the MALDI-ToF mass spectra of the two polymers. Given the fact that the dielectric constants of the two solvents are more or less equal and both solvents have relatively low donor strengths, the minimal differences seen in the extent of chlorination may be attributed to the difference in Lewis acid strength. Hence, polymer formed in nitrobenzene with an AN of 14.8 displays slightly more chlorination as compared to polymer formed in nitromethane, with an AN of 20.5, because of greater extent of interaction between nitromethane and any chloride anions (dimeric form) in the reaction solution. However, the small differences seen in the extent between chlorination as compared with P3HTs formed in more nonpolar solvents implies that the Lewis acidity of solvents having a high dielectric number does not affect the level of chlorination to the extent that it does in more nonpolar solvents.

Polymer formed in acetonitrile exhibited far more chlorination compared to that formed in either nitromethane or nitrobenzene. Acetonitrile has a dielectric constant similar to that of nitromethane and nitrobenzene. Acetonitrile also exhibits strong Lewis acid characteristics, having an AN of 19.3. Therefore, the differences seen in the extent of chlorination to materials

formed in acetonitrile may be attributed to the fact that acetonitrile also has a relatively high donor strength. The duality in the Lewis characteristics of acetonitrile–having both donor and acceptor capacity–could lead to competitive interactions between this solvent and the active forms of the oxidant species in solution, resulting in a higher percentage of chloride anions able to interact with the oxidized polymer chains.

The remaining solvents, benzene and hexane, are relatively inert solvents. Benzene and *n*-hexane are both very nonpolar solvents, having dielectric compounds of 2.27 and 1.9 at 25 °C. Benzene possesses an AN of 8.2 and a DN of 0.1. Hexane possesses an AN of 0 and a DN of 0. Therefore, the only appreciable difference between the two solvents lies with their Lewis acidity. Polymer formed in both benzene and hexane exhibited a large extent of chlorination (cf. Figures 2.24 and 2.27). It is difficult to determine the differences in the extent of P3HT chlorination due to the difficulties in obtaining high-quality MALDI-ToF mass spectra for polymer formed in benzene. This difficulty may be attributed to the fact that polymer formed in this solvent possessed a much larger average molecular weight (M_N ~ 92,000 Da) than polymer formed in hexane (M_N ~ 45,000 Da). Nonetheless, it may be the case that such a difference in acceptor strength seen between benzene and hexane may not dramatically affect the extent of chlorination for materials formed in such nonpolar solvents.

2.6.2 Solvent Influences on the Regioregularities of P3HTs Made by Means of Chemical Oxidation

In regards to regioregularity of P3ATs formed in solvents possessing different physical properties by means of chemical oxidation, it appears that regioregularity is affected mainly by the dielectric constant of the solvent, but also to a slight degree by the Lewis acid and base characteristics of the solvents. The regioregularities of materials formed in various solvents are listed in Table 2.1. In general, the use of less polar solvents–such as chloroform (77%

regioregular), carbon tetrachloride (74% regioregular), methylene chloride (75% regioregular), and 1,2-dichloroethane (81% regioregular)–produce polymers with greater structural regularity than those made in polar solvents, such as nitromethane (67% regioregular), and nitrobenzene (64% regioregular). Although, the ^{1}H-NMR data for P3HT formed in acetonitrile (75% regioregular) indicate that Lewis acid and base characteristics of the solvent may also influence regioregularities.

The exact nature of the mechanism for polymerization for thiophenes is still not fully understood, as discussed in Section 1.2.7. It is typically agreed that upon homocoupling of thiophenes and pyrroles occurs via a radical or radical cation coupling mechanism.[2] This may occur as a result of reactions between two radical species, or a radical species and a neutral monomer. Furthermore, these couplings may occur between monomers and oligomers, or oligomers and other oligomers after initial dimerization.[45-48] Lacroix et al. investigated the coupling rates for individual pyrrole oligomers of increasing chain length in various degrees of oxidation by means of electrochemical synthesis to determine the prominent means of coupling between either oligomers and monomer units (as a radical cation, RC, or neutral), or oligomers and other oligomers.[49] In these studies, initial gas-phase calculations were performed and then solvent effects were incorporated into the calculations by modeling the two extreme cases of solvation with water and hexane. Lacroix determined that in the formation of oligomers up to sexipyrrole (n = 6), the oligomer-monomer reactions are faster than oligomer-oligomer reactions regardless of the solvent used. This assumes that local concentrations of all reacting species remain similar throughout, which is not the case during the chemical oxidation of these materials.

Thus, Lacroix's results may not definitively reflect the exact nature of formation of long polymers by chemical oxidative coupling. Still, it is known that the oxidation potential of

oligomer chains decreases with increasing chain length.[47] Lacroix reported from his calculations that the pentapyrrole oligomer is oxidized to form a dication at a potential lower than that needed for the one-electron oxidation of pyrrole monomer.[49] Furthermore, it was shown that the formation of a monomer radical species is not necessary for electrochemical polymerization of pyrroles to occur.[47] It was proposed that once pyrrole dimers are formed–where dimer formation is the rate-determining step–the oxidized dimers (having a lower oxidation potential than monomers) attack neutral monomers and thereby continue chain growth. Furthermore, coupling solely between small oligomers (i.e. dimer-dimer and trimer-trimer) as starting material for polymerization compared to starting with monomer species of either pyrrole or thiophene has been shown to produce increasingly disordered polymer.[49] Lacroix noted that these empirical findings provide indirect proof that polymerization occurs via monomer-oligomer coupling because polymer formed using monomer substrate as a starting material displays higher degrees of regioregularity. Still, it is more likely that these different coupling mechanisms coexist and compete [25,27-29] to various degrees in a fashion that is dependent on the nature of the physical properties of the solvent employed for the polymerizations.[45,49]

Lacroix indicates from the molecular modeling used for his study it was suggested that for the electrochemical synthesis of long oligo(pyrrole)s from a solution containing pyrrole monomer as a starting substrate the predominant mechanism for chain growth may change during the growth process. Furthermore, the coupling mechanism is directly dependent on the solvent and the oligomer length.[49] Lacroix described a complex kinetic competition between coupling mechanisms including oligo(pyrrole) radical cations, monomer cations, and neutral monomers in solvents having different polarities that culminates in the presence of sexi(pyrrole) oligomers becoming the predominate species present in the reaction. He claimed that in water, an extremely polar solvent, the primary reaction to form sexi(pyrrole) will be the coupling

between the penta(pyrrole) dication + pyrrole RC. Whereas, in a nonpolar solvent the primary reaction to form sexi(pyrrole) involves coupling between the penta(pyrrole) dication + neutral pyrrole monomer. Lacroix further clarifies that his calculations suggest that the predominant mechanism involved in the electrosynthesis of long oligo(pyrrole)s may change during the growth process at some point, which will depend on the solvent the reaction is run and the length of the oligomer. He states that the solvent effects are strong enough in water to make oligo(pyrrole) radical cation dimerization slower as the oligomer chain length increases, while in nonpolar solvents additional reduction of the electrostatic interaction by counteranion effects or ion pairing will be needed to reach a similar situation.

Although Lacroix claimed that in water the polymer growth goes through the monomer-oligomer mechanism rather than the oligomer-oligomer mechanism, he admitted that this is assuming that concentrations of reacting all reacting species remains similar and he noted that the difference in solvent effects on the competing reactions is smaller in water than in nonpolar alkane solvent. Moreover, he suggests that there might be a solvent somewhere between water and alkane in which solvent and counteranion effects might be strong enough to critically influence the lifetimes of different radical cation species.

Again, Lacroix's calculations assumed that all local concentrations of reacting species involved remain constant throughout, although this is not the case in chemical oxidation. Therefore, if Lacroix's work is applied to thiophene coupling by chemical oxidation and it is assumed that a large concentration of monomer is consumed to form sexi(thiophene) regardless of solvent, at some point in the chemical oxidation reaction the primarily abundant reactive species in solution will be the sexi(thiophene). At this point, according to Lacroix's calculations, in nonpolar solvents the reaction may proceed at a faster rate by means of oligomer radical cation

+ neutral monomer coupling, which has been shown to be the synthetic pathway that results in increased the regioregularity of the polymer.[46,47]

In polar solvents, if it assumed that there exists an excess of sexi(thiophene) cations or dications, it is also be assumed that there is a smaller population of thiophene RC and neutral monomers as compared to thiophene radical-cation oligomers given the decrease in oxidation potential of oligomers with increasing chain length. Furthermore, the stability of the dication species not only increases with oligomer length, but through contributions by electrostatic interaction from the polar solvent, which is suggested as the major contributor of radical cation/solvent interactions outlined by Lacroix. Thus in polar solvents, the dication species may become the primary species and it is reasonable to predict that the main source of long polymer growth may be radical-cation oligomer-to-radical-cation oligomer interactions, which would proceed at a slower rate than dication + RC or neutral monomer coupling but predominate due to population issues. Hence, the decrease in regioregularity seen in materials formed in more polar solvents may be the result of RC oligomer-RC oligomer coupling that has been shown to form more irregular materials. This scenario may also explain the slower kinetic rates of polymerization measured in acetonitrile compared to chloroform.[5]

This explanation may help to explain the differences observed here in the regioregularity between P3HTs formed in nonpolar and polar solvents. It is likely that polymerization proceeds more so by RC oligomer-to-monomer coupling in nonpolar solvents, whereas RC oligomer-to-RC oligomer coupling occurs predominantly in polar solvents. Furthermore, the role of the alkyl chain on the 3-position of the thiophene ring to sterically direct coupling must be accounted for. For instance, the conformation of the alkyl chain should be dependent on the polarity of the solvent employed. In nonpolar solvents the alkyl chain should be fully extended, and in polar solvents the chain may fold in upon itself due to hydrophobic interactions with the solvent. As a

result, coupling in nonpolar solvents would tend to occur between the 2 and the 5 positions of the aryl ring in a head-to-tail fashion, as it is the least sterically hindered approach between monomer units and/or coupling between monomer units and oligomers.

This reasoning does not fully explain the regioregularity of materials formed in acetonitrile, which display regularities similar to those seen for more nonpolar solvents. Acetonitrile has a dielectric constant similar to nitromethane, but it has more donor strength (DN = 14.1) and slightly Lewis acid characteristic (AN = 19.5). The complex effects of the dual acceptor-donor nature of this solvent are made clear by the extent of chlorination to the resulting polymer formed in acetonitrile, which is considerably more than that seen for nitromethane. Lacroix explains that ion pairing, which was not modeled in his experiments and reduces electrostatic interactions may greatly effect radical cation lifetimes.[49] In fact, he indicates that there may be solvents some where between water and alkane in which solvent and counterion effects may be strong enough to make pyrrole, bipyrrole, and terpyrrole radical lifetimes identical.[49] This may offer some insight into the complex equilibrium of polymerization mechanisms encountered when acetonitrile is used as a solvent medium for the production of P3HTs by means of chemical oxidation with ferric chloride.

2.7 Conclusions

Poly(3-hexylthiophene)s formed by chemical oxidation with iron(III) chloride using different solvents possessing contrasting physical properties display various structural characteristics that may be attributed to contributions from solvent effects. However, there are difficulties making concrete determinations as to which physical properties of a given solvent directly impact the structural variations seen in the assorted P3HTs presented here. The difficulty arises in part due to the variability of parameters in the physical properties of the solvents. For instance, while considering a particular pair of solvents with which to examine the

affect of Lewis basicity, there may be a considerable difference in the dielectric constants of each solvent as well. Therefore, a consistent trend in physical properties between a series of different solvents is not easy to obtain. Secondly, it appears that the influences of a particular solvent to the physical properties of the resulting polymer must be considered as a result of a combination of all physical properties (i.e. dielectric constant, Lewis acidity, and Lewis basicity) simultaneously and individual physical properties cannot alone be credited as influencing the final properties of the polymer. However, inferences may be made as to the broader impact of a solvent's physical properties on the characteristics of the resulting P3HTs formed by chemical oxidation with ferric chloride in various solvents.

These results have shown that the extent of chlorination seen for the resultant P3HTs is affected by the polarity of the solvents. For instance, polymers formed in nitromethane and nitrobenzene have considerably less chlorination than those formed in more nonpolar solvents, such as chloroform and carbon tetrachloride. It is less clear whether or not the Lewis acidity of a solvent contributes to the extent of chlorination as well. However, it seems reasonable to expect solvents with stronger Lewis acid characteristics to produce material displaying less chlorination because the solvent may interact with the chloride ions in solutions and inhibit nucleophilic addition to the polymer through complexation, or by decreasing the donicity of the anion. The comparison of polymers produced in nonpolar solvents with similar dielectric constants, such as chloroform and carbon tetrachloride, but that vary in acceptor characteristics display this behavior to some extent. Furthermore, polymers produced in more polar solvents, such as nitomethane and acetonitrile that have appreciable differences in Lewis acid characteristics also display an increase in chlorination with a decrease in acceptor number. However, acetonitrile possesses a greater Lewis basicity than is exhibited by nitromethane. Finally, solvents

possessing a donor number that outweighs the solvent's AN do not allow for polymerization at all, due to the strong interactions of the solvents with the oxidant.

The regioregularity of polymers produced in different solvents seems to be a direct result of the polarity of the solvent. For instance, polymers formed in more nonpolar solvents–such as chloroform, carbon tetrachloride, methylene chloride, and 1,2-dichloroethane–tend to have a greater degree of regioregularity than those produced in more polar solvents, such as nitromethane and nitrobenzene. This phenomenon may be a result of the mechanistic pathway with which the material couples during the formation of longer polymer chains. A reasonable assumption is that materials formed in more polar solvents grow as a result of oligomer-to-oligomer coupling, whereas materials formed in more nonpolar solvents couple together by oligomer-to-monomer reactions. However, materials formed in acetonitrile, a polar solvent with a dielectric constant of 36.6, are the exception because they possess greater regioregularity compared to other polymers formed in more polar solvents. It would seem then that Lewis acidity and basicity may impact the mechanisms of polymer formation via a complicated combination of effects.

The effects of solvent interactions on the molecular weights of these materials are also difficult to explain. It would seem that materials formed in more nonpolar solvents produce higher weight materials over all, with chloroform being the exception, as compared to those produced in more polar solvents. This may be attributed to the regioregularity of the materials as polymers formed in more nonpolar solvents display greater regioregularity than those formed in more polar solvents. The coupling mechanism that influences the regioregularity of these materials may also contribute to the extent to which they couple and the same coupling mechanisms that result in more structural defects within that polymer may also contribute to the early termination of the polymerization. Furthermore, materials that exhibit the largest

molecular weights were those formed in the most nonpolar solvents, such as carbon tetrachloride, benzene, and hexane. This may be due to the insolubility of the oxidant in these solvents, which would facilitate polymerization to occur directly on the surface of the solid crystalline ferric chloride. The close proximity of polymerization events on the surface of the solid oxidant could contribute to the higher molecular weights exhibited by the resulting polymers.

Despite the fact that no clear trend or correlation was observed between the physical properties of the solvents investigated within this work (i.e. dielectric constant, acceptor number, and donor number) and the resulting structural characteristics of the P3HTs formed in those solvents, perhaps there exists an empirical scale of solvent polarity that may still aid in explaining the phenomena characterized in this Chapter. One such empirically determined scale is the $E_T(30)$ scale, which is defined as the molar transition energy, in kcal mol^{-1}, for the long wavelength electronic transition of 2,6-diphenyl-4-(2,4,6-triphenylpyridinio)phenolate dye (Dimroth-Reichardt's betaine dye) as a solution in the solvent under investigation at 25 °C and a pressure of 0.1 MPa.[50] The $E_T(30)$ values for the solvents investigated within this Chapter are included in Table 2.1. Unfortunately, there exists no well-defined correlation between the $E_T(30)$ values and the structural characteristics of the resulting polymers formed in the corresponding solvents. However, there are at least 183 other empirically determined quantitative measures of solvent polarity reported in the literature.[51]

Christian Reichardt defined "solvent polarity" as "the overall solvation capability (or solvation power) for reactants and activated complexes, as well as for molecules in the ground and excited states, which in turn depends on the action of all possible, specific and nonspecific, intermolecular forces between solvent and solute molecules, including Coulomb interactions between ions, directional interactions between dipoles, and inductive, dispersion, hydrogen

bonding, and charge-transfer forces, as well as solvophobic interactions. Only those interactions leading to definite chemical alterations of the solute molecules through protonation, oxidation, reduction, complex formation, or other chemical processes are excluded."[51,52] Reichardt's definition clearly suggests that solvent polarity cannot be uniquely assessed quantitatively by any single physical constant.[51] Although three different solvent properties, specifically dielectric constant, acceptor number, and donor number, were investigated in these works, it is clear from the results of this study that the solvent effects encountered during chemical oxidation with ferric chloride to form P3HTs play an intricate role in the very complicated reaction equilibrium involved for this type of polymerization.

In general, it has been shown that the effects of the physical properties of the solvent employed to form P3HTs by chemical oxidation with iron(III) chloride can greatly impact the structural characteristics of the resulting polymer in a variety of ways. The differences in structural properties seen for the various polymer products cannot be attributed to a particular property of a given solvent. Nonetheless, a solid foundation has been built for further inquiry into the matter. Because chemical oxidation of poly(3-alkythiophene)s is such a valuable method for the formation of these unique materials, an understanding of the influence from a particular solvent is crucial for the ability to vary the physical properties of the polymers produced by this method. These results show that chemical oxidation holds much promise to remain the most prominent means for the formation of P3ATs due to its ease and affordability, and the potential to tailor the physical properties of polymers formed by this means increases the value of the technique, as well as making polymer formed in this manner more applicable to a broader range of applications and devices. Still, further inquiry into the ability to tailor these materials through manipulation of solvent parameters will undoubtedly reveal even more valuable knowledge on the matter.

2.8 References

(1) Sugimoto, R.; Takeda, S.; Gu, H. B.; Yoshino, K. Preparation of Soluble Polythiophene Derivatives Utilizing Transition Metal Halides as Catalysts and Their Property. *Chemistry Express*. **1986**, *1*, 635-638.

(2) Skotheim, T. A.; Elsenbaumer, R. L.; Reynolds, J. R. *Handbook of Conducting Polymers*; 2 ed.; Marcel Dekker Inc.: New York, 1998,

(3) Niemi, V. M.; Knuuttila, P.; Osterholm, J. E.; Korvola, J. Polymerization of 3-Alkylthiophenes with Ferric Chloride. *Polymer*. **1992**, *33*, 1559-1562.

(4) Myers, R. E. Chemical Oxidative Polymerization as a Synthetic Route to Electrically Conducting Polypyrroles. *Journal of Electronic Materials*. **1986**, *15*, 61-69.

(5) Olinga, T.; Francois, B. Kinetics of Polymerization of Thiophene by Fecl3 in Chloroform and Acetonitrile. *Synthetic Metals*. **1995**, *69*, 297-298.

(6) Brauch, R. M. Structural Characterization of Poly (Heterocycle)S Formed Using Oxidative Methods. Ph.D. Dissertation, Louisiana State University and A&M College, Baton Rouge, 2006.

(7) Lewis, G. N. Valence and the Electron. *Transactions of the Faraday Society*. **1923**, *19*, 452-458.

(8) Zuffanti, S.; Luder, W. F. Generalized Acids and Bases in Organic Chemistry. I. Catalytic Condensation of Aldehydes. *Journal of Chemical Education*. **1944**, *21*, 485-487.

(9) Rice, R. V.; Zuffanti, S.; Luder, W. F. Acids and Bases. *Analytical Chemistry*. **1952**, *24*, 1022-1024.

(10) Gutmann, V. *The Donor-Acceptor Approach to Molecular Interactions*; Plenum Press: New York, 1978,

(11) Lindqvist, I.; Zackrisson, M. Relative Donor Strengths: A Thermochemical Study. *Acta Chemica Scandinavica*. **1960**, *14*, 453-456.

(12) Branden, C. I.; Lindqvist, I. The Crystal Structures of the Adducts Sbcl5.Pocl3, Sbcl5.(Ch3)3po, and Nbcl5.Pocl3. *Acta Chemica Scandinavica*. **1963**, *17*, 353-361.

(13) Gutmann, V.; Wychera, E. Coordination Reactions in Nonaqueous Solutions. The Role of the Donor Strength. *Inorganic and Nuclear Chemistry Letters*. **1966**, *2*, 257-260.

(14) Gutmann, V. Properties of Donor Solvents and Coordination Chemistry in Their Solutions. *New Pathways in Inorganic Chemistery*. **1968**, 65-86.

(15) Mayer, U.; Gutmann, V.; Gerger, W. Acceptor Number. Quantitative Empirical Parameter for the Electrophilic Properties of Solvents. *Monatshefte fuer Chemie*. **1975**, *106*, 1235-1257.

(16) Maine, P. A. D. D.; Koubek, E. Inorganic Salts Dissolved in Nonaqueous or in Mixed Solvents. I. Spectrophotometric and Conductometric Studies of Anhydrous Ferric Chloride Dissolved in Pure Nitromethane or in Nitromethane-Carbon Tetrachloride. *Journal of Inorganic and Nuclear Chemistry*. **1959**, *11*, 329-335.

(17) Fajer, J.; Linschitz, H. State of Iron(Iii) Chloride in Nonaqueous Solvents. *Journal of Inorganic and Nuclear Chemistry*. **1968**, *30*, 2259-2262.

(18) Friedman, H. L. The Visible and Ultraviolet Absorption Spectrum of the Tetrachloroferrate(Iii) Ion in Various Media. *Journal of the American Chemical Society*. **1952**, *74*, 5-10.

(19) Drago, R. S.; Hart, D. M.; Carlson, R. L. Spectrophotometric Studies of Iron(Iii) Chloride in Nonaqueous Solvents. *Journal of the American Chemical Society*. **1965**, *87*, 1900-1904.

(20) Swanson, T. B.; Laurie, V. W. Electron Magnetic Resonance and Electronic Spectra of Tetrachloroferrate(Iii) Ion in Nonaqueous Solution. *Journal of Physical Chemistry*. **1965**, *69*, 244-250.

(21) McCusker, P. A.; Kennard, M. S. Interaction of Iron(Iii) Compounds with Ethers. Ii. Spectrophotometric Study of Anhydrous Iron(Iii) Chloride and Tetrachloroferric(Iii) Acid in Dioxane and Other Ethers. *Journal of the American Chemical Society*. **1959**, *81*, 2976-2982.

(22) Vertes, A.; Nagy-Czako, I.; Burger, K. Moessbauer Study of Equilibrium Constants of Solvates. 3. Solvent-Solute Interactions in Nonaqueous Solutions of Iron(Iii) Chloride. *Journal of Physical Chemistry*. **1978**, *82*, 1469-1473.

(23) Work, R. A., III; McDonald, R. L. Nature of Iron(Iii) Chloride in Benzene. *Inorganic Chemistry*. **1973**, *12*, 1936-1938.

(24) Carlson, R. L. I. Molecular Complexes of Iodine Ii. The Behavior of Ion (Iii) Chloride in Non-Aqueous Solvents. Ph.D. Dissertation, University of Illinois, Urbana, 1962.

(25) Wells, A. F. *Structural Inorganic Chemistry*; 3 ed.; Clarendon Press: Oxford, 1962,

(26) Stanke, D.; Hallensleben, M. L.; Toppare, L. Oxidative Polymerization of Some N-Alkylpyrroles with Ferric Chloride. *Synthetic Metals*. **1995**, *73*, 267-272.

(27) Hanton, S. D. Mass Spectrometry of Polymers and Polymer Surfaces. *Chemical Reviews (Washington, D. C.)*. **2001**, *101*, 527-569.

(28) *Maldi-Tof Mass Spectrometry of Synthetic Polymers*; Pasch, H., Schrepp, W.; Springer: New York, 2003,

(29) Nielen, M. W. F. Maldi Time-of-Flight Mass Spectrometry of Synthetic Polymers. *Mass Spectrometry Reviews*. **1999**, *18*, 309-344.

(30) McCarley, T. D.; McCarley, R. L.; Limbach, P. A. Electron-Transfer Ionization in Matrix-Assisted Laser Desorption/Ionization Mass Spectrometry. *Analytical Chemistry*. **1998**, *70*, 4376-4379.

(31) Macha, S. F.; McCarley, T. D.; Limbach, P. A. Influence of Ionization Energy on Charge-Transfer Ionization in Matrix-Assisted Laser Desorption/Ionization Mass Spectrometry. *Analytica Chimica Acta*. **1999**, *397*, 235-245.

(32) McCarley, T. D.; Noble, C. O.; DuBois, C. J., Jr.; McCarley, R. L. Maldi-Ms Evaluation of Poly(3-Hexylthiophene) Synthesized by Chemical Oxidation with Fecl3. *Macromolecules*. **2001**, *34*, 7999-8004.

(33) Liu, J.; Loewe, R. S.; McCullough, R. D. Employing Maldi-Ms on Poly(Alkylthiophenes): Analysis of Molecular Weights, Molecular Weight Distributions, End-Group Structures, and End-Group Modifications. *Macromolecules*. **1999**, *32*, 5777-5785.

(34) Montaudo, G.; Samperi, F.; Montaudo, M. S. Characterization of Synthetic Polymers by Maldi-Ms. *Progress in Polymer Science*. **2006**, *31*, 277-357.

(35) Dass, C. *Principle and Practices of Biological Mass Spectrometry*; Wiley-Interscience; New York, 2001,

(36) Belu, A. M.; DeSimone, J. M.; Linton, R. W.; Lange, G. W.; Friedman, R. M. Evaluation of Matrix-Assisted Laser Desorption Ionization Mass Spectrometry for Polymer Characterization. *Journal of the American Society for Mass Spectrometry*. **1996**, *7*, 11-24.

(37) Sakurada, N.; Fukuo, T.; Arakawa, R.; Ute, K.; Hatada, K. Characterization of Poly(Methyl Methacrylate) by Matrix-Assisted Laser Desorption/Ionization Mass Spectrometry. A Comparison with Supercritical Fluid Chromatography and Gel Permeation Chromatography. *Rapid Communications in Mass Spectrometry*. **1998**, *12*, 1895-1898.

(38) Knochenmuss, R.; Zenobi, R. Maldi Ionization: The Role of in-Plume Processes. *Chemical Reviews (Washington, DC, United States)*. **2003**, *103*, 441-452.

(39) Zenobi, R.; Knochenmuss, R. Ion Formation in Maldi Mass Spectrometry. *Mass Spectrometry Reviews*. **1999**, *17*, 337-366.

(40) Chen, H.; He, M.; Pei, J.; Liu, B. End-Group Analysis of Blue Light-Emitting Polymers Using Matrix-Assisted Laser Desorption/Ionization Time-of-Flight Mass Spectrometry. *Analytical Chemistry*. **2002**, *74*, 6252-6258.

(41) Holdcroft, S. Determination of Molecular Weights and Mark-Houwink Constants for Soluble Electronically Conducting Polymers. *Journal of Polymer Science, Part B: Polymer Physics*. **1991**, *29*, 1585-1588.

(42) Pearson, D. L.; Schumm, J. S.; Tour, J. M. Iterative Divergent/Convergent Approach to Conjugated Oligomers by a Doubling of Molecular Length at Each Iteration. A Rapid Route to Potential Molecular Wires. *Macromolecules*. **1994**, *27*, 2348-2350.

(43) Andersson, M.; Wittgren, B.; Wahlund, K.-G. Accuracy in Multiangle Light Scattering Measurements for Molar Mass and Radius Estimations. Model Calculations and Experiments. *Analytical Chemistry*. **2003**, *75*, 4279-4291.

(44) Qi, Z.; Pickup, P. G. Reactivation of Poly(3-Methylthiophene) Following Overoxidation in the Presence of Chloride. *Journal of the Chemical Society, Chemical Communications*. **1992**, 1675-1676.

(45) Andrieux, C. P.; Audebert, P.; Hapiot, P.; Saveant, J. M. Identification of the First Steps of the Electrochemical Polymerization of Pyrroles by Means of Fast Potential Step Techniques. *Journal of Physical Chemistry*. **1991**, *95*, 10158-10164.

(46) Guyard, L.; Hapiot, P.; Neta, P. Redox Chemistry of Bipyrroles: Further Insights into the Oxidative Polymerization Mechanism of Pyrrole and Oligopyrroles. *Journal of Physical Chemistry B*. **1997**, *101*, 5698-5706.

(47) Wei, Y.; Chan, C. C.; Tian, J.; Jang, G. W.; Hsueh, K. F. Electrochemical Polymerization of Thiophenes in the Presence of Bithiophene or Terthiophene: Kinetics and Mechanism of the Polymerization. *Chemistry of Materials*. **1991**, *3*, 888-897.

(48) Wei, Y.; Tian, J.; Yang, D. A New Method for Polymerization of Pyrrole and Derivatives. *Makromolekulare Chemie, Rapid Communications*. **1991**, *12*, 617-623.

(49) Lacroix, J.-C.; Maurel, F.; Lacaze, P.-C. Oligomer-Oligomer Versus Oligomer-Monomer C2-C2' Coupling Reactions in Polypyrrole Growth. *Journal of the American Chemical Society*. **2001**, *123*, 1989-1996.

(50) Reichardt, C. Solvatochromic Dyes as Solvent Polarity Indicators. *Chemical Reviews (Washington, D. C.)*. **1994**, *94*, 2319-2358.

(51) Katritzky, A. R.; Fara, D. C.; Yang, H.; Taemm, K.; Tamm, T.; Karelson, M. Quantitative Measures of Solvent Polarity. *Chemical Reviews (Washington, DC, United States)*. **2004**, *104*, 175-198.

(52) Reichardt, C. *Solvents and Solvent Effects in Organic Chemistry*; 2nd ed.; VCH: Weinheim, Germany, 1988,

Chapter 3

Overcoming the Challenges Encountered in the Molecular Weight Determination of P3HTs

3.1 Introduction

3.1.1 Mass Discrimination in the MALDI-ToF-MS Analysis of Synthetic Polymers

The effect of the molecular weight of poly(3-hexylthiophene), P3HT, with regard to the electrical and optical properties of the material–that influence its functionality and therefore aid in determining its applicability in relevant and purposeful modern applications–has been discussed in Section 1.2.9. The use and benefits of matrix-assisted laser desorption/ionization time-of-flight (MALDI-ToF) mass spectrometry for the analysis of synthetic and conducting polymers has been discussed in Sections 1.31, 1.3.2, 1.33, and 2.3.1. MALDI-ToF-MS is an invariably powerful analytical tool for the characterization of the chemical composition (repeat units), molecular weight, and molecular weight distribution of synthetic polymers, as well as endgroup (α-) and backbone (β-) additions to such systems. Because it has been shown that the structure of poly(3-alkylthiophene)s, P3ATs, determines their physical properties and hence their functionality,[1] MALDI-ToF-MS is a particularly important utility for the development of these unique materials for purposeful applications. The analysis of the molecular weight and molecular weight distribution of P3ATs by use of MALDI-ToF-MS is of utmost interest, due to the fact that these characteristics contribute greatly to the polymers overall electrical and optical properties (cf. Section 1.2.9). However, MALDI-ToF-MS has been shown to have limitations in its ability to definitively provide correct molecular weight information for synthetic polymers, due to a variety of preparation, desorption/ionization, and instrumental issues.[2-4]

MALDI-ToF-MS has the capability to provide absolute molar mass measurements and potentially garner molecular weight distributions of synthetic polymers that are more accurate than other conventional methods, such as size-exclusion chromatography (SEC) (cf. Section

2.3.2). However, synthetic polymers are typically comprised of an assortment of different length oligomer or polymer chains that vary not only in molecular weight, but also chemical composition (α- and β-substituents) and often structure (branching). These considerations are a particular concern for the analysis of poly(3-hexylthiophene)s formed by chemical oxidative methods, and the exact determination of their molecular weight or the molecular weight of any synthetic polymer by means of MALDI-ToF-MS demands that both the molar mass and the relative abundance of all species comprising the entire mass range of the polymer sample be accurately measured. Unfortunately, this is not an easy endeavor for polymer samples having a wide molecular weight distribution or a polydispersity index, *PDI*, (cf. Sections 1.3.1 and 2.3.2, Equation 1.3) greater than 1.1.[2,3,5,6]

Historically, the accuracy of MALDI-ToF-MS measurements of the molecular weight for a polymer sample have been evaluated by the use of polymer standards with given molar masses provided by the manufacturer of the polymer and obtained by the use of SEC. Still, much ambiguity between the observed results for molecular weights of synthetic polymer standard samples measured using SEC as compared to those observed by use of MALDI-ToF-MS has been reported. To further exacerbate this dilemma, one of the greatest difficulties in determining the accuracy of molecular weight data gathered via MALDI-ToF-MS is the lack of well-characterized standards with which to use as a comparative marker for such purposes.

Montaudo et al. performed a study using a variety of synthetic polymers having a wide range of polydispersity indices including poly(methylmethacrylate), PMMA, or poly(styrene), PS, and poly(ethyleneglycol), PEG.[6] Measurements obtained by MALDI-ToF-MS were used to estimate the molecular weights and molecular weight distributions of the polymer samples, and they were compared to measurements obtained by SEC. Montaudo et al. clarified that the estimation of molecular weights by means of MALDI-ToF-MS poses several dilemmas. First,

the intensity of mass peaks shown in MALDI-ToF mass spectra of mixtures of samples is proportional to the molar amount of each species, and therefore the mass spectra of polymers yield number-average molecular weights (cf. Section 1.3.1). Conversley, conventional SEC–used as a relative method and employing calibration curves determined with molecular weight standards–gives weight-average molecular weights, and this must be taken into consideration when comparing the two. Next, in order to achieve accurate molecular weight measurements by use of MALDI-ToF-MS, ionization yields of various oligomer species within the polymer sample must not undergo any discrimination with respect to their mass values. Finally, the MALDI-ToF-MS detector must show a constant response to ions over the entire range of mass numbers. These, concerns have been mentioned previously in Sections 1.3 and 2.3.1.

Montaudo et al. reported that for samples of PMMA having a narrow polydispersity (PDI < 1.10)–that are typically employed as standards for calibration of molecular weights for comparative concentration-based SEC measurements (cf. Section 2.3.2)–M_P values obtained by MALDI-ToF-MS were consistently lower than molecular weights acquired via SEC. Polymer samples are often identified by their M_P value or the mass value for the most probable (abundant) point in the SEC chromatogram. Specifically, PMMA samples having polydispersity indices between 1.04–1.06 showed M_P values in the range of 2.1–11.8% lower in molecular weight when analyzed by MALDI-ToF-MS as compared to those obtained by SEC. Furthermore, congruity between M_P values for PMMA samples having polydispersity index values between 1.08–1.10 as compared by SEC and MALDI-ToF-MS worsened, wherein measurements made by MALDI-ToF-MS were shown to be 10.6–20.5% lower in molecular weight. The results were very similar for samples of PEG and PS having narrower molecular weight distributions. Polymer samples of PEG and PS with polydispersities between 1.02–1.06 were shown to have

disparities in molecular weight that were 0.1–11.5% lower when obtained by MALDI-ToF-MS as compared to those acquired by SEC. These differences are in good agreement with the results obtained for PMMA samples.

Polymer samples having much broader molecular weight distributions were also analyzed. A PMMA sample was determined to possess a *PDI* of 2.5 and a M_P of 33,000 Da by means of comparative SEC. This same sample was then analyzed by MALDI-ToF-MS and shown to have a M_P of 2,200 Da with a *PDI* of 1.15. These values are far smaller than those obtained by SEC, giving rise to an error measurement between the two methods of 93.3%. Similarly, a PS sample with a polydispersity index of 2.0 and a M_P of 9,000 Da as determined by means of conventional SEC was evaluated using MALDI-ToF-MS. Measurements obtained via MALDI-ToF-MS determined that the PS sample possessed a M_P of 2,000 Da with a *PDI* of 1.06, indicating an error in the M_P between the two techniques of 74%. These results clearly show that MALDI-ToF-MS as a technique for the analysis of average molecular weights and molecular weight distributions of synthetic polymers, particularly those with a broad molecular weight distribution, may be unreliable and caution should be used when estimating these values by MALDI-ToF-MS.

The disparity between such observations has been attributed to several different instrumental, preparation, or processing issues. For instance, the way in which processed data is displayed and compared between measurements obtained by SEC and MALDI-ToF-MS has been scrutinized and argued to be the cause of the discrepancies between these techniques. Jackson et al. performed a study wherein they compared the molecular weight measurements for poly(methylmethacrylate), PMMA, samples of narrow polydispersity (*PDI* = 1.08) by use MALDI-ToF-MS and SEC.[7] Jackson et al. examined the variations in the M_P of the PMMA samples (as provided by the manufacturer and obtained by SEC) with their own measurements

obtained by MALDI-ToF-MS. Jackson et al. looked at a variety of PMMA samples ranging in molecular weight from 1,270–15,100 Da (PMMA1270–PMMA15100). The results of this work showed that the M_P values for PMMA polymer standards obtained by MALDI-ToF-MS were consistently lower (~ 2 repeat units) than those obtained by the manufacturer using SEC.

This study also investigated the differences seen between molecular weight measurements using SEC and MALDI-ToF-MS for polymer samples having a wide molecular weight distribution. Jackson et al. compared the size-exclusion chromatogram of commercially obtained poly(tetramethylene ethylene glycol) with the spectrum obtained for the molecular weight distribution obtained by MALDI-ToF-MS. They showed that the M_P for this sample obtained by MALDI-ToF-MS was 1,400 Da, but by SEC the same sample was shown to have an M_P of 4,000 Da. However, plotting the same SEC data as a number-fraction intensity versus a linear (or square root) mass scale had a considerable influence on the M_P as seen by SEC and was determined by this means to be 1,450 Da, which is in good agreement with the M_P obtained by MALDI-ToF-MS.

They went on to argue that the discrepancies between M_P values obtained by MALDI-ToF-MS and SEC seen for the polymer samples examined are a function of how the data are displayed between the two methods. Jackson et al. noted that M_P values used in their study and described by SEC, based on weight fractions or concentrations obtained by use of a differential refractometer or a UV photometer, are displayed as weight-fraction intensity versus a log mass scale. Whereas M_P values obtained via MALDI-ToF-MS are described in terms of a number-fraction abundance versus a linear mass axis. They went on to explain that the conversion between a linear to a log mass scale or from weight-fraction to number-fraction intensity changes the mass at which the most probable peak (M_P) appears. Jackson et al. showed that for polymer samples having narrow molecular weight distributions, the differences seen in

M_P by use of SEC and MALDI-ToF-MS are expected to be small (~ 2 repeat units), although these discrepancies increase with an increase in polydispersity. They further clarify that for polymer samples having a wide polydispersity the M_P as obtained by SEC more so represents the M_W (cf. Section 1.3.1), and therefore the term M_P should be reserved for weight-fraction versus log mass plots and not applied to molecular weight distribution obtained by MALDI-ToF-MS, because a number-fraction versus linear mass scale is employed.

Montaudo et al. later attempted to deal with the underestimation of molecular weights and molecular weight distributions encountered by the use of MALDI-ToF-MS through an off-line procedure of data manipulation.[8] This method of MALDI-ToF mass spectra processing included: (i) signal smoothing to improve the recorded traces of the spectra up to high *m/z* values, (ii) a subtraction of the misleading contribution to the signals introduced by the offset used in spectrum recording, and (iii) examination of the spectra up to the highest possible *m/z* value for better accuracy in estimating the molecular weight values. In fact, Montaudo et al. did obtain results for the average molecular weight and molecular weight distributions by use of MALDI-ToF-MS that were in fairly good agreement with those provided by the manufacturer for polydisperse PMMA samples (SEC) after applying their novel "cleaning" procedure. However, in the treatment of the data obtained by MALDI-ToF-MS, Montaudo et al. assumed that no mass discrimination occurred as a result of sample preparation, desorption/ionization, transmission, or detection issues. Furthermore, baseline subtraction, and signal smoothing on a very noisy and decaying signal is a difficult endeavor and is subject to significant errors as well as poor reproducibility.[5]

Nevertheless, because a synthetic polymer sample with a polydispersity index greater than 2 may be comprised of oligomer and polymer chains with molar masses over a *m/z* range from a few hundred to a few hundred thousand Daltons[5] and there are more often than not great

discrepancies seen between molecular weight data obtained from MALDI-ToF-MS and SEC, researchers have expended much effort in uncovering the reasons for mass discrimination seen in MALDI-ToF-MS. Nielen points out that the high molecular weight end in the mass spectrum of a polydisperse polymer sample will "disappear" much earlier into the baseline noise than the high molecular weight side of the SEC distribution, due to the fact that a small population of high molecular weight species represents only a few ions in a MALDI-ToF mass spectrum, whereas the same population will possess significant bulk properties as detected by a refractive index detector used for SEC analysis.[5] Therefore, low molecular weight data is to be expected in such a circumstance and a decaying number-fraction distribution of ions seen in MALDI-ToF mass spectra of a synthetic polymer is clearly indicative of a sample having a broad molecular weight range ($PDI > 1.1$). Still, there are many variables involved in the acquisition of reliable MALDI-ToF-MS molecular weight data of polydisperse polymer samples that contribute to the accuracy of the measurements and must be taken into account in order to obtain purposeful information regarding a polymer's molecular weight.

In regards to poly(3-alkylthiophene)s, several reports in the literature have presented MALDI-ToF mass spectra having molecular weight distributions characteristic of mass discrimination in the form of an under-representation of higher molecular weight components with the indicative decay in the signal intensity for the number-fraction distribution as the m/z increases. Lui et al. reported on the MALDI-ToF-MS analysis of highly regioregular P3HTs, having a M_N of 12,200 Da and a PDI of 1.94 determined by conventional SEC.[9] However, the M_N and PDI obtained for the same material by means of MALDI-ToF-MS were calculated to be 4,956 Da and 1.74. The MALDI-ToF mass spectrum for this sample displayed signal intensity for the number-fraction distribution decaying sharply at roughly m/z 3,000 with increasing decay as the m/z increased until the ion signal was obscured in the baseline noise at approximately m/z

16,000. Furthermore, McCarley et al. reported on the MALDI-ToF-MS evaluation of P3HTs synthesized by chemical oxidation with $FeCl_3$.[10] Their work also compared the average molecular weight measurements for a P3HT sample obtained by means of both MALDI-ToF-MS and conventional SEC. The M_N of the polymer as calculated by means of SEC was 49,000 Da, whereas the calculation by means of MALDI-ToF-MS gave an M_N of 5,500 Da. The mass distribution seen in the MALDI-ToF mass spectrum for this polymer displayed signal intensity for the number-fraction distribution decaying sharply at roughly *m/z* 4,500 with increasing decay as the *m/z* increased until the ion signal was obscured in the baseline noise soon after *m/z* 10,000.

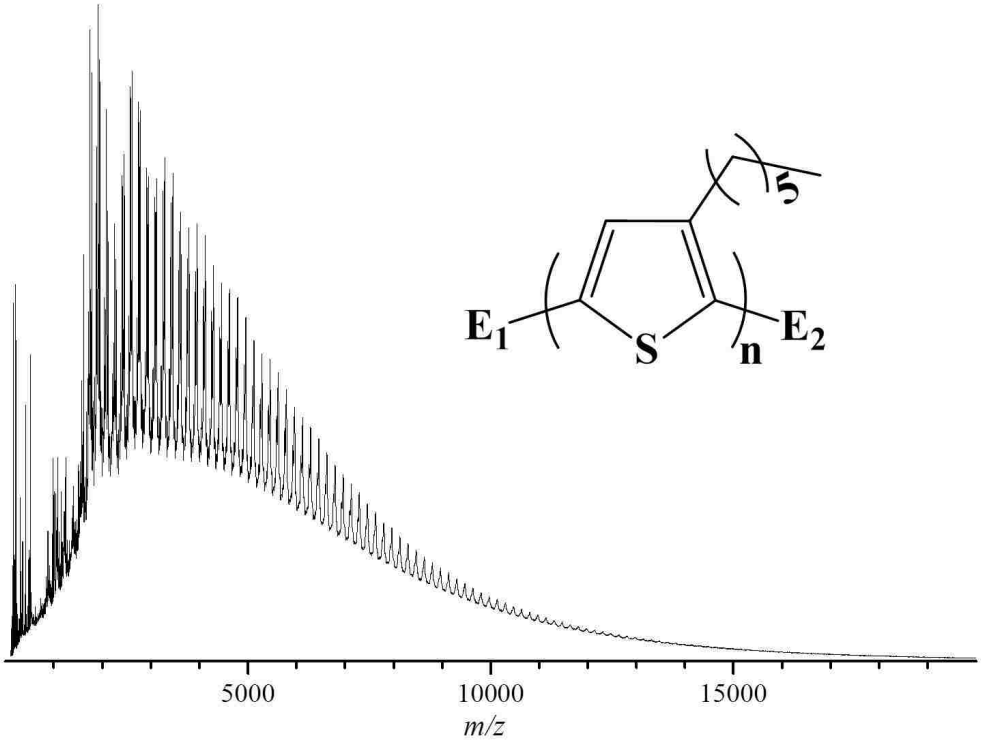

Figure 3.1 MALDI-ToF mass spectrum acquired in linear mode for polydisperse P3HT having a M_N = 66,000 Da and a *PDI* = 1.89 determined by analytical SEC-MALLS analysis.

The MALDI-ToF mass spectra presented throughout this Dissertation indicate that mass discrimination during MALDI-ToF-MS analysis of P3HTs is occurring. The mass spectra displayed herein follow a similar pattern of number-fraction distribution decay as discussed

above with large discrepancies between average molecular weights when calculated by SEC and MALDI-ToF-MS analysis. Figure 3.1 is the MALDI-ToF mass spectrum obtained in linear mode (cf. Section 2.3.1) of P3HT formed by chemical oxidation with $FeCl_3$ using chloroform as a reaction solvent that is later analyzed later in this Chapter in Section 3.4.2. The M_N of this material was determined by use of SEC–employing a multiangle laser light scattering (MALLS) detector in conjunction with a differential refractive index (DRI) detector–to be 66,000 Da with a *PDI* of 1.89. However, the MALDI-ToF-MS spectrum of this sample indicates a M_N of roughly 4,500 Da.

The mass distribution seen in the MALDI-ToF mass spectrum for this polymer is an excellent example of the common spectral characteristics encountered when higher-mass discrimination occurs during MALDI-ToF-MS analysis of a polydisperse polymer. The spectrum clearly exhibits a steep decay in ion signal intensity for the number-fraction distribution that in this case begins at about *m/z* 3,000 and increases with increasing *m/z* until the ion signal is obscured in the baseline noise, in this case at approximately *m/z* 15,000. Similar examples of this discrimination along with large discrepancies in observable average molecular weight data between SEC and MALDI-ToF-MS analysis are apparent throughout Chapter 2 of this Dissertation as well. The abundance of mass discrimination encountered throughout the breadth of this study has lead to the work presented within this Chapter; I will attempt to obtain a better understanding of the reasons for discrimination encountered in the MALDI-ToF-MS analysis of P3HTs.

3.1.2 Mass Discrimination in MALDI-ToF-MS Resulting from Sample Preparation

It has been shown that mass discrimination of polymer samples can result due to the manner in which the sample is prepared for analysis and the proper selection of the matrix, solvent, cationization agent, mixing ratios, and technique for deposition of the analyte onto the

MALDI target plate may all critically influence the data obtained via these means.[2,5,11-13] First, the chemical nature of the matrix employed is essential in order to obtain viable signals from synthetic polymer samples using MALDI-ToF-MS and the proper choice of matrix for a given polymer sample is crucial, as some compounds that act as effective matrices for certain classes of polymers are ineffective for others.[13-15] When considering the choice of proper matrix for a particular synthetic polymer sample, it is often an issue of trial and error, although there are listed in the literature[5] and in a database on the National Institute of Standards and Technology's (NIST) website,[16] potential matrixes and preparation recipes for given polymers that are a function of the chemical characteristics of such samples. When considering a proper matrix for a given polymer sample, it has been suggested that the matrix performs three important functions for the ionization/desorption event: (i) the incorporation leading to isolation of the analyte into matrix crystals, (ii) the collective absorption of laser light and subsequent ablation of the analyte, and (iii) an active role of the matrix in the ionization of the analyte.[17-19] Likewise, it is generally agreed that an ideal matrix should have: (i) high electronic absorption at the laser wavelength employed for analysis, (ii) good vacuum stability, (iii) low vapor pressure, (iv) good solubility in solvents that also dissolve the analyte, and (v) good miscibility with the analyte in the solid state.[15,19]

For instance, Belu et al. evaluated previously reported sample preparation procedures[20,21] for the analysis of poly(styrene), PS, by means of MALDI-ToF-MS using various matrices in an attempt to optimize the sample preparation methods for the procedure.[14] Belu et al. employed a variety of matrices including 2-nitrophenyl octyl ether (NPOE), *trans*-3-indole acrylic acid (IAA), 2,5-dihydroxybenzoic acid (DHB), sinapinic acid, 2-(4-hydroxyphenylazo)-benzoic acid (HABA), and dithranol for these purposes using silver trifluoroacetate (AgTFA) as a cationizing agent. Given the many different variables involved with MALDI-ToF-MS analysis that can

affect the molecular weight data obtained by these means, all other instrumental parameters were held as close to constant as possible during their investigation. For lower molecular weight PS (PS5000 ~ M_N = 5,000 Da) very low signal was observed for the PS5000 sample when IAA was the matrix and no signal was observed for the sample with DHB, HABA, and sinapinic acid as matrices. However, PS5000 prepared in dithranol gave well-resolved ion signals with twice the signal-to-noise ratio using 50% less laser power than signal obtained using NPOE.

Rashidzadeh and Guo also investigated the role that matrix plays in obtaining accurate molecular weight measurements for poly(methylmethacrylate), PMMA, samples having broad molecular weight distributions by means of MALDI-ToF-MS.[22] In order to simulate a polydisperse polymer sample, Rashidzadeh and Guo prepared a two-component blend of narrowly-distributed PMMA standards (PDI < 1.1) having number average molecular weights (M_N) of 12,500 and 46,000 Da (PMMA12500 and PMMA46000, respectively). They prepared this blend using a weight ratio of 1:10 of PMMA12500 (0.5 g L^{-1}) to PMMA46000 (5 g L^{-1}), and measurements were acquired keeping all other experimental and instrumental factors constant, with the detector voltage optimally adjusted to prevent detector saturation. 2-(4-hydroxyphenylazo)-benzoic acid (HABA) and *trans*-3-indole acrylic acid (IAA) were chosen for use in this analysis as they were previously shown to be effective matrices for narrowly-distributed PMMA standards.[6,23]

Rashidzadeh and Guo examined the MALDI-ToF mass spectra obtained for the blended polymer samples using both matrixes and observed significantly different PMMA distributions for each of the matrices employed, with the signal ratio of PMMA46000 to PMMA12500 being much smaller when HABA was used as a matrix. To determine which spectrum more faithfully represented the true distribution of the sample, Rashidzadeh and Guo used a novel method for the comparison of the peak ratios from the MALDI-ToF mass spectra for the individual

components of PMMA standards with their molar ratio. In short, they determined that the measured peak area ratio of low- to high-mass PMMAs was larger than the corresponding molar ratio in both cases, indicative of mass discrimination against high-mass PMMA in both cases. In fact, the error for IAA was ~70% and the error for HABA was ~230%. While Rashidzadeh and Guo admitted that some part of this error could be from instrumental factors, they emphasized that the contribution from instrumental issues should be less than 70% and therefore the majority of error seen for HABA was a result of the matrix itself.

With regards to poly(3-alkylthiophene)s, P3ATs, several different compounds have been reported for use as a matrix for MALDI-ToF-MS analysis. Liu et al. employed MALDI-ToF-MS for the analysis of molecular weight, molecular weight distributions, endgroup structures (cf. Section 2.3.1), and endgroup modifications for highly regioregular (cf. Sections 1.2.4, 1.2.5, and 1.2.6) poly(3-alkylthiophene)s.[9] Liu et al. reported employing dihydroxybenzoic acid (DHB), dithranol, 9-nitroanthracene, *trans*-3-indole acrylic acid (IAA), and sinapinic acid for this analysis. However, they reported that only dithranol and 9-nitroanthracene were found to assist in desorption of P3AT systems, and that the use of dithranol gave the best results. As a footnote, they went on to say that they soon there after employed terthiophene as a matrix as well and found it to be as effective as dithranol for the same analysis.

McCarley et al. employed MALDI-ToF-MS analysis for the evaluation of poly(3-hexylthiophene)s, P3HTs, synthesized by chemical oxidation with $FeCl_3$. McCarley et al.[10] reported evaluating several MALDI matrices, including dithranol, anthracene, and terthiophene in order to achieve the highest quality P3HT spectra and also to compare the spectra obtained from a traditional proton-transfer matrix versus matrices that they had previously introduced as electron-transfer agents.[24,25] Electron-transfer cationization is the accepted means by which P3ATs undergo ionization during the MADLI process.[9,10,24,25] McCarley et al. reported that

dithranol, terthiophene, and anthracene matrices produced similar ions and molecular weight averages and distributions, but terthiophene matrix was preferred because of the higher signal-to-noise ratio and resolution routinely obtained with its use.[10] Brauch came to similar conclusions in her report regarding the structural characterization of poly(heterocycle)s formed using oxidative methods.[26]

Some work done in this dissertation by means of MALDI-ToF-MS was performed using terthiophene as a MALDI matrix. However, the majority of the spectra obtained by MALDI-ToF-MS presented in the bulk of this work, and all the spectra obtained and presented in this Chapter of the dissertation, were acquired by the use of *trans*-2-[3-(4-*tert*-butylphenyl)-2-methyl-2-propenylidine] malonitrile, commonly referred to as DCTB. Very recently DeWinter et al. published their finding as to the effectiveness of DCTB for use as a MALDI matrix in the MALDI-ToF-MS analysis of highly regioregular P3HTs synthesized by use of the GRIM[27] method.[28] DeWinter et al. conducted an in-depth investigation into this matter and concluded DCTB to be a superior MALDI matrix for the ionization/desorption of P3HTs compared to terthiophene, as well as dithranol. They attributed the superior nature of DCTB as a matrix for these purposes to the high absorption of the DCTB molecule (λ_{max} = 346 nm and $\varepsilon_{337nm} \sim 26{,}300$ L mol^{-1} cm^{-1}) at the given laser wavelength employed (337 nm). Moreover, DeWinter et al. credited the ionization efficiency seen for P3HTs by use of DCTB to the bulky *tert*-butyl group of the DCTB molecule, which they stated is likely to limit the intermolecular interactions between the matrix molecules and the P3HT polymer chains in the condensed phase, thus rendering desorption/ionization easier.

Schriemer et al. also reported on mass discrimination of synthetic polymer samples with broad molecular weight distributions giving consideration to the effect of sample preparation in conjunction with the desorption/ionization phenomenon involved during MADLI-ToF-MS

analysis.[2] Schriemer et al. prepared multicomponent blends of PS using equimolar amounts of PS molecular weight standards having narrow polydispersity indices ($PDI < 1.1$) in such a fashion as to mimic a polydisperse polymer sample. They noted that multicomponent blends of PS from 3,000–12,000 Da provided spectra demonstrating excellent agreement between experimental and expected M_N values. Although, addition of high-mass PS components (20,000–22,000 Da) to the multicomponent blend resulted in a large drop in the experimental M_N value compared to the expected value. Furthermore, analysis of a blend in which the mid-mass components were removed resulted in spectra that showed a relative increase of the high-mass component with respect to the low-mass components. Schriemer et al. concluded that because the suppression of the high-mass component in the polymer blend arises from the nature of the sample itself, this indicates the existence of a sample preparation and/or desorption/ionization issue, which they noted are intimately related.[29]

Schriemer et al. reported that one factor influencing the discrimination of high-mass components was the formation of multimers in the MALDI-ToF-MS desorption/ionization process. Polymeric species can give rise to multimer formation in much the same way as has been observed for proteins,[30] and a multimer for these purposes is defined as an aggregation of two or more polymer distributions as seen in MALDI-ToF mass spectra.[2] Schriemer et al. noted that mass discrimination in the extent of multimer formation of high-mass polymer distributions was not surprising as entanglement is a function of polymer chain length.[20] They describe one method for the minimization of multimer formation involving the decrease in the concentration of polymer in the matrix, or in other words, increasing the matrix-to-analyte ratio (cf. Section 2.3.1).

In order to demonstrate this phenomenon, Schriemer et al. prepared a two-component blend of PS composed of PS having equimolar amounts of PS5050 (5,050 Da) and PS28,500

(28,500 Da) that was expected to have a M_N of 16,575 Da. They varied the matrix-to-analyte ratio for MALDI-ToF-MS analysis of this blend from roughly 200:1–8,000:1. This investigation showed that although increasing the matrix-to-analyte ratio did give rise to a slight decrease in multimer intensity even at the highest matrix-to-analyte ratios, multimers were still very much present as shown by the mass spectra. Furthermore, Schriemer et al. reported that the measured M_N increased with an increase in matrix-to-analyte ratio and was considerably overestimated at higher matrix-to-analyte ratios ($M_N > 19{,}000$ Da).

Schriemer et al. noted that the decrease in multimer formation would partially contribute to the increase in the measured M_N with the increase in matrix-to-analyte ratio, as more matrix molecules per polymer chain would serve to better isolate individual high-mass polymer chains. Although, the expected M_N was overestimated and multimers were still present at the highest matrix-to-analyte ratio, they admitted there must exist a fundamental difference between low- and high-mass components with respect to their desorption/ionization efficiency. Nevertheless, this work served to show that variables in sample preparation for synthetic polymers investigated by means of MALDI-ToF-MS, such as changes in the matrix-to-analyte ratio, may contribute greatly to discrepancies seen in molecular weight and molecular weight distribution measurements obtained by these means.

Liu et al. investigated the effects of the matrix-to-analyte ratio using dithranol and terthiophene as matrices for the analysis of P3ATs by means of MALDI-ToF-MS on the resulting spectra.[9] They had expected that a very high matrix-to-analyte concentration ratio would be necessary to insure dilution and separation of P3AT chains, because as they noted regioregular P3ATs have a strong tendency to self assemble. Conversely, they found this was not the case, and their experimental results showed that matrix-to-analyte ratios as low as 100:1 gave successful MALDI-ToF-MS results. In this work, Liu et al. also examined some low

molecular weight P3AT samples prepared from three different matrix-to-analyte ratios of 200:1, 2000:1, and 20,000:1 to see whether the matrix-to-analyte ratio had any effect on endgroup fragmentation. Mass discrimination has been shown to be a result of the nature of the endgroups attached to some polymers (cf. Section 1.3.2). Although Liu et al. kept all MALDI-ToF-MS experimental conditions constant with the exception of the matrix-to-analyte ratio, they did not observe any changes in the peak area ratios of oligomers possessing solely hydrogen-terminated endgroups to those having one hydrogen-terminated end and one bromine-terminated end, suggesting that the matrix-to-analyte ratio did not influence endgroup fragmentation in P3ATs.

Martin et al. investigated the influence of the laser power used in the MALDI-ToF-MS analysis of synthetic polymers and its contribution to discrepancies seen in average molecular weight measurements obtained by this means for polymers with broad molecular weight distributions.[31] Martin et al. noted that the laser power required for the desorption/ionization process in MALDI-ToF-MS is ideally adjusted slightly above the threshold power needed in order to obtain MALDI-ToF mass spectral results (i.e., ionization). However, they go on to add that this is only possible in the case of monodisperse samples and when examining polydisperse polymer sample there is no well-defined value for a threshold. To simulate a polymer sample having a broad molecular weight distribution, Martin et al. prepared a multicomponent blend of equimolar amounts of well-defined, narrowly-distributed poly(styrene), PS, standards. The low molecular weight component of the mixture was a PS standard having a M_P of 5,500 Da (PS5500), which was held constant during the experiment. Whereas, the high molecular weight component was increased from M_P = 20,000 Da to 100,000 Da to simulate increasing polydispersity of the polymer sample.

In their investigation using a blend of PS5500 and a PS standard having a M_P of 46,000 Da (PS46000), Martin et al. showed that at low laser power only the low molecular weight

distribution (PS5500) appeared in the MALDI-ToF mass spectrum of the sample. However, as the laser power was increased, a small peak due to the PS46000 appeared, which increased in intensity as the laser power increased to an optimal point where the high-mass peaks ceased to further increase in intensity. They further explained that if the laser power was increased past the optimal point, the low molecular weight distribution became broader and shifted to lower masses, which they attributed to fragmentation of the lower mass polymer. Furthermore, Martin et al. showed that with increasing peak area of the PS46000, a distribution of doubly-charged PS46000 with m/z 23,000 increased in intensity. They mentioned that this doubly-charged distribution did not interfere with the analysis of the low molecular weight distribution in this case, although they added that if in fact there existed a broader distribution of polymer, this doubly-charged distribution would change the "true" peak intensities for singly-charged ions in the region around m/z 23,000.

Martin et al. also performed this analysis using PS5500 and PS98000 (M_p = 98,000 Da), noting that at the minimum laser power required to produce a signal for the PS98000 the lower mass distribution showed broadening and mass shifts in the spectrum that were indicative of fragmentation and therefore it was not possible to make the high molecular weight peaks visible in the MALDI-ToF mass spectra without fragmentation of low weight material. Furthermore, a comparison of the low and high molecular peak areas in all spectra examined clearly showed that the signal of high molecular weight PS was always suppressed and the suppression becomes more evident as the molecular weight increases. Finally, for sample blends consisting of PS5500 and PS20800 (M_p = 20,800 Da), Martin et al. observed a signal peak at a m/z value twice that of the PS20800 ($m/z \sim 41{,}600$) indicating singly-charged PS20800 dimeric clusters, which they stated may disturb the shape of a broader, "real" distribution of polymer.

Martin et al. concluded that the high molecular weight portion for a polymer sample having a broad molecular weight distribution is always underestimated by MALDI-ToF-MS analysis. They also concluded that because of the different laser powers required for low and high molecular weight distributions and the resulting differences visible in the distribution of ions seen in the MALDI-ToF mass spectra, the experimental average molecular weight measurements M_N and M_W will always vary depending on the laser power employed. Additionally, they surmised that the signals from doubly-charged molecules and singly-charged clusters overlap with singly-charged ion peaks in polydisperse distributions, which gives erroneous average molecular weight data for these systems as seen by MALDI-ToF-MS. From these observations, Martin et al. summarized that MALDI-ToF-MS should only be considered an absolute method for the determination of molecular weight and molecular weight distributions for narrowly-disperse samples ($PDI < 1.1$) and not for polymers with broad molecular weight distributions.

Solubility is also an important factor to consider in sample preparation for MALDI-ToF-MS analysis of synthetic polymers and the solvent employed in the sample preparation has been identified as a potential source of mass discrimination.[12,32-34] The preparation of a polymer sample for MALDI-ToF-MS analysis typically involves dissolving the polymer in a solvent in which the full mass range of oligomers is completely soluble. Because a polymer sample having a broad molecular weight distribution consists of oligomers having appreciable variation in lengths and molar masses this is particularly important. The polymer solution is then mixed with a matrix (and metal salt or cationizing agent if necessary) solution. It is strongly recommended that single solvent systems be employed to prepare the polymer/matrix sample. This is not always possible in the analysis of synthetic polymers by these means, in which case the incompatibility of the solvent used to dissolve the polymer and that used to

dissolve the matrix becomes an issue that may lead to mass discrimination.[32,33] The sample is then spotted on the MALDI target where evaporation of the solvent and recrystallization of the polymer/matrix mixture occurs.

Guo et al. explain that depending on the choice of solvent used for sample preparation, during evaporation the varying solubility of different length oligomers may become significant because the polymer/matrix solution becomes very concentrated.[35] They further clarified that if the matrix and a certain fraction of the polymer crystallize before the rest of the polymer, or if a certain fraction of polymer alone crystallizes first, the result would be a separation of a certain fraction of the polymer from the matrix that lead to mass discrimination against that fraction of the polymer. Guo et al. also specified that solubility of polymer in the matrix crystals needs to be carefully considered as the polymer must be properly incorporated into the matrix crystals, and varying solubility of polymer oligomers having different size in the matrix may cause mass discrimination in the sample.[35] King et al. suggested that any factor affecting the solubility of polymer in the polymer/matrix mixture including the type of matrix or analyte, solvent composition, presence of other constituents in the solution, temperature, and crystallization rate will affect the incorporation of polymer into the matrix crystals.[36]

Guo et al. demonstrated mass discrimination due to improper incorporation of certain fractions of polymer sample into the matrix, leading to the doping of smaller amounts of these fractions in the matrix crystals and reducing their desorption/ionization, which they believed to have occurred during the solvent evaporation and crystallization process.[35] In this study they prepared a PMMA molecular weight standard having a M_P of 4,000 Da using tetrahydrofuran (THF) as a solvent and HABA for a matrix. Guo et al. noted that THF is an excellent solvent for their PMMA sample, so varying solubility should not have been a problem during the sample preparation, although they added that varying solubility could become a problem during the

solvent evaporation and recrystallization stages since the solution becomes very concentrated. The PMMA solution was prepared to make a 1 mg L^{-1} concentration and the HABA prepared to make a 20 mg L^{-1} concentration, which were mixed in a 2:1 (v/v) ratio of matrix to polymer. Additionally, a small amount of NaCl dissolved in methanol was added to the polymer solution for enhancing cationization.

Guo et al. recorded the MALDI-ToF mass spectra for the same PMMA sample taken from the same target spot but obtained by laser ablation of different areas of that target spot, thereby maintaining all other instrumental variables identical for all spectra with the exception of the area where desorption/ionization occurred. Although the spectra were obtained under identical experimental conditions, they qualitatively displayed very different ion distributions indicating substantial mass discrimination. One of the targeted areas for the PMMA sample gave an experimental number-average molecular weight (M_N) for the sample of 3,718 Da, which was in good agreement with the manufacturers M_N of 3,750 Da obtained by SEC. Whereas results gathered from a different targeted area for the identical sample gave a M_N of 2,968 Da. Although the conclusions drawn by Guo et al. as to the reasons for this mass discrimination are undoubtedly interesting, they do fail to address the addition of the small amount of methanol in the cationizing metal salt solution employed in the study, which would likely contribute to the observed results.

Chen et al. further examined mass discrimination of polydisperse synthetic polymer samples as a function of the solvents used to prepare the polymer sample for MALDI-ToF-MS analysis.[32] In this work Chen et al. were focusing on the affects of mass discrimination encountered when using binary solvent systems for sample preparation. Binary solvents systems are often employed when a cationizing agent is required for successful MALDI-ToF-MS analysis of a polymer, which for many synthetic polymers is usually the case. The metal salt is

incorporated into the MALDI sample preparation by dissolving the salt in a polar solvent then adding a small amount of the metal salt solution to the polymer solution of interest to be examined by MALDI-ToF-MS. Furthermore, Chen et al. examined the effects of contamination of the solvent in the form of water, which was found to be a major source of mass discrimination during the analysis of synthetic polymers by means of MALDI-ToF-MS analysis.

Using methanol as a single solvent and HABA as the matrix for the analysis of a PMMA standard sample having a M_N of 3,750 Da (provided from the manufacturer by means of conventional SEC), Chen et al. showed that as little as 1% addition of water (v/v) produced dramatic variation in the observed ion distributions seen in the MALDI-ToF mass spectra for the sample. In fact, a difference in the M_N calculated by MALDI-ToF-MS from 3,674 Da for the sample without water contamination to 2,851 Da for the sample having 1% water contamination was observed. Chen et al. also examined the effect of water contamination using acetone and THF, two other solvents often employed for the MALDI-ToF-MS analysis of PMMA. They found that the presence of water in these solvents could also cause significant mass discrimination, although the smallest amount of water that could lead to discrimination was found to be ~4% (v/v). This work clearly indicated that contamination of a polymer sample in the form of water leads to large discrepancies in molecular weight data obtained by MALDI-ToF-MS. Although this is a large concern when employing binary solvent systems for use in MALDI-ToF-MS analysis of synthetic polymers, there are other scenarios that can lead to this type of contamination. For instance, a high-quality solvent should be employed for these purposes, such as an HPLC- or pesticide-grade solvent. Also, repeated cooling and warming of the polymer sample, such as occurs from repeated transfer to and from refrigeration, may cause water contamination in the form of condensation from the air. In this case, care should be taken to ensure the polymer remains under an inert gas environment during the warming period.

With regards to the sample preparation of poly(3-hexylthiophene), P3HT, samples investigated in this chapter, a single solvent system of chloroform is employed for all MALDI-ToF mass spectra obtained herein. The use of a cationizing agent, such as a metal salt, is not necessary for efficient desorption/ionization of poly(3-alkythiophene)s[9,10,26] and hence for all MALDI-ToF-MS analysis found within this dissertation none have been employed. Chloroform was used as a solvent for MALDI sample preparation because it has been shown that P3AT oligomers ranging from low to high molecular weight are soluble in chloroform,[9] as well as the matrix employed for these investigations, DCTB. Pesticide-grade chloroform was used in this work, which was stored over activated molecular seives under a blanket of argon in order to ensure a minimal amount of water contamination to the solvent.

3.1.3 Mass Discrimination in MALDI-ToF-MS Resulting from Instrumental Issues

Instrumental factors also contribute to mass discrimination encountered during the characterization of molecular weights and molecular weight distributions for synthetic polymers having broad molecular weight distributions by means of MALDI-ToF-MS. These factors include transmission and detection issues inherent to MADLI-ToF-MS due to variations in instrumental parameters.[3,5,22,35,37] The influence of laser power on the desorption/ionization event is often categorized as an instrumental factor that can contribute to this mass discrimination. However, because desorption/ionization is so intimately related to sample preparation, the effects of laser power with regard to mass discrimination were previously discussed in Section 4.1.1.

The typical detector encountered in a MALDI-ToF mass spectrometer is a microchannel plate (MCP), which has a relatively limited signal-response dynamic range and may be easily saturated by low-mass analyte components, such as matrix ions and/or small oligomers.[5] This is especially so when analyzing synthetic polymers having a broad molecular weight distribution, where the majority of ions are of low molecular weight. A MCP is a multichannel version of a

channel electron multiplier (CEM). A CEM is a continuous arrangement of electrodes constructed of glass–that has been heavily doped with lead or coated on its inner surface with beryllium–drawn into a horn shape to which a high voltage between 1.8–2.0 kV is applied creating a uniform field throughout the length of the tube.[38] When an ion beam within the mass analyzer of a mass spectrometer strikes the surface of the entrance to the detector several electrons are ejected and then attracted along the length of the detector towards the opposite end, consequently ejecting an increasing number of electrons throughout their travel and thus amplifying the signal current or increasing the gain.[38] A MCP consists of millions of individual channels made of very small diameter (~10μm) fiberoptic cables of metal-doped glass that tremendously increase the gain of each channel as compared to a conventional CEM due to the increase in length of each channel.[38]

This type of detection system relies on ion-to-electron conversion, which is predominate at velocities above ~20–30 km s^{-1}.[4] During MALDI-ToF-MS analysis, two different ions both possessing single charges but having different molecular weights that are accelerated using the same voltage potentials will arrive at the detector at different times due to the fact that they each have different velocities imparted by the same accelerating potential (cf. Equation 2.4). Furthermore, the number of ejected secondary electrons at the detector surface is a function of the incident ion mass and velocity and therefore ions of differing masses will often cause a different number of secondary electrons to be ejected, which will yield different signal amplitudes from the detector.[4] This is not a huge concern for varying analytes within a similar sample where the molecular weight distribution is not large, although it becomes a consideration for samples such as synthetic polymer samples in which different analyte species may have differences in molecular weight up to 100,000 Da.

Detector saturation is also a concern when analyzing polydisperse synthetic polymer samples and it can contribute to the discrimination of high-mass distributions resulting from large abundances of low-mass materials in the sample, such as the matrix ions and smaller oligomer ions. A detector is basically a high-gain amplifier capable of amplifying ion signals by 10^7–10^8.[19,38] As mentioned above, the detector relies on a reserve of secondary electrons in order to amplify a signal–in the case of MALDI-ToF-MS an ion beam–and a depletion of secondary electrons due to an increase in signal constitutes a saturation of the detector. The presence of low-mass compounds in a polymer sample can cause detector saturation, which diminishes the amplification of signals seen for higher mass distributions. Detectors based on MCP technology are more prone to loss of gain with an increase of signal strength than other conventional electron multiplying detectors, due to time required for recovery of individual channels before their maximum gain can be reestablished.[3]

McEwen et al. investigated the instrumental effects encountered in the analysis of polymers possessing wide polydispersities by MALDI-ToF-MS, and the possible sources of mass discrimination seen for PMMA samples. McEwen et al. prepared a PMMA sample with a manufacture's reported M_N of 17,000 Da and a polydispersity index of 1.8 and then evaluated it by MALDI-ToF-MS analysis using both linear and reflectron modes (cf. Section 2.3.1). McEwen et al. noted that in the mass spectra of this sample obtained both in reflectron and linear modes the observed ion current (MALDI-ToF-MS ion signal) disappeared into the noise at approximately 20,000 Da, whereas the SEC chromatogram showed the presence of polymer to at least 40,000 Da. They further went on to demonstrate that PMMA molecules with molecular weights in excess of 25,000 Da that were obtained by collecting the early eluting fraction from the high-mass tail of an SEC separation of this PMMA sample, were observable by means of MALDI-ToF-MS.

McEwen et al. went on to show that ions above *m/z* 25,000 from the same PMMA sample could also be observed without SEC fractionation by means of gating the signal so that only a narrow pulse of ions in a selected mass range reach the detector in reflectron mode. They concluded that ions were being produced over the molecular entire weight range, but since the high-mass polymer was not observed in the spectra when low-mass ions were allowed to reach the detector a detector response problem caused by a continuous stream of particles impacting the detector might be responsible for the high-mass discrimination observed.

To investigate this issue further, in the same paper McEwen et al. prepared a PMMA sample using equimolar amounts of three PMMA molecular weight standards having narrow molecular weight distributions so that the concentration of each standard in the sample was approximately 2 pm μL^{-1}, then characterized them using MALDI-ToF-MS. The MALDI-ToF mass spectra for this sample showed that the areas of the ion signals were approximately equal using similar instrumental parameters employed previously. From this evidence they further concluded that detector saturation for the narrowly-disperse PMMA mixture was not occurring unless detector recovery was being achieved in the null periods between ions from each distribution striking the detector, thereby conferring that the continuous stream of particles impacting the detector seen for "true" polydisperse polymer samples might be responsible for the high-mass discrimination observed.

In order to investigate the effects of detector saturation on mass discrimination encountered in the MALDI-ToF-MS analysis of molecular weights for synthetic polymers, Schriemer et al. designed an experiment to determine the effect of the matrix and the MCP voltages on the M_N of a three-component blend of poly(styrene), PS. The sample was composed of molecular weight standards having narrow molecular weight distributions so as to simulate a polydisperse PS sample.[3] A blend of PS standards having M_N of 5,050, 16,00, and 35,000 Da

was prepared and a number of MALDI-ToF-MS analyses performed on them. In the first experiment, the blend was run under identical conditions with the exception that in the first MALDI-ToF-MS analysis, a deflection pulse was applied immediately postsource for removal of matrix ions, whereas in the second analysis the matrix ions were retained for detection. The results showed that deflecting the matrix led to lower M_N values than if the matrix was retained. Schriemer et al. explained that with retention of the matrix the detector is at least partially saturated and begins recovery after all the transmitted matrix ions have reached the detector, which is within the timeframe of the experiment, ~100 μs. They added that retaining the matrix results in lower mass distributions of PS being suppressed more than the higher masses, which leads to the increase in the M_N value. They also noted that even when the matrix ions are deflected an appreciable matrix signal is still observable, suggesting that the full influence of detector saturation by matrix ions might not be removed with deflection.

In the second set of experiments, Schriemer et al. analyzed the three-component PS blend by MALDI-ToF-MS while adjusting the MCP voltages of the instrument–which was equipped with a dual MCP detector–and deflecting the matrix. In the former matrix deflection experiment above the voltages were operated in the standard configuration with the voltage drop across the first MCP two-thirds that of the voltage dropped across the second MCP, which was operated at 1 kV. In this second set of experiments, the voltage drop across the second MCP was fixed at 1 kV, and in the first analysis the voltage of the first MCP was adjusted to one-third (0.33 kV) that of the second MCP; in the second analysis, the voltage drop across the first MCP was adjusted to match the voltage of the second MCP at 1 kV.

The calculated M_N for the analysis of the PS blend using matched voltage drops across the dual MCPs was found to be significantly higher than the M_N obtained for the sample using a 0.33 kV drop across the first MCP. Schriemer et al. explained that operating the detector using

matched voltage drops clearly implies operation of the detector under saturated conditions because the M_N values were significantly higher than those seen while analyzing the sample using the standard MCP voltage configuration and deflecting the matrix, as was done in the first set of experiments. They go on to make clear that although when the first MCP voltage is decreased to 0.33 kV, there is a considerable weakening of signal intensity that renders the instrument's sensitivity too poor to reliably detect the PS distribution having a M_N of 35,000; the calculated M_N for the two lower-mass components was in good agreement with the calculations for the same components observed in the first set of experiments where matrix was deflected, implying nonsaturating conditions. Schriemer et al. concluded that the extent of detector saturation does significantly affect the M_N determination for polydisperse synthetic polymer samples by means of MALDI-ToF-MS.

Rashidzadeh and Guo also performed experiments to determine the effect of detector saturation on mass discrimination to molecular weight measurements for synthetic polymers with wide molecular weight distributions by use of MALDI-ToF-MS.[22] Rashidzedah and Guo described two different sets of experiments in which they varied the high voltage applied to the detector while examining PMMA polymer samples. In the first set of experiments, Rashidzedah and Guo prepared a polydisperse (PDI = 1.5) PMMA sample having a M_N of 8,500 Da using IAA as a matrix. The MALDI-ToF mass spectra were compared for examples when spectra were obtained from the same desorption spot while keeping all instrumental parameters constant with the exception of adjusting the detector voltage from 1.5 kV in the first spectrum to 1.9 kV in the second spectrum. They observed two significantly different distributions for each of these spectra. They also correlated the observed m/z signals with the time of flight for the given ions to reach the detector.

In the first spectra where the detector was operated under low-gain conditions at 1.5 kV, Rashidzadeh and Guo observed that the low-mass matrix signal was relatively weak and the highest PMMA peak was at 16 μs, which roughly correlated to m/z 2,000. Whereas for the spectrum obtained under high-gain conditions with the detector voltage adjusted to 1.9 kV the signal for the matrix peaks became much stronger and a distinctly different distribution pattern of PMMA oligomers was observed with the highest PMMA peak shifting to 25 μs, which approximately correlated to m/z 4,500. This shift was explained in terms of detector saturation at high-gain detector conditions. The results were comparable to those seen by Schiemer et al.[3] where under detector saturation conditions the M_N of the sample was increased due to the lack of observable low-mass oligomers, which are obscured during the rise time (recovery period) of the channel detectors after the influx and detection of the population of matrix ions.

In their second set of experiments, Rasidzedah and Guo prepared a poly(ethylene glycol), PEG, sample consisting of two narrowly-distributed (PDI < 1.1) PEG molecular weight standards having a M_N of 1,450 (PEG1450) and 3,350 (PEG3350) Da in order to simulate a polydisperse PEG sample. They prepared this sample using HABA as a matrix and acquired the MALDI-ToF- mass spectra from the same desorption spot and under identical conditions, with the exception that the detector voltage was adjusted from low-gain conditions (1.5 kV) to high-gain conditions (1.9 kV). The results from the mass spectra obtained under low-gain (1.5 kV) conditions show that the signal for the PEG1450 was much weaker in intensity than the signal for the PEG3350 having a peak intensity ratio of PEG1450 to PEG3350 of 1:10. However, under high-gain (1.9 kV) conditions the signal intensity of the PEG1450 was significantly increased, and the peak intensity ratio of PEG1450 to PEG3350 was calculated to be 1:2.

Furthermore, Rashidzedah and Guo noted that the strongest peak signal of the PEG3350 was shifted from 24 μs under low-gain conditions to 22 μs under high-gain conditions, and more

importantly, under high-gain conditions the signal intensity from 22–26 μs for the PEG3350–roughly relating to a range between *m/z* 3000–3800–drops to almost zero. Thereafter in the same spectrum, the PEG3350 signal gradually increased in the higher mass range–roughly *m/z* 3800–4200–due to detector gain recovery, although Rashidzedah and Guo noted the gain recovery was very slow. Rasidzadeh and Guo suggested that the shift in the signal of the PEG3350 from 24 to 22 μs, and the consequential loss of signal from 22–26 μs under high-gain conditions, was a result of a diminution of ion detection efficiency due to detector saturation during the course of collection, which was primarily attributable to the strong signals of the PEG1450 and the low-mass oligomers of PEG3350. They went on to explain that the relative comparison of the highest peak intensity for PEG1450 at 17 μs versus the diminishing signal of the high-mass components of the PEG3350 at 30 μs under both low- (unsaturated) and high-gain (saturated) conditions implied that at 30 μs under high-gain conditions the detector is far from operating under complete gain recovery. They further clarify that under these conditions it would take the detector more than 6 μs to fully recover from major saturation, which would become a serious hindrance to the analysis of a very polydisperse synthetic polymer sample, because a 6 μs time window could encompass a mass range over 6,000 Da at a flight time of 80 μs.

3.1.4 Fractionation of Polydisperse Polymers for Molecular Weight Analysis by MALDI-ToF-MS

Prefractionation of synthetic polymer samples with broad molecular weight distributions (large *PDI*s) has become a popular solution in attempts to overcome the difficulties observed by measuring the average molecular weights and molecular weight distributions of these polymer samples using MALDI-ToF-MS. The most relevant separation technique employed for these purposes is the off-line coupling of size-exclusion chromatography, SEC, with subsequent

MALDI-ToF-MS characterization.[5,19] This method involves separating a polydisperse polymer sample–by means of collecting the eluting fractions of the polymer during SEC separation–into several fractions of the polymer having more narrow molecular weight distributions ($PDI < 1.1$). The molecular weight data of these polymer fractions can then be accurately assessed by means of MALDI-ToF-MS.

As discussed previously in Section 2.3.2, the use of conventional SEC employing solely colligative means of detection–such as DRI and UV-Vis absorption detectors–for the assessment of molecular weight data of synthetic polymers, depends on accurate molecular weight calibration using synthetic polymer standards having narrow molecular weight distributions and known molecular weights. Typically five or more of these polymer standards are injected into the SEC apparatus and the resulting measurements for elution volumes are plotted versus the logarithm of the molecular weight for each standard. These measurements are then used to derive the parameters that are used to determine the calibration line employed for future interpretation of the molecular weight data for unknown polymer samples.[19]

Historically, accurate determination of molecular weight data by means of conventional SEC using these detection methods has been obstructed because of the limited availability of well-characterized calibration standards.[5,19] Furthermore, the reliability of SEC results not only depends on the use of a set of primary polymer standards that possess known molecular weights and molecular weight distributions, but those standards must also possess a structure similar to the polymer of interest.[19] However, more often than not a set of polymer standards exhibiting all of these qualifications is not available for a specific polymer of interest. Therefore, most of the reports found throughout the literature deal with the use of SEC/MALDI-ToF-MS coupling in order to accurately assess polymer samples of interest; this is implemented when no well-characterized standards are available for SEC calibration purposes. Fractions are used that have

been collected during SEC separation for which the absolute molecular weights have been established using MALDI-ToF-MS in order to calibrate the SEC column for accurate assessment of molecular weight data by means of SEC.[5,19,39-43]

For Instance, Nielen and Malucha demonstrated the applicability of this technique by investigating the off-line coupling of SEC with MALDI-ToF-MS analysis of several synthetic polymers having PDIs ranging from 1.7–3.0, including poly(styrene), PS, and poly(butylacrylate), PBA.[40] The polymers were separated using conventional SEC employing differential refractive index (DRI) or ultra-violet/visible (UV-Vis) absorption detectors; 40 fractions were collected over the polymer distribution. Then, ten of the fractions were analyzed by means of MALDI-ToF-MS. The *m/z* data obtained from the MALDI-ToF mass spectra of a given polymer sample were then used for calibration of the SEC instrument in order to accurately assess the average molecular weight and polydispersity index of that particular polymer sample.

Nielen and Malucha made clear that the characterization of PS is not a problem because there exists a wide availability of well-characterized, narrowly-distributed PS molecular weight standards having known M_P values. Nevertheless, they included PS in their study for validation of the SEC/MALDI-ToF-MS technique of calibration because of the availability of reference data for PS. Nielen and Malucha used two PS standards having M_N provided by the manufacturer of 6,000 and 22,000 Da with *PDI*s of 2.5 and 2.1, respectively. The M_P values obtained by MALDI-ToF-MS for the selected fractions of the PS standard with an M_N of 6,000 Da collected during SEC separation were used for the calibration of the SEC column.

This calibration was subsequently applied for the calculations of the average molecular weight and molecular weight distribution measurements of the unfractionated PS sample using SEC. The results using the SEC/MALDI-ToF-MS calibration were found to be in good

agreement with the molecular weight data provided by the manufacturer. The same SEC/MALDI-ToF-MS calibration procedure was performed for the PS standard having a M_N of 22,000 Da. The calibration lines acquired by the SEC/MALDI-ToF-MS method for both PS samples were merged together, and the resulting calibration line was then used for the analysis of the PS standard having an M_N of 22,000 Da. The molecular weight averages and *PDI* for this sample were calculated within 1% of the original values for this sample provided by the manufacturer, thereby validating the accuracy of the SEC/MALDI-ToF-MS calibration method.

Nielen and Malucha performed this experiment using PBA as well because at the time very little data was available in the literature regarding the characterization of the polymer by MALDI-ToF-MS. They used a PBA sample that had a M_N of 19,900 Da and a *PDI* of 3.0 as provided by the manufacturer. The calculated average molecular weight and molecular weight distribution data obtained by SEC after calibrating the SEC column using the SEC/MALDI-ToF-MS calibration method was in fairly good agreement with the values provided by the manufacturer. However, there was a greater degree of error seen with the PBA than was noticed for the PS samples. The M_N for the PBA sample as determined by SEC/MALDI-ToF-MS calibration method was found to be 16,500 Da, and the M_W calculated by this technique was determined to be 62,200 Da; however, the manufacturer determined the M_W to be 59,200 Da. From these data, the *PDI* determined by the SEC/MALDI-ToF-MS calibration method was found to be 3.76; this was considerably larger than the *PDI* of 3.0 provided by the manufacturer. Nonetheless, the SEC fractionation and consequent MALDI-ToF-MS determination of molecular weight data for the collected fractions of synthetic polymers having broadly distributed molecular weights has provided a means of more accurately calibrating a SEC system for analysis of broadly distributed polymer samples when there does not exist a well-characterized set of molecular weight standards for a particular polymer of interest.[5,19,39-42]

However, the problem of inaccurate determination of molecular weight data encountered when employing SEC connected to purely concentration-sensitive detectors (as described above) may be avoided by the use of molecular weight sensitive detection, such as a light scattering detector. A light scattering detector is a very convenient means of detection and characterization of polydisperse polymer samples by means of SEC because it can provide absolute measurement of molecular weight without requiring calibration.[44-48] A multiangle light scattering (MALS) detector offers the additional advantage that the molecular dimensions of the polymer, or radius of gyration, may be determined from the angular dependence of the scattered light.[44] The combination of molecular weight data and the dimensions (radius of gyration) for the polymer within the sample can also be used to obtain important information about size, shape, and conformation of the polymer chains in solution.[49] A drawback to the use of light scattering detection is that the detector response is proportional to molecular weight and so it works very well for high molecular weight materials, but unfortunately it is less useful for smaller oligomers.[44,45] In this Dissertation, a multiangle laser light scattering (MALLS) detector was used in conjunction with a differential refractive index (DRI) detector for all SEC molecular weight and molecular weight distribution determinations. It has been reported that the combination of a concentration-sensitive detector and a molecular-weight sensitive detector provides the ability to obtain the absolute molecular weight data for a given polymer sample directly for each fraction or slice across a sample peak in the size-exclusion chromatogram.[45,49]

There are virtually no reports in the literature regarding the prefractionation of poly(3-alkylthiophene)s, P3ATs, having broad molecular weight distributions in order to investigate the discrepancies seen in molecular weight and molecular weight distributions observed in their MALDI-ToF-MS analysis as compared to those obtained by SEC. Lui et al. employed MALDI-ToF-MS on a poly(3-hexylthiophene)–formed via the McCullough[50-52] method of polymerization

and having a M_N of 12,200 Da and a *PDI* of 1.94 as determined by conventional SEC–for the analysis of the polymer's average molecular weight and molecular weight distribution.[9] Lui et al. compared the SEC results for this P3HT sample using MALDI-ToF-MS and observed that the molecular weight distribution in the size-exclusion chromatogram was skewed towards higher molecular weight material, whereas the molecular weight distribution observed in the MALDI-ToF mass spectrum was skewed towards lower molecular weight material. In fact, the M_N was 4,956 Da as calculated by means of MALDI-ToF-MS, a value less than half that of the M_N determined by SEC, and the *PDI* was 1.74. They attributed the differences seen by the two different techniques to many of the reasons outlined in Section 4.1.1 and 4.1.2, including the way in which the results are presented, the mass dependence of the desorption/ionization process in MALDI, and mass-dependent detection efficiency in MALDI-ToF-MS analysis. The latter two result in an under-representation of higher mass components with respect to lower mass components observed in the MALDI-ToF mass spectrum of the P3HT.

Lui et al. reduced the polydispersity of the P3HT by subjecting the sample to several sequential soxhlet extractions using a variety of organic solvents. They employed acetone and hexane to dissolve the P3HT oligomers and low molecular weight P3HT then they used methylene chloride in order to dissolve moderate molecular weight material. Finally, they used tetrahydrofuran, THF, and chloroform in order to dissolve large molecular weight polymer chains. They thereby fractionated the P3HT into five different samples with increasing average molecular weight having narrower molecular weight distributions that ranged from *PDI* = 1.1–1.29 as the M_N increased. Sequential soxhlet fractionation of regioregular P3HTs was previously reported by Trznadel et al.[53], although their study was focused on the examination of the effect of molecular weight on the spectroscopic and spectroelectrochemical properties of the

material for which they employed fourier-transform infrared (FTIR) and ultraviolet-visible (UV-Vis) spectroscopies along with cyclic voltammetry.

Lui et al. compared the SEC and MALDI-ToF-MS results for the five P3HT fractions. They reported that for all polymer samples examined SEC always gave higher molecular weights than MALDI-ToF-MS. Lui et al. observed that when the molecular weight of the materials was low–such as in the cases of the acetone and hexane fractions–the M_N calculated by SEC was 1.2–1.5 times higher than the MALDI-ToF-MS results. For higher weight materials, Lui et al. observed that the M_N calculated by SEC was 1.5–2.3 times higher than the MALDI-ToF-MS results. The *PDI*s for the five fractions were very similar or slightly higher when calculated by means of MALDI-ToF-MS as compared to those calculated by SEC.

The differences observed by Lui et al. for average molecular weights and molecular weight distributions of the P3HT fractions were attributed to the rigid-rod conformation of the material for which it has been reported that conventional SEC–requiring calibration using molecular weight standards–lacks the ability to correctly characterize rigid-rod polymers.[54-56] Lui et al. note that their findings were in very good agreement with those presented by Pearson et al. regarding the analysis of rigid-rod oligo(thiophene)-ethynylene systems that lead to the conclusion that conventional SEC overestimates the actual molecular weight of these systems by a factor of 1.5–2.0.[54] Furthermore, Holdcroft observed that conventional SEC overestimated the absolute molecular weight of P3HTs formed by chemical oxidation with $FeCl_3$ as compared to embulliometry methods by a factor of 1.8–2.0.[56] This was attributed to the stiffness of the polymer chains in solution and the difference in the intrinsic viscosities between P3HTs and the poly(styrene) standards used for calibration in SEC.[56]

As discussed above, conventional SEC requiring calibration using poly(styrene) standards was not employed for determination of the molecular weight data presented within this

Dissertation. Instead, MALLS in conjunction with DRI detection was used as it did not require calibration–with the exception of the determination of the specific refractive index increment, SRII, otherwise known as the $\delta n/\delta c$ for P3HT (cf. Section 2.3.2)–in order to provide absolute molecular weight measurements. Nonetheless, the P3HT discussed within the pages of this Chapter was fractionated by collecting aliquots of the eluting polymer during semipreparative SEC separation in order to narrow the molecular weight distributions of the material so that they could be studied in-depth using MALDI-ToF-MS analysis. This was done in an attempt to better understand the sources leading to the apparent mass discrimination seen in the MALDI-ToF mass spectra of these materials resulting in the extreme discrepancies in average molecular weights observed between SEC and MALDI-ToF-MS analysis throughout the body of this work.

3.2 Methods and Materials

3.2.1 Chemicals

Solvents employed for the purposes of polymerization or analytical charaterization of P3HTs were either chromatographic or pesticide grade and were used as received unless noted otherwise. Once opened, solvents used for polymerization and characterization were stored over activated molecular sieves (4Å, 8–12 mesh, beads, Fisher Chemical) and degassed with argon for one hour prior to use. 3-*n*-hexylthiophene monomer was purchased from Sigma-Aldrich (#399051, 99%) and distilled under vacuum prior to use. Ferric chloride was purchased from Sigma-Aldrich (#451649, anhydrous, powder, ≥99.9%, trace metal basis) and was opened under argon in a glove bag then stored under argon in a dessicator. The matrix employed for MALDI-ToF-MS analysis was *trans*-2-[3-(4-tert-butylphenyl)-2-methyl-2-propenylidine]malonitrile (DCTB) purchased from Sigma-Aldrich (#727881, ≥98% respectively) and used as received.

3.2.2 Synthetic Methods: Chemical Oxidation of 3-Hexylthiophene

Polymerizations were carried out according to previously reported procedures in the literature for chemical oxidative polymerization of thiophenes and pyrroles with some modifications.[26,57,58] The polymerization reaction was performed in a 250mL round bottom flask (RBF). The solvent employed was chloroform (pesticide grade, Fisher Scientific #C603), and the molar ratio of oxidant-to-monomer employed was 1:2.5. 3-*n*-hexylthiophene was purified prior to experiments via vacuum distillation. Iron(III) chloride consistently remained under a blanket of argon from the moment it was opened as received from the supplier. The chloroform was degassed with argon for a period of one hour prior to the reactions.

First, an oxidant suspension was prepared by the addition of 406.0 mg (2.5 mmol) of iron(III) chloride into 12.5 mL of chloroform. The mixture was allowed to stir for one hour at room temperature under a blanket of argon. A monomer solution was prepared by the addition of 168.3 mg (1.0 mmol) of 3-*n*-hexylthiophene to 12.5 mL of chloroform. This was allowed to stir at room temperature under argon for one hour. The monomer solution was then cannulated into the stirring oxidant mixture under argon. The reaction was then allowed to proceed for one hour while stirring at room temperature under a blanket of argon.

After one hour, the reaction was quenched by the addition of 200 mL of anhydrous methanol and allowed to stir at room temperature under argon for 24 hours; during which time the polymer is reduced and precipitates out of solution. The solid polymer was then thoroughly separated by vacuum filtration and rinsed well with methanol in order to remove residual $FeCl_3$. The soluble material remaining in the filtrate was discarded (cf. Section 2.2.2) and the solid polymer was then redissolved in 250 mL of chloroform. The polymer solution in chloroform was next washed three times in a separatory funnel with 250 mL 2.0 N HCl. The chloroform

was then rotary-evaporated to leave a thin, reddish-violet film of polymer that was then vacuum-dried to constant mass overnight.

3.3 Instrumentation

3.3.1 MALDI-ToF-MS

MALDI-ToF-MS analysis of synthetic polymers and its use for determination of molecular weights, molecular weight distribution, and endgroup analysis have been previously discussed in Sections 1.3 and 2.3.1. Mass spectrometric measurements were obtained by use of a Bruker UltraFlextreme MALDI-ToF-ToF mass specrometer. The instrument was equipped with a 355-nm Nd:YAG (solid state) 1 kHz smart beam II laser. For the purposes of the work covered within Chapter 3 of this Dissertation the linear mode (cf. Section 2.3.1) of the instrument was employed. The UltraFlextreme possesses multichannel plate (MCP) detectors with a limit of detection (LOD) of 1 fmol ACTH and is capable of mass accuracy up to 1 ppm depending on the mass range observed. The instrument is capable of mass resolution up to 40,000 depending on the *m/z* observed and the mode employed. The resolving power of the instrument in linear mode is up to 1200 fwhm.

The matrix employed for MALDI-ToF-MS inquiries was *trans*-2-[3-(4-tert-butylphenyl)-2-methyl-2-propenylidine]malonitrile, DCTB. Samples were prepared by dissolving the analyte and the matrix in pesticide grade chloroform (Fisher Scientific #C-603). A saturated solution of matrix was prepared in this solvent using matrix:analyte ratios > 1000:1, although for the analysis of higher mass polymer samples ratios were employed up to 10,000:1. A small aliquot (~ 2 μL) of analyte sample was added to the matrix solution (~ 4–6 μL) then they were thoroughly mixed prior to spotting onto the target plate using the dried drop method, where a 1 μL drop of a given sample was spotted on the target plate and allowed to air dry. The instrument was calibrated prior to each measurement using peptide standards (Bruker, #222570) in the

molecular weight range *m/z* 700–3,200 for analysis of lower mass materials and protein standards (Bruker #207234) in the molecular weight range *m/z* 20,000–70,000 for higher mass material. However, internal standards were not used for these experiments in order to avoid high-mass discrimination, due to the fact that oligo(ferrocenyldimethylsilane)s (cf. Section 2.4.1) ionize much more readily than the P3HTs under investigation.

3.3.2 Size-Exclusion Chromatography (SEC)

The use of size-exclusion chromatography for the determination of molecular weight data for synthetic polymers has been previously discussed in Section 2.3.2. Size-exclusion chromatography experiments were performed through the use of an Agilent 1100 series autosampler and isocratic pump system. In some experiments ultraviolet-visible absorption measurements were taken using a Waters 490E ultraviolet-visible detector (set to 430 nm). Light scattering measurements were obtained with a Wyatt Dawn Heleos (Wyatt Technologies Corporation, Santa Barbara, California) thermostatically-controlled multiangle laser light lcattering (MALLS) detector, with a 50-mW GaAs linearly-polarized laser (658 nm) and a K5 cell. The MALLS detectors were calibrated using toluene and normalized with poly(styrene) standards having a distinct monodisperse molecular weight of 30,000 Da prior to experiments. A Wyatt Optilab Rex refractive index detector was used in conjunction with light scattering measurements and it was positioned after the Dawn Helios MALLS detector. For analytical SEC experiments the two in-line columns employed were Phenogel columns (30 cm × 7.8 mm) from Phenomenex. Both columns possessed packing material consisting of 10-μm diameter particles. The first column contained a linear bed of packing material having mixed pore sizes in the range of 50–10^6 Å, and the second column contained beads with solely 10^5 Å pores. These columns were preceded by a Phenomenex guard (10-μm diameter) guard-column. For semipreparative SEC experiments a semipreparative PLgel column (600 × 25 mm) from Polymer Laboratories

(#1210-8130) with a bed of packing material (600 × 2.5 mm) consisting of 10-μm diameter particles having pore sizes of 10^3 Å was employed. A PLgel Prep-Guard from Polymer Laboratories (#1210-1120, 25 × 25 mm) was employed preceeding the semipreparative column. The solvent employed for the separations was tetrahydrofuran, THF, (HPLC grade, Mallinckrodt Analytical #2858-06), which was degassed prior to experiments using helium sparging and/or an in-line vacuum degasser. The flow rate of the solvent for analytical analyses was maintained at 1.0 mL min^{-1} and the injection volume for the investigated samples was 100 μL. For semipreparative analysis the flow rate was maintained at 10 mL min^{-1} using a sample injection volume of 1 mL. A DRI detector alone was used to monitor the elution of the P3HT sample during the collection of the fractions of this material by semipreparative SEC. The collected data was processed using the Astra V software provided from Wyatt Technologies Corporation.

3.3.3 Specific Refractive Index Increment (SRII) Measurements

Determination of $\delta n/\delta c$ for bulk and fractionated P3HTs was done using the Wyatt Optilab Rex refractive index detector (Wyatt Technologies Corporation, Santa Barbara, California) used for SEC analysis (cf. Section 2.4.1). Measurements were made at a wavelength of 658 nm and a temperature of 25 °C. The $\delta n/\delta c$ employed for the purposes of the work within this chapter were empirically determined using the unfractionated bulk P3HT polymer sample and was found to be 0.227 ± 0.008.

3.3.4 Proton Nuclear Magnetic Resonance (^{1}H-NMR)

The use of ^{1}H-NMR for the analysis of the regioregularity of poly(3alkylthiophene)s has been previously discussed in Sections 1.2.4 and 2.3.3. ^{1}H-NMR analyses were performed on either a Bruker DPX-400 (400 MHz) or AV-4 (400 MHz) liquid spectrometer. Samples of P3HTs were dissolved in deuterated chloroform ($CDCl_3$) purchased from Sigma-Aldrich for all ^{1}H-NMR experiments.

3.4 Results and Discussion

3.4.1 Comparison of Molecular Weight Data for P3HTs Formed by Chemical Oxidation with $FeCl_3$ Employing MALDI-ToF-MS and SEC-MALLS Analysis

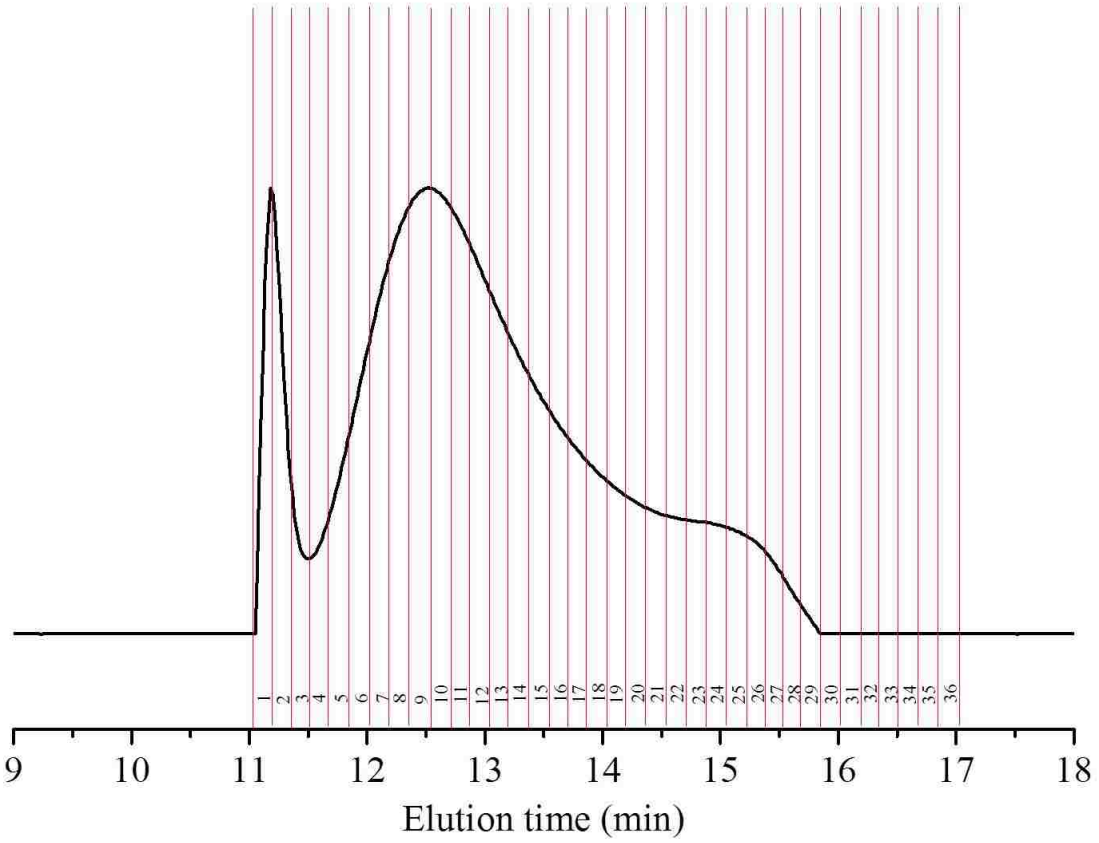

Figure 3.2 Chromatogram of the semi-preparative SEC separation of polydisperse P3HT having a M_N = 66,000 Da and a *PDI* = 1.89 determined by analytical SEC. Fractions of the eluting P3HT were collected in ten-second intervals and are delineated by the red-lined sections.

The sample of P3HT formed by chemical oxidation with $FeCl_3$ using chloroform as a reaction solvent and having a M_N 66,000 Da with a *PDI* of 1.89 shown in the mass spectrum presented in Figure 3.1 was fractionated using semipreparative SEC by collecting the eluting polymer as it left the DRI detector. Each polymer fraction was collected over a period of 10-seconds beginning with the eluting high-mass material seen by the DRI detector so as to yield 36 1.67-mL fractions of polymer solution. Figure 3.2 is the chromatogram of the semipreparative

SEC separation for this material denoted with the weight fractions collected during the separation. The collected polymer fractions were immediately placed and consistently stored under a blanket of argon gas in scintillation vials with Teflon-sealed caps that were further sealed using Parafilm. They were stored in a dark refrigerator between analyses and allowed to thermally equilibrate to room temperature before opening for analyses to avoid water condensation in the polymer.

P3HT Fraction #	M_W (Da)	M_W error (± %)	M_N (Da)	M_N error (± %)	*PDI*
1	789,700	2.3	720,000	2.3	1.1
3	238,900	1.0	210,600	0.9	1.13
5	139,300	2.1	122,000	1.6	1.14
7	83,300	2.8	80,260	2.5	1.04
9	71,790	2.6	70,020	2.4	1.03
10	66,230	2.5	64,530	2.3	1.03
13	47,990	5.0	47,540	5.0	1.01
15	43,330	5.0	42,870	4.0	1.01
18	33,860	6.0	33,440	6.0	1.01
21	32,900	6.0	32,650	6.0	1.01
24	29,160	10.0	28,630	9.0	1.02
27	23,780	15.0	23,240	15.0	1.02
30	26,780	13.0	26,390	13.0	1.02
BULK	125,800	1.4	66,640	1.2	1.89

Table 3.1 Average molecular weight and molecular weight distribution data for selected fractions of polydisperse P3HT collected during semi-preparative SEC obtained by analytical SEC analysis.

Thirteen representative P3HT samples were chosen for analytical SEC and MALDI-ToF-MS analysis. These samples were subjected to analytical SEC characterization in order to obtain the average molecular weights and molecular weight distributions for the individual polymer fractions. These data are shown in Table 3.1. The polydispersity index of all of the P3HT fractions examined was dramatically narrowed (PDI < 1.1) with the exception of fractions 1, 3,

and 5 that contained the highest molecular weight P3HT components. The average molecular weights, M_N and M_W, of fractions 1 and 3 seem exceptionally large. However, the chromatogram of the semipreparative separation (cf. Figure 3.2) indicates these fractions elute early within a peak that is not congruous with the rest of the separating materials. This fact combined with the extremely large average molecular weights for fractions 1 and 3 may indicate a degree of entanglement or aggregation occurring for the long chain polymers within these fractions. Furthermore, there exists a large degree of error associated with the later eluting fractions that may be attributed to the fact that MALLS detection is less efficient for the examination of smaller weight materials.[44,47-49] Moreover, the concentrations of the later eluting fractions were much less compared to the earlier eluting fractions. The decreased concentrations combined with the inefficiency of MALLS to correctly characterize small molecular weight materials made the reliable determination of molecular weight data for fractions eluting later than fraction 30 very difficult by these means.

The MALDI-ToF-MS analysis of fractions 1 and 3 provided no observable ion signals in a range up to *m/z* 400,000. Many attempts were made in an effort to produce discernable ion signals for these fractions, and in doing so, a variety of sample preparation and instrumental variables were adjusted. For instance, the polymer concentration for both of these fractions was diluted several times, thereby increasing the matrix-to-analyte ratio, in attempts to prevent entanglement or aggregation of the polymer chains that may inhibit efficient desorption/ionization during the MALDI event. However, the dilution of the polymer concentration in the analyte/matrix mixture did not yield any observable ion signal for these materials. Also, the laser power was adjusted throughout the range of the power gain for each serial dilution in further attempts to ionize the material (cf. Section 3.1.2). Nevertheless, manipulation of the laser power for any of the diluted polymer samples failed to produce

observable ion signals. Finally, the detection range was gated (cf. Section 3.1.3) by adjusting the range of *m/z* detection for the MCP detectors via diversion of ions outside of the selected range for each of the diluted polymer samples. The *m/z* range was gated incrementally in small *m/z* segments–for instance from *m/z* 75,000 to 100,000 or from *m/z* 100,000 to 125,000 and so forth–throughout the entire range up to *m/z* 400,000 for all diluted polymer samples, while varying the laser power through the entire range of gain in attempts to produce an ion signal for these materials. Still, no observable ion signals were detected for these fractions.

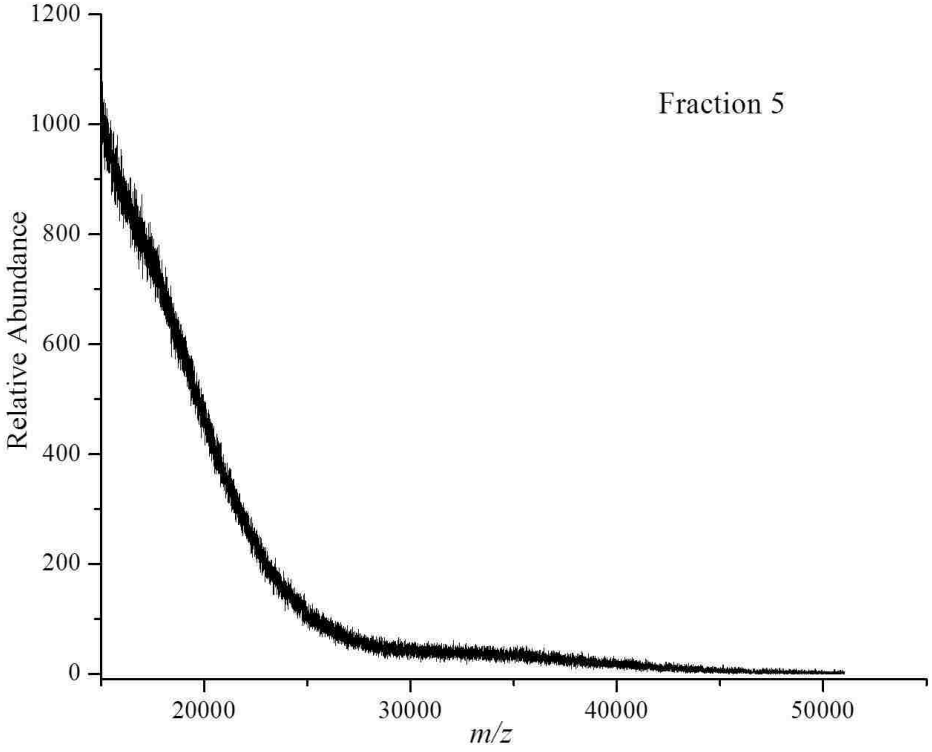

Figure 3.3 MALDI-ToF mass spectrum of P3HT fraction #5 having a M_N = 122,000 Da and a *PDI* = 1.14 determined by analytical SEC-MALLS analysis.

It is very likely that these high-mass P3HTs simply do not ionize with enough efficiency for qualitative analysis by means of MALD-ToF-MS, indicating to some degree that mass discrimination of higher molecular weight materials occurs due to desorption/ionization discrimination that may be dependent on sample preparation. However, because a multitude of

attempts to ionize these fractions via manipulation of sample preparation and desorption/ionization variables were made it is most probable that the higher molecular weight materials aggregates or become entangled during sample preparation and this phenomenon inhibits ionization.

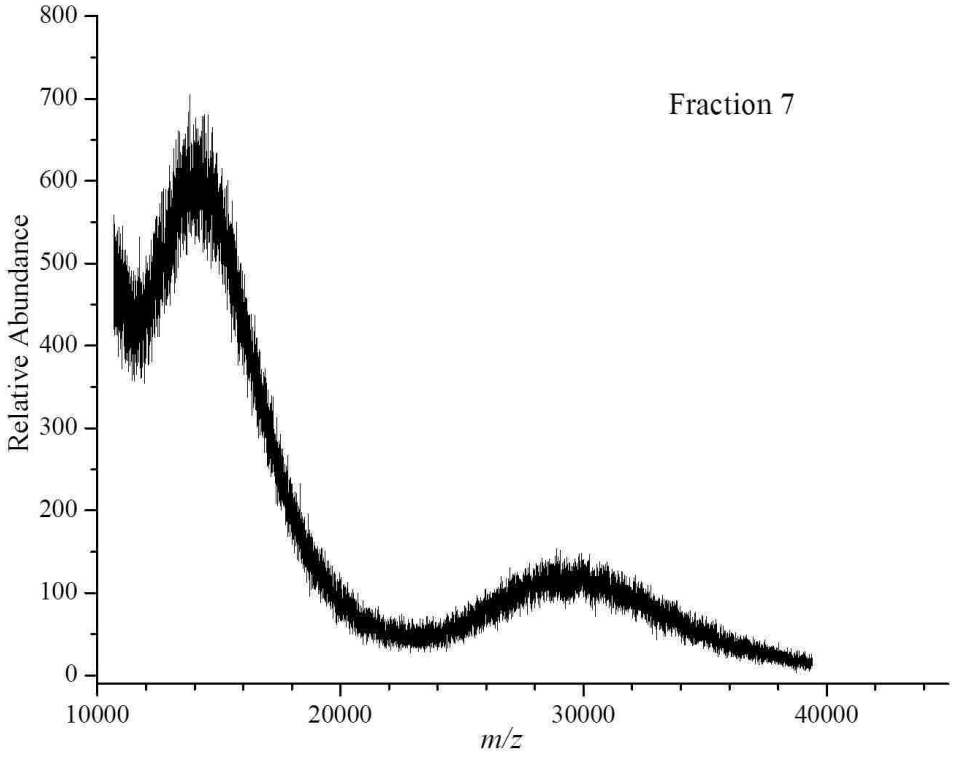

Figure 3.4 MALDI-ToF mass spectrum of P3HT fraction #7 having a M_N = 80,260 Da and a *PDI* = 1.04 determined by analytical SEC-MALLS analysis.

The observable ion signal obtained for fraction 5 is shown in the MALDI-ToF mass spectrum presented in Figure 3.3. In order to obtain this spectrum the instrument was gated between a range of *m/z* 15,000–50,000. There appears the glimpse of an ion signal at approximately *m/z* 35,000 with an unusual exponential increase in the signal as the *m/z* decreases. The first discernable ion signal detected for any of the fractions, albeit not well resolved, is shown in the MALDI-ToF mass spectrum of fraction 7 presented in Figure 3.4. This spectrum was obtained using ion gating between *m/z* 10,000–40,000. The mass spectrum of fraction 7 shows two ion signal peaks; one with a M_P at *m/z* 29,000 and a larger peak with a M_P at

m/z 14,500. The appearance of the second peak at *m/z* 14,500 in the mass spectrum of fraction 7 gives some insight into the sharply increasing baseline signal seen in the mass spectrum of fraction 5 (cf. Figure 3.3). Although MALDI-ToF-MS is a soft ionization technique that is thought to produce primarily singly-charged ions, there are a very limited number of reports in the literature that indicate multiply-charged ions can be produced in the MALDI-ToF-MS analysis of synthetic polymers.[31,59,60] However, there are no reports in the literature concerning multiple charging of poly(thiophene)s. The signal peak *m/z* 14,500 in the mass spectrum of fraction 7 is indicative of doubly-charged P3HT having the molecular weight in the range of 29,000 Da. The presence of doubly-charged species could explain the signals observed in the mass spectrum of fraction 5 in Figure 3.3.

The mass spectra of both fraction 5 and 7 provide molecular weight data that is exceedingly below the average molecular weights provided by means of SEC (cf. Table 3.1). Fraction 5 was found to have a number-average molecular weight, M_N, of 122,000 Da determined by SEC, whereas an estimate of the M_N for the same material by means of MALDI-ToF-MS is roughly 35,000 Da. Likewise, Fraction 7 was found to have a number-average molecular weight, M_N, of 80,260 Da determined by SEC, whereas an estimate of the M_N for the same material by means of MALDI-ToF-MS is roughly 30,000 Da. Thus for these fractions the M_N determined by SEC is 2.5–3.5 times that determined by MALDI-ToF-MS.

The MALDI-ToF mass spectrum of fraction 10 is shown in Figure 3.5. This spectrum was obtained using ion gating between 5,000–29,000 *m/z*. There are at least two ion signal peaks present in the spectrum. An ion signal peak having a M_P near *m/z* 22,000 is clearly present along with a more prominent peak at one-half the *m/z* of the former with a M_P at approximately *m/z* 11,000, indicating the possible presence of doubly-charged ions. There is also a glimpse of an ion signal peak emerging around *m/z* 7,000 that possibly could indicate the presence of triply-

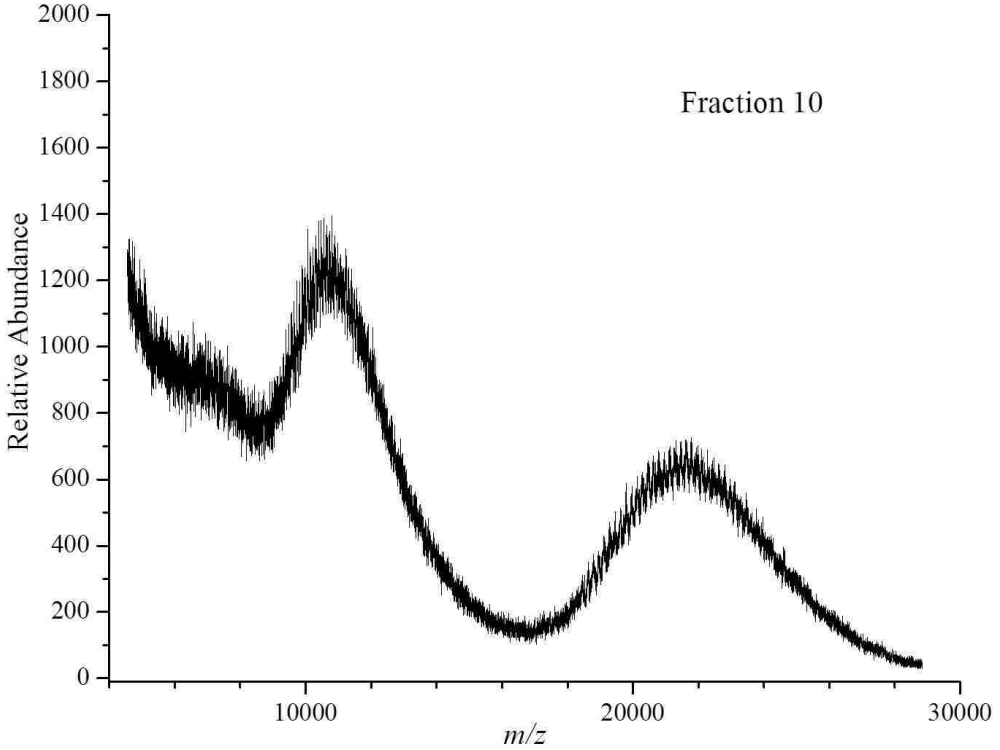

Figure 3.5 MALDI-ToF mass spectrum of P3HT fraction #10 having a M_N = 64,530 Da and a *PDI* = 1.03 determined by analytical SEC-MALLS analysis.

charged material, although this signal does not possess a sufficient signal-to-noise ratio to confirm this. Still, the increasing baseline as the *m/z* decreases in this area lends credence to this possibility. Again there is a large discrepancy between the average molecular weight of fraction 10 obtained by MALDI-ToF-MS as compared to that determined by SEC. The M_N of fraction 10 calculated by SEC was 64,530 Da, whereas the M_N estimated from the MALDI-ToF mass spectrum of fraction 10 is on the order of 22,000 Da; this is presuming the ion signal peak at *m/z* 22,000 is representative of singly-charged material. In such a case the number-average molecular weight (M_N) for this fraction determined by SEC is 3 times that determined by MALDI-ToF-MS.

The MALDI-ToF mass spectrum of fraction 13 is shown in Figure 3.6. This spectrum was obtained using ion gating between *m/z* 4,000–22,000. There are again at least two ion signal peaks present in the spectrum shown in Figure 3.6. An ion signal peak having a M_P at *m/z*

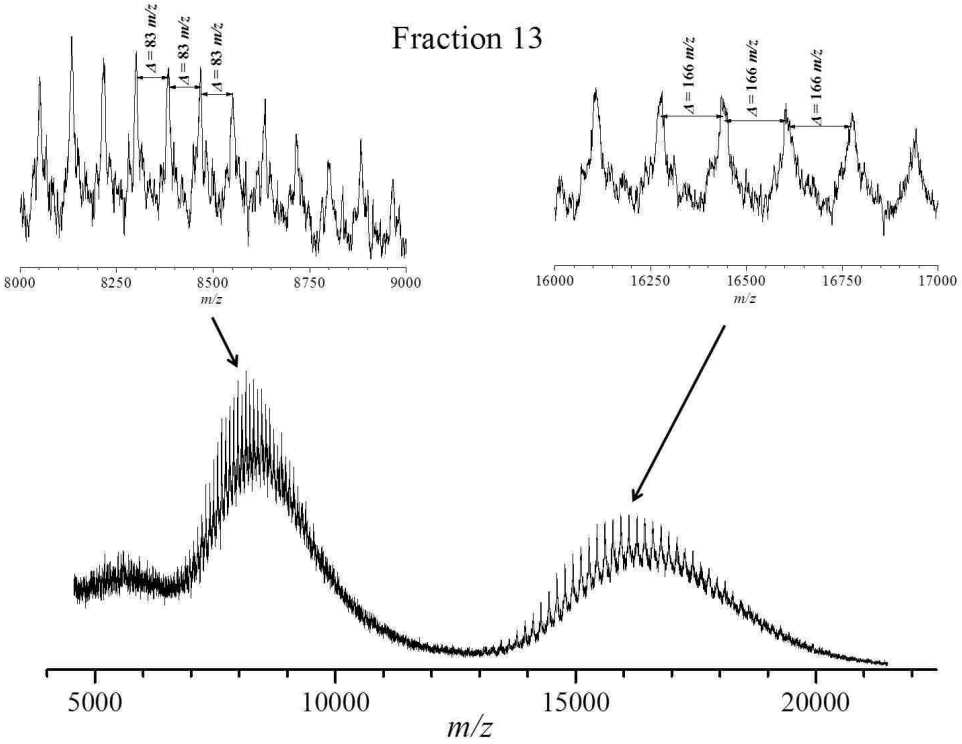

Figure 3.6 MALDI-ToF mass spectrum of P3HT fraction #13 having a M_N = 47,540 Da and a *PDI* = 1.01 determined by analytical SEC-MALLS analysis. The insets show the mass-to-charge difference for the ion series resulting from singly-charged P3HT (right) and doubly-charged P3HT (left).

16,500 is clearly present along with a more intense peak at one-half the *m/z* of the former with a M_P at *m/z* 8,250, indicating the presence of doubly-charged ions. The presence of doubly-charged species is now strongly evidenced as shown in the inset spectrum of Figure 3.6. The ion signals shown in the insets are now resolved well enough to discern the differences in *m/z* for the representative repeat units within the signal peaks. The repeat units for the signal at approximately *m/z* 8,250 differ by *m/z* 83–one-half the molar mass of the 3-*n*-hexylthiophene unit (166.2 amu)–whereas the ion series at approximately *m/z* 16,500 differ by *m/z* 166*;* clearly indicating the signal situated around *m/z* 8,2500 results from doubly-charged ions (cf. Section 2.3.1, Equation 2.4).

There is also ion signal emerging at *m/z* 5,500 that perhaps indicates the presence of triply-charged material, although this signal does not possess a sufficient signal-to-noise ratio to

confirm this. Again there is a large discrepancy between the average molecular weight of fraction 13 obtained by MALDI-ToF-MS as compared to that determined by SEC. The M_N of fraction 13 calculated by SEC was 47,540 Da, whereas the M_N estimated from the MALDI-ToF mass spectrum of fraction 13 is estimated at approximately 16,500 Da. The number-average molecular weight (M_N) for this fraction determined by SEC is approximately 3 times that determined by MALDI-ToF-MS.

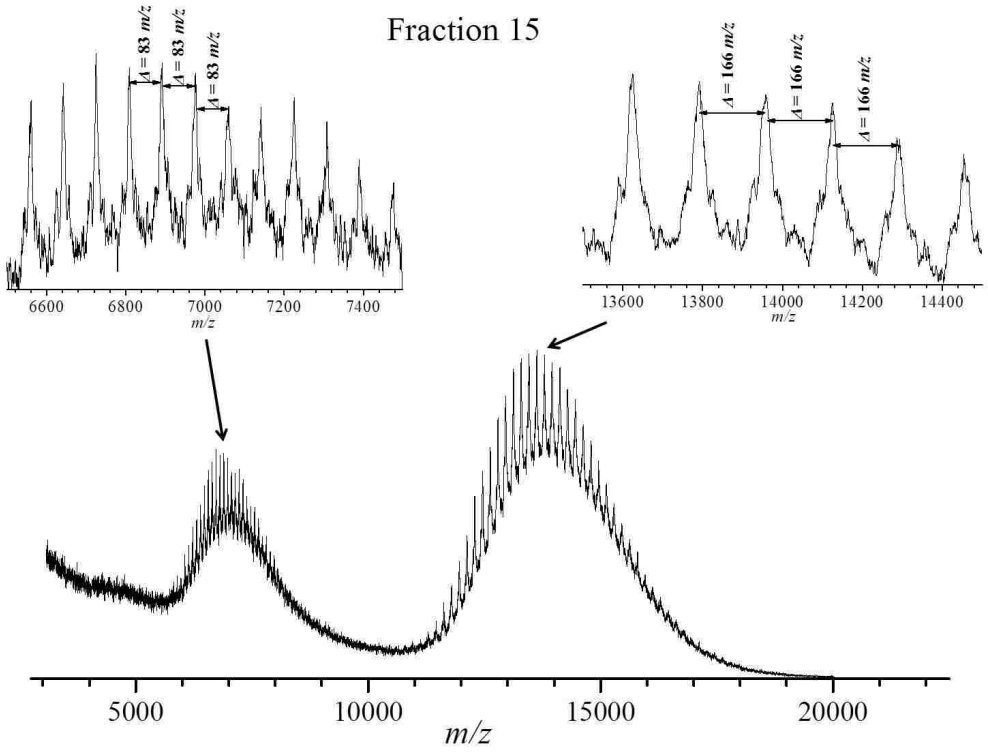

Figure 3.7 MALDI-ToF mass spectrum of P3HT fraction #15 having a M_N = 42,870 Da and a *PDI* = 1.01 determined by analytical SEC-MALLS analysis. The insets show the mass-to-charge difference for the ion series resulting from singly-charged P3HT (right) and doubly-charged P3HT (left).

The MALDI-ToF mass spectrum of fraction 15 is shown in Figure 3.7. This spectrum was obtained using ion gating between *m/z* 3,000–20,000. There are again at least two ion signals present in the lower spectrum in Figure 3.7. An ion signal peak having a M_P at roughly *m/z* 13,800 is clearly present along with a less intense peak at one-half the *m/z* of the former with a M_P at *m/z* 6,900 indicating the presence of doubly-charged ions. The presence of doubly-

charged species is again evidenced by ion signals shown in the insets, which are now resolved well enough to discern the differences in the *m/z* for the representative repeat units within the signal peaks. The ion series at approximately *m/z* 6,900 differ by *m/z* 83–one-half the molar mass of the 3-*n*-hexylthiophene unit (166.2 amu)–whereas the ion series at approximately *m/z* 13,800 differ by *m/z* 166*;* clearly indicating the ion series situated around *m/z* 6,900 results doubly-charged ions (cf. Section 2.3.1, Equation 2.4). There is also an ion series emerging at *m/z* 4,600 that might indicate the presence of triply-charged material, although this signal does not possess a sufficient signal-to-noise ratio to confirm this. Again there is a large discrepancy between the average molecular weight of fraction 15 obtained by MALDI-ToF-MS as compared to that determined by SEC. The M_N of fraction 15 calculated by SEC was 42,870 Da, whereas the M_N estimated from the MALDI-ToF mass spectrum of fraction 15 is estimated at approximately 13,800 Da. The number-average molecular weight (M_N) for this fraction determined by SEC is approximately 3 times that determined by MALDI-ToF-MS.

The MALDI-ToF mass spectrum of fraction 18 is shown in Figure 3.8. This spectrum was obtained using ion gating between *m/z* 3,000–15,000. There are at least two ion series signals present in the lower spectrum of Figure 3.8. An ion series signal having a M_P at roughly *m/z* 10,800 is clearly present along with a less intense ion series signal at one-half the *m/z* of the former with a M_P at *m/z* 5,400 indicating the presence of doubly-charged ions. The presence of doubly-charged species is again evidenced by ion signals shown in the insets, which are now resolved well enough to discern the differences in the *m/z* for the representative repeat units within the ion series signals. The ion series at approximately *m/z* 5,400 differ by *m/z* 83–one-half the molar mass of the 3-*n*-hexylthiophene unit (166.2 amu)–whereas the ion series at approximately *m/z* 10,800 differ by *m/z* 166*;* clearly indicating the peak situated around *m/z* 5,400 results from doubly-charged ions (cf. Section 2.3.1, Equation 2.4). There is also an ion

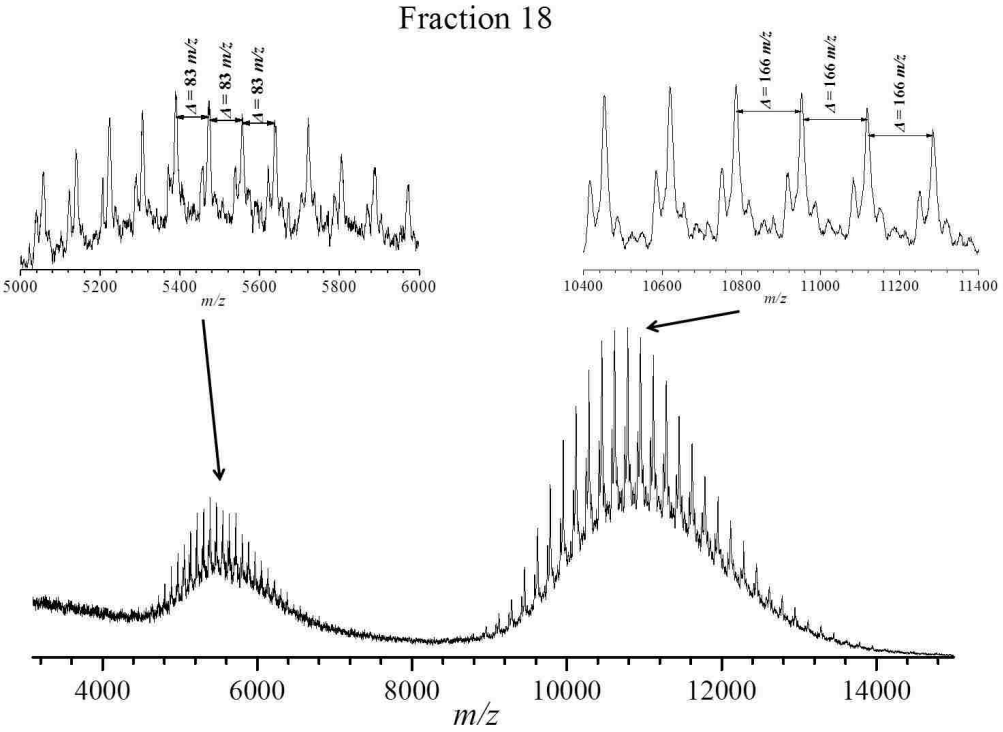

Figure 3.8 MALDI-ToF mass spectrum of P3HT fraction #18 having a M_N = 33,440 Da and a *PDI* = 1.01 determined by analytical SEC-MALLS analysis. The insets show the mass-to-charge difference for the ion series resulting from singly-charged P3HT (right) and doubly-charged P3HT (left).

series emerging at *m/z* 3,600 that perhaps indicates the presence of triply-charged material, although this signal does not possess a sufficient signal-to-noise ratio to confirm this. Again there is a large discrepancy between the average molecular weight of fraction 18 obtained by MALDI-ToF-MS as compared to that determined by SEC. The M_N of fraction 18 calculated by SEC was 33,440 Da, whereas the M_N estimated from the MALDI-ToF mass spectrum of fraction 18 is estimated at approximately 10,800 Da. The number-average molecular weight (M_N) for this fraction determined by SEC is approximately 3 times that determined by MALDI-ToF-MS.

The MALDI-ToF mass spectrum of fraction 24 is shown in Figure 3.9. This spectra was obtained using ion gating between *m/z* 2,000–8,000. There are two ion series signals present in the lower spectrum shown in Figure 3.9. An ion series signal having a M_P at roughly *m/z* 7,000 is present along with a slightly less intense signal at one-half the *m/z* of the former with a M_P at

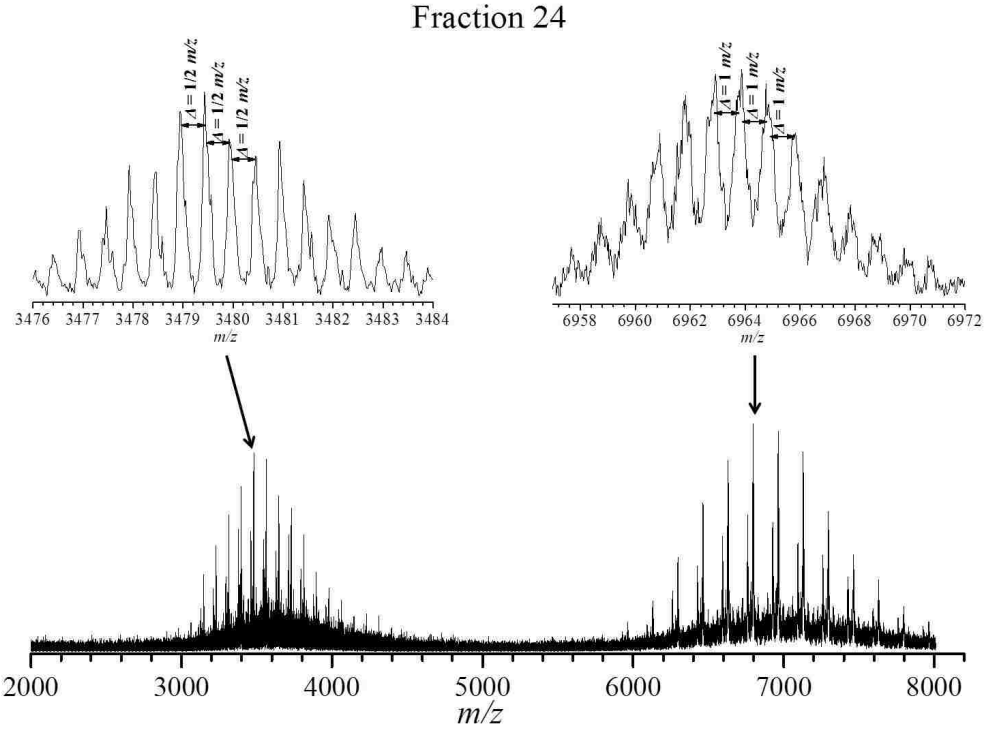

Figure 3.9 MALDI-ToF mass spectrum of P3HT fraction #24 having a M_N = 28,630 Da and a *PDI* = 1.02 determined by analytical SEC-MALLS analysis. The insets show the mass-to-charge difference for the ion series resulting from singly-charged P3HT (right) and doubly-charged P3HT (left).

m/z 3,500 indicating the presence of doubly-charged ions. The presence of doubly-charged species is now surely confirmed as shown in the inset spectra of Figure 3.9. The ion series signals shown in the insets are now resolved well enough to discern the isotopic differences in the *m/z* for the individual ion signals within the ion series.

The individual ion signals comprising the series at approximately *m/z* 3,500 differ by *m/z* ½, whereas the ion series at approximately *m/z* 7,000 differ by *m/z* 1; this undoubtedly indicates that the peak situated around *m/z* 3,500 results from doubly-charged ions (cf. Section 2.3.1, Equation 2.4). Again there is a large discrepancy between the average molecular weight of fraction 24 obtained by MALDI-ToF-MS as compared to that determined by SEC. The M_N of fraction 24 calculated by SEC was 28,630 Da, whereas the M_N estimated from the MALDI-ToF mass spectrum of fraction 24 is approximately 7,000 Da. The number-average molecular weight

(M_N) for this fraction determined by SEC is approximately 4 times that determined by MALDI-ToF-MS.

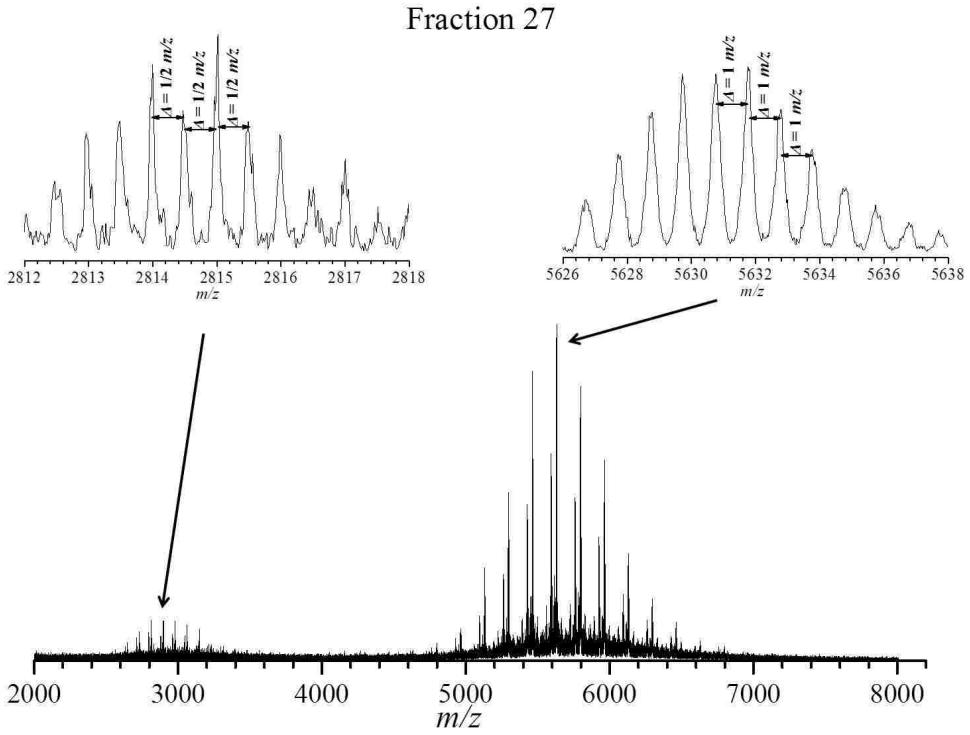

Figure 3.10 MALDI-ToF mass spectrum of P3HT fraction #27 having a M_N = 23,240 Da and a *PDI* = 1.02 determined by analytical SEC-MALLS analysis. The insets show the mass-to-charge difference for the ion series resulting from singly-charged P3HT (right) and doubly-charged P3HT (left).

The MALDI-ToF mass spectrum of fraction 27 is shown in Figure 3.10. This spectrum was obtained using ion gating between *m/z* 2,000–8,000. There are two ion series signals present in the lower spectrum shown in Figure 3.10. An ion series signal having a M_P at roughly *m/z* 5,600 is present along with a much less intense signal at one-half the *m/z* of the former with a M_P at *m/z* 2,800 indicating the presence of doubly charged ions. The presence of doubly-charged species is again confirmed by the ion series signals shown in the insets, which are resolved well enough to discern the isotopic differences in the *m/z* for the individual ion signals within the ion series. The individual ion signals comprising the ion series at approximately *m/z* 2,800 differ by *m/z* ½, whereas the ion series at approximately *m/z* 5,600 differ by *m/z* 1*;* undoubtedly indicating

that the peak situated around *m/z* 2,800 results from doubly-charged ions (cf. Section 2.3.1, Equation 2.4). Again there is a large discrepancy between the average molecular weight of fraction 27 obtained by MALDI-ToF-MS as compared to that determined by SEC. The M_N of fraction 27 calculated by SEC was 23,240 Da, whereas the M_N estimated from the MALDI-ToF mass spectrum of fraction 27 is estimated at approximately 6,000 Da. The number-average molecular weight (M_N) for this fraction determined by SEC is approximately 4 times that determined by MALDI-ToF-MS.

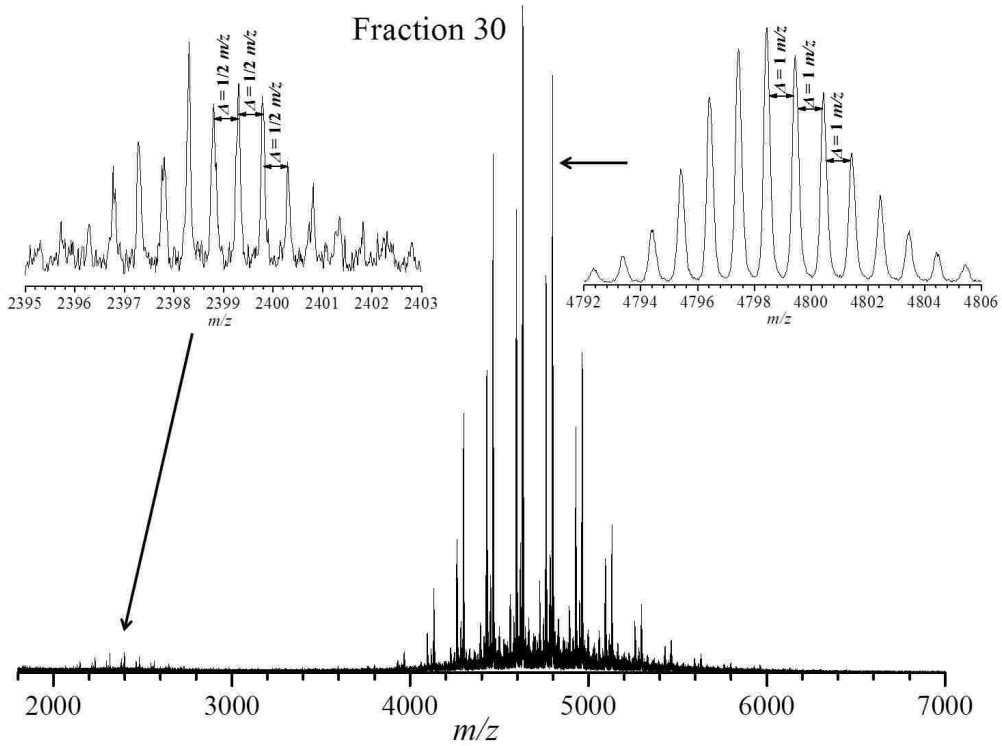

Figure 3.11 MALDI-ToF mass spectrum of P3HT fraction #30 having a M_N = 26,390 Da and a *PDI* = 1.02 determined by analytical SEC-MALLS analysis. The insets show the mass-to-charge difference for the ion series resulting from singly-charged P3HT (right) and doubly-charged P3HT (left).

The MALDI-ToF mass spectrum of fraction 30 is shown in Figure 3.11. Ion gating was not employed for the acquisition of this spectrum. There are two ion series signals present in the lower spectrum shown in Figure 3.11. An ion series signal having a M_P at roughly *m/z* 4,800 is

present along with a much less intense ion series signal at one-half the *m/z* of the former with a M_P at *m/z* 2,400 indicating the presence of doubly-charged ions. The presence of doubly-charged species is again confirmed by the ion series signals shown in the insets, which are resolved well enough to discern the isotopic differences in the *m/z* for the individual ion signals within the ion series. The individual ion signals comprising the ion series at approximately *m/z* 2,400 differ by *m/z* ½, whereas the ion series at approximately *m/z* 4,800 differ by *m/z* 1; undoubtedly indicating that the peak situated around *m/z* 2,800 results from doubly-charged ions (cf. Section 2.3.1, Equation 2.4). There is a large discrepancy between the average molecular weight of fraction 30 obtained by MALDI-ToF-MS as compared to that determined by SEC. The M_N of fraction 30 calculated by SEC was 26,390 Da, whereas the M_N estimated from the MALDI-ToF mass spectrum of fraction 30 is estimated at approximately 5,000 Da. The number-average molecular weight (M_N) for this fraction determined by SEC is approximately 5 times that determined by MALDI-ToF-MS.

The MALDI-ToF mass spectrum of fraction 33 is shown in Figure 3.12. Ion gating was not employed for the acquisition of this spectrum. There are two ion series signals present in the lower spectrum shown in Figure 3.12. An ion series signal having a M_P at roughly *m/z* 4,000 is present along with a much less intense ion series signal at one-half the *m/z* of the former with a M_P at *m/z* 2,000 indicating the presence of doubly-charged ions. The presence of doubly-charged species is again confirmed by the ion signals shown in the insets, which are resolved well enough to discern the isotopic differences in the *m/z* for the individual ion signals within the ion series. The individual ion series at approximately *m/z* 2,000 differ by *m/z* ½, whereas the ion series at approximately *m/z* 4,000 differ by *m/z* 1; undoubtedly indicating that the ion series signal situated around *m/z* 2,000 results from doubly-charged ions (cf. Section 2.3.1, Equation 2.4).

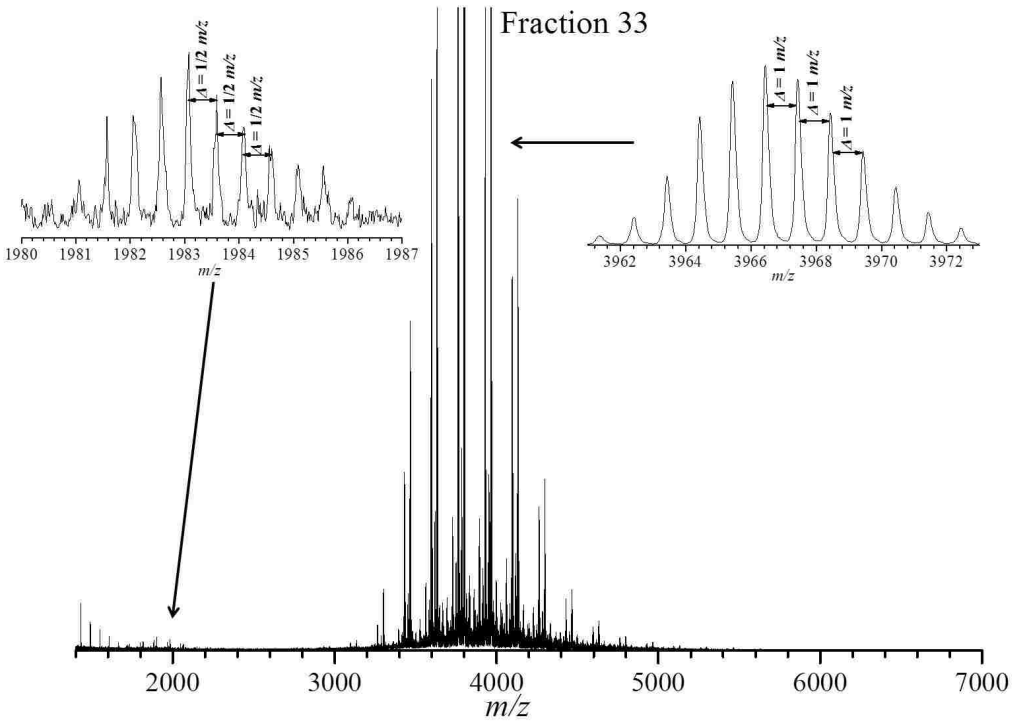

Figure 3.12 MALDI-ToF mass spectrum of P3HT fraction #33. The insets show the mass-to-charge difference for the ion series resulting from singly-charged P3HT (right) and doubly-charged P3HT (left).

The intensity of the ion series signal at *m/z* 2,000 possessing doubly-charged ions is severely diminished. In fact, signal intensity for doubly charged materials began to steadily diminish for fraction eluting later than fraction 24. This phenomenon may be a function of oligomer chain length as it has been reported there needs to be at least between 6–10 monomer units in an oligomer to minimize the coulombic repulsion and structural distortion effects (cf. Section 1.2.8) of dication formation in order to stablize the bipolaron structure of P3ATs.[61,62] Still, the material in fraction 33 having a M_p determined by MALDI-ToF-MS to be around 4,000 Da is primarily comprised of oligomers consisting of approximately 21–27 monomer units. Therefore, the diminishing signal for doubly charged species might also be attributed to the decrease in oxidation potential with the increase in chain length seen for these materials[53,63] and

the probability of producing doubly-charged species is likely influenced by a combination of both functions.

The SEC determination of the average molecular weights and molecular weight distribution for fraction 33 was unattainable, due to the fact that the MALLS detector was unable to provide a sufficient detection signal for this fraction and light scattering data measurements could not be obtained for fractions eluting later than fraction 30. This may be attributed to the fact that MALLS is not an efficient means for measuring the hydrodynamic radius of smaller molecules[44,47-49] but undoubtedly is also due to the fact that the later eluting fractions were much less concentrated than the earlier eluting fractions.

The most striking result obtained from the study presented in Section 3.4.1 is the existence of multiply-charged ions in the gas phase during the MALDI-ToF-MS analysis of P3HTs. Nonetheless, The above comparisons of molecular weight data obtained by means of SEC-MALLS and MALDI-ToF-MS for the P3HT fractions examined herein clearly show massive discrepancies involving the apparent overestimation of the average molecular weight calculated by means of SEC-MALLS that is on the order of 3-4 times greater than those estimated by means of MALDI-ToF-MS. The exact reasons for this phenomenon are still not fully understood, although there may multiple factors contributing to this problem.

First, with light scattering the molar mass can be directly obtained from R_θ/K_C when $\sin^2(\theta/2)$ equals zero (cf. Section 2.3.2). However, it is not feasible to measure the scattered light at 0° and higher angles must be used to perform the light scattering measurements. Therefore, in order to obtain the molar mass and root-mean-square radius from multiangle light scattering (MALLS), measurements at multiple angles greater than zero are performed and then extrapolated to zero. This extrapolation is done using a Debye,[64] Zimm,[65] or Berry[66] plot in which R_θ/K_C is plotted as a function of $\sin^2(\theta/2)$ where the intercept will be a function of the

molar mass and the slope at $\sin^2(\theta/2) = 0$ is a function of both molar mass and the root-mean-square radius. There are several methods of preparing these extrapolation plots that each depend on parameter fitting to a given function, which demands a prior knowledge of the polymers conformation (i.e. random-coil, spherical, or rigid-rod) for the accurate characterization of the light scattering data collected.[44,48] It is has been shown in the literature that the choice of extrapolation method and empirically determined parameter fitting can have a large impact on the accuracy of the results obtained by MALLS.[48] Therefore, it is quite possible that the extrapolation of $\sin^2(\theta/2) = 0$ used for the analysis of the fractions investigated in Section 3.4.1 may have been erroneous for the conformational nature of P3HTs examined.

Exacerbating this condition is the fact that the SRII ($\delta n/\delta c$), or the change in refractive index as a function of the change in the materials concentration, for P3HTs is dependent on the molecular weight of the material and is very likely dependent on the regioregularity and conformational structure of the polymer as well. The $\delta n/\delta c$ employed for the purpose of SEC-MALLS analysis performed within this Chapter was empirically evaluated using a bulk polymer sample (unfractionated) of P3HT and was determined to be 0.227. However, initial experiments performed in the course of this work indicated that the $\delta n/\delta c$ for differing molecular weight fractions of P3HT vary immensely. For example, fractions of P3HT that were separated by means of soxhlet extractions using various organic solvents were collected and then the $\delta n/\delta c$ for lower molecular weight material extracted in acetone and *n*-hexane was determined. The $\delta n/\delta c$ for the acetone fraction that included the distribution of the smallest molecular weight material ($M_N \sim$ 11,400 Da calculated by analytical SEC-MALLS) was determined to be 0.119, whereas the $\delta n/\delta c$ for the *n*-hexane fraction that contained the distribution of the next-larger molecular weight material ($M_N \sim$ 36,000 Da calculated by analytical SEC-MALLS) was found to be 0.202.

The $\delta n/\delta c$ for subsequent larger molecular weight P3HTs–extracted using methylene chloride and then chloroform[9] –was not determined.

However, the large change in the $\delta n/\delta c$ for the two fractions examined has great implications on the accurate determination of molecular weight data for P3HTs obtained by SEC-MALLS. First of all, the optical constant, K, used for the mathematical calculation of molecular weight from the intensity of scattered light is proportional to the square of the $\delta n/\delta c$ (cf. Section 2.3.2, Equation 2.6). Since the molecular weight calculated from MALLS is inversely proportional to the optical constant, K, (cf. Section 2.3.2, Equation 2.8) employing a $\delta n/\delta c$ half as large as the "true" $\delta n/\delta c$ will result in calculated molecular weights twice as large as the "true" molecular weight of that material. This may possibly aid in explaining the large overestimations of larger molecular weight materials observed for the early eluting fractions examined within this Chapter.

Still, this does not help to explain the overestimations of molecular weight for the later eluting fractions obtained by means of SEC-MALLS having smaller molecular weight polymer. However, the extrapolation of the intensity of scattered light at $\sin^2(\theta/2) = 0$ in the Debye plot–or similar plot where R_θ/K_C is plotted as a function of $\sin^2(\theta/2)$–is also dependent on the concentration of the material under examination. The concentration of the eluting material during SEC-MALLS determined using the DRI detector relies solely on the $\delta n/\delta c$ of the eluting material. If a large $\delta n/\delta c$ is employed for this determination and the material actually exhibits a much smaller change in refractive index as a function of concentration then the concentration of the material will be greatly underestimated. This phenomenon is clearly evidenced in the semipreparative SEC chromatogram shown in Figure 3.2 where there is no appreciable signal response from the DRI detector for the final eluting fractions of P3HT despite the observable presence of small molecular weight material. Because the molecular weight calculated by

MALLS is inversely proportional to concentration, c, (cf. Section 2.3.2, Equation 2.8) employing a $\delta n/\delta c$ that is too large will result in overestimations of the actual molecular weight of the material. However, It is likely that the inefficiency of MALLS to correctly assess the molecular weight of materials having a small hydrodynamic volumes (< 10,000 Da)[44,48] plays a large role in the erroneous average molecular weights seen for the later eluting fractions as calculated by SEC-MALLS.

Furthermore, it is very possible that aggregation of P3HTs could be occurring during the SEC-MALLS analysis leading to the erroneous average molecular weight data seen in Section 3.4.1. It is well known that poly(3-alkylthiophene)s have a strong tendency to self assemble due to π-π interchain interactions.[9,67,68] Reports have shown that P3HTs can undergo extensive π-stacking to form aggregates in solution up to 1000 molecules, assembled in side-by-side stacking mode.[69,70] Aggregation to this extent is shown to typically occur only upon the introduction of small amounts a nonsolvent–or one in which P3HT is less soluble–such as methanol into a solution of P3HT dissolved in a good solvent, such as chloroform. However, aggregation to this extreme extent is not necessary in order to cause large overestimations of molecular weight by MALLS analysis.

However, P3HTs have been shown to still possess a rigid-rod conformation when they are dissolved in a good solvent[69,70] that would afford the material the opportunity for π-π interchain interactions that could lead to some degree of π-stacking or aggregation. Furthermore, extensive aggregation up to thousands of molecules is not necessary in order to give the overestimation of molecular weight data seen in Section 3.4.1. In fact, possibly only several P3HT chains would have to aggregate to produce the results presented above depending on the true molecular weight of the polymer chains examined. Some unusual behavior that may be evidence of aggregation of P3HTs appears in the semipreparative SEC chromatogram presented

in Figure 3.2. The front of the chromatogram trace shows a clear separation of early eluting material that results in a unique peak eluting prior to the main separation peak for the bulk of the P3HT. This may be indicative of the largest molecular weight material that would be most likely to aggregate leading to the exorbitant molecular weights for these fractions calculated by analytical SEC. Furthermore, the tailing seen in the chromatogram for the late eluting P3HT fractions is also very curious. This could be an indication of some enthalpic interaction between the polymer and the column, although the mechanism of SEC is based on the premise that the separation is purely entropic (cf. Section 2.3.2). However, it could possibly be an indication of some degree of conformational change in the material that might be caused by aggregation of the polymer as well. In any case, given the electronic structure of P3HTs and their rigid-rod like conformation the probability that they are aggregating during the SEC separations is not beyond the realm of possibility.

3.4.2 Mass Discrimination of P3HTs During MALDI-ToF-MS Analysis

The data presented in Section 3.4.1 may provide further insight into the mass discrimination of higher molecular weight materials observed during the MALDI-ToF-MS analysis of bulk P3HT samples for which multiply-charged ions may play an integral role. To more closely examine the role of multiply-charged material in the mass discrimination of P3HTs an experiment was performed in which fractionated P3HT samples having narrow molecular weight distributions were combined in equal volumetric proportions in order to simulate polydisperse P3HT samples. The MALDI-ToF-MS analyses for all samples were performed under similar preparation and instrumental conditions. The matrix-to-analyte ratio was kept in the same proportion throughout the experiment. Likewise, the laser power was maintained just above the threshold needed for observable ion detection for all spectra acquired. The results of this experiment are shown in the MALDI-ToF mass spectra compiled in Figure 3.13.

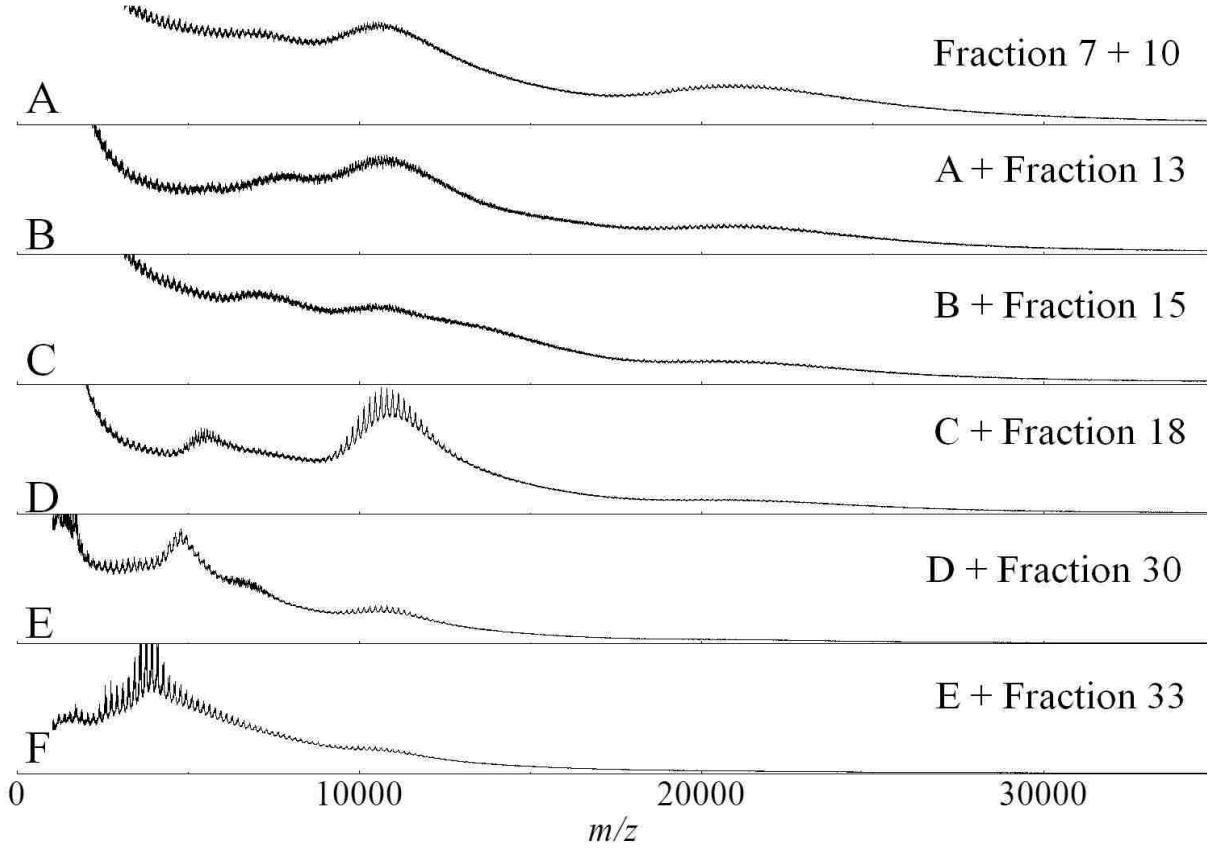

Figure 3.13 MALDI-ToF mass spectra showing sequential addition of equal volumetric portions of lower molecular weight fractions of P3HT to higher molecular weight fractions.

In Figure 3.13A is the mass spectrum for the sample comprised of equal volumetric portions of fractions 7 and 10. Individual MALDI-ToF-MS examination of fraction 7 (cf. Figure 3.4) indicated this fraction contains P3HT having a M_P around *m/z* 29,000, where as fraction 10 (cf. Figure 3.5) was comprised of P3HT having a M_P at roughly *m/z* 22,000. In the mass spectrum shown in Figure 3.1.3A there is no clear evidence of the ion series signal representing singly-charged P3HT from fraction 7 (*m/z* 29,000), although the elevated baseline in that *m/z* region tailing from the prominent ion series signal at roughly *m/z* 22,000–representing singly-charged P3HT from fraction 10–may be attributed to some degree from the presence of the material at *m/z* 29,000 from fraction 7. There is a prominent ion series signal at ~ *m/z* 22,000 which is likely the product of the singly-charged material from fraction 10 along with a clear

peak at ~11,000 that likely represents the doubly-charged material from the same fraction. The elevated baseline between these two ion series signals might be attributed to the presence of doubly-charged species from fraction 7 (*m/z* 14,500). Furthermore, there exists an emerging peak around *m/z* 7,000 that implies the presence of triply-charged material from fraction 10. This presumption is strengthened by the very high baseline between *m/z* 7,000–11,000 that could be caused by triply-charged P3HT from fraction 7. Furthermore, the sharply increasing baseline below *m/z* 7,000 may very well be a result of multiply-charged ($> 3^+$) P3HT.

Figure 3.13B is the mass spectrum for a polymer blend containing equal volumetric portions of fractions 7, 10, and 13 ($M_P \sim$ *m/z* 29,000, 22,000, and 16,500). There is no distinguishable ion series signal present in Figure 3.13B that can be identified for the singly-charged material from fraction 13 (*m/z* 16,500), although the baseline in the region for this ion series signal is somewhat elevated as compared to the same region in Figure 3.13A. However, the relative intensity of the doubly-charged species (*m/z* 8,250) for fraction 13 seen in mass spectrum in Figure 3.6 is close to twice that of the singly-charged species. In fact the presence of the doubly-charged ion series signal from fraction 13 is seen in the MALDI-ToF mass spectrum in Figure 3.13B by the increase and shift towards higher *m/z* in the baseline in the region of *m/z* 7000–11,000 as compared to Figure 3.13A. In the mass spectrum in Figure 3.13B there appears a decrease in the intensity of the ion series signal at ~ *m/z* 22,000 representing the singly-charged P3HT from fraction 10 compared to the intensity for the same ion series signal in Figure 3.13A. This is evidence to some degree that mass discrimination of higher mass material may be occurring in the presence of excess lower mass materials. Furthermore, the increase in the slope of the elevating baseline below *m/z* 7,000 still points towards the presence of multiply-charged ($> 3^+$) P3HT.

The MALDI-ToF mass spectrum for the polymer blend containing fractions 7, 10, 13, and 15 ($M_P \sim m/z$ 29,000, 22,000, 16,500, and 13,800) is shown in Figure 3.13C. The overall effect to the spectrum upon addition of fraction 15 ($M_P \sim m/z$ 13,800, cf. Figure 3.7) is the broadening and smoothing of the baseline over the entire m/z range of the material. There is the indication of the ion series signal for the singly-charged species from fraction 15 by the increase in the baseline between m/z 12,000–15,000. This has the effect of giving the baseline an appearance of increasing almost linearly from the front of the ion series signal at $\sim m/z$ 22,000 for the singly-charged species from fraction 10. There also is an indication of a decrease in the intensity of the ion series signal at $\sim m/z$ 22,000, although this is difficult to discern because of the overall increase in the baseline. There is also an apparent signal increase in the m/z region for the doubly-charged P3HT from fraction 15 between m/z 6,000–8,000–that is now a combination of doubly-charged signal from fractions 13 and 15, as well as triply-charged material from fraction 10–that exceeds the signal at $\sim m/z$ 11,000 for the doubly-charged material from fraction 10. The constructive addition of signals from all three of these fractions may help to explain the large increase in signal for this region. The baseline below m/z 6,000 also continues to increase compared to the former mass spectra presented, most likely due to the constructive addition of multiply-charged species providing further evidence for the existence of species having charges greater than 3^+.

In Figure 3.13D is shown the mass spectrum of the polymer blend comprised of fractions 7, 10, 13, 15, and 18 ($M_P \sim m/z$ 29,000, 22,000, 16,500, 13,800, and 10,800). In the mass spectrum shown in Figure 3.13D there arises a dramatic increase in the signal situated in the region around m/z 11,000 that exceeds all other discernable signals within the spectrum. This ion series signal may be comprised of signals from both the singly-charged P3HT from fraction 18, as well as the signals from the doubly-charged species from fraction 10, and the constructive

addition of signals from both samples would explain the very high intensity of this ion series signal. The ion series signal at ~ *m*/*z* 22,000 representing the singly-charged species of fraction 10 observably diminishes as does the baseline in the region where there appeared signals in the form of increasing baseline intensity for the singly-charged species of fractions 13 and 15 (M_P ~ *m*/*z* 16,500, and 13,800) between *m*/*z* 13,000–18,000.

A strong ion series signal also appears in the *m*/*z* region expected for the doubly-charged species of fraction 18 (~*m*/*z* 5,400), although its width and intensity point to the fact that this ion series signal is the result of constructive addition of the signals from singly-charged P3HT from fraction 18, doubly-charged species from fraction 15, and triply-charged P3HT ions from fraction 10. This speculation is reinforced by the largely elevated almost level baseline signal in the region of *m*/*z* 7,000–9,000 between the two most prominent ion series signals that is likely the result of the constructive addition of signals arising from doubly- or triply-charged and possibly higher-charged species from all of the fractions within the polymer blend. The idea of constructive addition of signals by various multiply-charged species from the different polymer fractions would also aid in explaining the sharp increase in the baseline seen in the low *m*/*z* region (<*m*/*z* 5,000) that appears in all of the MALDI-ToF mass spectra presented so far.

The decrease in the ion signals for the singly-charged species of fractions 10, 13, and 15 (M_P ~ *m*/*z* 22,000, 16,500, and 13,800) seen in the MADLI-ToF mass spectrum presented in Figure 3.13D give an indication that mass discrimination for the higher-weight P3HT is occurring upon the sequential addition of fractions possessing lower molecular weight material. However, the intensity of the ion series signal situated at ~ *m*/*z* 11,000 clearly implies that there is constructive addition of ion signals for differently charged P3HT ions from different fraction samples occurring; in this case singly-charged species from fraction 18, and doubly-charged species from fraction 10. This implies that these higher-mass materials are still being ionized in

the MALDI event, although they are not being detected. This is further evidenced by the elevated baseline in the region of *m/z* 13,000–18,000 that is probably comprised of overlapping and constructively added signals for a variety of multiply-charged ions from several P3HT fractions including the higher-mass fractions (i.e. fractions 10, 13, and 15–$M_P \sim m/z$ 22,000, 16,500, and 13,800). Therefore, it would appear that the source of discrimination lies in detection and not ionization efficiency. These facts point to the probable source of discrimination as being a result of the lack of detector response for the higher-weight materials due to saturation of the detector (cf. Section 3.1.3) because of the exceedingly continuous stream of ions resulting from the many varieties of multiply charged species produced in the MALDI event.

In Figure 3.13E is shown the mass spectrum of the polymer blend comprised of fractions 7, 10, 13, 15, 18 and 30 ($M_P \sim m/z$ 29,000, 22,000, 16,500, 13,800, 10,800, and 4,800). With the addition of fraction 30 the signal peaks for the singly-charged ions from fractions 10, 13, and 15 ($M_P \sim m/z$ 22,000, 16,500, and 13,800) are no longer apparent. There still remains the trace of a ion series signal in the region of *m/z* 11,000 where it has been proposed the ion series signal is comprised of signals for both singly-charged ions from fraction 18 and doubly-charged ions from fraction 10, although the ion series signal in this region is significantly diminished from the previous spectrum (cf. Figure 3.13D). The appearance of an ion series in the region between *m/z* 6,000–8,000 indicate the presence of doubly-charged ions from fractions 15 and 18 ($M_P \sim m/z$ 13,800, and 10,800) despite the fact that the singly-charged ions from both of these fractions are no longer observable in the mass spectrum. Furthermore, the elevated baseline between the ion series signals situated at *m/z* 6,000–8000 and *m/z* 11,000 indicate the presence of doubly-charged P3HT ions from fraction 13 ($M_P \sim m/z$ 16,500).

The fact that the singly-charged ions from fractions 10, 13, and 15 are no longer apparent in the MALDI-ToF mass spectrum shown in Figure 3.13E, whereas the doubly-charged ions from the same fraction are still evident shows that the P3HT in these fractions is being ionized during the MALDI event, although there is lack of a sufficient detector response for the singly-charged species. This further supports the argument that detector saturation is the primary source of mass discrimination of higher molecular weight materials seen in the analysis of bulk P3HTs by MALDI-ToF-MS and not desorption/ionization discrimination. The excessive decrease in the ion series signal around *m/z* 11,000 reinforces the idea that successive addition of lower molecular weight materials to the polymer blend causes a predictable decrease in the signal for higher-mass material, as a result of a larger population of lower mass material that creates a continuous stream of particles striking the detector thereby diminishing the amplification of signals seen for higher-mass distributions due to the absence of sufficient time required for detector recovery. Furthermore, this phenomenon is extremely aggravated by the presence of multiply charged polymer ions that are now clearly shown to exist in the gas phase during MALDI-ToF-MS analysis of P3HTs.

The mass spectrum presented in Figure 3.13E also clearly shows a prominent ion series at roughly *m/z* 4,800 arising from singly-charged ions of P3HT from fraction 30 ($M_P \sim m/z$ 4,800), although the intensity and width of this ion series signal would imply the presence of signals for multiply-charged ions from higher-mass fractions that have constructively added to the signal. The individual examination of fraction 30 by MALDI-ToF-MS (cf. Figure 3.11) showed a tremendous decrease in the intensity for the signals arising for doubly-charged species. In fact, signal for doubly-charged materials began to steadily diminish for fractions eluting later than fraction 24.

As mentioned above, the observed decrease in the population of doubly-charged species that are formed during MALDI-ToF-MS analysis may be a function of oligomer chain length, as it has been reported there needs to be a minimum of 6–10 monomer units in an oligomer to minimize the coulombic repulsion and structural distortion effects (cf. Section 1.2.8) of dication formation in order to stablize the bipolaron structure of P3ATs.[61,62,71] Still, the material in fraction 30 having a M_P determined by MALDI-ToF-MS to be around 4,800 Da is primarily comprised of oligomers consisting of approximately 27–34 monomer units. However, it has been shown that it is energetically favorable to localize the charges that appear on P3AT chains, producing a local distortion (quinoidal structure) of the polymer lattice around the charge,[72] which necessitates a coplanar arrangement of the monomer rings in order for a small band gap and high conductivities to be achieved.[72-74]

Hence, the probability of the formation of doubly-charged species may also be a function of the regioregularity (cf. Sections 1.2.3–1.2.6) of the material. ^{1}H-NMR analysis of similar fractions from a different P3HT sample formed in the identical fashion to those presented within this Chapter and collected during semipreparative separation did show some variation in regioregularity between the different fractions. The analysis of the unfractionated bulk P3HT yielded a regioregularity of 77%. The ^{1}H-NMR analysis of early eluting fractions showed regioregularities that were on the order of 81%, whereas the ^{1}H-NMR analysis of later eluting fractions were shown to have regioregularities as low as 70%. Thus the differences in regioregularity between the fractions may play a role in influencing the formation of doubly-charged species seen throughout this Chapter.

Finally, the diminishing signal for doubly-charged species might also be a function of the decrease in oxidation potential with increasing chain length seen for these materials.[53,63] In fact the UV-Vis spectrometric analysis of fractions very similar to those presented within this chapter

did show a blue shift in absorption from 440 nm to roughly 405 nm for later eluting fractions. Therefore, the probability of producing doubly-charged species is most likely influenced by a combination of all three of the above-mentioned functions. Nonetheless, in the mass spectrum presented in Figure 3.13E, there appears an unusually elevated baseline signal below *m/z* 4,000 that must be due to the constructive addition of multiply-charged ion signals arising from a combination of higher molecular weight material from the former fractions. This fact aids to reinforce the premise that multiply-charged species are a primary contributor to detector saturation leading to the mass discrimination of higher-mass materials during the MALDI-ToF-MS analysis of P3HTs.

In Figure 3.13E is shown the mass spectrum of the polymer blend comprised of fractions 7, 10, 13, 15, 18, 30 and 33 ($M_P \sim m/z$ 29,000, 22,000, 16,500, 13,800, 10,800, 4,800 and 4,000). Upon the addition of fraction 33, the mass spectrum takes on an appearance strikingly similar to the MALDI-ToF-MS mass spectrum for the unfractionated P3HT sample, which is presented in Figure 3.1. The ion series signal once at *m/z* 22,000 representing the singly-charged ions from fraction 10 is no longer observable and the response where there was once an indication of signal for singly-charged species from fractions 13 and 15 is very much diminished. The ion series signal near *m/z* 11,000, presumably comprised of singly-charged species from fraction 18, and doubly-charged species from fraction 10, is also diminished to the point that it has virtually "disappeared" into the baseline. In fact the spectrum shows a more or less flat baseline increasing in intensity from around *m/z* 15,000 back to approximately *m/z* 4,000–where the baseline culminates in an apex that clearly shows ion signals for the singly charged species from fraction 33–and then diminishes in intensity at a similar rate back towards zero. The result is the appearance of one ion series signal with a width of nearly 15,000 amu that is indicative of a broadly disperse polymer sample.

Although there are no discernable ion series signals providing evidence that this distribution is comprised of multiply-charged species of higher-mass material, the intensity and breadth of the baseline before and after the observable ion series signal arising from fraction 33 provides strong evidence to their existence. The characteristics of the mass spectrum in Figure 3.13F–along with the evidence provided by the five former mass spectra in Figure 3.13–leave little doubt that the signals from multiply charged ion species play an integral role in the extreme mass discrimination seen for higher-mass materials in the MALDI-ToF-MS analysis of P3HTs that might otherwise be mistaken for and attributed to simple background noise. Furthermore, the data presented here clearly indicate that detector saturation–aggravated by the phenomenon of multiply charged P3HT ions in the gas phase–is likely the primary cause of this discrimination.

3.5 Conclusions

The body of work presented in this Chapter has raised some very interesting questions with regards to the ability to correctly characterize the absolute molecular weights and molecular weight distributions of poly(3-hexylthiophene)s, P3HT, by means of both SEC-MALLS and MALDI-ToF-MS. First, although SEC-MALLS is suppose to be a means to accurately obtain the absolute molecular weight and molecular weight distribution without having to use poly(styrene), PS, molecular weight standards such as is the case with conventional SEC–which has been shown to provide erroneous molecular weight data due to the conformational differences between PS and P3HT–the results presented herein indicate this is not the case.

The extreme discrepancies observed in the calculated molecular weights of P3HT fractions calculated by analytical SEC-MALLS compared to MALDI-ToF-MS clearly show that there is a large degree of error involved in one or the other technique. Given the fact that the fractions were collected in a manner that undoubtedly produced very narrowly-distributed

polymer samples it is likely that the average molecular weight data estimated by MALDI-ToF-MS analysis is very close to the true weights and distributions for these materials as mass discrimination during the analysis of the individual polymer fractions may be discounted. This lends itself to the likelihood that very large errors are encountered during the evaluation of average molecular weight data for the P3HTs examined here by means of SEC-MALLS that lead to overestimations 4 times that of the absolute molecular weight of the P3HTs examined by MALDI-ToF-MS.

The exact reason for the excessive discrepancies is still unknown, although there are several possible explanations. First, the overestimation of the molecular weights of the P3HT fractions may be a result of employing a fit to the extrapolated data for the Debye plot used for the estimation of the intensity for scattered light at the angle of 0°–a basic requirement in order to obtain the molecular weight for a particle directly from R_θ/K_C–that did not well represent the conformational structure of P3HT. Secondly, it is very likely that the $\delta n/\delta c$ of P3HT is a function of the materials molecular weight and that the $\delta n/\delta c$ varies excessively for the different P3HT fractions examined. Finally, it is possible that the P3HTs observed during SEC-MALLS analysis undergo aggregation due to π-π interchain interactions leading to π-stacking that result in the overestimation of molecular weight by means of light scattering examination. Furthermore, if aggregation of the material is occurring then the conformational structure of the P3HTs may be changing during the SEC analysis in which case the extrapolated data used in the Debye plot may not at certain times during the analysis best reflect the conformation of the material. It is probable that the overestimations of molecular weights obtained by SEC-MALLS throughout this work are a result of the combination of all three scenarios.

The observation of multiply-charged P3HT ions in the gas phase during the MALDI-ToF-MS analysis of the P3HT fractions–even though MALDI-ToF-MS has been acclaimed as a

soft-ionization technique that produces unfragmented, singly-charged species, which renders the technique valuable for molecular weight determinations of synthetic polymers–is an extremely important find that has aided in part to explain the reasons for the tremendous mass discrimination of higher molecular weight distributions seen in the MALDI-ToF mass spectra of polydisperse P3HTs. The existence of doubly charged P3HTs was unequivocally proven during the analysis of the individual P3HT fractions, although there was convincing evidence that P3HT ions having charges greater than 2^+ are formed during the MALDI event throughout all of the MALDI-ToF-MS experiments presented within this Chapter. The importance of this discovery and the implications it has on the accurate characterization of poly(3-alkylthiophene)s by MALDI-ToF-MS cannot be overemphasized.

The experiments shown in Section 3.4.2 of this Dissertation clearly indicate that the existence of multiply charged P3HT ion species greatly impacts the ability to correctly interpret the molecular weigh data for these materials obtained by MALDI-ToF-MS. This is due to the fact that signals for multiply charged ions coincide in the same *m*/*z* regions as those produced by the singly charged species for which molecular weight determination is being performed. The coinciding and overlapping ion signals combine through a constructive addition of signal intensity to obscure the observation of neighboring ion signals. Furthermore, the creation of multiply charged species creates and over abundance of lower *m*/*z* ions that greatly increases the number of small *m*/*z* ions that the MCP detectors encounter in the form of a continuous stream of smaller *m*/*z* ions made up largely of multiply charged species. This in turn does not allow the detectors enough recovery time before the arrival of higher molecular weight distributions so that the detectors can produce a signal for the higher-mass components having sufficient amplification of gain within the time frame of the MALDI-ToF-MS experiment. In other words,

the detector becomes saturated with small *m/z* ions comprised of multiply charged species and cannot recover in time to detect the higher-mass components.

There was also good evidence that mass discrimination for higher-weight P3HTs is due to sample preparation or desorption/ionization issues because of the fact that P3HTs from fractions 1 and 3 could not be ionized during MALDI-ToF-MS analysis of the individual polymer fractions. Many attempts to overcome the typical reasons for ionization discrimination due to sample preparation were performed during the analysis of these materials. For instance, the matrix-to-analyte ratio was increased through serial dilutions of both polymer fractions thereby decreasing the concentration of the polymer sample in the matrix/analyte mixture in order prevent entanglement or aggregation of these larger materials. Also, the instrument's laser power was adjusted through the full range of gain for each diluted sample in attempts to ionize the materials. Furthermore, each diluted sample was examined using detection gating in small increments throughout the *m/z* ranges expected for these fractions while varying the laser power through the full range of gain. Nonetheless, the ion signals for the materials from these higher-mass fractions were not observable by MALDI-ToF-MS analysis, leading to the conclusion that the longer polymer chains comprising these fractions most likely do become entangled or aggregate inhibiting their ability to undergo efficient desorption/ionization during the MALDI event.

The effects of molecular weight to the electronic and optical properties of poly(alkylthiophene)s has been previously discussed in Section 1.2.9. Needless to say, the ability to correctly characterize the molecular weight and molecular weight distributions of these materials is critical to their application in relevant and purposeful contemporary devices and technologies. It is now clear that the fractionation of these materials prior to the MALDI-ToF-MS analysis for the purposes of molecular weight determination is necessary in order to achieve

accurate results, and semipreparative SEC is a convenient method to do so. Also, it has been shown that employing analytical SEC-MALLS does not guarantee that absolute molecular weights will be obtained, although that is the theory behind light scattering.[44] In fact, for the purposes of gaining correct molecular weight data by means of SEC it may be more beneficial to employ conventional SEC using P3HT fractions that have been characterized for their molecular weight by means of MALDI-ToF-MS as molecular weight standards, and for these purposes semipreparative SEC would be extremely useful.

3.6 References

(1) Skotheim, T. A.; Elsenbaumer, R. L.; Reynolds, J. R. *Handbook of Conducting Polymers*; 2 ed.; Marcel Dekker Inc.: New York, 1998.

(2) Schriemer, D. C.; Li, L. Mass Discrimination in the Analysis of Polydisperse Polymers by Maldi Time-of-Flight Mass Spectrometry. 1. Sample Preparation and Desorption/Ionization Issues. *Analytical Chemistry*. **1997**, *69*, 4169-4175.

(3) Schriemer, D. C.; Li, L. Mass Discrimination in the Analysis of Polydisperse Polymers by Maldi Time-of-Flight Mass Spectrometry. 2. Instrumental Issues. *Analytical Chemistry*. **1997**, *69*, 4176-4183.

(4) Axelsson, J.; Scrivener, E.; Haddleton, D. M.; Derrick, P. J. Mass Discrimination Effects in an Ion Detector and Other Causes for Shifts in Polymer Mass Distributions Measured by Matrix-Assisted Laser Desorption/Ionization Time-of-Flight Mass Spectrometry. *Macromolecules*. **1996**, *29*, 8875-8882.

(5) Nielen, M. W. F. Maldi Time-of-Flight Mass Spectrometry of Synthetic Polymers. *Mass Spectrometry Reviews*. **1999**, *18*, 309-344.

(6) Montaudo, G.; Montaudo, M. S.; Puglisi, C.; Samperi, F. Characterization of Polymers by Matrix-Assisted Laser Desorption/Ionization Time-of-Flight Mass Spectrometry: Molecular Weight Estimates in Samples of Varying Polydispersity. *Rapid Communications in Mass Spectrometry*. **1995**, *9*, 453-460.

(7) Jackson, C.; Larsen, B.; McEwen, C. Comparison of Most Probable Peak Values as Measured for Polymer Distributions by Maldi Mass Spectrometry and by Size Exclusion Chromatography. *Analytical Chemistry*. **1996**, *68*, 1303-1308.

(8) Montaudo, G.; Scamporrino, E.; Vitalini, D.; Mineo, P. Novel Procedure for Molecular Weight Averages Measurement of Polydisperse Polymers Directly from Matrix-Assisted Laser Desorption/Ionization Time-of-Flight Mass Spectra. *Rapid Communications in Mass Spectrometry*. **1996**, *10*, 1551-1559.

(9) Liu, J.; Loewe, R. S.; McCullough, R. D. Employing Maldi-MS on Poly(Alkylthiophenes): Analysis of Molecular Weights, Molecular Weight Distributions, End-Group Structures, and End-Group Modifications. *Macromolecules*. **1999**, *32*, 5777-5785.

(10) McCarley, T. D.; Noble, C. O.; DuBois, C. J., Jr.; McCarley, R. L. Maldi-MS Evaluation of Poly(3-Hexylthiophene) Synthesized by Chemical Oxidation with $FeCl_3$. *Macromolecules*. **2001**, *34*, 7999-8004.

(11) Raeder, H. J.; Schrepp, W. Maldi-Tof Mass Spectrometry in the Analysis of Synthetic Polymers. *Acta Polymerica*. **1998**, *49*, 272-293.

(12) Danis, P. O.; Karr, D. E. A Facile Sample Preparation for the Analysis of Synthetic Organic Polymers by Matrix-Assisted Laser Desorption/Ionization. *Organic Mass Spectrometry*. **1993**, *28*, 923-925.

(13) He, M.; Chen, H. Current Mass Spectrometry of Synthetic Polymer. *Current Organic Chemistry*. **2007**, *11*, 909-923.

(14) Belu, A. M.; DeSimone, J. M.; Linton, R. W.; Lange, G. W.; Friedman, R. M. Evaluation of Matrix-Assisted Laser Desorption Ionization Mass Spectrometry for Polymer Characterization. *Journal of the American Society for Mass Spectrometry*. **1996**, *7*, 11-24.

(15) Hanton, S. D. Mass Spectrometry of Polymers and Polymer Surfaces. *Chemical Reviews (Washington, D. C.)*. **2001**, *101*, 527-569.

(16) National Institute of Standards and Technologies-Material Measurement Laboratory, Synthetic Polymer Maldi Recipes Search Form. http://polymers.nist.gov/maldirecipes/index.cfm (accessed September 2011).

(17) Bauer Barry, J.; Guttman Charles, M.; Liu, D.-w.; Blair William, R. Tri-Alpha-Naphthylbenzene as a Crystalline or Glassy Matrix for Matrix-Assisted Laser Desorption/Ionization: A Model System for the Study of Effects of Dispersion of Polymer Samples at a Molecular Level. *Rapid communications in mass spectrometry : RCM*. **2002**, *16*, 1192-1198.

(18) Zhang, J.; Zenobi, R. Matrix-Dependent Cationization in Maldi Mass Spectrometry. *Journal of mass spectrometry : JMS*. **2004**, *39*, 808-816.

(19) Montaudo, G.; Samperi, F.; Montaudo, M. S. Characterization of Synthetic Polymers by Maldi-Ms. *Progress in Polymer Science*. **2006**, *31*, 277-357.

(20) Danis, P. O.; Karr, D. E.; Xiong, Y.; Owens, K. G. Methods for the Analysis of Hydrocarbon Polymers by Matrix-Assisted Laser Desorption/Ionization Time-of-Flight Mass Spectrometry. *Rapid Communications in Mass Spectrometry*. **1996**, *10*, 862-868.

(21) Bahr, U.; Deppe, A.; Karas, M.; Hillenkamp, F.; Giessmann, U. Mass Spectrometry of Synthetic Polymers by Uv-Matrix-Assisted Laser Desorption/Ionization. *Analytical Chemistry*. **1992**, *64*, 2866-2869.

(22) Rashidzadeh, H.; Guo, B. Use of Maldi-Tof to Measure Molecular Weight Distributions of Polydisperse Poly(Methyl Methacrylate). *Analytical Chemistry*. **1998**, *70*, 131-135.

(23) Juhasz, P.; Costello, C. E.; Biemann, K. Matrix-Assisted Laser Desorption Ionization Mass Spectrometry with 2-(4-Hydroxyphenylazo)Benzoic Acid Matrix. *Journal of the American Society for Mass Spectrometry*. **1993**, *4*, 399-409.

(24) McCarley, T. D.; McCarley, R. L.; Limbach, P. A. Electron-Transfer Ionization in Matrix-Assisted Laser Desorption/Ionization Mass Spectrometry. *Analytical Chemistry*. **1998**, *70*, 4376-4379.

(25) Macha, S. F.; McCarley, T. D.; Limbach, P. A. Influence of Ionization Energy on Charge-Transfer Ionization in Matrix-Assisted Laser Desorption/Ionization Mass Spectrometry. *Analytica Chimica Acta*. **1999**, *397*, 235-245.

(26) Brauch, R. M. Structural Characterization of Poly (Heterocycle)S Formed Using Oxidative Methods. Ph.D. Dissertation, Louisiana State University and A&M College, Baton Rouge, 2006.

(27) Loewe, R. S.; Ewbank, P. C.; Liu, J.; Zhai, L.; McCullough, R. D. Regioregular, Head-to-Tail Coupled Poly(3-Alkylthiophenes) Made Easy by the Grim Method: Investigation of the Reaction and the Origin of Regioselectivity. *Macromolecules*. **2001**, *34*, 4324-4333.

(28) De Winter, J.; Deshayes, G.; Boon, F.; Coulembier, O.; Dubois, P.; Gerbaux, P. Maldi-Tof Analysis of Polythiophene: Use of Trans-2-[3-(4-T-Butyl-Phenyl)-2-Methyl- 2-Propenylidene]Malononitrile-Dctb-as Matrix. *Journal of Mass Spectrometry*. **2011**, *46*, 237-246.

(29) Dreisewerd, K.; Schuerenberg, M.; Karas, M.; Hillenkamp, F. Influence of the Laser Intensity and Spot Size on the Desorption of Molecules and Ions in Matrix-Assisted Laser Desorption/Ionization with a Uniform Beam Profile. *International Journal of Mass Spectrometry and Ion Processes*. **1995**, *141*, 127-148.

(30) Hillenkamp, F.; Karas, M.; Beavis, R. C.; Chait, B. T. Matrix-Assisted Laser Desorption/Ionization Mass Spectrometry of Biopolymers. *Analytical Chemistry*. **1991**, *63*, 1193A-1203A.

(31) Martin, K.; Spickermann, J.; Raeder, H. J.; Muellen, K. Why Does Matrix-Assisted Laser Desorption/Ionization Time-of-Flight Mass Spectrometry Give Incorrect Results for Broad Polymer Distributions? *Rapid Communications in Mass Spectrometry*. **1996**, *10*, 1471-1474.

(32) Chen, H.; Guo, B. Use of Binary Solvent Systems in the Maldi-Tof Analysis of Poly(Methyl Methacrylate). *Analytical Chemistry*. **1997**, *69*, 4399-4404.

(33) Yalcin, T.; Dai, Y.; Li, L. Matrix-Assisted Laser Desorption/Ionization Time-of-Flight Mass Spectrometry for Polymer Analysis: Solvent Effect in Sample Preparation. *Journal of the American Society for Mass Spectrometry*. **1998**, *9*, 1303-1310.

(34) Hoteling, A. J.; Mourey, T. H.; Owens, K. G. Importance of Solubility in the Sample Preparation of Poly(Ethylene Terephthalate) for Maldi Tofms. *Analytical Chemistry*. **2005**, *77*, 750-756.

(35) Guo, B.; Chen, H.; Rashidzadeh, H.; Liu, X. Observation of Varying Molecular Weight Distributions in Matrix-Assisted Laser Desorption/Ionization Time-of-Flight Analysis of Polymethyl Methacrylate. *Rapid Communications in Mass Spectrometry*. **1997**, *11*, 781-785.

(36) King, R. C.; Goldschmidt, R.; Xiong, Y.; Owens, K. The Role of Solubility in the Preparation of Synthetic Polymer Samples for Analysis by Matrix-Assisted Laser Desorption/Ionization Time-of-Flight Mass Spectrometry. In *Proceedings of the 43rd Annual Meeting of the American Society of Mass Spectrometry*; ASMS: Santa Fe, 1995, p. 689.

(37) McEwen, C. N.; Jackson, C.; Larsen, B. S. Instrumental Effects in the Analysis of Polymers of Wide Polydispersity by Maldi Mass Spectrometry. *International Journal of Mass Spectrometry and Ion Processes*. **1997**, *160*, 387-394.

(38) Dass, C. *Principle and Practices of Biological Mass Spectrometry*; Wiley-Interscience; New York, 2001.

(39) Montaudo, M. S.; Puglisi, C.; Samperil, F.; Montaudo, G. Application of Size Exclusion Chromatography Matrix-Assisted Laser Desorption/Ionization Time-of-Flight to the Determination of Molecular Masses in Polydisperse Polymers. *Rapid Communications in Mass Spectrometry*. **1998**, *12*, 519-528.

(40) Nielen, M. W. F.; Malucha, S. Characterization of Polydisperse Synthetic Polymers by Size-Exclusion Chromatography/Matrix-Assisted Laser Desorption/Ionization Time-of-Flight Mass Spectrometry. *Rapid Communications in Mass Spectrometry*. **1997**, *11*, 1194-1204.

(41) Mourey, T. H.; Hoteling, A. J.; Balke, S. T.; Owens, K. G. Molar Mass Distributions of Polymers from Size Exclusion Chromatography and Matrix-Assisted Laser Desorption/Ionization Time-of-Flight Mass Spectrometry: Methods for Comparison. *Journal of Applied Polymer Science*. **2005**, *97*, 627-639.

(42) Montaudo, G.; Garozzo, D.; Montaudo, M. S.; Puglisi, C.; Samperi, F. Molecular and Structural Characterization of Polydisperse Polymers and Copolymers by Combining Maldi-Tof Mass Spectrometry with Gpc Fractionation. *Macromolecules*. **1995**, *28*, 7983-7989.

(43) Kassis, C. E.; DeSimone, J. M.; Linton, R. W.; Remsen, E. E.; Lange, G. W.; Friedman, R. M. A Direct Deposition Method for Coupling Matrix-Assisted Laser Desorption/Ionization Mass Spectrometry with Gel Permeation Chromatography for Polymer Characterization. *Rapid Communications in Mass Spectrometry*. **1997**, *11*, 1134-1138.

(44) Wyatt, P. J. Light Scattering and the Absolute Characterization of Macromolecules. *Analytica Chimica Acta*. **1993**, *272*, 1-40.

(45) Trathnigg, B. Determination of Mwd and Chemical Composition of Polymers by Chromatographic Techniques. *Progress in Polymer Science*. **1995**, *20*, 615-650.

(46) Tarazona, M. P.; Saiz, E. Combination of Sec/Mals Experimental Procedures and Theoretical Analysis for Studying the Solution Properties of Macromolecules. *Journal of Biochemical and Biophysical Methods*. **2003**, *56*, 95-116.

(47) Barth, H. G.; Boyes, B. E.; Jackson, C. Size Exclusion Chromatography and Related Separation Techniques. *Analytical Chemistry*. **1998**, *70*, 251R-278R.

(48) Andersson, M.; Wittgren, B.; Wahlund, K.-G. Accuracy in Multiangle Light Scattering Measurements for Molar Mass and Radius Estimations. Model Calculations and Experiments. *Analytical Chemistry*. **2003**, *75*, 4279-4291.

(49) Laguna, M. T. R.; Medrano, R.; Plana, M. P.; Tarazona, M. P. Polymer Characterization by Size-Exclusion Chromatography with Multiple Detection. *Journal of Chromatography, A*. **2001**, *919*, 13-19.

(50) McCullough, R. D.; Lowe, R. D. Enhanced Electrical Conductivity in Regioselectively Synthesized Poly(3-Alkylthiophenes). *Journal of the Chemical Society, Chemical Communications*. **1992**, 70-72.

(51) McCullough, R. D.; Lowe, R. D. The Synthesis of Well-Defined Conducting Poly(3-Alkylthiophenes). *Polymer Preprints (American Chemical Society, Division of Polymer Chemistry)*. **1992**, *33*, 195-196.

(52) McCullough, R. D.; Lowe, R. D.; Jayaraman, M.; Ewbank, P. C.; Anderson, D. L.; Tristram-Nagle, S. Synthesis and Physical Properties of Regiochemically Well-Defined, Head-to-Tail Coupled Poly(3-Alkylthiophenes). *Synthetic Metals*. **1993**, *55*, 1198-1203.

(53) Trznadel, M.; Pron, A.; Zagorska, M.; Chrzaszcz, R.; Pielichowski, J. Effect of Molecular Weight on Spectroscopic and Spectroelectrochemical Properties of Regioregular Poly(3-Hexylthiophene). *Macromolecules*. **1998**, *31*, 5051-5058.

(54) Pearson, D. L.; Schumm, J. S.; Tour, J. M. Iterative Divergent/Convergent Approach to Conjugated Oligomers by a Doubling of Molecular Length at Each Iteration. A Rapid Route to Potential Molecular Wires. *Macromolecules*. **1994**, *27*, 2348-2350.

(55) Raeder, H. J.; Spickermann, J.; Kreyenschmidt, M.; Muellen, K. Maldi-Tof Mass Spectrometry in Polymer Analytics. Part 2. Molecular Weight Analysis of Rigid-Rod Polymers. *Macromolecular Chemistry and Physics*. **1996**, *197*, 3285-3296.

(56) Holdcroft, S. Determination of Molecular Weights and Mark-Houwink Constants for Soluble Electronically Conducting Polymers. *Journal of Polymer Science, Part B: Polymer Physics*. **1991**, *29*, 1585-1588.

(57) Sugimoto, R.; Takeda, S.; Gu, H. B.; Yoshino, K. Preparation of Soluble Polythiophene Derivatives Utilizing Transition Metal Halides as Catalysts and Their Property. *Chemistry Express*. **1986**, *1*, 635-638.

(58) Stanke, D.; Hallensleben, M. L.; Toppare, L. Oxidative Polymerization of Some N-Alkylpyrroles with Ferric Chloride. *Synthetic Metals*. **1995**, *73*, 267-272.

(59) Frankevich, V.; Zhang, J.; Dashtiev, M.; Zenobi, R. Production and Fragmentation of Multiply Charged Ions in "Electron-Free" Matrix-Assisted Laser Desorption/Ionization. *Rapid Communications in Mass Spectrometry*. **2003**, *17*, 2343-2348.

(60) Schriemer, D. C.; Li, L. Detection of High Molecular Weight Narrow Polydisperse Polymers up to 1.5 Million Daltons by Maldi Mass Spectrometry. *Analytical Chemistry*. **1996**, *68*, 2721-2725.

(61) Zade, S. S.; Bendikov, M. Theoretical Study of Long Oligothiophene Dications: Bipolaron Vs Polaron Pair Vs Triplet State. *Journal of Physical Chemistry B*. **2006**, *110*, 15839-15846.

(62) Moro, G.; Scalmani, G.; Cosentino, U.; Pitea, D. On the Structure of Polaronic Defects in Thiophene Oligomers: A Combined Hartree-Fock and Density Functional Theory Study. *Synthetic Metals*. **2000**, *108*, 165-172.

(63) Osawa, S.; Ito, M.; Iwase, S.; Yajima, H.; Endo, R.; Tanaka, K. Effects of Molecular Weight on the Electrical Properties of Electrochemically Synthesized Poly(3-Hexylthiophene). *Polymer*. **1992**, *33*, 914-919.

(64) Debye, P. Molecular-Weight Determination by Light Scattering. *Journal of Physical and Colloid Chemistry*. **1947**, *51*, 18-32.

(65) Zimm, B. H. Apparatus and Methods for Measurment and Interpretation of the Angular Variation of Light Scattering; Preliminary Results on Polystyrene Solutions. *Journal of Chemical Physics*. **1948**, *16*, 1099-1116.

(66) Berry, G. C. Thermodynamic and Conformational Properties of Polystyrene. I. Light-Scattering Studies on Dilute Solutions of Linear Polystyrenes. *Journal of Chemical Physics*. **1966**, *44*, 4550-4564.

(67) Melis, C.; Colombo, L.; Mattoni, A. Self-Assembling of Poly(3-Hexylthiophene). *Journal of Physical Chemistry C*. **2011**, *115*, 576-581.

(68) Sato, T.; Kishida, H.; Nakamura, A.; Fukuda, T.; Yamamoto, T. Strong Stacking Behavior and Large Third-Order Nonlinear Optical Susceptibility χ(3) of Head-to-Head-Type Poly(3-Alkynylthiophene-2,5-Diyl), HH-P3(CCR)Th. *Synthetic Metals*. **2007**, *157*, 318-322.

(69) Yamamoto, T.; Komarudin, D.; Kubota, K.; Sasaki, S. Stacking of Poly(3-Alkylthiophene)S and Poly(4-Alkylthiazole)S in a Colloidal Solution and in the Solid. *Chemistry Letters*. **1998**, 235-236.

(70) Yamamoto, T.; Komarudin, D.; Maruyama, T.; Arai, M.; Lee, B.-L.; Suganuma, H.; Asakawa, N.; Inoue, Y.; Kubota, K.; Sasaki, S.; Fukuda, T.; Matsuda, H. Extensive Studies on π-Stacking of Poly(3-Alkylthiophene-2,5-Diyl)S and Poly(4-Alkylthiazole-2,5-Diyl)s by Optical Spectroscopy, NMR Analysis, Light Scattering Analysis, and X-Ray Crystallography. *Journal of the American Chemical Society*. **1998**, *120*, 2047-2058.

(71) Fichou, D.; Xu, B.; Horowitz, G.; Garnier, F. Generation of Stabilized Polarons and Bipolarons on Extended Model Thiophene Oligomers. *Synthetic Metals*. **1991**, *41*, 463-469.

(72) Bredas, J. L.; Street, G. B. Polarons, Bipolarons, and Solitons in Conducting Polymers. *Accounts of Chemical Research*. **1985**, *18*, 309-315.

(73) McCullough, R. D.; Lowe, R. D.; Jayaraman, M.; Anderson, D. L. Design, Synthesis, and Control of Conducting Polymer Architectures: Structurally Homogeneous Poly(3-Alkylthiophenes). *Journal of Organic Chemistry*. **1993**, *58*, 904-912.

(74) Barbarella, G.; Bongini, A.; Zambianchi, M. Regiochemistry and Conformation of Poly(3-Hexylthiophene) Via the Synthesis and the Spectroscopic Characterization of the Model Configurational Triads. *Macromolecules*. **1994**, *27*, 3039-3045.

Chapter 4

Characterization of P3HTs Formed at Low Temperatures by Chemical Oxidation

4.1 Introduction

4.1.1 An Overview of Low-Temperature Synthesis of P3HTs

Reports in the literature concerning the low-temperature synthesis of poly(3-alkylthiophene)s, P3ATs, by means of chemical oxidation with ferric chloride are virtually nonexistent.[1] Amou et al. reported the use of low-temperature conditions combined with lower monomer concentrations during chemical oxidation of 3-*n*-hexylthiophene in order improve the regioregularity of the resulting polymer.[1] Amou et al. prepared poly(3-hexylthiophene)s, P3HTs, by chemical oxidation with ferric chloride using chloroform as a reaction solvent and initially employing an oxidant-to-monomer ratio of 4:1; this was done by suspending 4.0 mmol of ferric chloride in 1.0 mL of chloroform under nitrogen in a 25 mL round-botom flask and then adding 1 mmol 3-*n*-hexylthiophene via syringe and allowing the misture to stir for 24 hours under nitrogen. The reaction mixture was then poured into methanol containing a 10% concentrated Hydrochloric acid. The precipitate was collected by filtration and washed with methanol in a soxhlet extractor for 24 hours.

Amou et al. went on to perform a series of similar polymerization reactions while decreasing the monomer concentration and the reaction temperatures while extending the reaction time. They reported that while performing the polymerization reactions at –45 °C, as the monomer concentrations decreased the number average molecular weight, M_N, of the resulting polymer decreased unless the reaction time increased, whereby the M_N increased as a function of time. Performing the reaction at –45 °C and using a monomer concentration of 0.02 mol L^{-1} while allowing the reaction to proceed for a period of 200 hours reportedly gave polymer in 100% yields with a M_N of 68,000 Da, a *PDI* of 1.9, and regioregularity (cf. Sections

1.2.3–1.2.6) of 88%. Structure-function relationships in P3ATs have been previously discussed within Chapter 1. Nonetheless, the explanation of the influence of low temperature provided by Amou et al. was somewhat ambiguous and was based more in terms of the monomer concentrations; however, they concluded that the observed effect of temperature should result from the enhancement of selectivity in oxidative coupling between monomer molecules and oligomer molecules resulting in chain growth during chemical oxidative polymerization with ferric chloride to form P3HTs. The coupling between monomers and oligomers, compared to coupling between oligomers and other oligomers, during chain growth of P3ATs has been shown to be the most likely route to the formation of more regioregular P3ATs (cf. Section 2.6.2).[2-4]

The work presented within this Chapter involves the low-temperature synthesis of P3HT by means of chemical oxidation with ferric chloride. In light of the results presented within Chapter 2 of this Dissertation, low-temperature polymerizations in Chapter 4 were performed using different solvents for the reaction medium. It has been shown in Chapter 2 that the physical properties of specific solvents employed for reactions performed via chemical oxidation with ferric chloride have markedly different impacts on the physical properties of the resulting polymer. Expectations of the work presented herein were not only to determine if the combination of a specific solvent with low-temperature synthesis might yield P3HT with superior physical properties (cf. Sections 1.2.3–1.2.6 and 1.2.9), but also to potentially elucidate further information as to the mechanisms (cf. Section 1.2.7 and 2.6.2) that are responsible for the creation of high-quality polymers.

4.2 Methods and Materials

4.2.1 Chemicals

Solvents employed for the purposes of polymerization or analytical characterization of P3HTs were either chromatographic grade, reageant grade, or pesticide grade and were used as

received unless noted otherwise. Once opened, solvents used for polymerization and characterization were stored over activated molecular sieves (4Å, 8–12 mesh, beads, Fisher Chemical) and degassed with argon for one hour prior to use. 3-*n*-hexylthiophene monomer was purchased from Sigma-Aldrich (#399051, 99%) and distilled under vacuum prior to use. Ferric chloride was purchased from Sigma-Aldrich (#451649, anhydrous, powder, ≥99.9%, trace metal basis) and was opened under argon in a glove bag, then stored under argon in a dessicator. Matrices employed for MALDI-ToF-MS analysis were either 2,2':5',2''-terthiophene, or *trans*-2-[3-(4-tert-butylphenyl)-2-methyl-2-propenylidine]malonitrile (DCTB). Both matrices were purchased from Sigma-Aldrich (#311073, 99%, and #727881, ≥98% respectively) and used as received.

4.2.2 Synthetic Methods: Low-Temperature Chemical Oxidation of 3-Hexylthiophene

Polymerizations were carried out according to previously reported procedures in the literature for chemical oxidative polymerization of thiophenes and pyrroles,[5-7] with some modifications. The reactions were performed in a 250 mL round bottom flask (RBF). The solvents employed varied, depending on their physical properties for individual experiments. The molar ratio of oxidant-to-monomer remained constant at 1:1 throughout all polymerizations in order to compare the physical properties of the polymers formed in Chapter 4 of this Dissertation with those discussed in Chapter 2. Oxidant-to-monomer ratios employed for these polymerizations are small compared to those used for typical oxidative polymerizations of P3ATs found throughout the literature; this was discussed previously in Section 2.2.2. 3-*n*-hexylthiophene was purified prior to experiments via vacuum distillation. Iron(III) chloride consistently remained under a blanket of argon from the moment it was opened as received from the supplier. All solvents used were degassed with argon for a period of one hour prior to the reactions.

Temperature variations for this study were controlled through use of a Lauda RE107 thermostatically-controlled bath, with the unit set for external circulation. The model RE107 is capable of maintaining a minimum temperature of –35 °C for an indefinite period of time operating in ambient conditions (i.e. room temperature). Low-temperature reactions were conducted inside a thermally insulated environment in very close proximity to the thermostatically-controlled bath using insulated circulation tubing and jacketed reaction vessels. The polymerization reactions were performed at a temperature of –30 °C with the exception of those reactions conducted using carbon tetrachloride, which has a freezing point of ~23 °C. Reactions performed employing carbon tetrachloride were successfully conducted at –25 °C without any indication of phase change occurring.

First, an oxidant solution or suspension, depending on the nature of the solvent, was prepared by the addition of 162.2 mg (1.0 mmol) of iron(III) chloride into 12.5 mL of a given solvent. The mixture was allowed to stir and equilibrate to the reaction temperature for one hour under argon atmosphere. A monomer solution was prepared by the addition of 168.3 mg (1.0 mmol) of 3-*n*-hexylthiophene to 12.5 mL of the same solvent used for preparation of the iron(III) mixture. This was allowed to stir and equilibrate to the reaction temperature under argon atmosphere for one hour. The monomer solution was then cannulated into the stirring oxidant mixture under argon. The reaction was then allowed to proceed for 24 hours stirring at under argon atmosphere.

After one hour, the reaction was quenched by the addition of 200 mL of anhydrous methanol and allowed to stir at low temperature under argon for 24 hours; during which time the polymer is reduced and precipitates out of solution. The solid polymer was then thoroughly separated by vacuum filtration and rinsed well with methanol in order to remove residual $FeCl_3$. The soluble polymer remaining in the filtrate was not used for characterization as discussed in

Section 2.2.2 The solid polymer was then redissolved in 250 mL of chloroform. The polymer solution in chloroform was next washed three times in a separatory funnel with 250 mL of 2.0 N HCl. The chloroform was then rotary-evaporated to leave a thin, reddish-violet film of polymer that was then vacuum-dried to constant mass overnight.

4.3 Characterization

4.3.1 Endgroup Analysis

Endgroup analysis of poly(3-hexylthiophene)s was done by use of matrix-assisted laser desorption/ionization time-of-flight mass spectrometry (MALDI-ToF-MS). Some perspective of the use of MALDI-ToF-MS for the characterization of synthetic and conducting polymers has been discussed in Sections 1.3.1, 1.3.3, and 2.3.1. The limitations of MALDI-ToF-MS for the analysis of synthetic polymers, including P3HTs, have been thoroughly discussed throughout Chapter 3. The method of sample preparation for MALDI-ToF-MS analysis of polymers performed within this Chapter was outlined in Section 2.3.1.

4.3.2 Molecular Weight Analysis

Molecular weight measurements were done by means of gel-permeation chromatography (GPC), also referred to as size-exclusion chromatography (SEC), using a multiangle laser light scattering (MALLS) detector in conjunction with a differential refractive index (DRI) detector. The use of SEC for the characterization of the average molecular weights and molecular weight distributions of synthetic polymers has been previously discussed in Section 2.3.2 and throughout Chapter 3.

4.3.3 Determination of Regioregularity

The pattern of coupling between monomers of 3-*n*-hexylthiophene by means of chemical oxidative polymerization, called regioregularity, has been discussed in Section 1.2.3. The regioregularity of P3ATs has a marked impact on the materials electrical and optical properties,

as has been outlined in depth throughout Chapter 1. The analytical method for the determination of the materials regioregularity presented here is ^{1}H-NMR. With this technique, the integration and comparison of the relative ratio between the signal peaks for the α-methylenes (aryl methylenes) of polymer chains is used for this determination. Signals for these α-methylene peaks are typically present at a chemical shift of $\delta \sim 2.8$, or $\delta \sim 2.6$ if the coupling is regioregular or regiorandom, respectively. The extent of regioregularity is defined as the percentage of the ratio between the two peaks. A more extensive look at this application is found within Section 1.2.4.

4.4 Instrumentation

4.4.1 MALDI-ToF-MS

Mass spectrometric measurements were obtained in part by use of a Bruker OmniFlex MALDI-ToF mass specrometer. The instrument was equipped with a 337-nm nitrogen laser and it is capable of both linear and reflectron time-of-flight detection. The OmniFlex possesses multichannel plate (MCP) detectors with a limit of detection (LOD) of 1 fmol ACTH and it is capable of mass resolutions up to 10,000 depending on the *m/z* observed. Measurements were also performed using a Bruker ProFlexx III, which was also equipped with a 337-nm nitrogen laser, MCP detectors with a LOD of 100 fmol ACTH, and capable of linear and reflectron detection. The mass resolution of this instrument is up to 8,000 depending on the *m/z* investigated.

The matrices employed for MALDI-ToF-MS inquiries were either terthiophene or *trans*-2-[3-(4-tert-butylphenyl)-2-methyl-2-propenylidine]malonitrile, DCTB. DCTB was used for the majority of the experiments, as far greater signal intensities and signal-to-noise ratios were achieved employing this matrix. Samples were prepared by dissolving the analyte and the matrix in chloroform or methylene chloride. A saturated solution of matrix was prepared in

these solvents in matrix:analyte ratios > 1000:1. A small aliquot (~ 2 μL) of analyte sample was added to the matrix solution (~ 4–6 μL) and they were thoroughly mixed prior to spotting onto the target plate using the dried drop method, where a 1 μL drop of a given sample was spotted on the target plate and allowed to air dry. The instrument was calibrated prior to each measurement using peptide standards (Bruker, #222570) in the molecular weight range of *m/z* 700–3200 for analysis performed in reflectron mode. Internal standards were not used for these experiments.

Bruker's Xmass software was employed in order to calculate the isotopic masses, and patterns for oligo(3-hexylthiophene)s having different endgroup (α-), and backbone (β-) substituents. The calculated patterns were used in conjunction with Equations 1.4, and 1.5 for the determination of α-, and β-substituents and also referred to for mass accuracy determinations. The observed experimental signal intensities (relative abundances) were used as pseudo-N_i measurements and the *m/z* values were applied as pseudo-M_i measurements for the relative comparison of populations or extent of substitution. Observed experimental signal peaks were designated to be molecular radical cations ($M^{+\bullet}$) as a result of electron-loss ionization, as described in Section 2.3.1.

4.4.2 Size-Exclusion Chromatography (SEC)

Gel-permeation chromatography experiments were performed through the use of an Agilent 1100 series autosampler and isocratic pump system. In some experiments, ultraviolet-visible absorption measurements were taken using a Waters 490E ultraviolet-visible detector (set to 430 nm). Light scattering measurements were obtained with a Wyatt Dawn Heleos (Wyatt Technologies Corporation, Santa Barbara, California) thermostatically-controlled, multiangle laser light scattering (MALLS) detector, with a 50-mW GaAs linearly-polarized laser (658 nm) and a K5 cell. The MALLS detectors were calibrated using toluene and then normalized with poly(styrene) standards having a distinct monodisperse molecular weight of 30,000 Da prior to

experiments. A Wyatt Optilab Rex refractive index detector was used in conjunction with light scattering measurements and it was positioned after the Dawn Helios MALLS detector. The two in-line columns that were employed for these purposes were Phenogel columns (30 cm × 7.8 mm) from Phenomenex. Both columns possessed packing material consisting of 10-μm diameter particles. The first column contained a linear bed of packing material having mixed pore sizes in the range of 50–10^6 Å and the second column contained beads with solely 10^5 Å pores. These columns were preceded by a Phenomenex guard (10-μm diameter) guard column. The solvent employed for the separations was tetrahydrofuran, THF, which was degassed prior to experiments using helium sparging and/or an in-line vacuum degasser. The flow rate of the solvent for these analytical analyses was maintained at 1.0 mL min^{-1} and the injection volume for the investigated samples was 100 μL. The collected data was processed using the Astra V software provided from Wyatt Technologies Corporation.

4.4.3 Specific Refractive Index Increment (SRII) Measurements

Determination of $\delta n/\delta c$ for bulk and fractionated P3HTs was done using the Wyatt Optilab Rex refractive index detector (Wyatt Technologies Corporation, Santa Barbara, California) used for SEC analysis (cf. Section 2.4.1). Measurements were made at a wavelength of 658 nm and and a temperature of 25 °C. The $\delta n/\delta c$ used for the analysis of polymers within this Chapter was empirically determined and found to be 0.227; this was for a bulk polymer sample (unfractionated, cf. Section 3.1.4) formed by chemical oxidation with $FeCl_3$ using chloroform as a solvent.

4.4.4 Proton Nuclear Magnetic Resonance (^{1}H-NMR)

^{1}H-NMR analyses were performed on either a Bruker DPX-400 (400 MHz) or AV-4 (400 MHz) liquid spectrometer. Samples of P3HTs were dissolved in deuterated chloroform ($CDCl_3$) purchased from Sigma-Aldrich for all ^{1}H-NMR experiments.

4.5 Results

4.5.1 P3HTs Formed at –30 °C Using Chloroform as a Reaction Solvent

P3HTs investigated in this Section were prepared via the procedure outlined in Section 4.2.2 using chloroform ($CHCl_3$) as the solvent medium. Chloroform has historically been the solvent employed for chemical oxidative polymerization of P3ATs without much regard or explanation as to its qualifications for these purposes. Chloroform is a very nonpolar solvent with a dielectric constant of 4.8 at 25 °C (cf. Section 2.1.2). Iron(III) chloride is only slightly soluble in chloroform at room temperature, remaining for the most part in the solid state, but imparting a slight yellowish tint to the suspension. Chloroform has very strong Lewis acid characteristics and is assigned a Gutmann Acceptor number, AN, (cf. Section 2.1.2) of 23. It has virtually negligible Lewis base characteristics and therefore has a Guttman donor number, DN, (cf. Section 2.1.2) very near zero. Mass yields of polymer recovered from the preparation of P3HTs formed following the procedures outlined in Section 4.2.2 with chloroform were on the order of ~ 20% compared yields of P3HT formed under similar conditions at room temperature, which were on the order of ~30% (cf. Section 2.5.1).

As noted in Section 2.2.2, polymer yields are in general lower than others reported in the literature for the production of P3HTs by this method as a result of the low oxidant-to-monomer ratio used. This fact is magnified because of the low temperatures employed for polymer reactions found within this Chapter. Mass yields of P3HTs for the purposes of this work were regarded in a relative manner.

The MALDI-ToF mass spectra observed during the endgroup analysis of these materials indicate the presence of oligomers possessing α-terminal ends consisting of two hydrogens [H-$(C_{10}H_{14}S)_n$-H], as well as oligomers possessing one hydrogen and one chlorine [H-$(C_{10}H_{14}S)_n$-Cl] shown in Figure 4.1. The upper spectrum in Figure 4.1 is the MALDI-ToF mass spectrum of

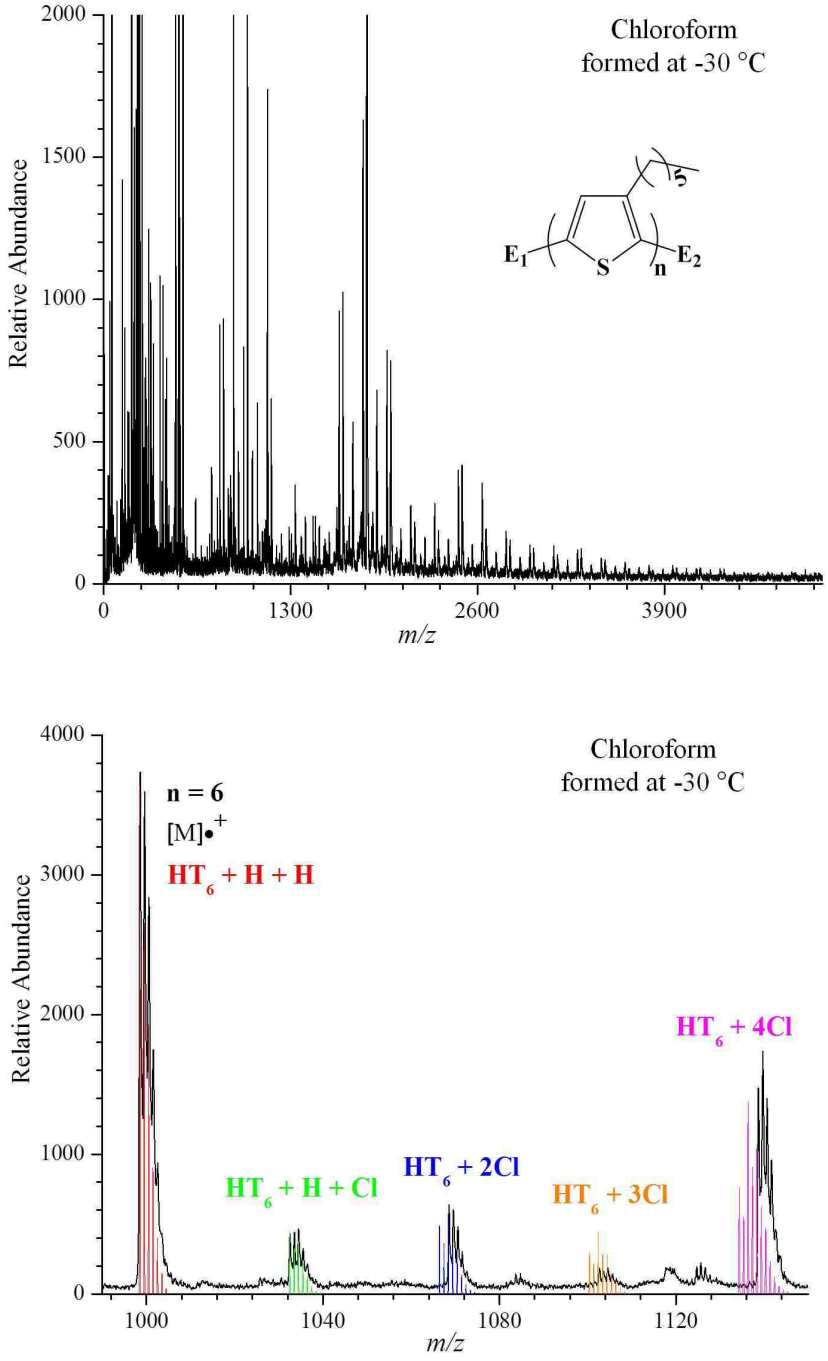

Figure 4.1 MALDI-ToF mass spectra of P3HT formed at –30 °C in chloroform observed by use of reflectron mode (upper). The inset (lower) shows expanded 6-mer region of the spectrum with colored peaks indicating the calculated isotope patterns of the 6-mer having different chlorine additions.

oligomers in the range of *m/z* 0–5200 by use of reflectron mode (cf. Section 2.3.1). There is a distinct decrease in the abundance of interstitial peaks between those that are indicative of

molecular radical cations ($M^{\bullet+}$) having solely hydrogen-terminated endgroups as compared to P3HT formed under similar conditions but at room temperature (cf. Figure 2.3).

The lower spectrum in Figure 4.1 is an inset to the spectrum for P3HT formed by chemical oxidation with ferric chloride at –30 °C using chloroform as a solvent and focuses on the $M^{\bullet+}$ peak for the oligomer $n = 6$. The overlays shown in various colors are the calculated isotopic patterns for the representation of the given species that were produced by the Bruker Xmass software. The calculated peaks are labeled in their respective color denoting the chemical composition of the calculated patterns, where HT_n indicates the repeat unit, which is a 3-*n*-hexylthiophene monomer unit minus 2 hydrogen atoms with a molar mass of 166.3 amu. These are shown in comparison to the experimental peaks observed for the polymer sample in the background. The spectrum shows excellent agreement with oligomers representing the hydrogen-terminated molecular radical cation, as well as the ion pattern indicating the presence of oligomers possessing one chlorine termination and one hydrogen endgroup. There is also some evidence shown in this spectrum for the presence of oligomers having a greater extent of chlorine additions.

The calculated patterns for oligomers having two or more chlorine additions do show some disagreement with the observed patterns. The differences seen in the calculated and observed patterns for the oligomers containing more than two chlorine additions may be accounted by the lack of deprotonation during polymerization as discussed in Section 2.5.1. There is an obvious decrease in the extent of chlorination for the P3HT formed at –30 °C apparent in the mass spectra shown in Figure 4.1 compared to those polymers formed under similar conditions at room temperature shown in the mass spectra in Figure 2.3 indicated by the comparison of the relative abundances of ion signals for the respective materials.

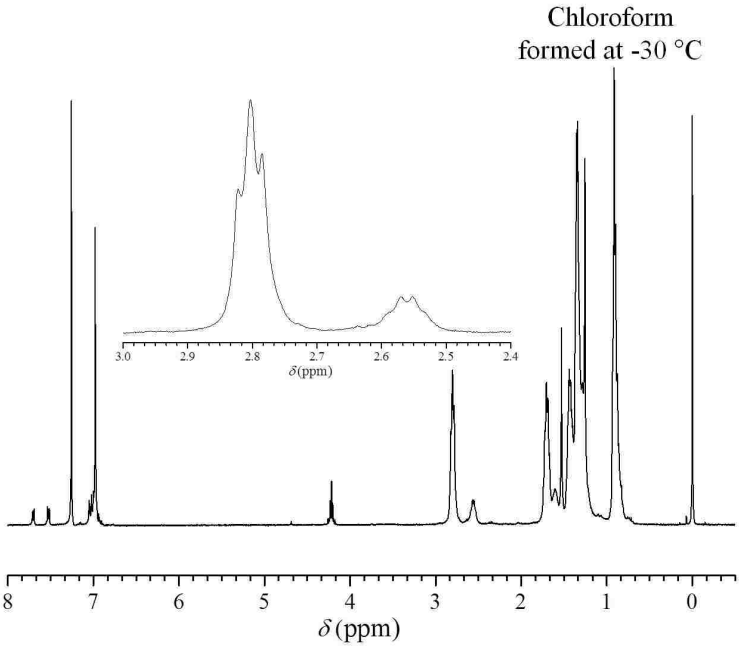

Figure 4.2 ^{1}H-NMR spectrum of P3HT formed at –30 °C in chloroform. The inset shows the α-methylene region used to determine the material's regioregularity of 83%.

The ^{1}H-NMR analysis of P3HTs formed by chemical oxidation with ferric chloride at –30 °C using chloroform is shown in Figure 4.2**.** The inset shows the peaks for signals arising from the α-methylene (aryl methylene) groups found at chemical shifts of $\delta \sim 2.8$ ppm and $\delta \sim 2.58$ ppm, indicating signal response from regioregular,and regioirregular material, respectively (cf. Section 1.2.3). The analysis of structural regularity by integration and relative comparison of these peaks is discussed in Section 1.2.4. From integration of the peak found at $\delta \sim 2.8$ ppm normalized as one (1.0) and integration of the peak found at $\delta \sim 2.58$ ppm, which was determined to be 0.20 as compared to the normalized peak, the percentage of the peak at $\delta \sim 2.8$ ppm is found to be 83% of the combined areas of the two peaks. Therefore, the regioregularity of P3HT formed by this chemical oxidative polymerization (cf. Section 4.2.2) using chloroform as a solvent can be regarded as 83% regioregular material. The regioregularity of the P3HT formed at –30 °C increased 6% compared to those formed under similar conditions at room temperature, which was shown to be 77% regioregular (cf. Figure 2.4).

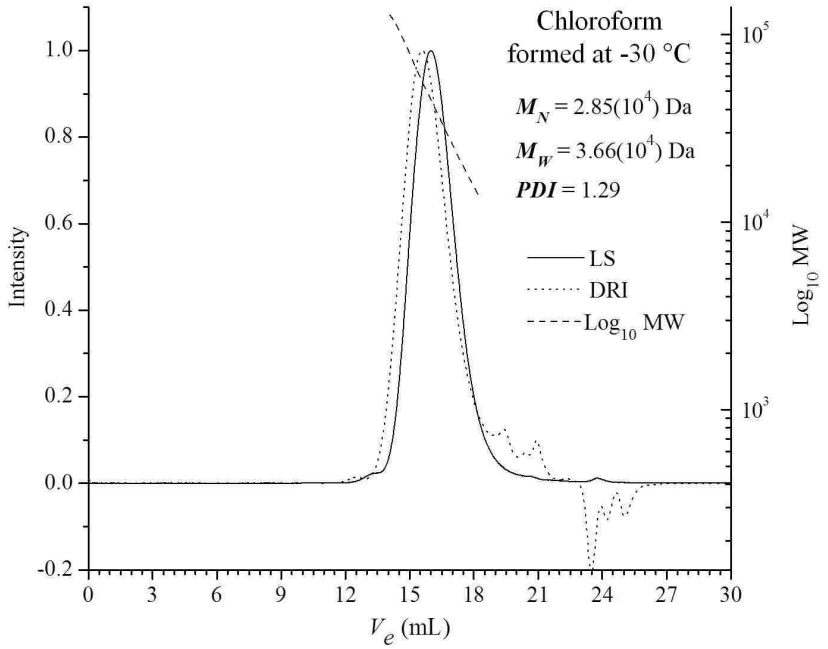

Figure 4.3 Plot of elution volume vs. Log_{10} of molar mass (dashed) and LS (solid) and DRI (dotted) chromatograms of P3HT formed at –30 °C in chloroform.

In Figure 4.3 is shown the chromatogram from the analytical GPC analysis of P3HT formed at –30 °C in chloroform; light scattering (LS) data is represented by the solid line trace, differential refractive index (DRI) data is traced with a dotted line, and the logarithm base 10 of the distribution of molecular weight data is shown by a dashed line. The number-average molecular weight (M_N) for this material as determined from the DRI data was found to be 28,500 Da compared to P3HT formed under similar conditions at room temperature, which was calculated to be 19,500 Da (cf. Figure 2.5). The weight-average molecular weight, M_W, calculated from light scattering (LS) data for P3HT formed at –30 °C is 36,600 Da compared to those formed at room temperature that was determined to be 36,600 Da (cf. Figure 2.5). Thus, the *PDI* for P3HTs formed by oxidative polymerization with iron(III) chloride at –30 °C using chloroform as a solvent is calculated to be 1.29, whereas those formed under similar conditions at room temperature had a *PDI* of 1.88 (cf. Figure 2.5).

4.5.2 P3HTs Formed at −25 °C Using Carbon Tetrachloride as a Reaction Solvent

P3HTs investigated in this section were prepared via the procedure outlined in Section 4.2.2 using carbon tetrachloride (CCl_4) as the solvent medium. Carbon tetrachloride is a more nonpolar solvent than chloroform with a dielectric constant at 25 °C (cf. Section 2.1.2) of 2.2. Iron(III) chloride is less soluble in carbon tetrachloride than it is in chloroform at room temperature, remaining for the most part in the solid state and imparting a very slight yellowish tint to the suspension. Carbon tetrachloride has more than two times less Lewis acid strength than chloroform and is assigned a Gutmann Acceptor number, AN, (cf. Section 2.1.2) of 8.6. Carbon tetrachloride has negligible Lewis base characteristics. Mass yields of polymer recovered from the preparation of P3HTs formed following the procedures outlined in Section 4.2.2 using carbon tetrachloride were on the order of ~ 20% compared yields of P3HT formed under similar conditions at room temperature, which were on the order of ~30% (cf. Section 2.5.2).

The MALDI-ToF mass spectra observed during the endgroup analysis of these materials indicate the presence of oligomers possessing α-terminal ends consisting of two hydrogens [H-$(C_{10}H_{14}S)_n$-H], along with oligomers having one hydrogen and one chlorine [H-$(C_{10}H_{14}S)_n$-Cl] at the α-terminals as shown in Figure 4.4. The upper spectrum in Figure 4.4 is the MALDI-ToF mass spectrum of oligomers in the range of m/z 0–5000 by use of reflectron mode (cf. Section 2.3.1). The overall ion pattern presented in the upper spectrum of Figure 4.4 indicates that the abundance of interstitial peaks (chlorinated oligomers) between those representing hydrogen terminated molecular radical cations has dramatically decreased compared to those found in the mass spectra of P3HT formed under similar conditions at room temperature (cf. Figure 2.6).

The lower spectrum in Figure 4.4 is an inset to the spectrum for P3HT formed by chemical oxidation with ferric chloride at −25 °C using carbon tetrachloride as a solvent and it

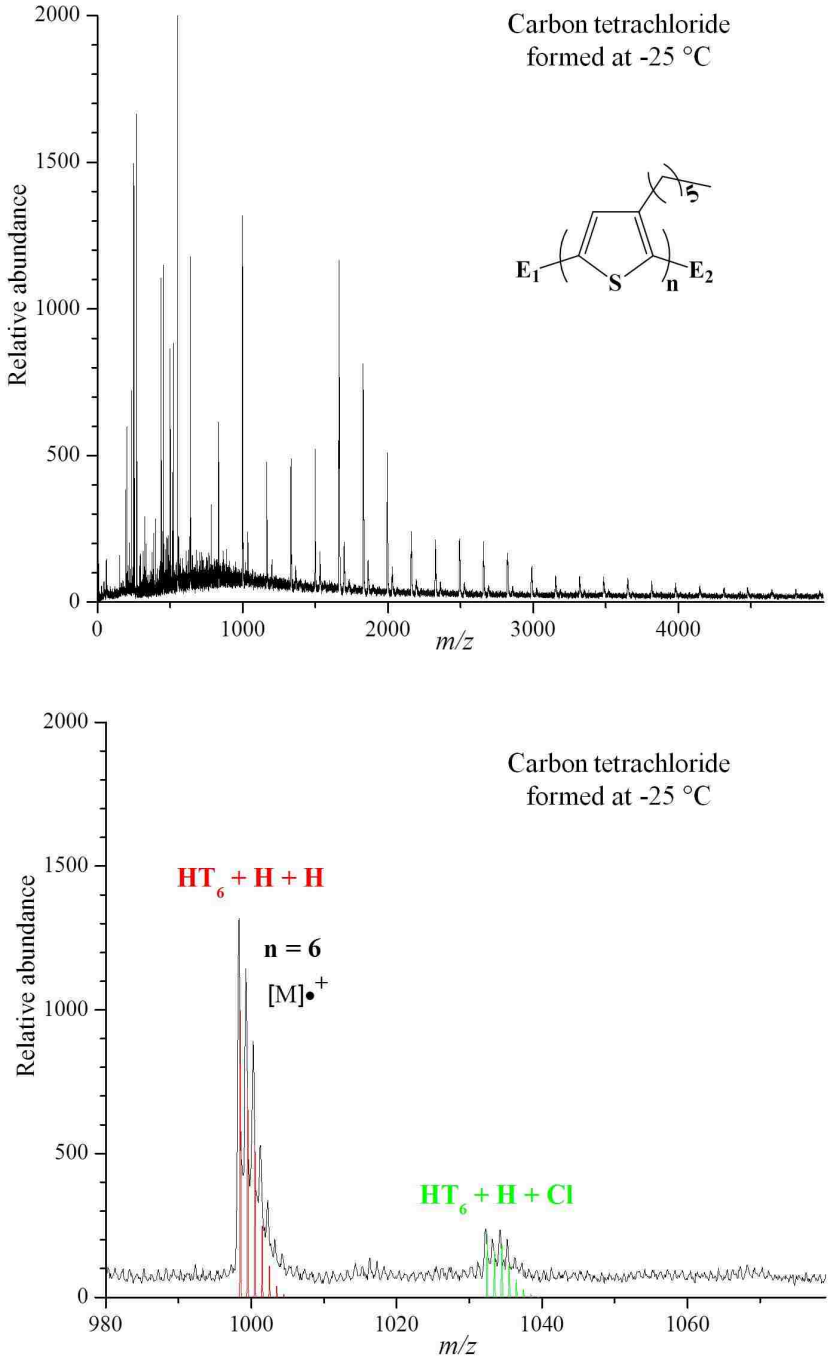

Figure 4.4 MALDI-ToF mass spectra of P3HT formed at –25 °C in carbon tetrachloride observed by use of reflectron mode (upper). The inset (lower) shows expanded 6-mer region of the spectrum with colored peaks indicating the calculated isotope patterns of the 6-mer having different chlorine additions.

focuses on the $M^{\bullet+}$ peak for the oligomer $n = 6$. The overlays shown in various colors are the calculated isotopic patterns for the representation of the given species, which were produced by

the Bruker Xmass software. The calculated peaks are labeled in their respective color denoting the chemical composition of the calculated patterns, where HT_n indicates the repeat unit, which is a 3-*n*-hexylthiophene monomer unit minus 2 hydrogen atoms and has a molar mass of 166.3 amu. These are shown in comparison to the experimental peaks observed for the polymer sample in the background. The spectrum shows excellent agreement with oligomers representing the hydrogen-terminated molecular radical cation, as well as ion patterns indicating oligomers possessing one chlorine termination and one hydrogen endgroup.

There appears a very extensive decrease in the ion signals observed for chlorinated oligomers of P3HT formed at –25 °C in the mass spectra shown in Figure 4.1 compared to those polymers formed under similar conditions at room temperature shown in the mass spectra in Figure 2.6 indicated by the comparison of the relative abundances of ion signals for the respective materials. In fact, there exists no observable ion signals for oligomers possessing 2 or more chlorine additions in the mass spectrum of P3HT formed at –25 °C using carbon tetrachloride, whereas the peak for doubly-chlorinated oligomers is evident in greater abundance than solely hydrogen-terminated oligomers for P3HT formed at room temperature (cf. Figure 2.6). Furthermore, the ion signal for singly-chlorinated P3HT formed at room temperature is more abundant than the signal for oligomers possessing solely hydrogen-teminated oligomers as shown in Figure 2.6, whereas the signal for singly-chlorinated P3HT oligomers formed at –25 °C (cf. Figure 4.4) is at most $1/6^{th}$ that seen for solely hydrogen-terminated oligomers formed at –25 °C.

The ^{1}H-NMR analysis of P3HTs formed by chemical oxidation with ferric chloride at –25 °C using carbon tetrachloride is shown in Figure 4.5. The inset shows the peaks for signals arising from the α-methylene (aryl methylene) groups found at chemical shifts of $\delta \sim 2.8$ ppm and $\delta \sim 2.58$ ppm, indicating signal response from regioregular and regioirregular material,

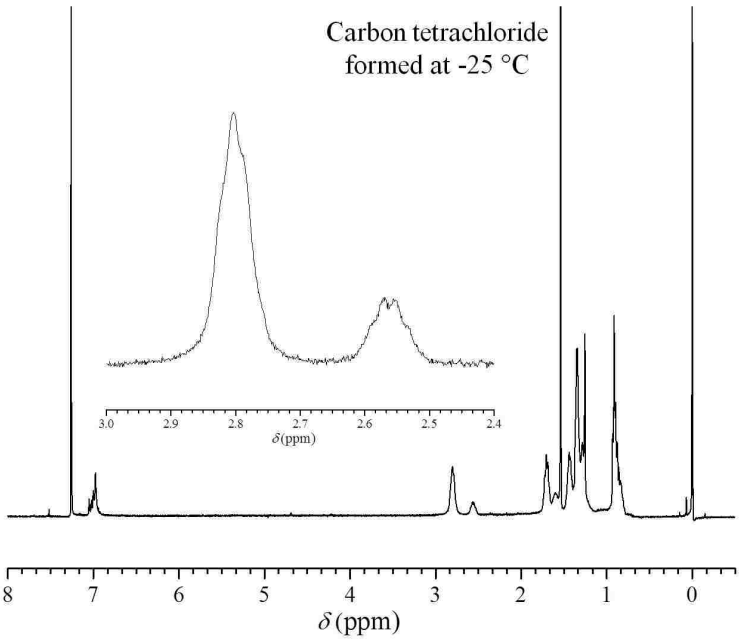

Figure 4.5 ^{1}H-NMR spectrum of P3HT formed at –25 °C in carbon tetrachloride. The inset shows the α-methylene region used to determine the material's regioregularity of 80%.

respectively (cf. Section 1.2.3). The analysis of structural regularity by integration and relative comparison of these peaks is discussed in Section 1.2.4. From integration of the peak found at δ ~ 2.8 ppm normalized as one (1.0) and integration of the peak found at δ ~ 2.58 ppm, which was determined to be 0.25 as compared to the normalized peak, the percentage of the peak at δ ~ 2.8 ppm is found to be 80% of the combined areas of the two peaks. Therefore, the regioregularity of P3HT formed by this chemical oxidative polymerization (cf. Section 4.2.2) at –25 °C using carbon tetrachloride as a solvent can be regarded as 80% regioregular material. The regioregularity of the P3HT formed at –25 °C using carbon tetrachloride increased 6% compared to those formed under similar conditions at room temperature, which was shown to be 74% regioregular (cf. Figure 2.7).

In Figure 4.6 is shown the chromatogram from the analytical GPC analysis of P3HT formed at –25 °C in carbon tetrachloride; light scattering (LS) data is represented by the solid

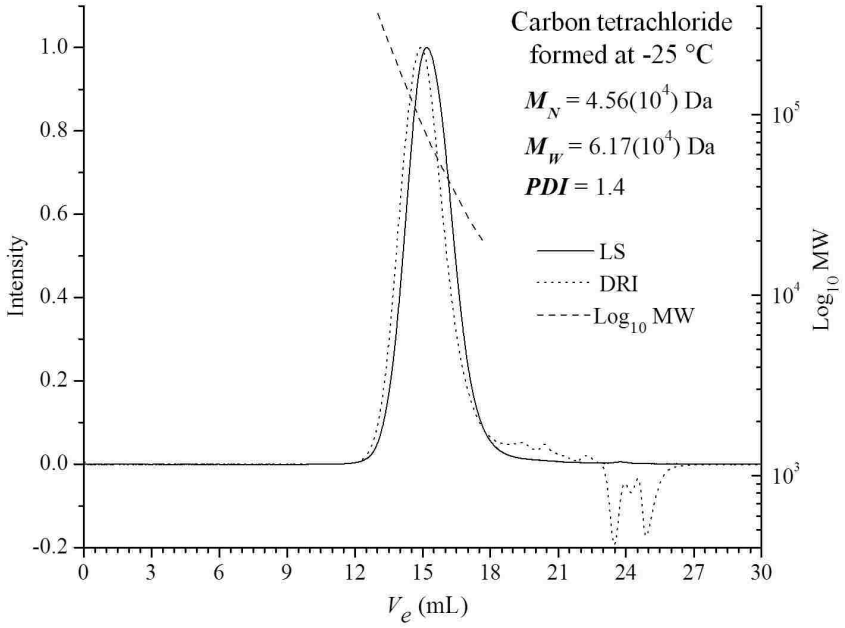

Figure 4.6 Plot of elution volume vs. Log_{10} of molar mass (dashed) and LS (solid) and DRI (dotted) chromatograms of P3HT formed at –25 °C in carbon tetrachloride.

line trace, differential refractive index (DRI) data is traced with a dotted line, and the logarithm base 10 of the distribution of molecular weight data is shown by a dashed line. The number-average molecular weight (M_N) for this material as determined from the DRI data was found to be 45,600 Da compared to P3HT formed under similar conditions at room temperature, which was calculated to be 56,600 Da (cf. Figure 2.8). The weight-average molecular weight, M_W, calculated from light scattering (LS) data for P3HT formed at –25 °C is 61,700 Da compared to those formed at room temperature that was determined to be 119,000 Da (cf. Figure 2.8). Thus, the *PDI* for P3HTs formed by oxidative polymerization with iron(III) chloride at –25 °C using carbon tetrachloride as a solvent is calculated to be 1.4, whereas those formed under similar conditions at room temperature had a *PDI* of 2.1 (cf. Figure 2.8).

4.5.3 P3HTs Formed at –30 °C Using 1,2-Dichloroethane as a Reaction Solvent

P3HTs investigated in this section were prepared via the procedure outlined in Section 4.2.2 using 1,2-dichloroethane, (DCE, $C_2H_4Cl_2$) as the solvent medium. DCE is more than two

times as polar as chloroform with a dielectric constant of 10.4 at 25 °C (cf. Section 2.1.2). Iron(III) chloride is more soluble in DCE than it is in chloroform at room temperature, imparting slightly more yellowish tint to the suspension as compared to chloroform. DCE is used as a reference with antimony (V) chloride for empirical determination of Guttman acceptor numbers and has arbitrarily been assigned an AN of 100 in that state (cf. Section 2.1.2) and is considered to have strong Lewis acid characteristics. It is also used as a supporting medium for determination of Guttman donor numbers (cf. Section 2.1.2) and is regarded as having negligible Lewis base strengths. Mass yields of polymer recovered from the preparation of P3HTs formed following the procedures outlined in Section 4.2.2 with DCE were on the order of ~ 20% compared yields of P3HT formed under similar conditions at room temperature, which were on the order of ~30% (cf. Section 2.5.4).

The MALDI-ToF mass spectra observed during the endgroup analysis of these materials indicate the presence of oligomers possessing α-terminal ends consisting of primarily two hydrogens [H-$(C_{10}H_{14}S)_n$-H], and oligomers having one hydrogen and one chlorine [H-$(C_{10}H_{14}S)_n$-Cl] α-terminal groups, as shown in Figure 4.7. The upper spectrum in Figure 4.7 is the MALDI-ToF mass spectrum of oligomers in the range of m/z 0–5200 by use of reflectron mode (cf. Section 2.3.1).

The lower spectrum in Figure 4.7 is an inset to the spectrum for P3HT formed by chemical oxidation with ferric chloride at –30 °C using DCE as a solvent and focuses on the $M^{\bullet+}$ peak for the oligomer n = 6. The overlays shown in various colors are the calculated isotopic patterns for the representation of the given species, which were produced by the Bruker Xmass software. The calculated peaks are labeled in their respective color denoting the chemical composition of the calculated patterns, where HT_n indicates the repeat unit, which is a 3-*n*-hexylthiophene monomer unit minus 2 hydrogen atoms and has a molar mass of 166.3 amu.

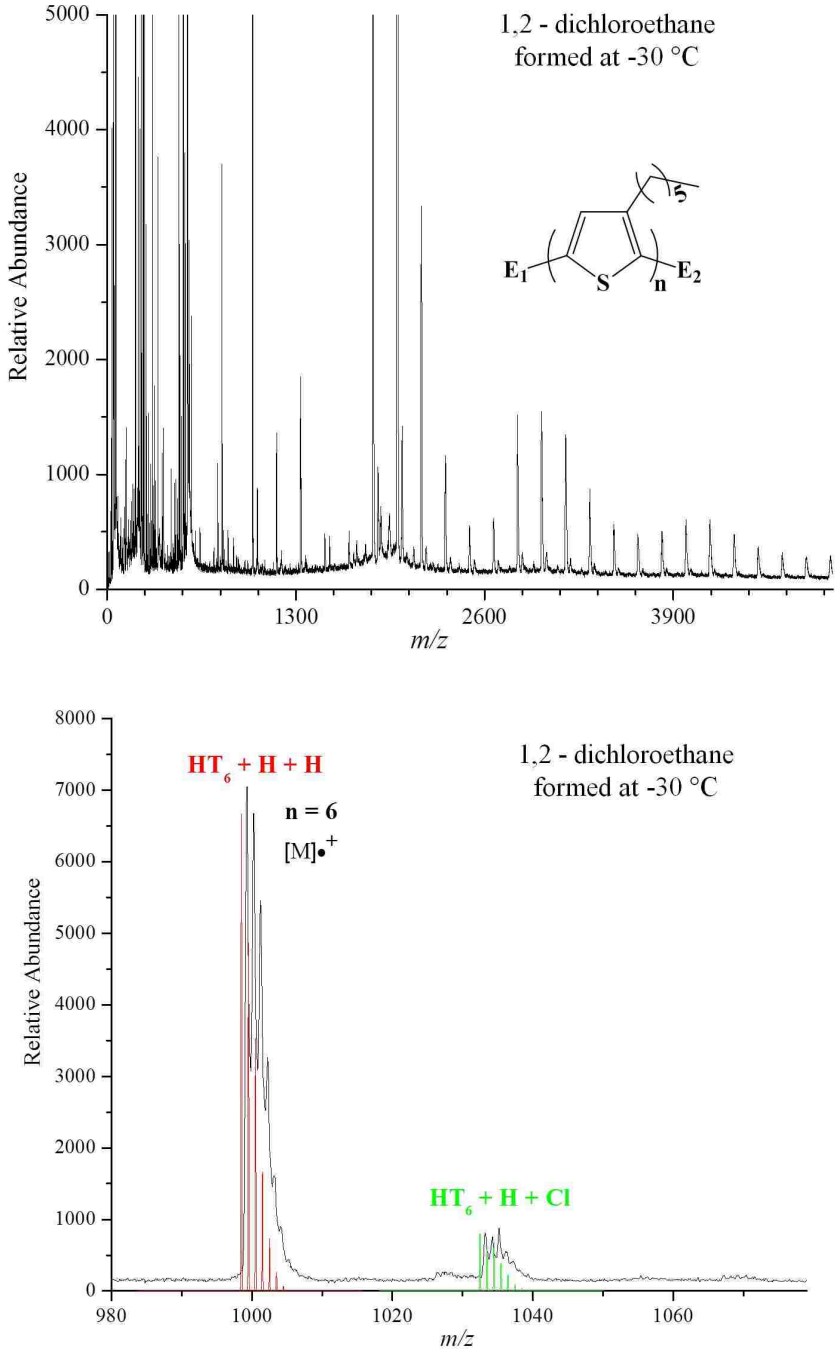

Figure 4.7 MALDI-ToF mass spectra of P3HT formed at –30 °C in 1,2-dichloroethane observed by use of reflectron mode (upper). The inset (lower) shows expanded 6-mer region of the spectrum with colored peaks indicating the calculated isotope patterns of the 6-mer having different chlorine additions.

These are shown in comparison to the experimental peaks observed for the polymer sample in the background.

The spectrum shows good agreement with oligomers representing the hydrogen-terminated molecular radical cation, as well as ion patterns indicating oligomers possessing one chlorine termination and one hydrogen endgroup. There is no indication by comparison of calculated and observed ion patterns for oligomers possessing two chlorine additions as was seen for P3HT formed under similar conditions at room temperature (cf. Figure 2.12). Hydrogen-terminated P3HT is the primary species observed in the MALDI-ToF mass spectrum of the material formed at –30 °C using DCE as a solvent with very limited observable signal for singly-chlorinated P3HT oligomers. In fact, the ion signal for singly-chlorinated P3HT formed at room temperature using DCE is almost half that of the signal for oligomers possessing solely hydrogen-teminated oligomers as shown in Figure 2.12, whereas the signal for singly-chlorinated P3HT oligomers formed at –30 °C (cf. Figure 4.7) is roughly 1/10th that seen for solely hydrogen-terminated oligomers formed at –30 °C.

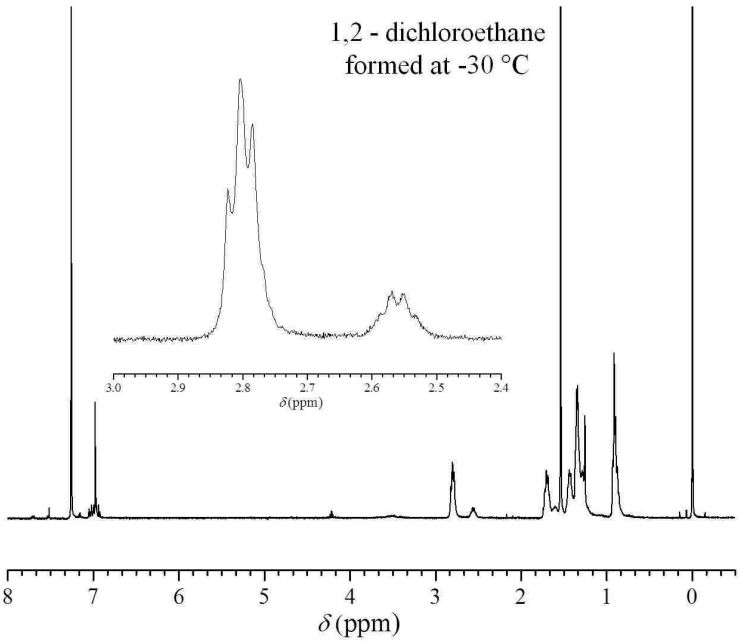

Figure 4.8 ^{1}H-NMR spectrum of P3HT formed at –30 °C in 1,2-dichloroethane. The inset shows the α-methylene region used to determine the material's regioregularity of 81%.

The ^{1}H-NMR analysis of P3HTs formed by chemical oxidation with ferric chloride at –30 °C using 1,2-dichloroethane is shown in Figure 4.8. The inset shows the peaks for signals arising from the α-methylene (aryl methylene) groups found at chemical shifts of $\delta \sim 2.8$ ppm and $\delta \sim 2.58$ ppm, indicating signal response from regioregular and regioirregular material, respectively (cf. Section 1.2.3). The analysis of structural regularity by integration and relative comparison of these peaks is discussed in Section 1.2.4. From integration of the peak found at $\delta \sim 2.8$ ppm normalized as one (1.0) and integration of the peak found at $\delta \sim 2.58$ ppm, which is was determined to be 0.24 as compared to the normalized peak, the percentage of the peak at $\delta \sim 2.8$ ppm is found to be 81% of the combined areas of the two peaks. Therefore, the regioregularity of P3HT formed by this chemical oxidative polymerization (cf. Section 4.2.2) using DCE as a solvent can be regarded as 81% regioregular material. There was no improvement in the regioregularity of P3HT formed at –30 °C using DCE as a reaction solvent as compared to P3HT formed under similar conditions at room temperature (cf. Figure 2.13) as was noticed for the previous two solvents employed for these low-temperature polymerization reactions.

In Figure 4.9 is shown the chromatogram from the analytical GPC analysis of P3HT formed at –30 °C in DCE; light scattering (LS) data is represented by the solid line trace, differential refractive index (DRI) data is traced with a dotted line, and the logarithm base 10 of the distribution of molecular weight data is shown by a dashed line. The number-average molecular weight (M_N) for this material as determined from the DRI data was found to be 18,800 Da compared to P3HT formed under similar conditions at room temperature, which was calculated to be 53,500 Da (cf. Figure 2.14). The weight-average molecular weight, M_W, calculated from light scattering (LS) data for P3HT formed at –30 °C is 25,600 Da compared to those formed at room temperature that was determined to be 86,100 Da (cf. Figure 2.14). Thus,

the *PDI* for P3HTs formed by oxidative polymerization with iron(III) chloride at –30 °C using DCE as a solvent is calculated to be 1.36, whereas those formed under similar conditions at room temperature had a *PDI* of 1.61 (cf. Figure 2.14).

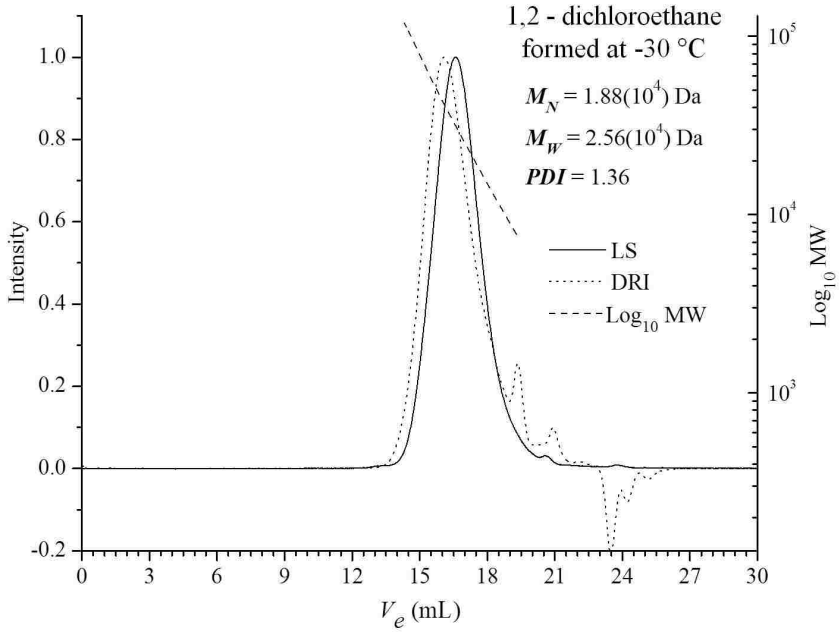

Figure 4.9 Plot of elution volume vs. Log_{10} of molar mass (dashed) and LS (solid) and DRI (dotted) chromatograms of P3HT formed at –30 °C in 1,2-dichloroethane.

4.5.4 P3HTs Formed at –30 °C Using Nitromethane as a Reaction Solvent

P3HTs investigated in this section were prepared via the procedure outlined in Section 4.2.2 at –30 °C using nitromethane (CH_3NO_2) as the solvent medium. Nitromethane is a very polar solvent with a dielectric constant of 37 at 25 °C (cf. Section 2.1.2). Iron(III) chloride is completely soluble in nitromethane at room temperature, forming a yellow/orange solution almost immediately upon addition of $FeCl_3$. Nitromethane is a strong Lewis acid strength and is assigned a Gutmann Acceptor number (AN) (cf. Section 2.1.2) of 20.5, slightly less than chloroform. Nitromethane has little Lewis base characteristics and has a Guttman donor number, DN, (cf. Section 2.1.2) of 2.7. Mass yields of polymer recovered from the preparation of P3HTs formed following the procedures outlined in Section 4.2.2 with nitromethane were on the order

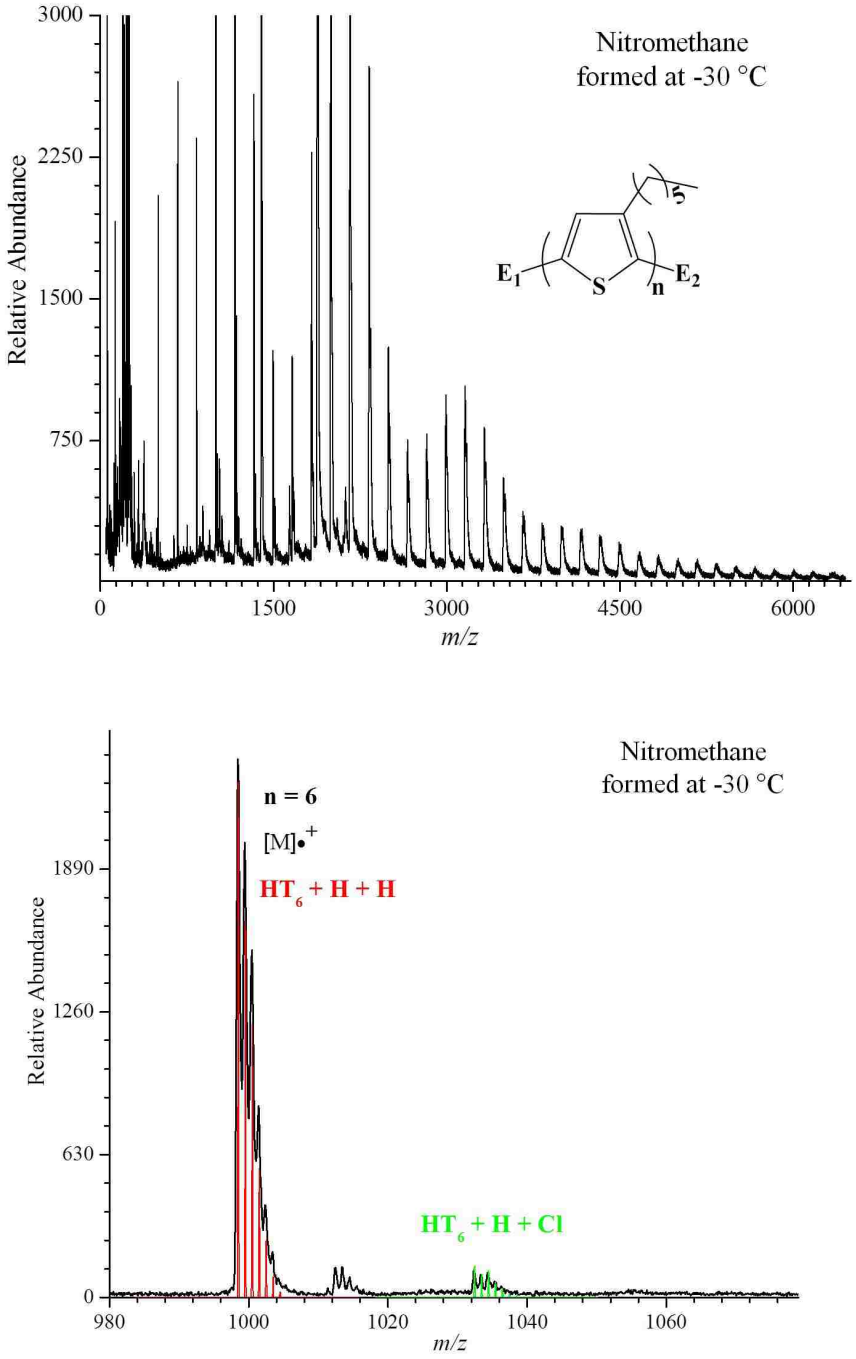

Figure 4.10 MALDI-ToF mass spectra of P3HT formed at –30 °C in nitromethane observed by use of reflectron mode (upper). The inset (lower) shows expanded 6-mer region of the spectrum with colored peaks indicating the calculated isotope patterns of the 6-mer having different chlorine additions.

of ~ 10% compared yields of P3HT formed under similar conditions at room temperature, which were on the order of ~25% (cf. Section 2.5.5).

The MALDI-ToF mass spectra observed during the endgroup analysis of these materials indicate the presence of oligomers possessing α-terminal ends consisting of primarily two hydrogens [H-$(C_{10}H_{14}S)_n$-H], and a limited number of oligomers having one hydrogen and one chlorine [H-$(C_{10}H_{14}S)_n$-Cl] α-terminal groups as shown in Figure 4.10. The upper spectrum in Figure 4.10 is the MALDI-ToF mass spectrum of oligomers in the range of m/z 0–6500 by use of reflectron mode (cf. Section 2.3.1). There is no observable abundance of interstitial peaks reflecting chlorinated oligomers between those observed that are indicative of molecular radical cations ($M^{\bullet+}$) having α-terminals with solely hydrogen-terminated endgroups.

The lower spectrum in Figure 4.10 is an inset to the spectrum for P3HT formed by chemical oxidation with ferric chloride at –30 °C using nitromethane as a solvent and it focuses on the $M^{\bullet+}$ peak for the oligomer $n = 6$. The overlays shown in various colors are the calculated isotopic patterns for the representation of the given species, which were produced by the Bruker Xmass software. The calculated peaks are labeled in their respective color denoting the chemical composition of the calculated patterns, where HT_n indicates the repeat unit, which is a 3-*n*-hexylthiophene monomer unit minus 2 hydrogen atoms and has a molar mass of 166.3 amu. These are shown in comparison to the experimental peaks observed for the polymer sample in the background. The spectrum shows excellent agreement with oligomers representing the hydrogen terminated molecular radicalcations [H-$(C_{10}H_{14}S)_n$-H], as well as ion patterns indicating oligomers possessing one chlorine termination and one hydrogen endgroup [H-$(C_{10}H_{14}S)_n$-Cl]. There is extremely limited chlorination as compared to materials formed at –30 °C using the other solvents employed for the studies within this Chapter. All chlorination to P3HT formed at –30 °C using nitromethane as a reaction solvent is in the form of the addition of one chlorine atom and the relative abundance as observed by MALDI-ToF-MS of this species is approximately $1/24^{th}$ that of the hydrogen-terminated oligomers. Whereas, the ion signal for

singly-chlorinated P3HT formed at room temperature using nitromethane is approximately 1/8th that of the signal for oligomers possessing solely hydrogen-teminated oligomers as shown in Figure 2.15.

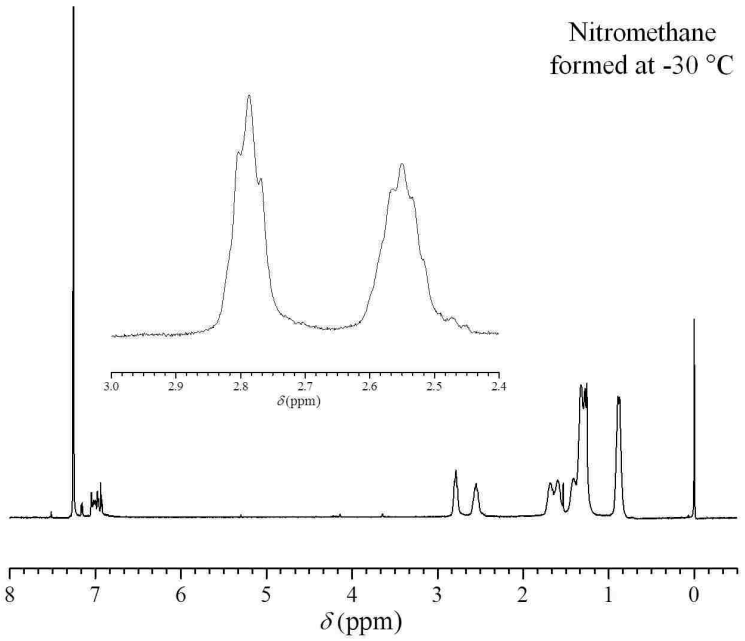

Figure 4.11 ^{1}H-NMR spectrum of P3HT formed at –30 °C in nitromethane. The inset shows the α-methylene region used to determine the material's regioregularity of 53%.

The ^{1}H-NMR analysis of P3HTs formed by chemical oxidation with ferric chloride at –30 °C using nitromethane is shown in Figure 4.11. The inset shows the peaks for signals arising from the α-methylene (aryl methylene) groups found at chemical shifts of $\delta \sim 2.8$ ppm and $\delta \sim 2.58$ ppm, indicating signal response from regioregular and regioirregular material, respectively (cf. Section 1.2.3). The analysis of structural regularity by integration and relative comparison of these peaks is discussed in Section 1.2.4. From integration of the peak found at $\delta \sim 2.8$ ppm normalized as one (1.0) and integration of the peak found at $\delta \sim 2.58$ ppm, which was determined to be 0.9 as compared to the normalized peak, the percentage of the peak at $\delta \sim 2.8$ ppm is found to be 53% of the combined areas of the two peaks. Therefore, the regioregularity of P3HT formed by this chemical oxidative polymerization at –30 °C (cf. Section 4.2.2) using

nitromethane as a solvent can be regarded as 53% regioregular material. The regioregularity of the P3HT formed at –30 °C using nitromethane decreased 14% compared to those formed under similar conditions at room temperature, which was shown to be 67% regioregular (cf. Figure 2.16).

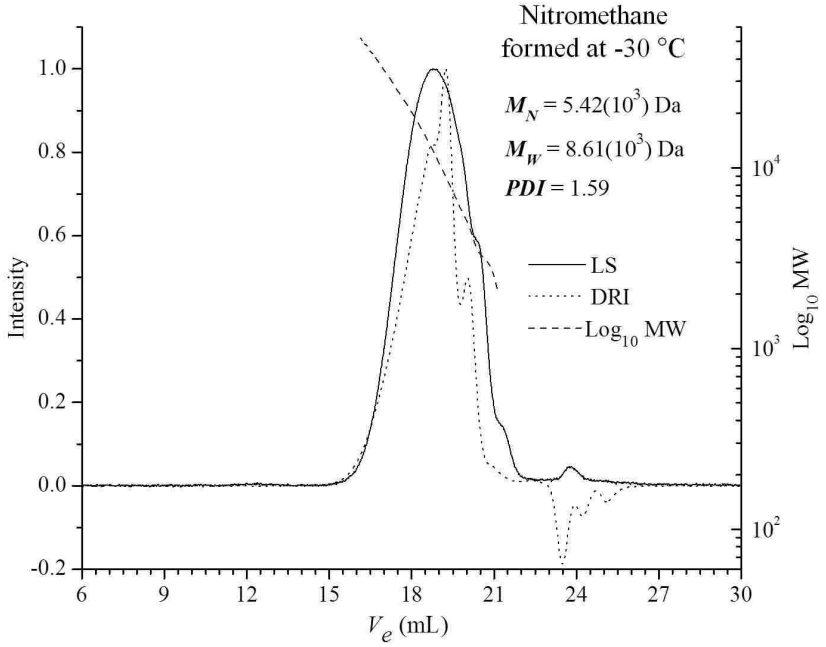

Figure 4.12 Plot of elution volume vs. Log_{10} of molar mass (dashed) and LS (solid) and DRI (dotted) chromatograms of P3HT formed at –30 °C in nitromethane.

In Figure 4.12 is shown the chromatogram from the analytical GPC analysis of P3HT formed at –30 °C in nitromethane; light scattering (LS) data is represented by the solid line trace, differential refractive index (DRI) data is traced with a dotted line, and the logarithm base 10 of the distribution of molecular weight data is shown by a dashed line. The number-average molecular weight (M_N) for this material as determined from the DRI data was found to be 5,420 Da compared to P3HT formed under similar conditions at room temperature, which was calculated to be 38,100 Da (cf. Figure 2.17). The weight-average molecular weight, M_W, calculated from light scattering (LS) data for P3HT formed at –30 °C is 8,600 Da compared to

those formed at room temperature that was determined to be 48,800 Da (cf. Figure 2.17). Thus, the *PDI* for P3HTs formed by oxidative polymerization with iron(III) chloride at –30 °C using DCE as a solvent is calculated to be 1.59, whereas those formed under similar conditions at room temperature had a *PDI* of 1.28 (cf. Figure 2.17).

4.6 Discussion

The most obvious and dramatic effect of low-temperature synthesis of P3HTs by means of chemical oxidation with ferric chloride–regardless of the solvent employed for the reaction–was the minimization to the extent of chloride addition to the resulting P3HTs. This phenomenon is still not fully understood. It was thought that possibly chloride anions were being sequestered via water remnants within the reaction mixtures, although extreme care was taken to conduct these experiments in the driest conditions. Therefore more experiments were conducted in order to attempt to eliminate possibility. Specifically, an experiment was performed where the solvent (nitromethane)–along with the monomer–was distilled immediately prior to the reaction. The solvent was then put over activated molecular sieves and examined via ^{1}H-NMR, which gave no indication to the presence of water in the solvent. The glassware used in the experiment was baked at 120 °C overnight before the polymerization reaction was conducted. The polymerization was performed inside a glove bag in an argon atmosphere. Finally, the sealed ampule of ferric chloride employed (#451649, anhydrous, powder, ≥99.9%, trace metal basis) for the experiment was opened and measured inside a glove bag under argon atmosphere immediately prior to the experiment. The results of this polymerization yielded the conclusion that water was not responsible for the decrease in chlorine addition during low-temperature polymerizations.

It is likely that a simple answer to this phenomenon may be found by examining the factors proposed for the chlorination of these materials at room temperature (cf. Section 2.6.1).

This explanation is based upon the conclusion that the extent of chlorination is dependent upon the species (physical state) of ferric chloride found in the reaction mixture that is dependent on the physical properties of the solvent employed for the reaction (cf. Section 2.1.3). The interaction between the solvent and oxidant are influenced by the physical properties of the solvent such as the dielectric constant and the acceptor and donor ability of that solvent (cf. Section 2.1.2 and 2.1.3). Therefore, the low temperatures employed for the reactions in experiments presented in Chapter 4 must affect the physical state of the oxidant in some manner.

A minor influence may stem from the slight increase of dielectric constant at low temperatures, although this in itself is probably not sufficient enough to significantly alter the physical state of ferric chloride in the low-temperature reaction mixtures (cf. Section 2.1.2 and 2.1.3). Next, the extended reaction time (24 hours) may allow for either: (i) more oxidant to dissolve and go into solution taking on the monomeric state (tetrachloroferrate, cf. Section 2.1.3); or (ii) the larger crystals of solid oxidant to break apart into smaller pieces–although remaining predominantly in a crystalline form–that increases the overall surface area of solid oxidant in suspension where oxidation occurs and decreases the probability that oxidation of reacting 3-*n*-hexylthiophene species occurs directly on the surface of large pieces of solid oxidant where chlorination of the resulting polymer is more likely to occur (cf. section 2.1.1).[8] Finally, the reduction of temperature removes energy from the reacting system and slows the kinetics of the polymerization sufficiently in order to allow the former factors to occur before nucleophilic chlorination (cf. Section 1.2.9) of the resulting polymer. However, it is likely that the minimization of chlorine addition to P3HTs formed at low temperatures via chemical oxidation with ferric chloride is the result of a combination of all of these factors.

The ^{1}H-NMR studies provided interesting results as to the effect of lower temperatures to the regioregularity of P3HTs formed by chemical oxidation with ferric chloride as shown in

Table 4.1. P3HTs formed under these conditions using the nonpolar solvents chloroform and carbon tetrachloride were observed to have increased regioregularity compared to those P3HTs formed under similar conditions at room temperature. The regioregularity of P3HT formed in chloroform at –30 °C was observed to increase to 83% from 77% for the polymer formed at room temperature. Similar results were observed for polymer formed in carbon tetrachloride. These results lend credence to reports by Amou et al.[1] that regioregularities upwards of 88% are achievable for P3HTs formed by chemical oxidation with ferric chloride at –45 °C. For P3HT formed by chemical oxidation at low temperatures using 1,2-dichloroethane as a reaction solvent there was no change in regioregularity compared to P3HT formed under similar conditions at room temperature. Interestingly, the regioregularity of P3HT formed by chemical oxidation with ferric chloride at low temperature using nitromethane as a reaction solvent dramatically decreased from 67% for polymer produced at room temperature to 53% for those produced at low temperatures.

Solvent	Dielectric Constant @ 25 °C	AN[3]	DN[4]	M_N (Da) RT[2]	M_N (Da) –30 °C*	*PDI* RT[2]	*PDI* –30 °C*	RR[1] RT[2]	RR[1] –30 °C*
chloroform	4.8	23	negligible	19,500	36,600	1.88	1.29	77%	83%
carbon tetrachloride	2.2	8.6	negligible	56,600	119,000	2.1	1.4	74%	80%
1,2-dichloroethane	10.4	100[a]	–	53,500	86,100	1.61	1.36	81%	81%
nitromethane	37	20.5	2.7	38,100	48,800	1.28	1.59	67%	53%

*Reactions using carbon tetrachloride were performed at –25 °C.
[a]1,2-dichloroethane is used as a reference solvent with $SbCl_5$ for empirical DN measurements.
[1]Regioregularity
[2]Room temperature
[3]acceptor number
[4]donor number

Table 4.1 Solvents employed for the production of P3HTs by chemical oxidation with ferric chloride at low temperatures. The physical properties of solvents are included, along with physical properties of polymers resulting from polymerizations performed in each solvent at room temperature and low temperature.

It is reported that low temperatures[9] and more nonpolar solvents[10,11] stabilize the lifetimes of radical species. Also, reports in the literature demonstrate that the oxidation potential for the thiophene monomer (1.55 V versus Ag/AgCl)[12] is much greater than the oxidation potential for small thiophene oligomers having $n = 2–4$ (1.17 V for $n = 2$, 0.96 V for $n = 3$, and 0.90 V for $n = 4$ versus Ag/AgCl)[12]. Furthermore, the oxidation potential of longer 3-alkylthiophene oligomers has been reported to decrease as a function of increasing chain length.[13] With all of this in mind, transition-state calculations by Lacroix et al.[4]–regarding the coupling reactions involved in the polymerization of poly(pyrrole)–indicated that in nonpolar solvents the calculated energy barrier for the formation of a longer pyrrole oligomers was 2–10 times smaller for the coupling between a pyrrole oligomer radical cation and a pyrrole monomer radical cation than the energy barrier calculated for coupling between two pyrrole oligomer radical cations.

In regards to the improvement to the regioregularity observed for P3HTs formed by chemical oxidation at low temperatures–using chloroform and carbon tetrachloride as reaction solvents–it is possible that presence of monomer radical cations in the reacting mixture is increased due to their increased lifetime stability at low temperatures–as well as the similar influence from the polarity of the solvent–providing a sufficient population of reacting species to propagate by the preferred route outlined by Lacroix et al; the coupling route that has been reported to produce more regioregular P3ATs.[2-4]

In the case of P3HTs formed at low temperatures using nitromethane as a reaction solvent it may be the case that less thiophene monomer radical cations are present in the reacting mixture because of the combined effects of the higher oxidation potential of the monomer and the shorter lifetimes for monomer radical cation species that are formed, due to the greater polarity of the solvent. Therefore, although the low temperature may somewhat increase the lifetime of the monomer radical cations that are formed, less of these species are present in the reacting mixture.

It is obviously apparent that some monomer radical cations survive to form oligomers by the fact that polymer is formed. However, it is likely that the majority of reacting thiophene species present in the reaction mixture at some point during the polymerization becomes oligomeric species for which the lifetimes are stabilized because of their lower oxidation potential and the low-temperature effects. Thus, the coupling of oligomeric radical cation species with other oligomeric radical cation species would become the primary coupling route to form longer polymer chains, as these species are the predominant species in the reacting solution. The extreme decrease in regioregularity for the P3HT formed at low temperature using nitromethane may indicate a shift to primarily oligomer-to-oligomer radical cation coupling, whereas during the polymerization reaction conducted at room temperature there exists a competition during polymer chain growth between oligomer radical cation-to-monomer radical cation coupling and oligomer radical cation-to-oligomer radical cation coupling.

This scenario outlined for the formation of P3HTs formed at low temperatures using nitromethane as a reaction solvent may provide an insight into the diminished number average molecular weight for P3HTs formed at low temperature using nitromethane (M_N~5,400 Da). Whereas, the M_N for P3HT formed by chemical oxidation with ferric chloride at room temperature using nitromethane as a reaction solvent was calculated by SEC-MALLS to be roughly 38,000 Da. It is very likely that the coupling between monomer radical cations and oligomer radical cations not only is the pathway to forming more regioregular materials but also the route necessary for the formation of very long P3HT polymer chains.

The results presented for the P3HT formed by chemical oxidation with ferric chloride at low temperatures using 1,2-dichloroethane, DCE, indicate the difficulty in correctly assessing the experimental factors–such as solvent properties and temperature–that influence the physical properties of P3HT formed in this manner. For instance, the regioregularity of P3HTs formed at

a low temperature and those formed at room temperature using DCE as a reaction solvent did not differ; both methods produced material that was 81% regioregular. This might be explained by the fact that DCE possesses an intermediate polarity compared to either chloroform or carbon tetrachloride and nitromethane. However, the M_N of material formed in DCE at a low temperature decreased dramatically from 53,500 Da for P3HT formed at room temperature to 18,800 Da; this was similar to the decrease in M_N observed for materials formed in the polar solvent nitromethane, which also displayed a large decrease in regioregularity. Whereas, P3HT formed at low temperatures in nonpolar solvents where an increase in regioregularity was observed exhibited either an increase in M_N as compared to polymer formed under similar conditions at room temperature–such as is the case with chloroform–or a small decrease in M_N, such as is the case for carbon tetrachloride. In other words, if the regioregularity and the average molecular weights of the P3HTs presented within this work are both functions of the specific coupling route involved during chain growth then the regioregularity of those P3HTs formed at a low temperature using DCE would be expected to decrease as there was an observed decrease in the M_N of the material. Unfortunately, this anomaly is still not understood.

4.7 Conclusions

The use of low temperatures to form P3HTs by means of chemical oxidation with ferric chloride has proven to be a useful means to tailor the physical properties of the resulting polymers. The structural characteristics of P3HTs have been shown to directly impact their unique optical and electrical properties[14-16], which directly impacts their applicability in modern technological applications (cf. Section 1.2.2). Most striking is the diminishment to the extent of chlorination observed to the materials produced at low-temperatures regardless of the specific solvent employed for the polymerization. The nucleophilic addition of chlorine to P3ATs has

been reported to dramatically increase their oxidation potentials,[16] which has been shown to have a marked impact on their conductivity and optical properties as well.[15]

It has also been shown that the regioregularity of P3HTs may be increased by the use of low-temperature chemical oxidation with ferric chloride in certain nonpolar solvents. These findings are in good agreement with other reports for similar low-temperature polymerizations to form P3HTs by these means.[1] Therefore, it has now been shown that P3HTs can be formed by chemical oxidation with ferric chloride having sufficient structural regioregularity and possessing limited chlorination making them well-qualified candidates for application in contemporary devices.[17,18] The ability to employ chemical oxidation with ferric chloride as a means to produce P3ATs that are beneficial for use in modern technological applications is extremely important because of the ease and affordability of the polymerization technique.

The experiments performed within this Chapter employing low-temperature polymerizations using different solvents that possess different physical properties gave some further insight into the coupling mechanisms involved in chain growth during the polymerization of P3HT that were outlined in Chapter 2 (cf. Section 2.6.2). It seems likely that the influence to the selective coupling pathway to form P3HTs may stem primarily from the effects provided by the specific solvent employed for the reaction (cf. Section 2.6.2). For instance, evidence exists that indicates the primary coupling route to form longer polymer chains in nonpolar solvents involves the coupling between thiophene monomer neutrals or radical cations and oligo(thiophene) radical cations (cf. Section 2.6.2); this route is reported to form more regioregular materials.[2-4] Whereas, there is evidence that the primary coupling route to form longer polymer chains in polar solvents involves the coupling between oligo(thiophene) radical cations with other oligo(thiophene) radical cations (cf. Section 2.6.2). It is very likely that the effect of low temperatures employed during the chemical oxidation with ferric chloride is to

intensify the influence to the primary coupling route that is mainly directed by the physical properties of the solvent employed as opposed to the low temperatures directly directing the coupling route.

4.8 References

(1) Amou, S.; Haba, O.; Shirato, K.; Hayakawa, T.; Ueda, M.; Takeuchi, K.; Asai, M. Head-to-Tail Regioregularity of Poly(3-Hexylthiophene) in Oxidative Coupling Polymerization with Fecl3. *Journal of Polymer Science, Part A: Polymer Chemistry*. **1999**, *37*, 1943-1948.

(2) Barbarella, G.; Zambianchi, M.; Toro, R. D.; Colonna, M., Jr.; Iarossi, D.; Goldoni, F.; Bongini, A. Regioselective Oligomerization of 3-(Alkylsulfanyl)Thiophenes with Ferric Chloride. *Journal of Organic Chemistry*. **1996**, *61*, 8285-8292.

(3) Roncali, J.; Garnier, F.; Lemaire, M.; Garreau, R. Poly Mono-, Bi-, and Trithiophene: Effect of Oligomer Chain Length on the Polymer Properties. *Synthetic Metals*. **1986**, *15*, 323-331.

(4) Lacroix, J.-C.; Maurel, F.; Lacaze, P.-C. Oligomer-Oligomer Versus Oligomer-Monomer C2-C2' Coupling Reactions in Polypyrrole Growth. *Journal of the American Chemical Society*. **2001**, *123*, 1989-1996.

(5) Stanke, D.; Hallensleben, M. L.; Toppare, L. Oxidative Polymerization of Some N-Alkylpyrroles with Ferric Chloride. *Synthetic Metals*. **1995**, *73*, 267-272.

(6) Sugimoto, R.; Takeda, S.; Gu, H. B.; Yoshino, K. Preparation of Soluble Polythiophene Derivatives Utilizing Transition Metal Halides as Catalysts and Their Property. *Chemistry Express*. **1986**, *1*, 635-638.

(7) Brauch, R. M. Structural Characterization of Poly (Heterocycle)S Formed Using Oxidative Methods. Ph.D. Dissertation, Louisiana State University and A&M College, Baton Rouge, 2006.

(8) Niemi, V. M.; Knuuttila, P.; Osterholm, J. E.; Korvola, J. Polymerization of 3-Alkylthiophenes with Ferric Chloride. *Polymer*. **1992**, *33*, 1559-1562.

(9) Van Duyne, R. P.; Reilley, C. N. Low-Temperature Electrochemistry. III. Application to the Study of Radical Ion Decay Mechanisms. *Analytical Chemistry*. **1971**, *44*, 158-169.

(10) Lund, H. *Organic Electrochemistry*; Lund, H., Baizer, M. M.; 3rd ed.; Marcel Dekker: New York, 1991, 302.

(11) Hapiot, P.; Gaillon, L.; Audebert, P.; Moreau, J. J. E.; Lere-Porte, J. P.; Wong Chi Man, M. Solvent Effects on the Polymerization Kinetics of Some α-Silylated Thiophene Oligomers. Special Influence of the α-Silyl Group. *Synthetic Metals*. **1995**, *72*, 129-134.

(12) Camarada, M. B.; Jaque, P.; Diaz, F. R.; del Valle, M. A. Oxidation Potential of Thiophene Oligomers: Theoretical and Experimental Approach. *Journal of Polymer Science, Part B: Polymer Physics*. No pp yet given.

(13) Ten Hoeve, W.; Wynberg, H.; Havinga, E. E.; Meijer, E. W. Substituted 2,2':5',2":5",2"':5"',2"":5"",2""':5""',2""":5""",2"""':5"""',2"""":5""",2""""':5""",2""""":5"""- Undecithiophenes, the Longest Characterized Oligothiophenes. *Journal of the American Chemical Society*. **1991**, *113*, 5887-5889.

(14) McCullough, R. D.; Lowe, R. D.; Jayaraman, M.; Anderson, D. L. Design, Synthesis, and Control of Conducting Polymer Architectures: Structurally Homogeneous Poly(3-Alkylthiophenes). *Journal of Organic Chemistry*. **1993**, *58*, 904-912.

(15) Trznadel, M.; Pron, A.; Zagorska, M.; Chrzaszcz, R.; Pielichowski, J. Effect of Molecular Weight on Spectroscopic and Spectroelectrochemical Properties of Regioregular Poly(3-Hexylthiophene). *Macromolecules*. **1998**, *31*, 5051-5058.

(16) Qi, Z.; Pickup, P. G. Reactivation of Poly(3-Methylthiophene) Following Overoxidation in the Presence of Chloride. *Journal of the Chemical Society, Chemical Communications*. **1992**, 1675-1676.

(17) Kline, R. J.; McGehee, M. D.; Kadnikova, E. N.; Liu, J.; Frechet, J. M. J.; Toney, M. F. Dependence of Regioregular Poly(3-Hexylthiophene) Film Morphology and Field-Effect Mobility on Molecular Weight. *Macromolecules*. **2005**, *38*, 3312-3319.

(18) Woo, C. H.; Thompson, B. C.; Kim, B. J.; Toney, M. F.; Frechet, J. M. J. The Influence of Poly(3-Hexylthiophene) Regioregularity on Fullerene-Composite Solar Cell Performance. *Journal of the American Chemical Society*. **2008**, *130*, 16324-16329.

Chapter 5

Summary and Future Outlook

5.1 Summary and Conclusions

The purpose and primary focus of the work presented within this Dissertation was to garner a better understanding as to the effects of experimental conditions on the structure of poly(3-hexylthiophene), P3HT, formed by chemical oxidative coupling using $FeCl_3$ as an oxidant in hopes of improving the ability to tailor the physical properties of P3HTs formed via manipulation of oxidative coupling routes. Poly(3-alkylthiophene)s, P3ATs, are highly-valued materials and their molecular structure is of main concern when assessing and developing their applicability for realistic and relevant use in contemporary technologies as both microscopic and macroscopic structure directly impacts the electrical and optical properties of the polymer.[1-5] Specifically, the aim of this research was to determine the dependence of structural characteristics, such as endgroups, molecular weights, and regioregularities on the solvent employed for the reaction and the temperature the reaction was performed. In doing so, much of the research conducted herein was done with the application of matrix-assisted laser desorption/ionization time-of-flight mass spectrometry, MALDI-ToF-MS. Consequently, a large portion of this study was also focused on uncovering the factors, such as sample preparation and instrumental issues, that contribute to the high molecular weight mass discrimination observed in the MALDI-ToF-MS analysis of these materials and the inconsistency of other traditional methods, such as size-exclusion chromatography, SEC, to correctly characterize the molecular weights of poly(3-alkylthiophene)s.

Chemical oxidative polymerization of these materials remains the most popular and wide-spread method for the preparation of P3ATs, due to the method's affordability, ease, and ability to form large yields of high mass polymer. Therefore, the ability to utilize this synthetic

route with a better understanding of the effects of the experimental conditions that may be employed in order to augment the materials characteristics is of utmost importance. The work presented in this Dissertation has demonstrated that through the proper selection of solvent and/or adjustment to temperature this simple and convenient synthetic method can be employed to modify the properties of the resulting P3ATs. Furthermore, this study has provided enormous insight as to the necessary methodology required in order to obtain accurate molecular weight measurements for these materials both by MALDI-ToF-MS and SEC.

P3HTs having different structural characteristics were synthesized by chemical oxidation with ferric chloride using a variety of solvents possessing different polarites and Lewis acidities and basicities. It was demonstrated that P3HTs formed in very polar solvents having strong Lewis acidity with little Lewis basicity possess limited chlorination to their α-terminals. Whereas, P3HTs formed in very nonpolar solvents having strong Lewis acidity with little Lewis basicity exhibited much more chlorination to their α-terminals as well as perhaps chlorination extended to β-positions. This phenomenon is likely attributed to the active species of oxidant that is dependent on the polarity of the solvent and the interaction of the oxidant species with the solvent, depending on the Lewis acidity of that solvent. It was further demonstrated that the regioregularity of P3HTs formed in very nonpolar solvents improves as compared to those formed in polar solvents, which possibly results from differences in the coupling mechanism of the reactive thiophene species that propagates chain growth during the reaction and is dependent on the polarity of the solvent employed. However, there is some evidence that the Lewis acidity and basicity of the solvent does play a role in directing the coupling pathway.

Incidentally, it was also demonstrated that the methanol-soluble portion of P3HT remaining in the filtrate after vacuum filtration of the solid polymer produced during the chemical oxidation procedure contained very small (n = 5-7), very regioirregular (~50%

regioregular) oligomers that contribute to erroneous data during endgroup and molecular weight analysis of P3HTs by MALDI-ToF-MS and ^{1}H-NMR when this portion was included with the solid polymer for assessment. It was thus concluded that this soluble portion of polymer should not be included as recovered product from the chemical oxidation of P3HTs with ferric chloride, which is in good agreement with other reports in the literature.[6]

P3HTs having different structural characteristics were synthesized by chemical oxidation with ferric chloride at very low temperatures (–25 to –30 °C) using a variety of solvents possessing different polarites and Lewis acidities and basicities. It was demonstrated at low temperatures P3HTs are formed with very limited chlorination compared to those formed under similar conditions at room temperature regardless of the solvent used for the reaction. Although the exact reasons for this phenomenon are still not understood, it is likely that the combination of low temperatures, extended polymerization time, and the slow kinetics of the polymerization afforded by the low temperature are responsible.

It was further demonstrated that the regiorgularity of P3HTs formed at low temperatures by chemical oxidation improved compared to those formed under similar conditions at room temperature when the reaction was performed using very nonpolar solvents having strong Lewis acidity with little Lewis basicity. However, the regioregularity of P3HTs formed at low temperatures by chemical oxidation diminished compared to those formed under similar conditions at room temperature when the reaction was performed using a polar solvent having strong Lewis acidity with little Lewis basicity. The mechanisms influencing these results are not fully understood, although it is likely that low temperature may intensify the forces influencing the primary coupling routes of the reactive thiophene species that propagates chain growth during the reaction, which are more so dependent on the physical properties of the solvent employed for the reaction than the temperature at which it is performed.

During the MALDI-ToF-MS analysis of P3HTs formed by chemical oxidation with iron(III) chloride, it was unequivocally shown that multiply-charged P3HT species are formed during the MALDI event. It was further demonstrated that the presence of multiply-charged species strongly contribute to the mass discrimination of higher molecular weight distributions during the MALDI-ToF-MS analysis of broadly disperse P3HT samples because of extensive detector saturation stemming from these species. This work clearly proves the necessity of prefractionation of polydisperse P3HTs before accurate molecular weight and molecular weight distribution measurements can be obtained by these means. This works also provided evidence that some high mass discrimination occurs during the MALDI-ToF-MS anaylsis of P3HTs because of the lack of ionization efficiency and/or entanglement issues for very long chain polymers.

Furthermore, the comparison of average molecular weights for P3HT samples–that have been fractionated offline using semipreparative SEC–obtained by both MALDI-ToF-MS and analytical SEC analysis has shown that analytical SEC coupled with MALLS and DRI detection provides calculated molecular weight data for these materials that is overestimated by a factor of 3–4 times the estimations yielded by MALDI-ToF-MS. The overestimations of molecular weight data obtained by SEC-MALLS/DRI likely result from several factors including: (i) the inconsistent extrapolation of $\sin^2(\theta/2) = 0$ in the plot of R_θ/K_C versus $\sin^2(\theta/2)$ due to poorly fit shape factors; (ii) the changes in the $\delta n/\delta c$ of P3HTs as a function of molecular weight; (iii) enthalpic interactions between P3HTs and the SEC column bed; (iv) aggregation of P3HTs during the separation process that result directly in overestimations to the extent of scattered light from the aggregates, and/or changes in the shape of the material that impact the correct extrapolation of $\sin^2(\theta/2) = 0$ because of poorly fit shape factors.

Overall, the work described in this Dissertation has offered a greater insight into the means to produce P3ATs possessing tailored functionality by the facile and affordable method of chemical oxidation. These studies have also elucidated some of the challenges encountered during the analytical assessment of these materials and aided in providing the means to overcome these difficulties and accurately characterize P3ATS so that they may be better utilized in modern applications. The results I have made available within this Dissertation lay a strong foundation for future efforts to better understand the structural properties of P3ATs made by chemical oxidation, which will aid in the development of their use in relevant and purposeful technologies.

5.2 Future Work

In order to better understand the mechanisms driving the coupling of the reactive thiophene species that propagate chain growth during polymerization, which have been proposed to depend on the physical properties of the solvent and the temperature employed for chemical oxidation, the in-depth characterization of product species that evolve as a function of time during chemical oxidation could be conducted. Polymerizations could be performed using solvents employed for the studies presented in this Dissertation and aliquots of the reaction mixtures retrieved in sequence at different intervals of the reaction. The aliquots would then be quenched and processed for analysis, which would include the techniques outlined in this Dissertation.

Polymer chain formation via coupling between thiophene oligomers and thiophene monomers or, on the other hand, between thiophene oligomers and other thiophene oligomers–which have been speculated in this Dissertation to be the two pathways resulting in the differences observed for structural regioregularity and molecular weights of the P3HTs investigated–could be monitored using MALDI-ToF-MS and GC-MS. The two different

coupling routes should yield oligomer patterns at different times during the polymerization that are unique for one pathway or the other. For instance, polymer chain growth via oligomer-to-monomer coupling would be apparent by means of mass spectrometry from ion series signals resulting from incremental progression of growth (i.e. n = 6, 7, 8, 9…) differing by m/z 166. Whereas, polymer chain growth via oliomer-to-oligomer coupling could be evidenced by ion signals differing in repeating ion signal patterns indicative of oliomer-to-oligomer coupling (i.e. n = 5, 6, 10, 11, 12…). The reaction aliquots characterized by mass spectrometry could then be characterized by ^{1}H-NMR for structural determination and conclusions could be drawn as to the effects of coupling and therefore the effects of solvent and temperature to the regioregularity of the material. Once information as to the differences between coupling mechanisms and regioregularity stemming from solvent and temperature has been correlated, the effect of these experimental conditions to the molecular weight of the materials produced by chemical oxidation with ferric chloride at different temperatures using various solvents can be better determined.

Also, much effort should be placed on the in-depth characterization of fractions of P3HT obtained by semipreparative size-exclusion chromatography. These fractions should first be collected in smaller increments as they elute from the SEC column. Although the fractions examined within this dissertation were collected every ten seconds and possessed relatively narrow distributions, the MALDI-ToF-MS analysis indicated that there was still a large overlap of molecular weight distributions between polymer fractions; this is always the case with SEC but smaller fractions would allow better analytical evaluation of very narrowly-distributed fractions with distinct molecular weight ranges. Semipreparative SEC affords the ability to inject rather large concentrations (up to 10 mg) of polymer onto the column bed and therefore very small fractions (i.e. collected every 5 seconds) yield abundant amounts of fractionated material for analysis.

The fractions of P3HT obtained by semi-preparative size-exclusion chromatography used for MALDI-ToF-MS studies in this work afforded the observation of P3HT ion series signals only up to roughly *m/z* 35,000, albeit very little signal was achieved for the earlier eluting P3HT fractions between m/z 30,000–35,000. However, the MALDI-ToF-MS analysis of polymer above *m/z* 20,000 provided spectra wherein the ion series signals were not well resolved and displayed very broad ion series signals that indicate the fractions of these earlier eluting material were perhaps comprised of broad molecular weight distributions. This may be due to higher concentrations of P3HT within the earlier eluting fractions. Furthermore, the absence of observable ion signals for fractions from the earliest eluting material by MALDI-ToF-MS examination indicates a lack of ionization efficiency for these materials that may be caused by the broad range of molecular weight distributions within the fraction and/or entanglement of long polymer chains. In either case, collecting smaller fractions with more narrow distributions may assist in overcoming the difficulties encountered during the MALDI event and aid to promote ionization of the earlier eluting fractions of P3HT; it will at least better the resolution of the observable P3HT ion series signals in higher *m/z* ranges that are presented within this document.

Furthermore, P3HT fractions obtained by semipreparative SEC should be used to determine the differences in $\delta n/\delta c$ of P3HTs as a function of molecular weight. The preliminary studies concerning the change in $\delta n/\delta c$ for P3HTs as a function of molecular weight discussed in this Dissertation involved the fractionation of bulk polymer by means of soxhlet extraction using different organic solvents. The soxhlet-extracted fractions examined exhibited tremendous differences in $\delta n/\delta c$ for acetone- and *n*-hexane-extracted samples. However, the molecular weight distributions for these soxhlet-extracted fractions were very broad and overlapped considerably. As it has been previously discussed in this Dissertation, the impact that the $\delta n/\delta c$ has on the correct determination of molecular weight data by means of SEC-MALLS/DRI

necessitates that the accurate $\delta n/\delta c$ for the appropriate molecular weight distribution be employed for such analysis, as very small changes in $\delta n/\delta c$ result in large differences in the calculated molecular weight data. The correct determination of the $\delta n/\delta c$ for a particular molecular weight distribution may only be unquestionably accomplished using very narrow distributions of polymer that may be acquired via semi-preparative SEC.

Further studies should also be performed on the collected polymer fractions to obtain more detailed information about the electronic properties of the various molecular weight distributions. Fractionation by semipreparative SEC should be performed on polymers made under different experimental conditions in order to correlate the electronic properties for polymers with different degrees of regioregularity and endgroup substitution with their molecular weight distribution. Electrochemical studies could be performed to evaluate the electronic properties of different P3HT molecular weight distributions having different regioregularities and endgroup substituents in order to determine their oxidation and reduction potentials, as well as their conductivities. Electrochemical studies could be corroborated with UV-Vis spectrometric analysis. These studies would provide insight into the energy band levels (HOMO and LUMO) of P3HTs of different molecular weight distributions possessing different chemical structures and compositions.

Finally, much effort should also be placed towards outlining and implementing procedures in order to obtain accurate molecular weight information about P3ATs by use of analytical size-exclusion chromatography. Narrowly-dispersed fractions of P3HT collected by semipreparative SEC that have been well-characterized using MALDI-ToF-MS could be used as molecular weight standards for the determination of the average molecular weights of unknown P3AT samples using conventional-analytical SEC employing solely colligative detection methods. This would be useful for unknown P3AT samples that did not possess very large

average molecular weights, unless P3AT fractions of higher molecular weight distributions used as molecular weight standards could be successfully characterized by MALDI-ToF-MS.

However, the P3HT fractions collected by semipreparative SEC could also be used to modify the methods employed for the SEC-MALLS/DRI analysis of unknown polydisperse P3HT samples possessing large average molecular weights as well. As mentioned above, the correct determination of the $\delta n/\delta c$ for P3HTs as a function of molecular weight is the first crucial step required in order to accomplish this task. Once the correct $\delta n/\delta c$ has been established for a particular weight distribution, that weight distribution could be analyzed by analytical SEC-MALLS/DRI. For each weight fraction evaluated, careful examination of the Debye plots for each slice of the chromatogram for each weight fraction would allow a better determination of the best-fit shape function for that fraction–as well as offering information to conformational changes between different molecular weight fractions–and provide better extrapolated light scattering data from the Debye plot. The combination of the correct $\delta n/\delta c$ and fit function would enable more accurate determination of molecular weight data for future unknown P3AT samples possessing large average molecular weights, although the analysis of future samples would possibly require some degree of fractionation as well.

Issues concerning enthalpic interactions between P3HT and the column bed, along with aggregration of P3HT, during SEC analysis of these materials should also be addressed. In order to examine the effects of enthalpy between P3HT and the column material experiments could be performed using a SEC column wherein the bed material has a degree of hydrophilic composition incorporated. To examine the effects of the aggregation of P3HTs during SEC analysis experiments could be performed while elevating the temperature of the column and mobile phase.

5.3 References

(1) McCullough, R. D.; Lowe, R. D.; Jayaraman, M.; Anderson, D. L. Design, Synthesis, and Control of Conducting Polymer Architectures: Structurally Homogeneous Poly(3-Alkylthiophenes). *Journal of Organic Chemistry*. **1993**, *58*, 904-912.

(2) Trznadel, M.; Pron, A.; Zagorska, M.; Chrzaszcz, R.; Pielichowski, J. Effect of Molecular Weight on Spectroscopic and Spectroelectrochemical Properties of Regioregular Poly(3-Hexylthiophene). *Macromolecules*. **1998**, *31*, 5051-5058.

(3) Qi, Z.; Pickup, P. G. Reactivation of Poly(3-Methylthiophene) Following Overoxidation in the Presence of Chloride. *Journal of the Chemical Society, Chemical Communications*. **1992**, 1675-1676.

(4) Woo, C. H.; Thompson, B. C.; Kim, B. J.; Toney, M. F.; Frechet, J. M. J. The Influence of Poly(3-Hexylthiophene) Regioregularity on Fullerene-Composite Solar Cell Performance. *Journal of the American Chemical Society*. **2008**, *130*, 16324-16329.

(5) Kline, R. J.; McGehee, M. D.; Kadnikova, E. N.; Liu, J.; Frechet, J. M. J.; Toney, M. F. Dependence of Regioregular Poly(3-Hexylthiophene) Film Morphology and Field-Effect Mobility on Molecular Weight. *Macromolecules*. **2005**, *38*, 3312-3319.

(6) Amou, S.; Haba, O.; Shirato, K.; Hayakawa, T.; Ueda, M.; Takeuchi, K.; Asai, M. Head-to-Tail Regioregularity of Poly(3-Hexylthiophene) in Oxidative Coupling Polymerization with Fecl3. *Journal of Polymer Science, Part A: Polymer Chemistry*. **1999**, *37*, 1943-1948.

Vita

Warren Solfiell was born in Auburn, New York. He spent his childhood and adolescent years living in Westborough, Massachusetts, although he was lured by the beauty of the Finger Lakes back to New York as a young man where he spent the next decade. Warren returned to higher education as a nontraditional student at the age of 30. He obtained his Bachelor of Science in Chemistry from Framingham State University in 2004. He continued his effort towards an advanced degree in analytical chemistry at Louisiana State University, where he joined the research group of Professor Robin L. McCarley. Warren currently still resides in Baton Rouge, Louisiana.